UNIVERSITÀ
DI SIENA
1240

**Doctorate in Chemical and Pharmaceutical Sciences
Cycle XXXV (2019-2022)**

Exploration of the selective and multitarget inhibition

of the endocannabinoid system

catabolic enzymes as pharmacological tools

for central nervous system disorders

Coordinator: Prof. Maurizio Taddei

Department of Biotechnology, Chemistry and Pharmacy

Tutor: **PhD Candidate:**

Prof. Stefania Butini   Alessandro Papa

Table of contents

1. Introduction

1.1. The endocannabinoid system

The most important discoveries of modern science could be abridged as "Eureka moments" representing the convergent point of random observations, faux pas and serendipity made by talented scientists. The "Eureka moment" of Raphael Mechoulam, considered the father of modern studies on cannabis, was the identification of the main components of *Cannabis sativa*: delta-9-tetrahydrocannabinol (Δ^9-**THC**, **1 Figure 1**) and cannabidiol (**CBD**, **2 Figure 1**) [1].This discovery, dated back as 1969, increased the interest around the recreational and medicinal use of cannabis. Nevertheless, *Cannabis sativa* is a remarkable example of a socially divisive topic, confused by too many contrasting and sometimes incorrect viewpoints deriving from both scientific and non-scientific community. Several studies focused on **THC**, which is the main responsible of the psychotropic effects of cannabis, evidenced its high lipophilic structure, suggesting that THC mediated effects could be due to a non-specific interaction with membrane cells [2]. Afterwards at the discovery of the enantioselective pharmacological activity THC mediated, the idea of the potential presence of a specific cannabinoid receptor was put forward [3]. The first **THC** specific receptors was identified in 1988 and it was called cannabinoid receptor type 1 (CB$_1$R). Trough homology cloning process also a second receptor was identified, called cannabinoid receptor type 2 (CB$_2$R), which resulted rather different by CBR1 [4]. This information opened the way for further studies which were focused on the discovery of physiological ligands able to engage the CBRs. The first identified endogenous ligand was anandamide (**3**, **AEA**, **Figure 1**), followed by the 2-arachidonoylglycerol (**4**, **2-AG**, **Figure 1**) [5]. This resulted, in the late 1990s, in the identification of a rather complex endogenous signaling system, namely the

endocannabinoid system (ECS). The ECS is a widespread neuromodulatory network that plays an important role in the regulation of many cognitive physiological functions.
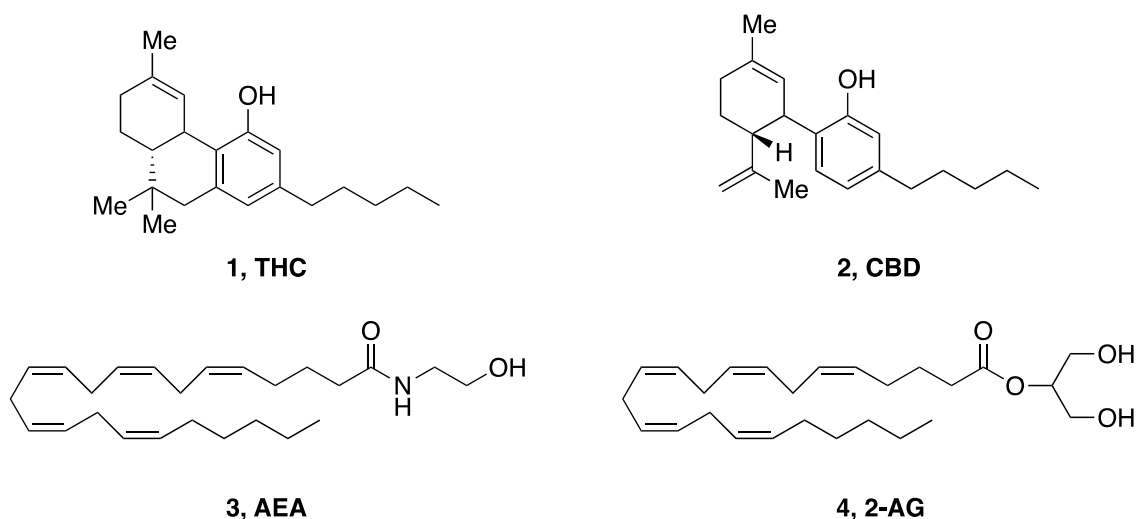
Figure 1. Chemical structure of exogenous (THC and CBD) and endogenous (AEA and 2-AG) ligands of CBRs.

The ECB includes: (1) two G-protein-coupled receptors (GPCR) known as CB_1R and CB_2R; (2) the endogenous lipidic ligands for these receptors, called endocannabinoids; (3) proteins and enzymes involved in the synthesis and in the catabolism of these endogenous ligands [6] [7]. Most of the ECS components are multifunctional; therefore, the ECS influences and is influenced by many other signaling pathways. It is a pleiotropic signaling system involved in all aspects of mammalian physiology and pathology, and for this reason represents a potential target for the design and development of new therapeutic drugs [8] [6].

1.1.1. Cannabinoid receptors

The CB_1R gene is located on chromosome 6 (6q15, HGNC:2159) and comprise of four exons. This receptor is coupled to inhibitory G protein, and it is composed by seven-transmembrane helical domain, extracellular and intracellular loops, an extracellular N-terminus and an intracellular carboxy terminal tail [9] [10]. It is expressed in all central

nervous system (CNS) area. CBR1 have been observed in the cerebral cortex (cingulate gyrus, prefrontal cortex, and hippocampus), basal ganglia (globus pallidus, substantia nigra), periaqueductal gray, hypothalamus, amygdala, and cerebellum [11]. Is highly expressed in brainstem medullary nuclei, such as the nucleus of the solitary tract and area postrema, serving as the primary integrative centers for the cardiovascular system and emesis, respectively [12]. The CB1Rs were found to be primarily located in the presynaptic terminals of GABAergic (amygdala and cerebellum) [13] glutamatergic (cortex, hippocampus and amygdala) [14], dopaminergic, GABAergic interneurons, cholinergic neurons, noradrenergic, and serotonergic neurons [15]. Low levels of presynaptic CB_1R were also detected in the nociceptive primary afferent fibers in the spinal cord. In addition to neuronal cells, CBRs were also identified in the perivascular and parasynaptic astroglia processes and oligodendrocytes [16] [17]. Apart from astrocytes, the CBR_1 was also identified in other cells of the blood brain barrier (BBB) such as the brain endothelial cells, pericytes, and vascular cells. Further, the CB_1R was also observed in the myelinating Schwann cells of the peripheral nervous system. The CB_1R can be also expressed at the post-synaptic level where it can form heterodimers in combination with other GPCRs including adenosine receptors and dopamine D_2 receptors [10][6]. The CB_1R is coupled with Gi/Go proteins whose activation determine an inhibition of adenylate cyclase and stimulation of Mitogen Activated Protein Kinase (MAPK), with subsequent opening of K^+ channels and closure of type P/Q Ca^{2+} channels [18]. These neuronal electric effects CB_1R mediated, resulting in the regulations of neurotransmitters release at the level of the synaptic cleft, especially at the level of glutamatergic and GABAergic neurons [19]. CB_2R is located in chromosome 1p36 in humans and the gene has a simple structure containing a single coding exon. The CB_2R

are also coupled with a Gi/Go GPCR protein. This receptor is highly expressed in immune cells and lymphoid tissue, modulating both innate and adaptative immune response [20]. CB_2R stimulation led to the inhibition of adenylate cyclase with following reduction of cAMP levels and attenuate activity of protein kinase A (PKA). Low levels of cAMP and PKA in the cytosol are closely connected with the regulation of variety of genes expression which promotes survival, proliferation, and differentiation of the immune cells. Hence, the CB2R activation results in a reduction of the immune system activity [21]. Under pathological conditions, CB_2R were detected in fibrotic kidney [22], and in active hepatic stellate cells [23]. However in physiological conditions the same receptor has an important role in the maintenance of homeostasis in pancreatic cells [24], adipocytes [25], skeletal muscle cells [26] and cardiomyocytes [27] (see **Figure 2**). The CBRs cross-connections with other neurotransmitters' signaling pathways highlight the strong neuromodultory activity of the ECS that underscore its pivotal role in cognition, memory, movement, and nociception [13].
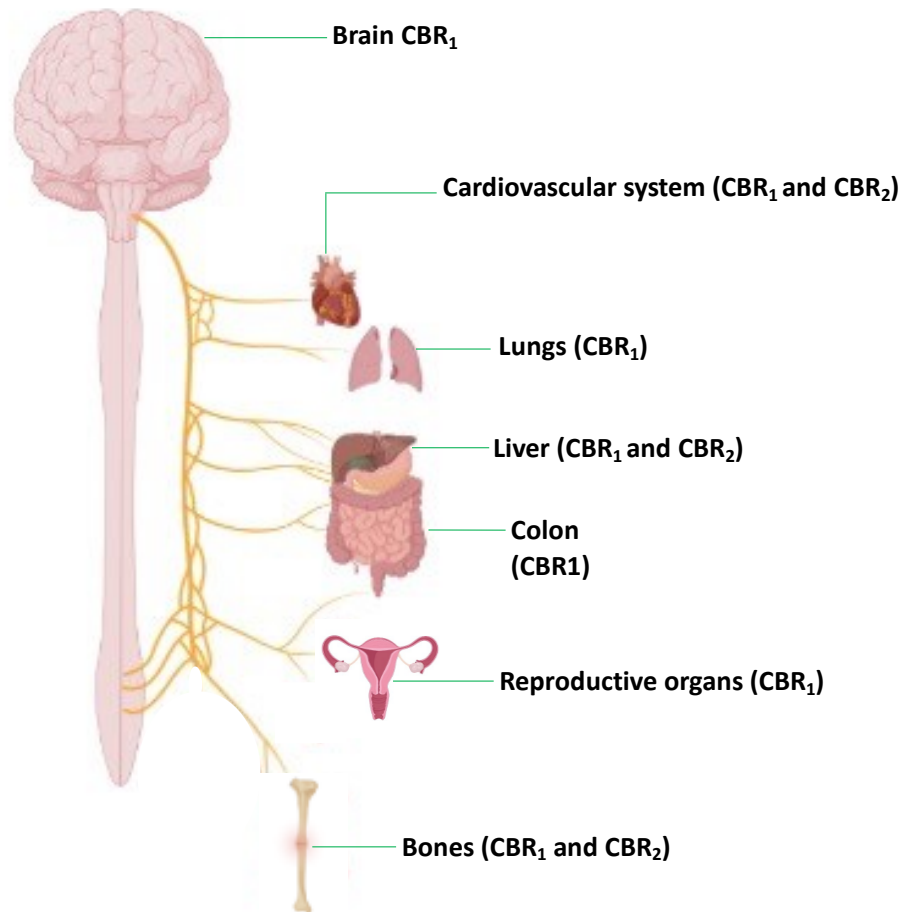
Figure 2. Cannabinoid receptors distribution through the human body.

Transient potential receptor type 1 vanilloid channel (TRPV1) and G protein-coupled receptor 55 (GPR55) have been identified as other suspected cannabinoid receptors. TRPV1 belongs to a subclass of ion channels characterized by weak voltage sensitivity and non-selective permeability to monovalent and divalent cations including Mg^{2+}, Ca^{2+}, and Na^+ [8]. TRPV1 activation contributes to pain transmission, neurogenic inflammation and, as suggested by more recent studies, also to synaptic plasticity, neuronal overexcitability and neurotoxicity [28]. TRPV1 channels are widely expressed in dorsal root ganglia and sensory nerve fibers, but also in non-neuronal cells and tissues such as keratinocytes and skeletal muscle. GPR55 belongs to the large GPCR family and is currently considered a potential cannabinoid receptor. The endogenous ligand of this receptor has been identified in lysophosphatidylinositol, but GPR55 appears to be

activated by **THC (1)** and by some synthetic agonists of CB_1R. The exact function of GPR55 is still not fully understood, but recent findings have suggested that activation of GPR55 may play an opposite role to that of CB_1R by increasing the release of neurotransmitters [29].

1.1.2. Endocannabinoids

The endocannabinoids are lipid mediators, mostly esters or amides of arachidonic acid (AA). AEA which is an ethanol amide of the AA and 2-AG [6] [30], which a glycerol ester of AA, are the most important endogenous ligands of CBRs. Particularly, 2-AG is the major endocannabinoid, because it is 100-1000-fold more abound than AEA. It is a full agonist of CB_1R (Ki = 440 nM) characterized by a lower activity but a better efficacy when compared with the partial CB_1R agonist AEA (Ki R = 240 nM) [6][31]. Both AEA and 2-AG are produced by the cleavage of plasma membrane phospholipids such as phosphatidylethanolamine (PE), phosphatilcoline (PC) or phosphatidylinositol 4,5-bifosfate (PI 4,5-bifosfate). The process starts from the Ca^{2+} dependent trans-acylase (Ca-TA) which transfers an acyl chain of AA from the 1-arachidynoilposphatisylcoline to the primary amino group of the PE, generating the *N*-acyl-phosphatidylethanolamine (NAPE). The hydrolytic activity of *N*-acyl- phosphatidylethanolamine-phospholipase D (NAPE-PLD) allows to obtain the AEA through a NAPE-PLD dependent process. However, AEA can be synthesized also by two NAPE-PLD independent biological route [32][33]. For the 2-AG, different biosynthetic processes were proposed, even if they are not completely characterized. Increased levels of Ca^{2+} lead to the activation of the membrane phospholipase C which hydrolyzes PI 4,5 biphosphate generating Inositol triphosphate (IP3) and diacylglycerol (DAG). Two serine hydrolases, diacylglycerolipase-α/ β (DAGL-α and DAGL-β) catalyzed the last step with the formation of 2-AG and AA [34]. However, also other endocannabinoids have been

identified: **2-arachidinoyl glycil ether (5, 2-AGE, Figure 3)**, **viridamine (6, Figure 3)**, **oleamide (7, Figure 3)**, **decoeseasanoilethanolammine (8, DHEA, Figure 3)** and *N*-**arachidonoildopamine (9, NADA, Figure 3)** [6]. In addition to the above mentioned CBRs ligands, also other endocannabinoid-like compounds were identified. Even if this latter do not show affinity for the CBRs, they can compete with the endocannabinoids for the active sites of their metabolizing enzymes, reducing the endocannabinoids degradations, resulting in that is called *entourage effect* [6] [35].
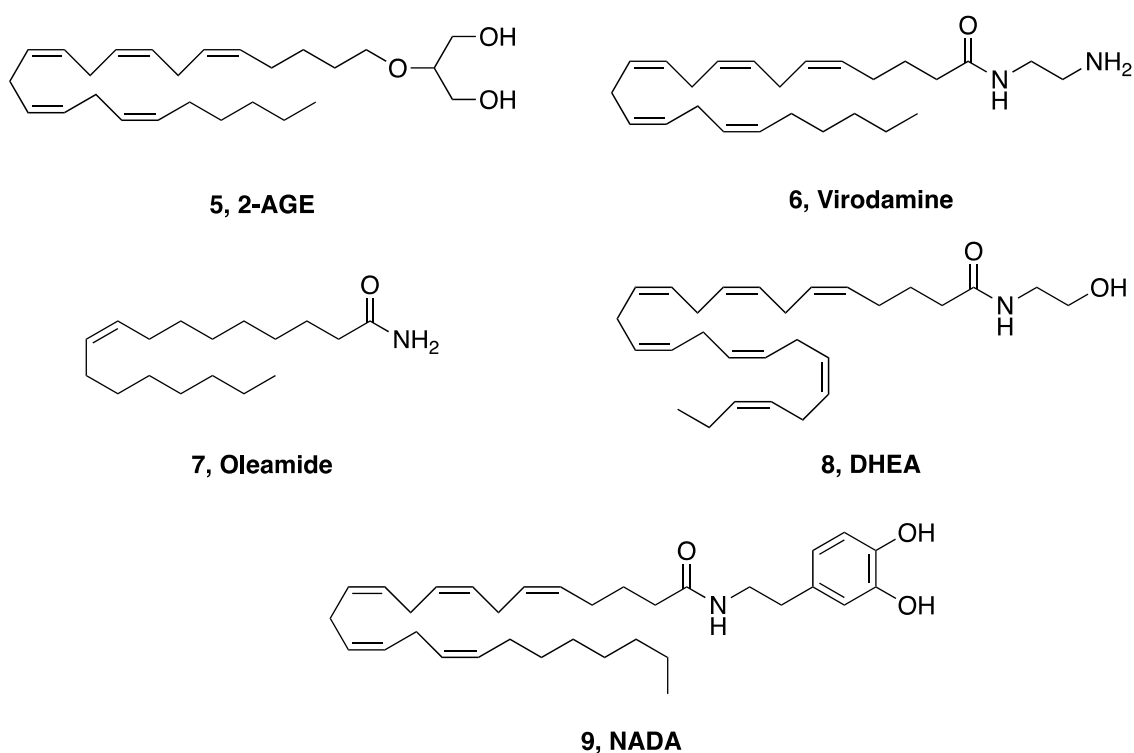
Figure 3. Chemical structure of endogenous ligands of the CBRs.

All these lipid mediators are synthetized "on demand" in the postsynaptic sites and released as result of increased levels of intracellular Ca^{2+}. After their release they migrate out of the neuron, by using the endocannabinoid membrane transporter (EMT), to stimulate the CB_1R at the presynaptic level. This retrograde activity leads to the activation of K^+ and inhibition of Ca^{2+} channels, regulating the duration of synaptic activities and,

subsequently, different forms of short- and long-term synaptic plasticity. In **Figure 4** a

schematic representation of ECS activity in a glutamatergic synapse is reported.
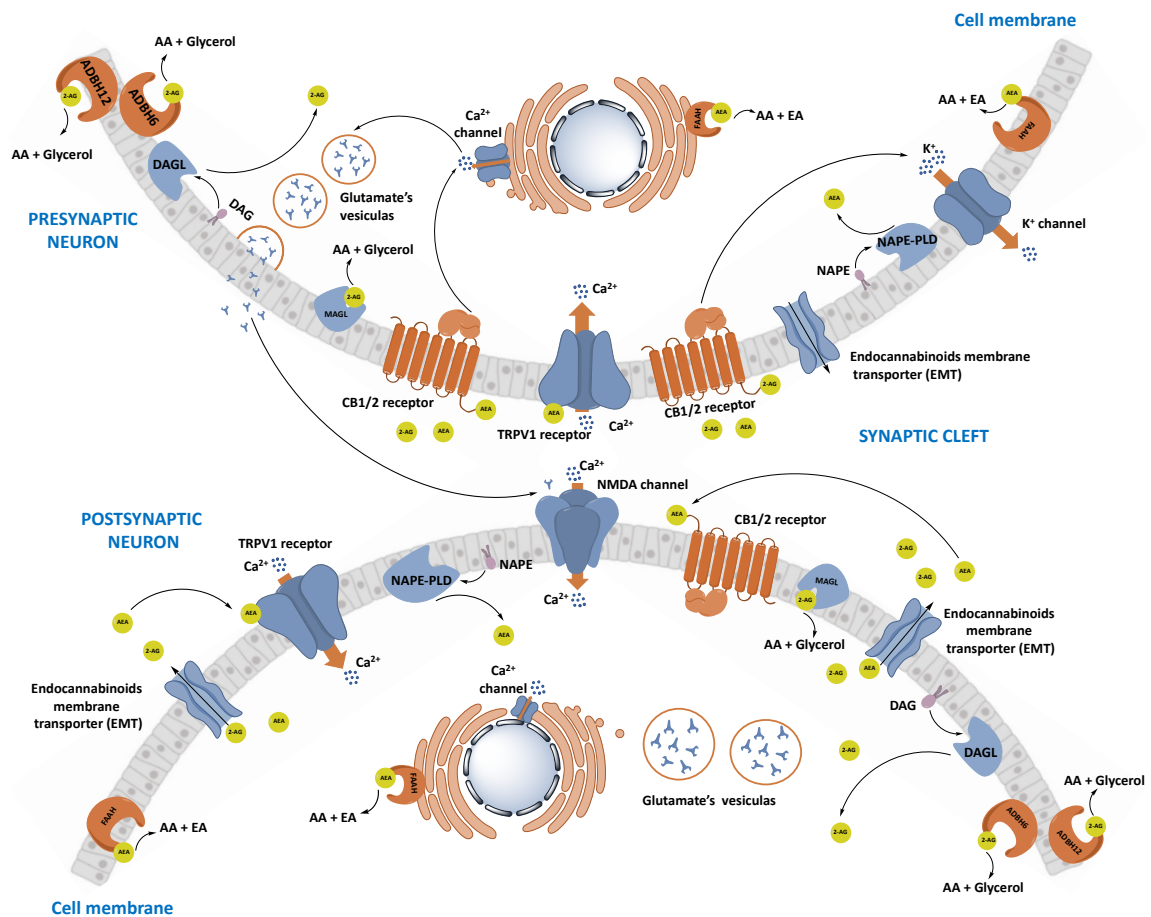
Figure 4. Retrograde signaling of ECS in a Glutamatergic synapse. Anandamide (AEA) and 2-arachidonoylglycerol (2-AG) are synthesized on demand in the postsynaptic neuron following an increment of Ca^{2+} concentration. AEA is synthesized starting from the membrane lipid N- acylphosphatidylethanolamine (NAPE) by N-acyl-phosphatidylethanolamine-hydrolyzing phospho- lipase D (NAPE-PLD) activity, while diacylglycerol lipase (DAGL) converts the diacylglycerol (DAG) in 2-AG. AEA and 2-AG move across the cell membrane through a purported endocannabinoid membrane transporter (EMT). Cannabinoid receptor type 1/2 (CB1/2) and transient receptor poten-tial vanilloid 1 (TRPV1), are the main receptor targets of AEA and 2-AG on the presynaptic neuron. Activation of CB1/2 receptors triggers the Ca^{2+}-mediated release of glutamate, in the presynaptic neuron, with subsequent activation of NMDA receptors in the postsynaptic neuron. Moreover, the transduction pathway of CB1/2-mediated determines the K^+ efflux which opposes the depolarization in the presynaptic neuron. AEA is hydrolyzed by FAAH enzyme while in the 2-AG catabolism are involved MAGL, ADBH6, and ADBH12 enzymes. The outcome of this process is the inhibition of glutamatergic activity. Moreover, endocannabinoid signaling can also proceed by a non-retrograde mechanism, in which AEA and 2-AG active CB1 receptors or TRPV1 channel on the postsynaptic neurons.

However, the presence of CB_1R and TPVR1 ion the post-synaptic neurons suggests that the endocannabinoid signaling can also proceed in a non-retrograde or autocrine manner [6]. After their activity, endocannabinoids are quickly removed from the synaptic cleft by an uptake process or passive diffusion and then inactivated by catabolic enzymes. The most important enzymes involved in the catabolism of AEA, and 2-AG are fatty acid amide hydrolase (FAAH) and monoacylglycerol lipase (MAGL) respectively (ref). However, also other enzymes take part at the endocannabinoids inactivation, and among these there are the alpha/beta-Hydrolase domain containing 6 and 12 (ABDH6 and ABDH12), manly involved in the catabolism of 2-AG [6].

1.1.3. The catabolic enzymes of the ECS

Inactivation of endocannabinoids rapidly occurs in vivo by cellular uptake and enzymatic hydrolysis. FAAH is primarily responsible for the degradation of AEA, while 2-AG inactivation preferentially occurs through hydrolysis by the presynaptically localized enzyme MAGL [36]. To a smaller extent, 2-AG is also metabolized by FAAH, alpha/beta-Hydrolase domain contain 6 (ABDH6), alpha/beta-Hydrolase domain contain 12 (ABDH12), and cyclooxygenase 2 (COX-2) [6][37].

1.1.4. FAAH enzyme

FAAH is a membrane-bound protein belonging to the serine hydrolase family. This enzyme plays a significant role in the catabolism of bioactive lipids called fatty acid amides (FAA) in both the CNS and peripheral tissues [37] [38]. FAAH is widely distributed throughout the body. In the rat, it was found in large quantities in the liver, followed by the small intestine, testes, uterus, kidneys, eye tissues, spleen, and possibly lungs, while skeletal muscle and heart lack this enzyme [6][37]. Immunohistochemical studies revealed that FAAH is widely localized in major neurons such as Purkinje cells

in the cerebral cortex, pyramidal cells in the cerebral cortex and hippocampus, and mitral cells in the olfactory bulb. The enzyme is also predominantly expressed within intracellular membranes such as the outer membrane of mitochondria and the smooth endoplasmic reticulum in the neuronal somatodendritic compartment. Most of the enzyme belonging to the hydrolase superfamily are soluble cytosolic enzymes, whilst FAAH is an integral membrane protein. It is composed by 579 amino acids with a 63 kDa molecular weight. The first crystal structure of the enzyme, which was resolved in 2002, shows the FAAH in complex with the irreversible inhibitor MAFP (see **Figure 5**, panel a). Its homodimeric nature is characterized by a protein *core* of a twisted β-sheet, surrounded by 24 α-helices.
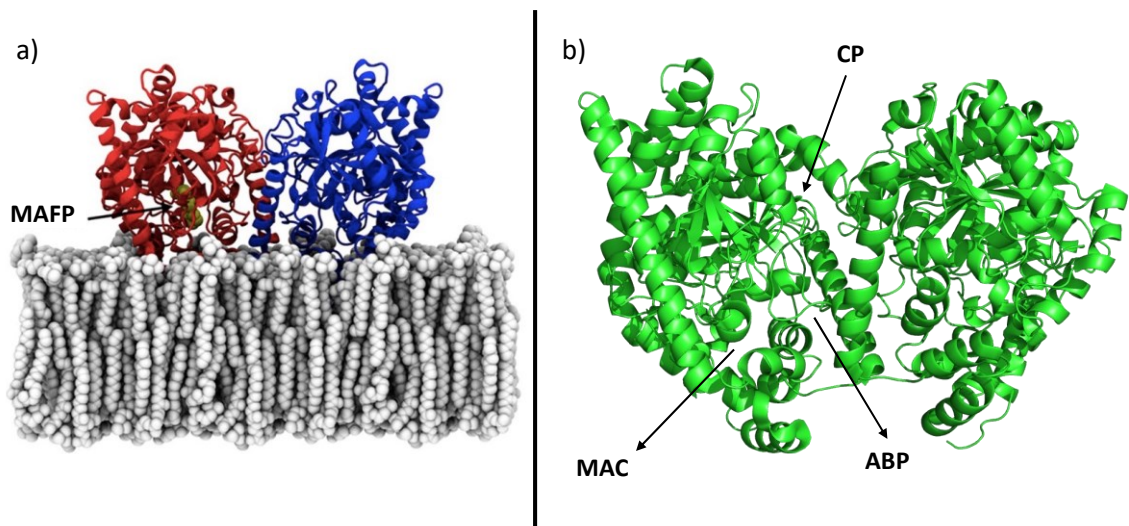
Figure 5. Dimeric structure of *h*FAAH enzyme. Panel a): FAAH enzyme in complex with the irreversible inhibitor MAFP. Panel b): identification of the different channels in the FAAH structure.

The protein shows multiple channels necessary for the input and/or output of substrates and catabolic products to both intracellular and extracellular compartment[37] [39]. The membrane access channel (MAC) is a lipophilic channel which connects the protein surface with the catalytic pocket of the enzyme. The cytosolic port (CP) connects the catalytic center to the intracellular space. It is composed by hydrophilic amino acids

which accommodates polar catabolic products. Finally, the acyl chain binding pocket (ABP) interacts with the lipophilic chain of the endogenous substrate. In the catalytic pocket of the FAAH enzyme is presents the catalytic triad responsible of the hydrolytic activity. It is composed by Ser241, Ser217, and Lys142 [37,39]. Close to the catalytic triad a circle of N-H forms the oxanion hole, which allowed the accommodation of the carbonylic moiety of the substrate After the discovery of the 3D structure of the enzyme the catalytic mechanism of FAAH was identify by means mutagenic and kinetic studies. In **Figure 6** the catalytic mechanism of FAAH enzyme is depicted.
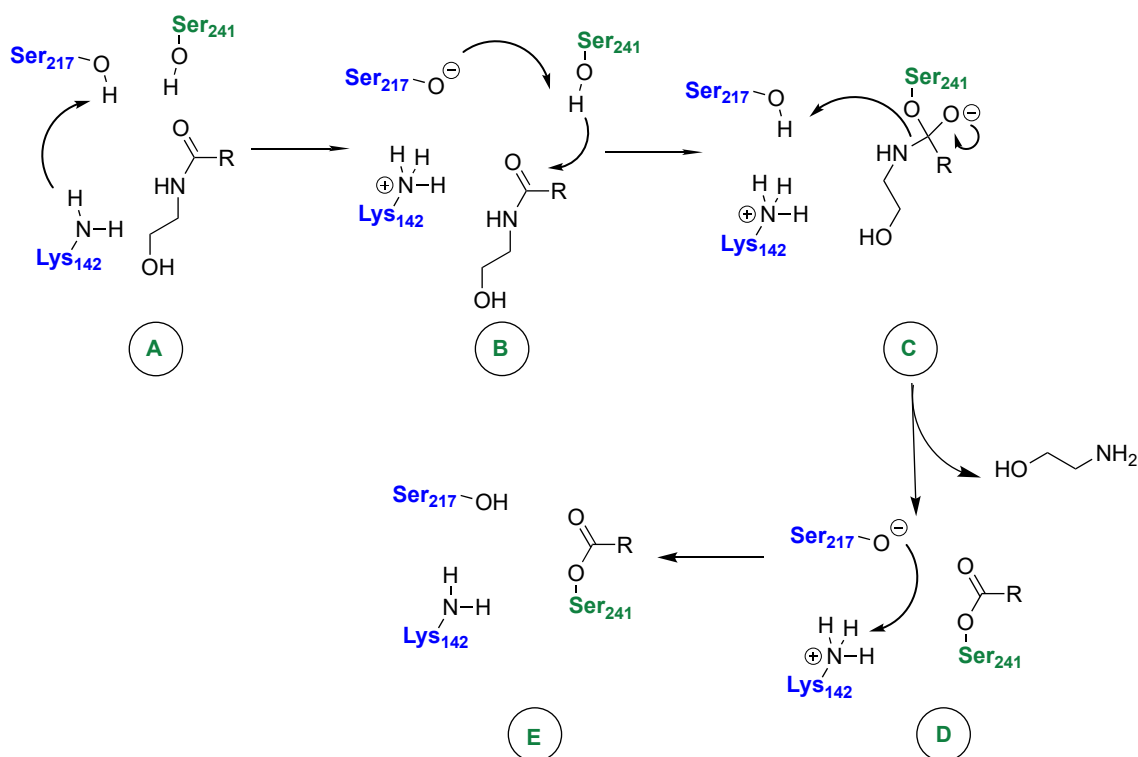
Figure 6. Catalytic mechanism of FAAH enzyme. Following the AEA entrance, the inactivation mechanism of AEA starts with the deprotonation of the Ser217 (step A) operated by Lys142, leading to the zwitterionic intermediate (step B). The alkoxide of Ser217 deprotonates the Ser217 residue activating this latter for a nucleophilic attack on the carbonylic group of AEA to form the tetrahedric intermediate C. The rearrangement of C lead to the release of ethanolamine and at the formation of *O*-acylated Ser241 (step D). A proton exchange from Lys142 and Ser 217 leads to the step E. Finally, Ethanol amine reach the cytosol by through the CP, while the entrance of a molecule of water in the active site, by using the same channel, will restore the FAAH catalytic activity [37][39].

1.1.5. MAGL enzyme

MAGL is a soluble membrane-associated enzyme of ~33 kDa, which belongs to the superfamily of serine hydrolase [6] [40]. MAGL preferentially hydrolyzes monoacylglycerols to glycerol and fatty acids. In most tissues, including the brain, more than 80% of the hydrolytic activity of 2-AG is prevented by the inhibition of MAGL, suggesting the dominant role of MAGL for the degradation of 2-AG [6][31]. MAGL is highly expressed in the brain, liver, adipose tissue, intestines, and others, and this was demonstrated by both genetic and pharmacological inhibition of MAGL in mice. In the brain, MAGL is expressed in neurons, astrocytes, and oligodendrocytes and, to a lesser extent, in microglia [40].
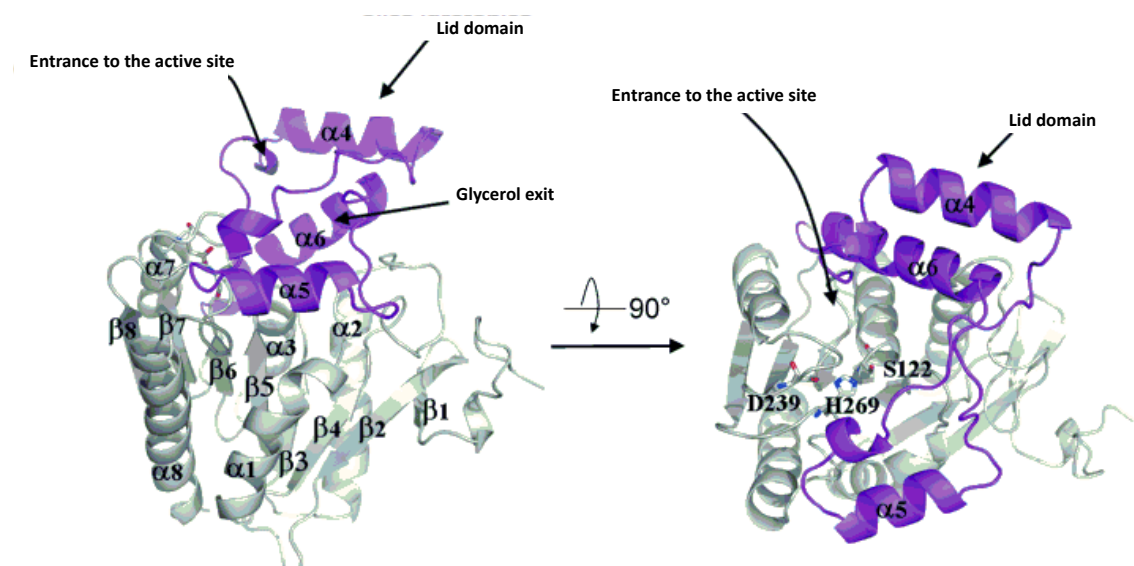
Figure 7. Crystallographic structure of *h*MAGL. On the left: monomeric structure of the enzyme. The catalytic triad is reported in sticks while the lid domain is depicted in magenta. On the right side: imagine of the same monomer rotate of 90°.

MAGL architecture is characterized by a homodimeric structure, composed eight β-sheet articulated in seven parallel and one antiparallel configuration. These are surrounded by eight a-helices. In the enzyme structure it is possible to identify a cap domain which works as a lid (see **Figure 7**). This allows the enzyme to exist in two main conformational states:

an open or closed form to regulate the substrate access [41]. The hydrolytic machinery of the MAGL enzyme is orchestrated by a catalytic triad, composed by Ser122, His269, and Asp239 which hydrolyses 2-AG in glycerol and arachidonic acid. It is in located in the center of the binding pocket (see **Figure 8**). The two Phe residues (Phe93 and Phe209) play a gate like function while a lipophilic channel localized alongside to the catalytic tread, accommodate the acyl chain of the glycerol. Also in this case, likely in the FAAH enzyme, a network of H-donors composes an oxyanion hole, necessary to stabilize the tetrahedral intermediate deriving from the 2-AG hydrolysis.
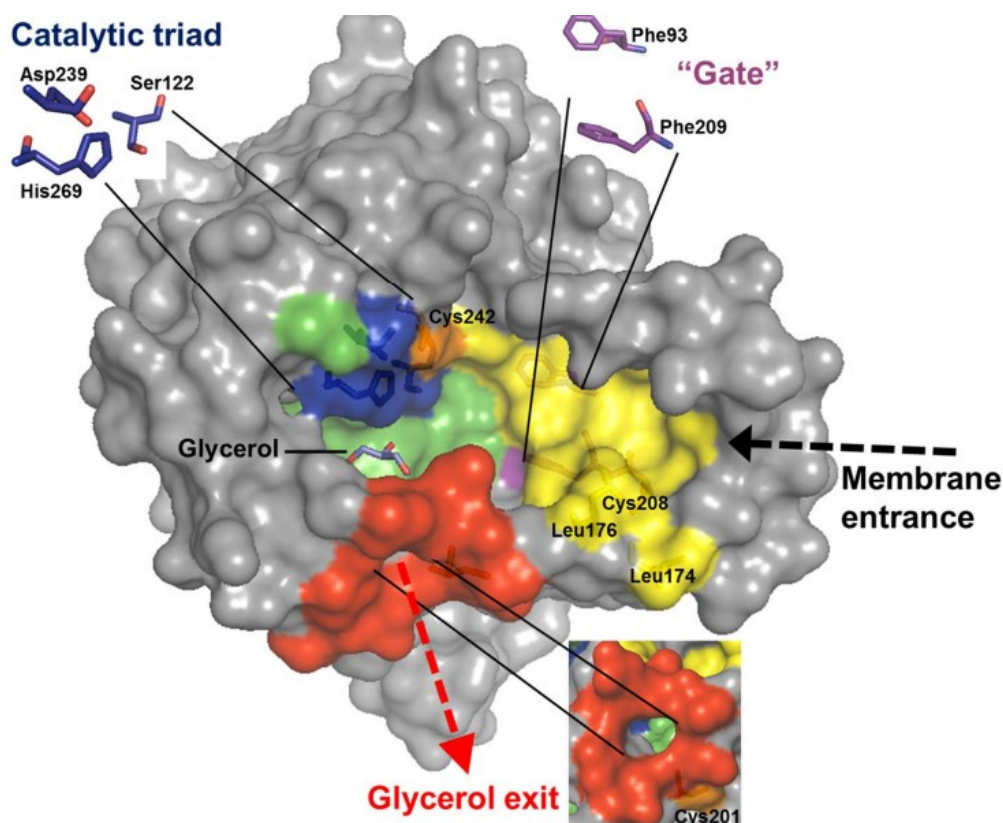
Figure 8. Key structural elements of MAGL enzyme.

The catalytic mechanism of 2-AG inactivation is reported in **Figure 9**.
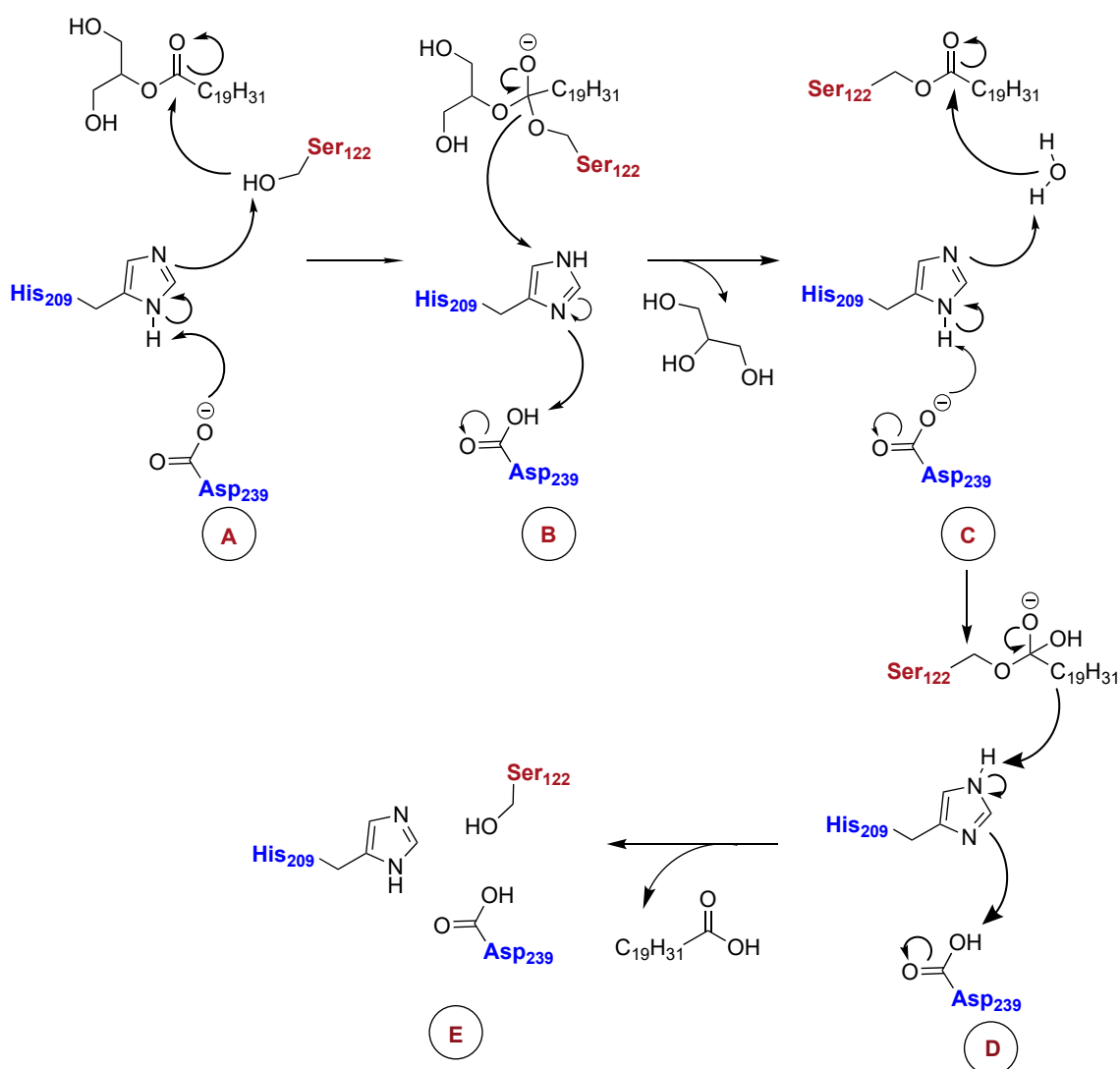
Figure 9. Catalytic mechanism of MAGL. Once the substrate reaches the active site, its ester bond is hydrolyzed by nucleophilic attack of the catalytic Ser 122 to the corresponding carbonyl carbon of the substrate. The acid-based proton transfer between Asp239 and His269, triggers the deprotonation of Ser122, which in its corresponding alkoxide form attacks the carbonyl carbon of the substrate (A). The rearrangement of the tetrahedral intermediate (B) favorite by the interaction with the His209 promotes the glycerol elimination (C) leading to the acylated enzyme. A hydroxy anion deriving from the interaction between His209 and a molecule of water, attack the enzyme-substrate covalent complex to form the tetrahedral intermediate D. The rearrangement of this latter restores the MAGL activity [41].

1.2. The ECS as a pharmacological target

The medicinal use of *Cannabis sativa* was introduced in England around the 1700. It uses find benefits for its analgesic, anti-inflammatory, antiemetic and anti-convulsing properties. However, the use of *Cannabis* fell out of favor in the early 20th century, largely due to concerns about its psychotropic activity and effects on behavior, motor co-ordination and memory and learning; such concerns led to cannabis removal from the British Pharmacopoeia in 1932 [42]. However, later, the discovery the CBRs and their endogenous ligands led to consider the ECS as promising pharmacological target. The emerging picture not only reinforces endocannabinoids as potent regulators of cellular metabolism but also reveals that ECS signaling is mechanistically more complex and diverse than originally thought [43]. In the CNS the ECS activity reduces the dopaminergic tone contributing at the Parkinson disease (PD) [44]. Other complex disease directly connected with dysregulation of ECS include multiple sclerosis (MS), Alzheimer's disease (AD), Huntington disease (HD) and psychiatric disorders such as schizophrenia[6][45]. Pain treatment is a well-established therapeutic application for the ECS. Stimulation of CB_1R in the interneurons and in the spinal cord reduce pain sensations whilst the CB_2R activity promotes an inflammatory activity, decreasing the production of pro-inflammatory cytokines [46]. Endogenous cannabinoids showed anti-proliferative, anti-inflammatory, and pro-apoptotic properties in several cancer cells and in animals. However, activators of the ECS are used in the cancer therapy only for the treatment of nausea and pain associated with the anticancer agents [47]. In the gastrointestinal system, the activation of CB_1R can produce an anti-inflammatory effect, potentially useful for the treatment of inflammatory bowel diseases [48]. CBRs activation also showed protective effects against hepatic ischemia-reperfusion injury [49]. Moreover, the abundance of CB_2R in osteocytes, osteoclasts and osteoblast suggests the

contribution of the ECS in bone mass maintenance [50]. The CBRs agonist were the first synthetic stimulators of the ECS used in therapy. The therapeutic applications for compounds or medical preparation such as, Bedrocan®, Bedrobinol®, Bediol®, Bedica®, Cesamet®, Marinol®, Sativex® regard anorexia, neuropathic pain, or MS. Their use depends on the country in which these drugs can be marketed. However, CBRs agonist administration show neurological side effects, including impairment of cognition, motor dysfunctions or psychoses, especially after long-term treatment [43,51]

The modern medicinal chemistry is strongly focused on the discovery of new synthetic compounds able to modulate the ECS, due to its universally recognized therapeutic opportunities [52]. However, the multitude of unwanted effects deriving from the use of CBRs agonist represents a burden to be overcome. For these reasons in the last 20 years, research interest was also focused on the ECS catabolic enzyme as potential therapeutic targets, this validating the pharmacological inhibition of FAAH and MAGL enzymes as a therapeutic alternative at the use of CBRs agonists. The main action of FAAH and MAGL inhibitors is to increase the endogenous levels of AEA and 2-AG thus extending the duration of their biological effect, representing a potential therapeutic strategy for various diseases. Chemical inactivation of these catabolic enzymes leads to an increase in neuronal transmission and/or counter controls to neuroinflammation and pain, including depression and anxiety. These activities take place without any changes in weight gain, motility, sleep, or other side effects typically seen with direct CBRs agonists [38,53].

1.3. ECS in neuroinflammatory and neurodegenerative conditions

Although the etiology and the pathogenesis of several CNS diseases such as AD, PD, and amyotrophic lateral sclerosis (ALS), is not always completely know, the common factor in these neurologic disorders is represented by a widespread neuroinflammation [54]. A progressive neuroinflammatory condition represents the starting pint of more complex biological dysfunctions then resulting in the loss of neuronal functions, atypical protein deposit, and cell death. The role of the ECS in these conditions has been deeply studied. Stimulation of CB_1R leads to a generally reduced glutamate-induced excitotoxicity, improving the neuronal viability [55]. An increased CB_2R activity is associated with active microglia and astrocytes inducing anti-inflammatory and neuroprotective effects in AD, PD, HD, and ALS [54,56,57]. These ECS-mediated beneficial effects can be trigged by a pharmacological inhibition of catabolic enzymes of the ECS such as FAAH and MAGL. Increased levels of AEA and 2-AG reduce the production of pro-inflammatory prostaglandins that promote neuroinflammation and attenuate the release tumor necrosis factor-α (TNF-α), IL-1β and nitric oxide (NO) [54,58]. Another important factor in the neuroinflammatory state is represented by the excess of oxygen and nitrogen reactive species (ROS and RNS). NO is produced in neurons, endothelial cells, and glial cells (astrocytes, oligodendrocytes, and microglia) in a Ca^{2+} dependent manner by the activity of NO synthase (NOS). It is involved in the regulation of neurotransmission, synaptic plasticity and in the regulation of cerebral blood flow. During neuroinflammation large amount of NO is produced in the brain by inducible NOs, playing a crucial role in the oxidative-nitrative stress [59]. The combination of ROS and RNS leads to the generation of peroxynitrite which promotes lipid peroxidation and mitochondrial damage, impairing the cells antioxidant capacity. The ROS are the result of neurons glutamatergic excitotoxicity which lead to mitochondrial dysfunction and at

oxidative stress (OS) condition. All these factors strongly contribute to the neuronal death and at the amplification of inflammatory response [59]. The ECS seems to have a crucial role in the management of the OS and the ROS and RNS production by means the control of the glutamatergic activity and the CB_2R signaling. In this context the stimulation of ECS can represent a valid therapeutic opportunity to mitigate the neuroinflammatory processes in complex diseases.

1.4. ECS in MS

MS is an immune-mediate, progressive neurodegenerative disease, whose main hallmark is represented by lesions of the myelin sheath in the CNS, due to exacerbate immunological response [60]. MS is determined by genetic, environmental, and social factors which can contribute to the disease progressions. The symptoms include spasticity, fatigue, tremor pain, memory impairment, sexual dysfunctions which can, in most of the cases, lead to depression and anxiety [60,61]. Based on these symptoms, four different forms of MS can be identified: the relapse remitting MS (RRMS), primary progressive MS (PPMS), secondary progressive MS (SPMS) and progressive relapse MS (PRMS). The most common (85% of the cases) is the RRMS, characterized by relapse of acute attacks and remitting stage [62,63]. The demyelination process is strongly related to neuroinflammatory process, as confirmed also in several animal model of MS [60]. Since the strong inflammatory nature, MS in considered to be a two-stage disease with a neuroinflammatory and a neurodegenerative phase. During the inflammatory phase, pro-inflammatory cytokines such as TNF-a and INF-y induce a series of modifications in the endothelial cells and astrocytes modifying the permeability of the BBB [64]. Once that BBB integrity is compromised, immune cells can reach the CNS and produce antibody and cytokines. Theses antibody attack certain protein of the myelin sheath, while T cells

produce TNF-α and other cytokines which trigger astrocytes to produce NO. The formation of antibody, in combination with NO free radicals and pro-inflammatory cytokines, induce the phagocytic action on myelin stealth by macrophages, that leads to the demyelination of neurons [65][66]. The demyelination of axon and nerve impair the signal transductions causing all the neurological disorders above mentioned. Various CBRs agonists are used as anti-inflammatory agents. Among these compounds, **WIN55212** showed also beneficial effects in the myelin repair in the cuprizone-based animal model of MS, when administrated at low doses. However, high compound concentration showed neurotoxicity effects probably due to at decreased neuronal Ca^{2+} influx as results of Gi/Go protein stimulation [67]. Moreover, recent studies suggest as the use of MAGL inhibitors in the experimental autoimmune encephalomyelitis (EAE) model of MS led to reduce pain a promotes myelin repair [68]. These highlight the potential use of ECS catabolic enzyme as new pharmacological tools for the treatment of MS.

1.5. Multiple neuronal connections of the ECS

The ECS is closely correlated with other systems cooperating to regulate many cognitive and physiological processes, primarily via controlling both GABAergic and glutamatergic neurons in the synaptic terminals of many brain areas involved in emotional behaviors included social and cognitive activity [30,69] An important interaction regards the ECS and the dopaminergic system. Dopamine is an important neurotransmitter in the brain which plays a major role in learning, motivation and reward, emotion, executive functions, and motor control [70,71]. ECS works as a filter of afferent input that acts locally at midbrain and terminal regions to shape how incoming information is conveyed into dopamine neurons and to output targets [72]. This regulation occurs through the ECS

activity in the GABAergic and glutamatergic circuits directly connected to the dopaminergic system [73][74]. The dopamine also has a critical role in the development of various substance addiction and withdrawal. The consumption of cocaine, amphetamine, morphine, nicotine, and alcohol, increases extracellular dopamine concentration in the striatum; thus, the ECS modulation can be beneficial as a novel therapeutic strategy in various scenarios of substance withdrawal and abuse [75]. Endocannabinoids also interact with the serotoninergic system in the regulation of stress, cognitive functions, food intake and sleep [76]. Moreover, recent studies have shown that GPCRs, including CBRs, can exist and function as higher-order dimers or complexes. The CB_1R-D_2R heteromers have been suggested to have physiological implications in neurodegenerative disorders such as AD, PD, epilepsy, autism, but also in neuropsychiatric pathologies such as anxiety, depression, and psychotic disorders [77] [78]. The multiple connections of the ECS with other signaling pathways in the CNS allow the consideration of the ECS as an optimal source of inspiration in the development of innovative multi-target compounds. This new approach could represent a valid therapeutic alternative for the treatment of multifactorial and complex disease, such as MS, AD, PD and cancer [6].

1.6. Polypharmacology of the ECS

Polypharmacology breaks up the classical paradigm of "one-drug, one target, one disease" electing multi-target compounds as potential therapeutic tools suitable for the treatment of complex diseases (see **Figure 10**), such as metabolic syndrome, psychiatric or degenerative CNS disorders, and cancer. Modern drug discovery has been strongly focused on the development of single target-drugs characterized by high affinity and selectivity. This approach is based on a direct cause−effect relationship between the

activity of a gene product and a particular phenotype. Consequently, a pharmacological agent able to specifically modulate the activity of a deregulated protein, should be able to revert a pathological phenotype [79,80].

However, many lines of evidence prove that complex pathologies are often polygenic and characterized by the dysregulation of various physiological processes. These diseases often require a combination therapy which may result in positive but also negative synergistic effects [81,82]. Now it is accepted that many approved drugs have, on average, close to six known targets to elicit their therapeutic effects. While current active compounds from medicinal chemistry sources with available high-confidence activity data are known to bind, on average, to only one/two targets [83]. The lack of success of highly potent and target-specific drugs in clinical development, and the limited therapeutic efficacy of single-target drugs are encouraging the design of multi-target compounds.
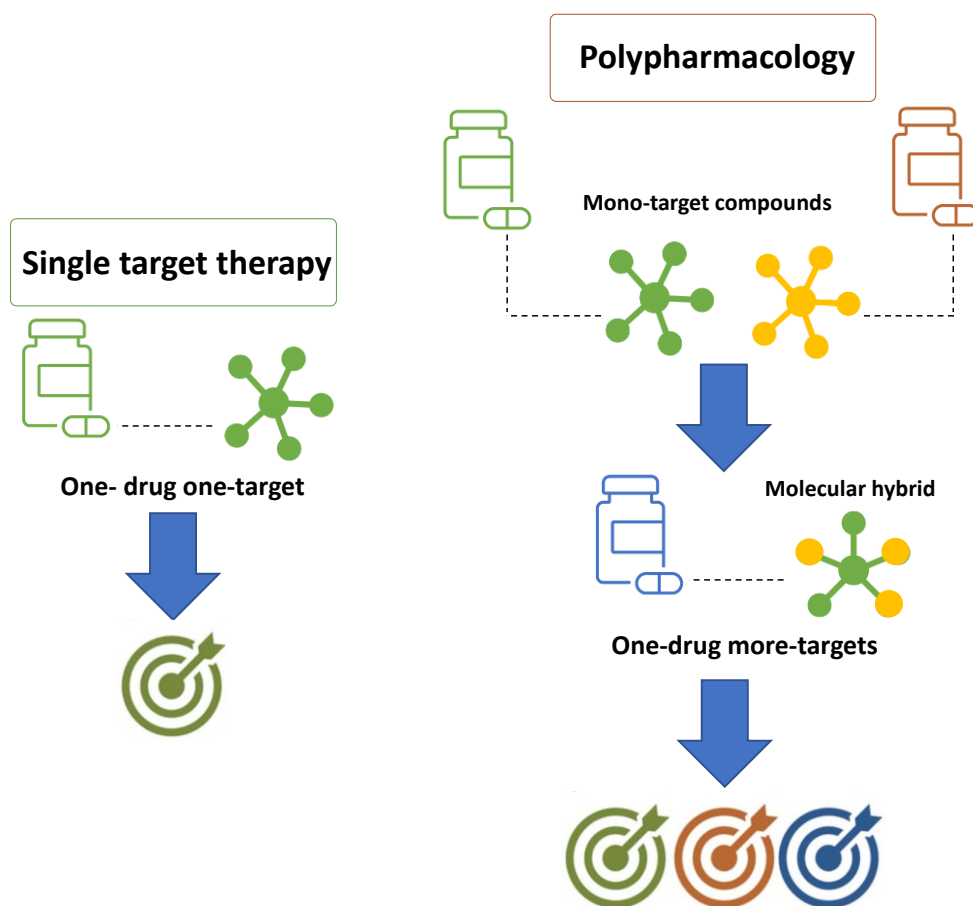
Figure 10. Single target therapy *vs.* polypharmacological approach

The multiple ECS neuro-connections provide an attractive opportunity to modulate the activity of FAAH or MAGL enzymes simultaneously to other relevant neuro-transmitting or enzymatic systems by using a polypharmacological approach. The involvement of CB_1R and COXs enzymes in the pain modulation has led to the development of dual FAAH/COXs inhibitors as possible therapeutic options for pain treatment [84] [85]. Activation of CB_2R by epoxidized fatty acids (EpFAs) together with the AEA effects on CBRs laid the rational basis for the development of multi-target FAAH/Soluble epoxide hydrolase (sEH) inhibitors, as antinociceptive agents [86]. The neuroprotective properties of FAAH inhibitors and the therapeutic efficacy of anti-cholinesterase agents were combined obtaining hybrid FAAH/ACh inhibitors, potentially useful for the treatment of AD [87]. Simultaneously targeting the ECS and the dopaminergic system could represent

an innovative strategy to fight drug abuse and the abstinence response [87]. Moreover, for the treatment of glaucoma the use of dual FAAH and melatonin receptors antagonists resulted in a new viable strategy [88].

1.7. FAAH inhibitors

The discovery of FAAH enzyme opened the way at the identification of new classes of compounds able to induce an indirect stimulation of the ECS by FAAH inhibition. The first identified FAAH inhibitors were electrophilic compounds able to interact with the nucleophilic Ser24, forming a covalent bond. Derivatives such as **10** and **11** (see **Figure 11**, panel A), although not particular relevant for a medicinal chemistry point of view, they resulted useful tools to completely understand the FAAH catalytic machinery [37]. The rational designee for the new FAAH inhibitors led to the development trifluoromethyl ketones or esters as derivative of the AA. Boger *et.al* identified compounds **12**, **13** and **14** (**Figure 11,** panel A) on which the first kinetic studies were conducted. The trifluoromethyl ketone **13** resulted a reversible inhibitor whilst the α-chlorine derivate **14** works as a noncompetitive FAAH inhibitor. These studies clarified that the inhibitory potency of the FAAH inhibitors is generally increased by increasing electrophilicity of the reactive carbonyl group [89].

Ketoheterocycles. The next step in the development of new FAAH inhibitors was done in 2000. Boger *et al.* replaced the trifluoromethylenic group of compound **13** with different ether cycles moieties, to modulate the inhibitory potency of the novel FAAH inhibitors [90]. This structural modification led to obtain the highly potent oxazolyl-ketone **15** (**Figure 11**, panel B) and the oxazolyl-pyridine **16** (**Figure 11**, panel B). The substitution of the oleic acid-based chain of compound **16** with the smaller phenyl-hexyl aliphatic portion represented a key point in the development of FAAH inhibitors. Indeed,

ketones **17** (**OL-92**, **Figure 11**, panel B) and **18** (**OL-135**, **Figure 11**, panel B) were two of the most potent inhibitors [91,92]. These compounds showed a reversible enzymatic inhibition, because, after the nucleophilic attack of Ser241 on the carbonyl center, the inhibitors are stabilized in a tetrahedral intermediate in the enzyme binding pocket [91,92].

A) *First generation of FAAH inhibitors*

10, PMSF

11, MAFP

12

13, (Ki = 1.2 nM)

14, (Ki = 700 nM)

B) *Ketoheterocycles*

15, (Ki = 370 nM)

16, (Ki = 2.3 nM)

17, OL-92 (Ki = 2.3 nM)

18, OL-135 (Ki = 4.7 nM)
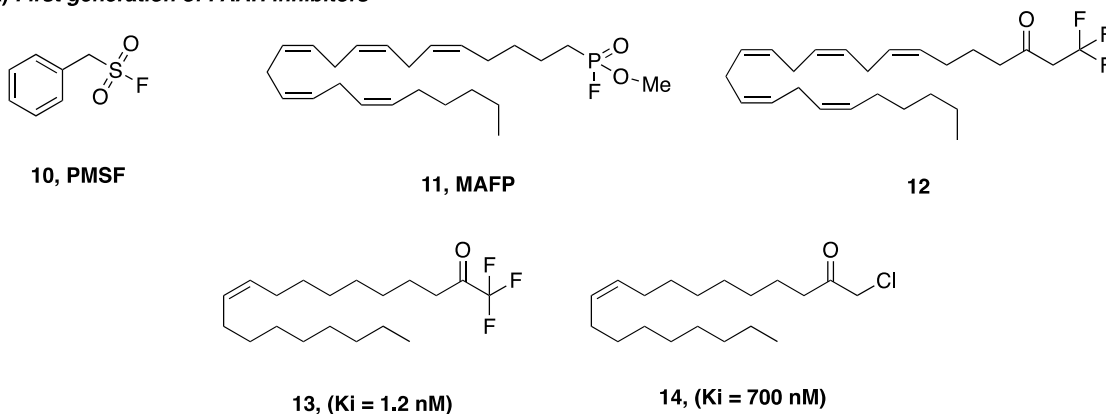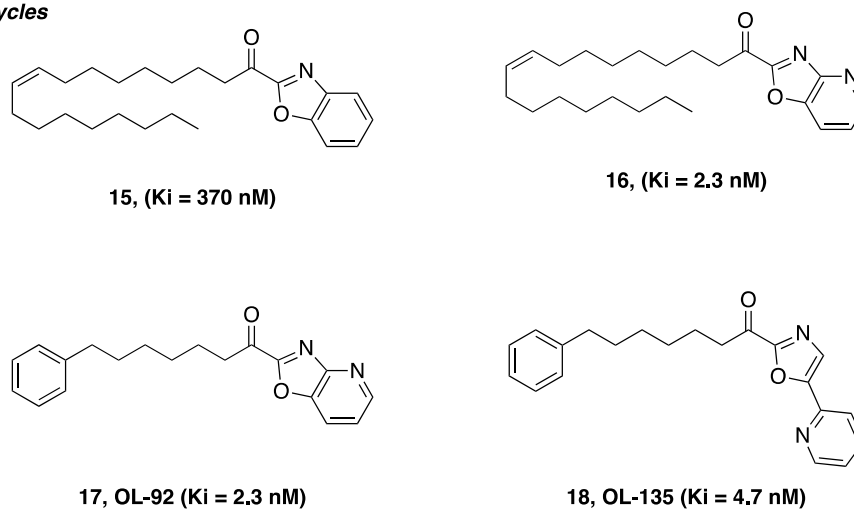
Figure 11. Chemical structure of FAAH inhibitors. Panel A: first generation of FAAH inhibitors. Panel B: ketohetrocycle-based FAAH inhibitors

A) *Carbamate-based FAAH inhibitors*
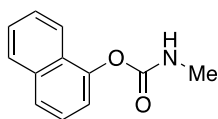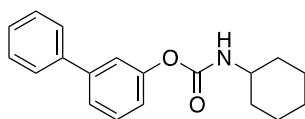
19, (IC$_{50}$ > 3000 nM)   **20, URB524 (IC$_{50}$ = 63 nM)**   **21, URB597 (IC$_{50}$ = 4.6 nM)**
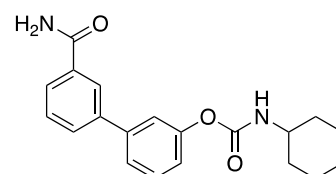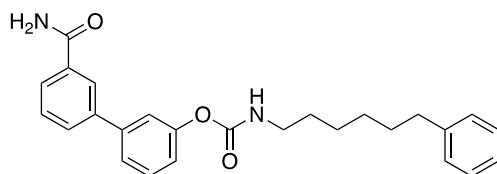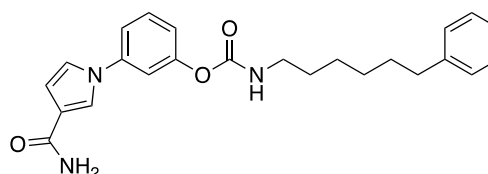
22, JP-83 (IC$_{50}$ = 14 nM)   **23, NF1245 (IC$_{50}$ = 3.3 nM)**

B) *Urea-based FAAH inhibitors*
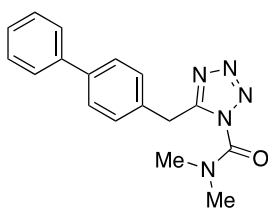
24, LY-218340 (IC$_{50}$ = 12.4 nM)   **25, PF-04457845 (IC$_{50}$ = 2.7 nM)**
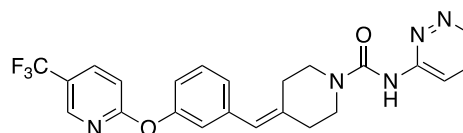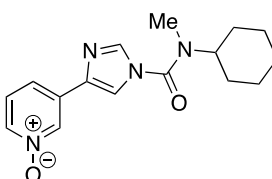
26, BIA 10-2474 (IC$_{50}$ > 1000 nM)

Figure 12. Chemical structure of FAAH inhibitors. Panel A: carbamate-based FAAH inhibitors. Panel B: urea-based FAAH inhibitors

Carbamate-based FAAH inhibitors. The rational designee for the carbamate-based FAAH inhibitors takes inspiration from the ketoheterocycles derivatives and the AchE inhibitor **19** (**Figure 12**, Panel A). This latter shows interesting structural elements which could be useful also for the FAAH inhibition. The methylammino moiety of compound **19** was replaced with the most lipophilic cyclohexylamine, obtaining compound **URB524** (**20**, **Figure 12**, Panel A) [93,94]. The introduction of a carboxamido group in the by-acrylic portion of **20** led to compound **URB597** (**21, Figure 12**, Panel A), the most studied

and characterized FAAH inhibitors. The irreversible mechanism of action of **URB597**, depicted in **Figure 13**, shows how the O-byarilic moiety works as leaving group as consequence of the nucleophilic attach operated by Ser241. The result is the carbomoylated enzyme [95].
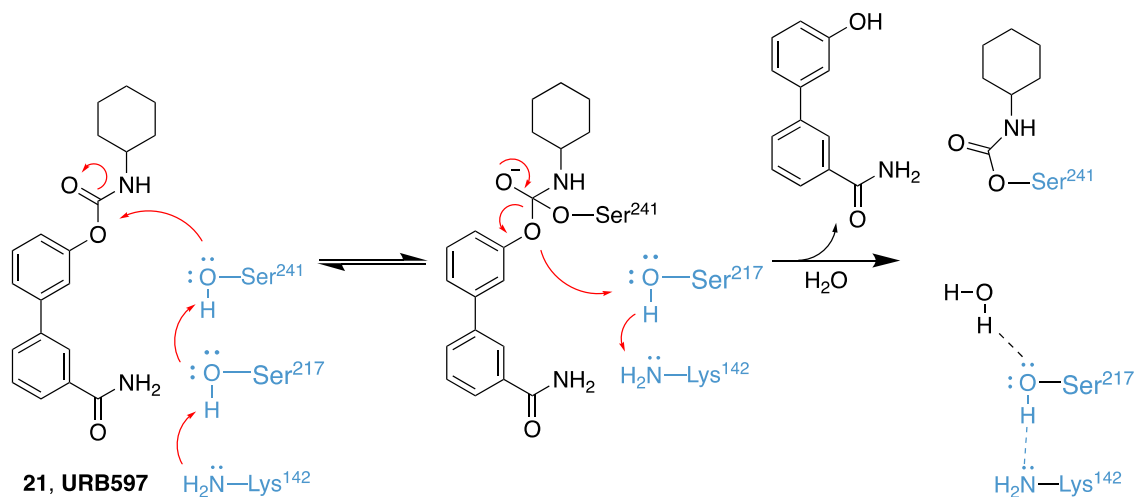
Figure 13. Mechanism of action of the irreversible carbamate-based FAAH inhibitor **URB697** (**21**). The carbonyl group of **21** undergoes the nucleophilic attack by Ser241 to form a tetrahedral intermediate. The protonation of the O-biaryl moiety, catalyzed by Lys^{142} and Ser^{217}, allows the collapse of the tetrahedral intermediate and the subsequent exit of the O-biarylic group, leading to the formation of the carbamoylated enzyme.

Finally, the combination of the phenylhexyl lateral chain with the **21** by-arylic core led to the discovery of compound **JP-83** (**22**, **Figure 12**, Panel A) [96]. Our research group focused its efforts in the developed of new carbamate-based FAAH inhibitors, taking inspiration from compounds such as **21** and **22**. Our FAAH inhibitors, typified by compound **NF1245** (**23**, **Figure 12**, Panel A) shows excellent activity against the target combined with a good selectivity profile [97].

Urea-based FAAH inhibitors. The urea-based FAAH inhibitors captured the interests of several pharmaceutical industries. Compounds **LY-2183240** (**24**, **Figure 12**, Panel B), developed by Lilly, was in first analysis reported as AEA transporter inhibitor and then identified to be a high potent FAAH inhibitor. Mass spectrometry studies demonstrated

the irreversible mechanism of action of this compound associated with a relevant analgesic effect [96]. Compound **PF-04457845** (**25**, **Figure 12**, Panel B) developed by Pfizer is an urea-based FAAH inhibitor that reached the clinical trials for the treatment of Tourette's syndrome. This inhibitor shows an irreversible mechanism of action combined with good drug-like properties. In the human treatment compound **25** did not show cognitive dysfunctions after administration at high doses, but it resulted completely ineffective for the treatment of osteoarthritic pain [38]. Of great interest is the story of the FAAH inhibitor **BIA-102472** (**26**, **Figure 12**, Panel B) that the Portuguese company Bial Pharmaceuticals studied in the clinic for the treatment of pain, motor disorders and neurodegenerative diseases [98]. During the clinical trial 90 patients out of 128 were treated with the compound while the other 38 used the placebo. Six people from the FAAH inhibitor-treated group showed severe adverse effects, and four of them manifested irreversible cerebral damage. Moreover, for one of this four the state of cerebral dead was declared [98]. Following this accident, the Food and Drug Administration (FDA) and the European Medicine Agency (EMA) worked together to identify the causes of the problem. Several studies showed as the observed unwanted effects deriving from the presence of off-targets. The compound is a covalent FAAH inhibitor, and its long time of action was strongly correlated to an irreversible inhibition also of other enzymes [98].

1.8. MAGL inhibitors

The great therapeutic interest of MAGL enzyme led to consider this latter as potential pharmacological target for the treatment of all the pathological condition in which the ECS is involved. MAGL inhibitors can be classified as reversible and irreversible ligands,

and among these latter we can mention cysteine-targeting compounds and serine122-targeting compounds [60].

Cysteine-targeting compounds. The earliest reported MAGL inhibitors were sulfuryl-containing derivatives able to interact with a cysteines close to the catalytic triad of the enzyme [53]. Among these we can find compounds such as **Disufiram** (**27**, **Figure 14**, Panel A), used for the treatment of alcoholism as aldehyde dehydrogenase inhibitors and then identified as MAGL inhibitors [53]. In the class of aril thioamides compound **CK16** (**28**, **Figure 14**, Panel A) showed good activity and selectivity profile against FAAH. Its irreversible mode of action is probably due to at the interactions with Cys208 and Cys242 [99].

Serine-targeting compounds. MAGL can be irreversibly inactivated by nucleophilic attack of the Ser122 by electrophilic moieties followed by the release of a leaving group and the formation of a stable adduct between the enzyme and the inhibitor. The carbamate-based MAGL inhibitor **URB602** (**29**, **Figure 14**, Panel B) belongs to this class of inhibitors, although it does not show any selectivity against FAAH [100]. With the aim to optimize the selectivity profile of the carbamate based MAGL inhibitors, Cravatt *et al.* identified the derivatives **JZL184** (**30**, **Figure 14**, Panel B). This compound did not show off-target effects towards cannabinoid receptors and other catalytic serine-containing enzymes [101]. Cravatt *et al.* reported the replacement of the O-*p*-nitrophenyl leaving group by an O-hexafluoroisopropyloxy (HIPF) carbamate, modification that yielded compound **KML29** (**31**, **Figure 14**, Panel B) [51], with enhanced MAGL activity and selectivity over FAAH and other serine hydrolases according to competitive activity-based protein profiling (ABPP) assays [102]. The identification by Sanofi-Aventis of the triazole urea **SAR629** (**32**, **Figure 14**, Panel B) derivate opened the way at the discovery

of new urea-based MAGL inhibitor. This compound was a useful tool to confirm the mechanism of inhibition of ureas, since the X-ray structure of **33** bound to human MAGL confirmed the formation of the carbamylated enzyme adduct through Ser122 [26]. Other compounds belonging to the urea superfamily were the piperazine and piperidine triazole derivatives such as **JJKK006** (**33**, **Figure 14**, Panel B) and **JJKK048** (**34**, **Figure 14**, Panel B)[103].More recently a new carbamate-based MAGL inhibitor named **ABX-1431** (**35**, **Figure 14**, Panel B), developed by Abide Therapeutics, completed a clinical trial (NCT03625453) for treatment of Tourette Syndrome or Chronic Motor Tic Disorder [104]. The research activity of our research group was also directed in the development of new MAGL inhibitors. In this field, we designed and synthesized a new series of urea-based MAGL inhibitors characterized by an azitin-2-one core. These inhibitors, typified by compound **NF1819** (**36**, **Figure 14**, Panel B) resulted potentially effective in the treatment of MS as demonstrated by their efficacy in an EAE model of MS [68].
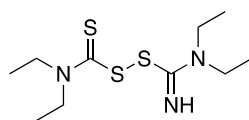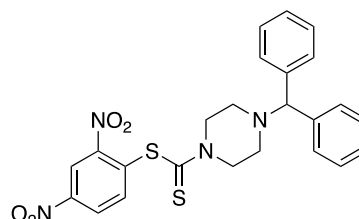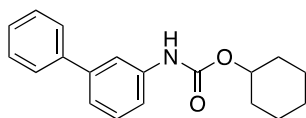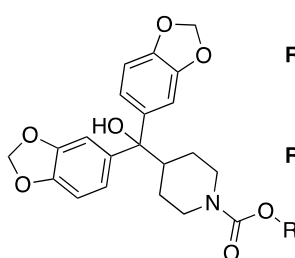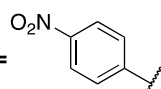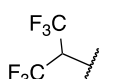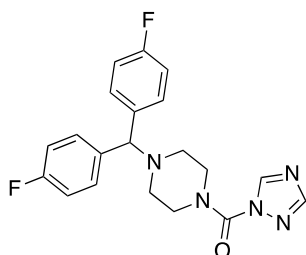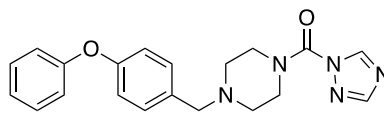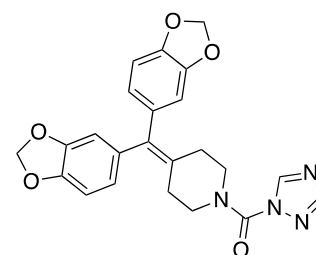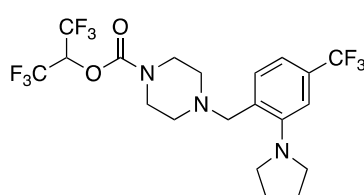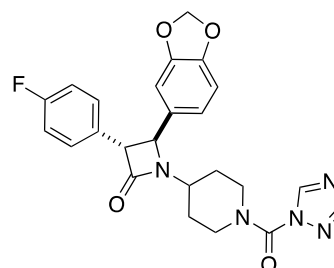
Figure 14. Chemical structure of cysteine-targeting MAGL inhibitors (Panel A) and serine targeting MAGL inhibitors (Panel B).

Reversible MAGL inhibitors. The reversible inhibition of the MAGL enzyme also could represent a valid therapeutic option to modulate the 2-AG levels. However, the development of reversible MAGL inhibitors is still scarce, and this approach could be useful to reduce the side effects deriving from an indirect overstimulation of the CBRs.

In 2010, Janssen Pharmaceuticals patented two high potent e reversible MAGL inhibitors **37** and **38** (**Figure 15**). The X-ray confirmed their reversible mode of action, highlighting as both compounds occupy the lid-domain of the enzyme, which regulates the access to the active site, while the carbonyl group is accommodated in the oxyanion hole [53] [105].

37 (IC$_{50}$ = 10 nM)   **38 (IC$_{50}$ = 5 nM)**
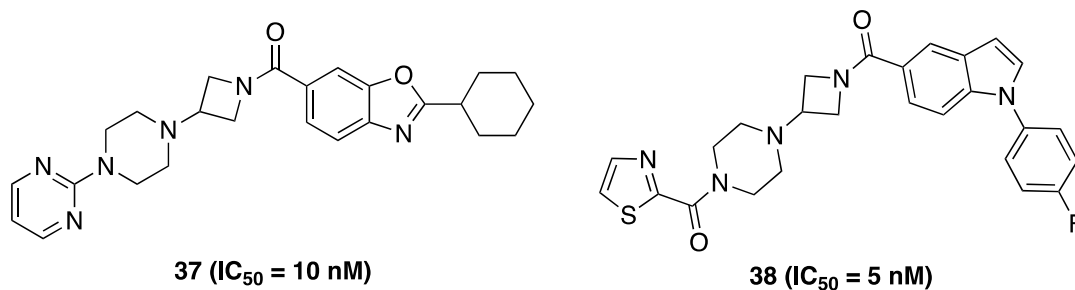
Figure 15. Chemical structure of reversible MAGL inhibitors **37** and **38**.

1.9. Dual FAAH/MAGL inhibitors

In the last few years, academic and industrial efforts have been strongly focused on the development of selective FAAH or MAGL inhibitors with potential therapeutic application in several diseases such as MS, epilepsy, neuropathic pain, and chronic pain disorders. However, the simultaneous inhibition of the two main ECS catabolic enzymes also appears as a promising therapeutic strategy. The polypharmacological approach to the development of dual FAAH/MAGL inhibitors remains still not particularly explored. Two relevant examples of hybrid FAAH/MAGL inhibitors, **JZL195 (39**, **Figure 16**) and **SA-57 (40**, **Figure 16**) were reported in literature and were in deep studied in several models of different diseases [6] [101]. Compound **39** represents the prototype of the covalent dual FAAH/MAGL inhibitors. When compared in the treatment with selective FAAH and/or MAGL inhibitors, compound **39** proved to be more efficacious of the single target therapy, especially for the analgesic effect [106] [107]. The *O*-hydroxyacetamide **40** developed by Sanofi-Aventis represented an innovative compound as pharmacological tool for the treatment of CNS disorders, indeed **40** showed to block a wide spectrum of

morphine withdrawal signs. This therapeutical benefit was discernible from the THC-like

side effects which resulted evident only with high doses [6] [108][109].

39, JZL195
IC$_{50}$ rFAAH = 13 nM,
IC$_{50}$ rMAGL = 19 nM

40 SA-57
IC$_{50}$ mFAAH = 1.0 nM
IC$_{50}$ mMAGL = 410 nM
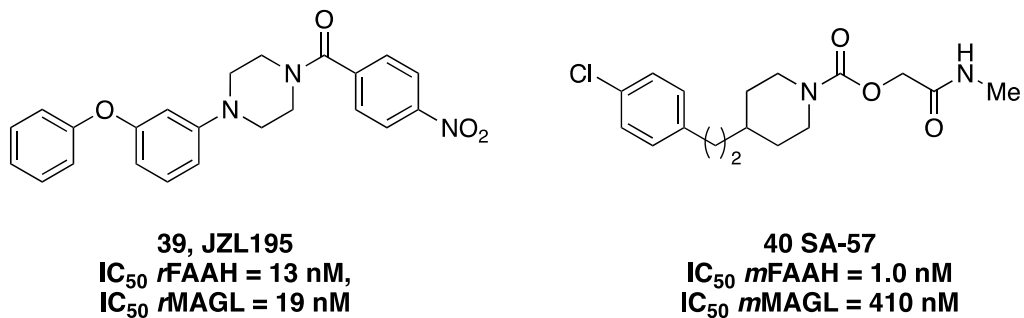
Figure 16. Chemical structure of dual FAAH-MAGL inhibitors **40** and **41**.

2. Overview of the thesis work

Since the establishment of the ECS as a promising pharmacological target, several compounds able to modulate the ECS activity were developed. Among these we can mention CBRs agonists, selective FAAH or MAGL inhibitors, dual FAAH/MAGL inhibitors and several examples of multi-targeting compounds involving FAAH or MAGL inhibition. During my PhD work I focused my efforts on the development of new selective and multitarget compounds having the ECS catabolic enzymes, FAAH and MAGL, as main pharmacological targets. This exploration in the ECS and its therapeutics opportunity resulted in the discovery of different library of compounds, which are following listed.

1. Development of new selective FAAH inhibitors. The discovery of novel FAAH inhibitors represents a pivotal challenge of our research group. In this framework, our recent research activity was directed toward the identification of carbamate based FAAH inhibitors characterized by high potency and an excellent selectivity profile towards MAGL and CBRs. Although the previously reported FAAH inhibitors showed an excellent pharmacodynamic profile, they also display a poor water solubility and chemical stability in aqueous media. Taking into account the scaffold of several FAAH inhibitors synthetized in our research group and taking inspiration from several compounds reported in the literature, I completed an exhaustive structure active relationship study (SARs), synthesizing novel carbamate based FAAH inhibitors characterized by improved drug-like proprieties. From this library of more than 20 compounds (derivatives **41a-t** in **Figure 17** and **Table1**), we selected the best 4 derivatives which showed efficacious anti-neuroinflammatory activity in cell and in ex vivo assays.
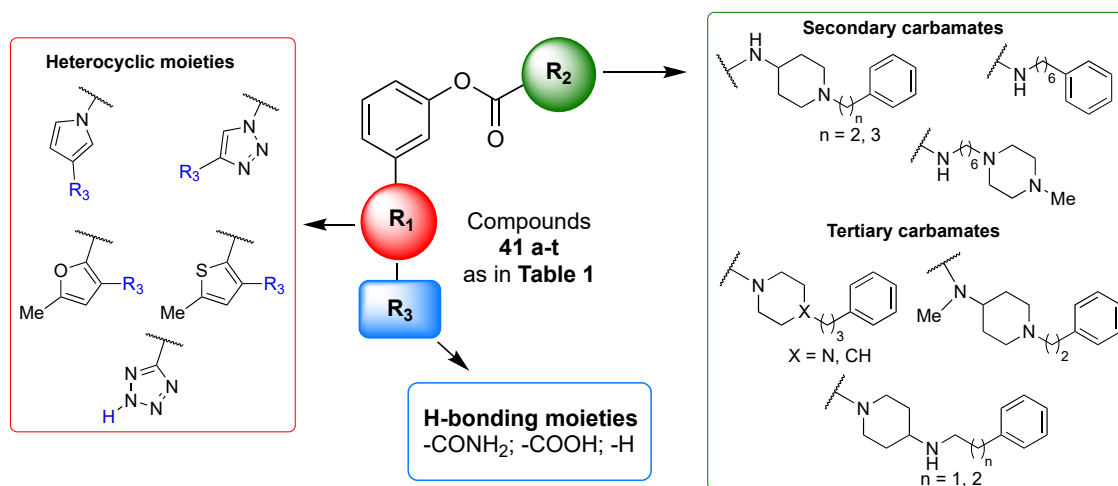
Figure 17. General structure of the new developed FAAH inhibitors

2. Development of new selective MAGL inhibitors. The MAGL inhibitors represent an important explored topic in our research group. Our research in this field led at the identification of high potent and selective MAGL inhibitors characterized by an azetidine-2-one scaffold. The next step in this field led us to perform a scaffold exploration finalized at the developed of new spiro β-lactam derivatives to which I contributed synthetizing two compounds (see **Figure 18**, compounds **42a-l**, and **Table 3**).
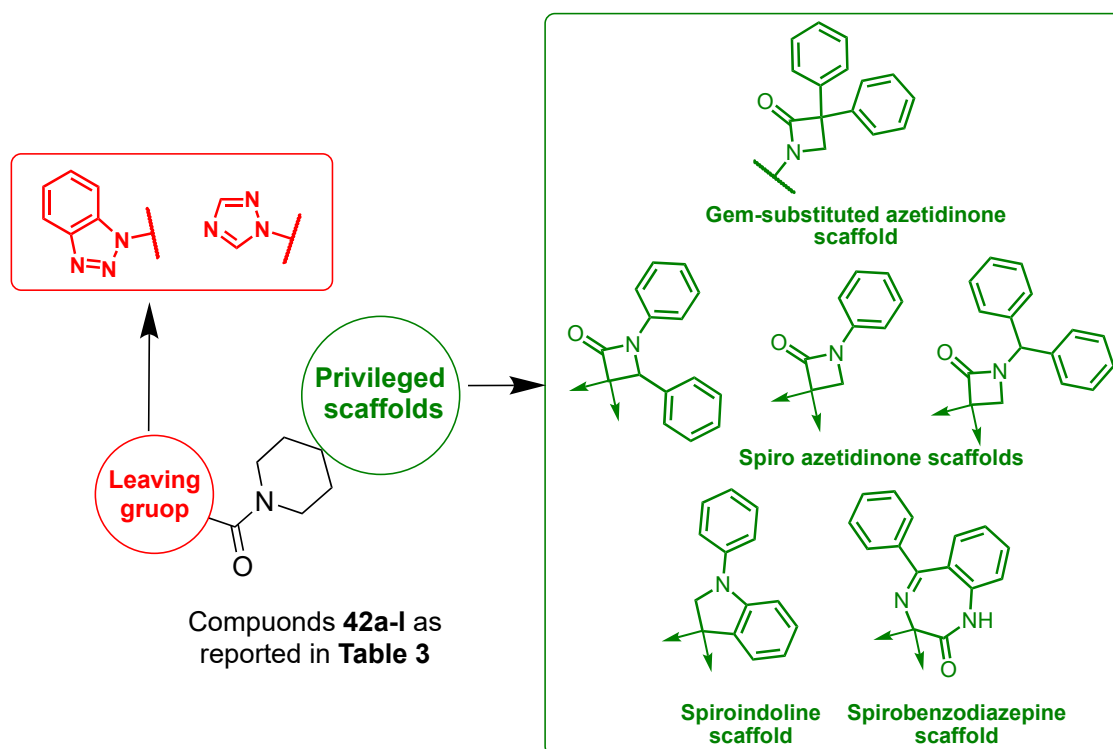
Figure 18. Representation of the new developed MAGL inhibitors

3. Development of dual FAAH/MAGL inhibitors. Polypharmacology is defined as the design or use of pharmaceutical agents acting on multiple targets. In the last years, its development can be ascribable to the lack of success of highly potent and target-specific drugs and to the limited therapeutic efficacy of single target drugs. These difficulties in the drug discovery encouraged the designee of innovative multitarget compounds which can offer a variety of advantages such as the reduction of treatment complexity, drug side effects, pharmacokinetic complexity, drug–drug interactions, and patients' compliance. The simultaneous inhibition of the two mains important ECS catabolic enzymes, FAAH and MAGL, also represents a promising polypharmanacologic opportunity for the treatment of several CNS disorders. In this field, I focused my efforts on the synthesis of a library of potential dual FAAH/MAGL inhibitors by means a scaffold simplification strategy started from our high potent and selective MAGL inhibitors (compounds **43 a-l** as in **Figure 19** and **Table 5**). For a subset of selected compounds, the anti-inflammatory activity was evaluated in rat organotypic hippocampal slice cultures. The first results for

these compounds showed their excellent anti-inflammatory effect in dose dependent manner.
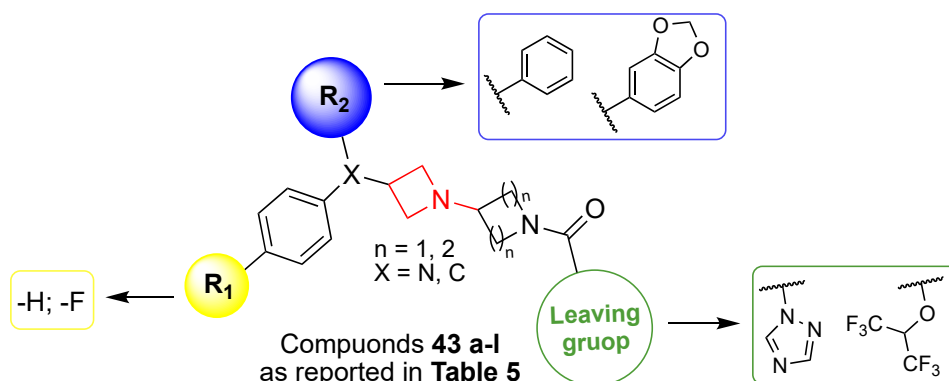
Figure 19. General structure of the new developed dual FAAH/MAGL inhibitors

4. Development of dual FAAH/Histone Deacetylase 6 (HDAC6) inhibitors. Several evidence highlight as dysregulations of the HDAC6 enzymatic activity is involved in several neuroinflammatory and neurodegenerative conditions. Considering the pivotal role of ECS in the maintenance of the CNS homeostasis in the context of complex diseases we decided to explore an innovative polypharmacological approach related to the synthesis of potential dual FAAH/HDAC6 inhibitors whose general structure is reported in figure **20** (compounds **44a-h**).
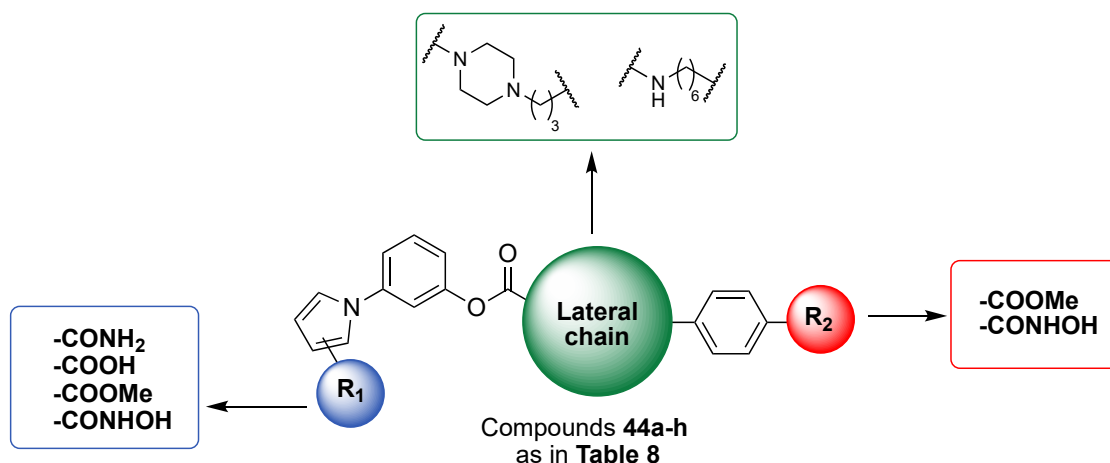
Figure 20. General structure of the new developed dual FAAH/HDAC6 inhibitors

5. Development of dual MAGL/Histaminergic 3 receptor (H₃R) ligands. The neuromodulation operated by both the histaminergic system and ECS occurs by

controlling the release of important neurotransmitters in the CNS. This connection between histaminergic and endocannabinoid system represented for us a source of inspiration to develop new compounds able to simultaneously modulate the activity of both neuromodulatory networks. These compounds behaving as dual MAGL/H3R ligands, and useful as potential tools for the treatment of MS, were developed in collaboration with Professor Holger Stark (at the University of Dusseldorf) who has strong knowledge on the histaminergic system. In fact, this series of analogues was completed during a period of three months that I spent, within my PhD, in the laboratories of Professor Holger Stark. The general structure of the two series of derivatives developed during this collaborative project (Set A compounds **45a-d** and Set B, compounds **46 a-g**) are reported in **Figure 21**.
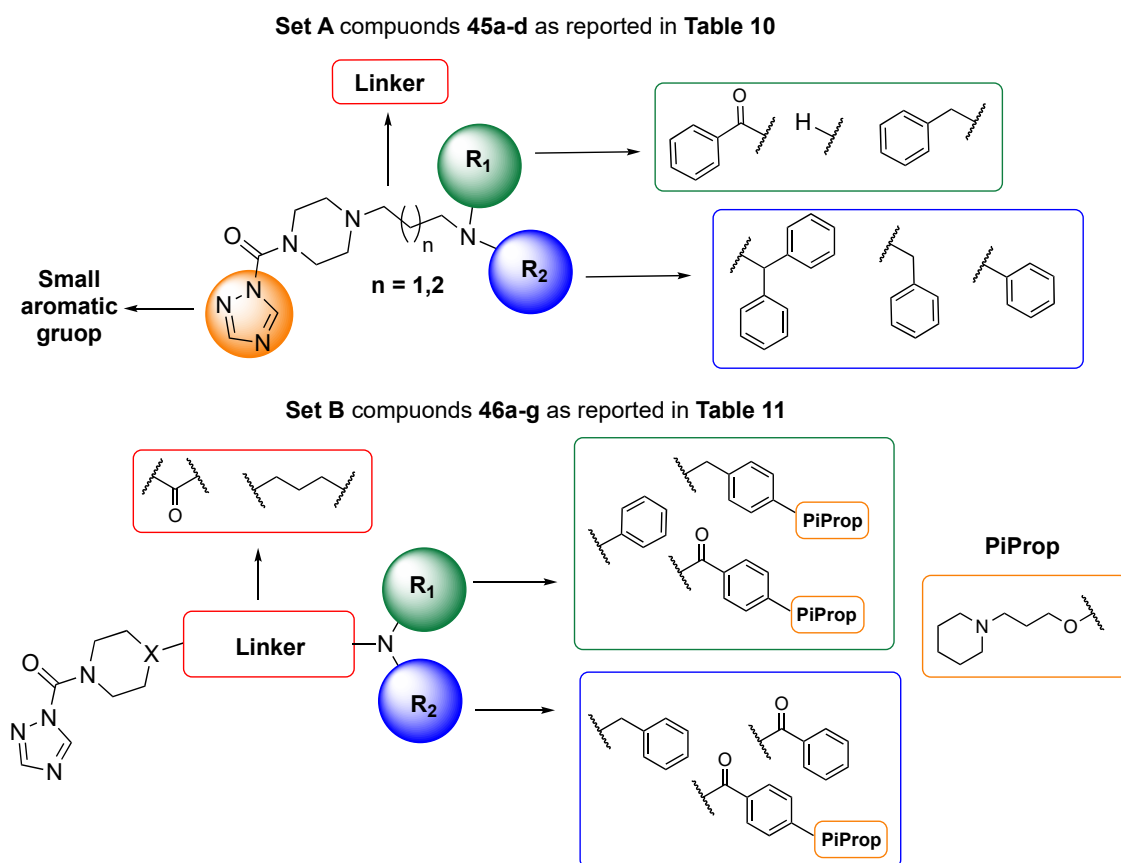
Figure 21. General structure of Set A and Set B compounds developed as potential dual MAGL/H3R ligands.

3. Development of new FAAH inhibitors

3.1. Background

As previously reported the research activity of our research developed high potent and selective FAAH inhibitors characterized by a carbamate-based structure and typified by compounds **23** and **NF1376** (**47**, **Figure 22**, panel A) [97,110]. The general structure of these compounds evidence three kay elements necessary for the FAAH inhibition: i) the electrophilic center, represented by the carbonyl group of the carbamate moiety; ii) the *O*-byarylic portion bearing a carboxamido group, which works as a leaving group; iii) a lipophilic phenylhexyl lateral chain. Docking pose of compounds **23** (**Figure 22**, panel B) clarified its binding mode in the enzyme pocket [97].
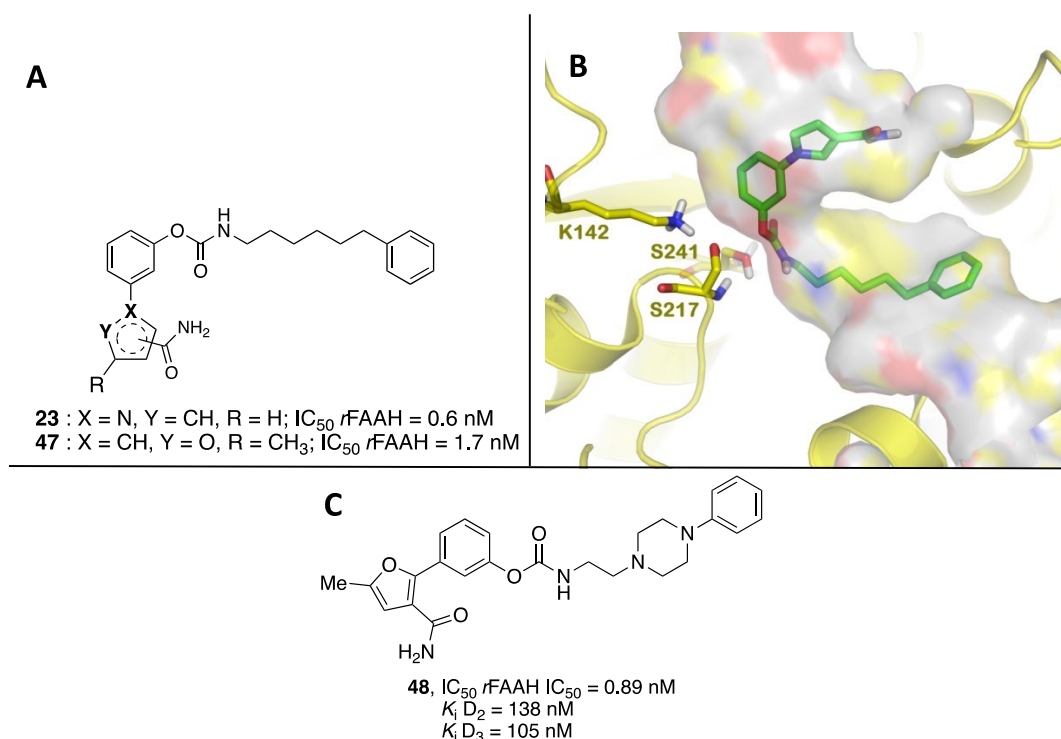
Figure 22. Panel A: general structure of the carbamate based FAAH inhibitor **23** and **47**; panel B: docking pose of the FAAH inhibitor **23** in the enzyme binding pocket; panel C: chemical structure of the dual FAAH/D_2-D_3 ligand **48**.

The carboxamido group on the *O*-byarylic moiety anchors the compound in the active site by means an H-bond. The phenyhexyl lateral chain is accommodate in the ABC

channel, and its terminal phenyl ring involved in a π-stalking interaction with the Phe381. This binding mode allowed the positioning of the carbamate moiety in proximity of the catalytic triad [97]. These inhibitors characterized by high potency and an excellent selectivity profile resulted effective in the treatment of a murine model epilepsy [111]. As a further aim, we recently embarked in a polypharmacological approach where FAAH inhibition was combined to dopamine receptor antagonism. To this end, we attached over the arylfurane-based scaffolds of our FAAH inhibitors a phenylpiperazine lateral chain (compound **48**, **Figure 22**, panel C) [112]. Multitarget FAAH/D_2D_3 ligands could found potential application for the treatment of complex and multifactorial diseases as well as for addictions and also smoke cessation. Our compounds showed an activity in the nanomolar range for the selected targets together with absence of unwanted interaction against the CBRs. Their inflammatory profile was evaluated in human cell line [112].

3.2. Development and biological characterization of compounds 41a-t as potential FAAH inhibitors

The previously reported carbamate-based FAAH inhibitors of our research group showed a nanomolar activity against the target, although they were characterized by poor drug-disposition properties. Given the poor water solubility and chemical stability of compounds such as **23** and **47**, we focused our efforts on the development of new FAAH inhibitors with improved key physico-chemical property, preserving inhibitory potency against the target. To achieve this aim, we designed novel classes of *O*-arylcarbamates in which basic and/or acidic fragments were inserted in the structure of our reference inhibitors **23** and **47**. The effect of tertiarization of the carbamate nitrogen was also explored to reduce the reactivity of the compounds in acidic and neutral media. This set of modifications led to the synthesis of compounds **41a-t** (see **Figure 23** and **Table 1**) which were evaluated for FAAH inhibitory potency, FAAH/MAGL selectivity,

solubility, and chemical stability. In this frame, I focused my efforts on the synthesis and in the experimental evaluation of the drug-like properties for the new developed compounds [113].
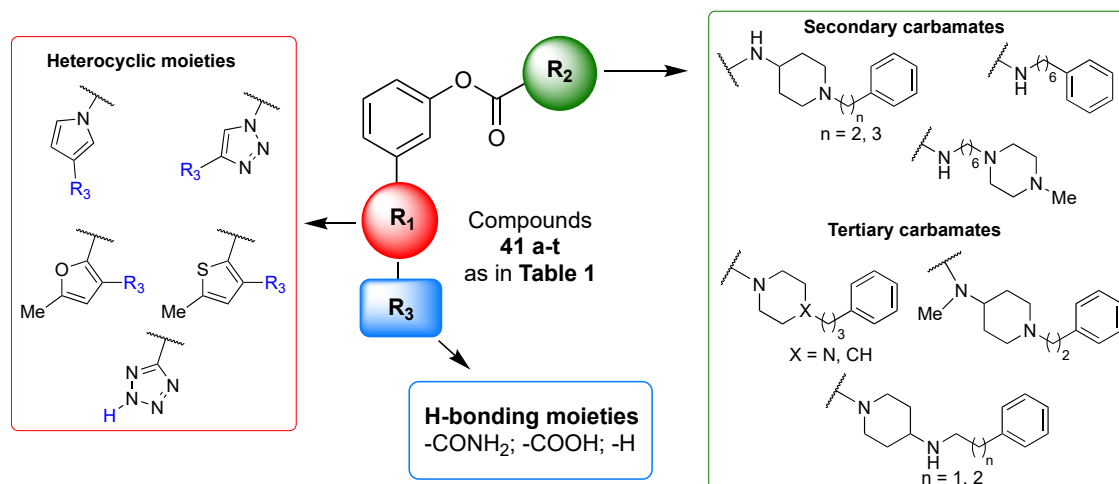
Figure 23. Development of new carbamate based FAAH inhibitors **41 a-t**

The activity of our new compounds toward FAAH and MAGL enzymes and the selectivity profile, towards cannabinoid CB_1R and CB_2R, was investigated in collaboration with research group of Professor Varani at University of Ferrara. Moreover, docking studies performed at the University of Parma, in collaboration with the research group of Professor Mor, allowed us to clarify the binding mode of the new derivatives. For selected analogues, cytotoxicity was evaluated in murine fibroblasts and in 1321N1 astrocytes. The most promising compounds **41e**, **41n** and **41s** effectively reduced ROS production in 1321N1 astrocytes. These cellular characterizations were performed by Varani and collaborators together with the study on the reversible mechanism of action for compound **41e** and **41g**, while the absence of cardiac side-effects was evaluated for compound **41n** at the University of Siena by Professor Saponara. Finally, we assessed the neuroprotective effects of compounds **41e**, **41g**, **41n** and **41s** against inflammation-induced neurodegeneration in *ex vivo* cultures of rat hippocampal explants. This ex vivo

study was conducted at the University Federico II of Napoli in by Prof Francesca Boscia [113].

3.3. Chemistry of the new FAAH inhibitors

The synthesis of compounds **41a-t** is reported in the **Schemes 1-6**, as described in our recent work [113]. According to our retrosynthetic analysis (**Figure 24**), all the compounds were obtained by using a convergent approach. The bisaryl phenols **49a-f** could be reacted with a multitude of primary (**50a-d**) or secondary amines (**50e-i**) in the presence of *p*-nitrophenyl chloroformate to generate the final compounds (**41a-f, 41i-p** and **41s-t**) or their appropriately protected analogues. The required non-commercially available amines (**50a-c,e-i**) could be synthesized by applying reductive amination protocols engaging the appropriate amine and the corresponding aldehydes or *N*-alkylation of the appropriate amines. Upon the need of different functional groups, an orthogonal protection strategy was applied for obtaining selective and effective deprotection in the different stages of the synthetic process as detailed in the **Schemes 2-5**.

Figure 24. Retrosynthetic analysis of the new FAAH inhibitors
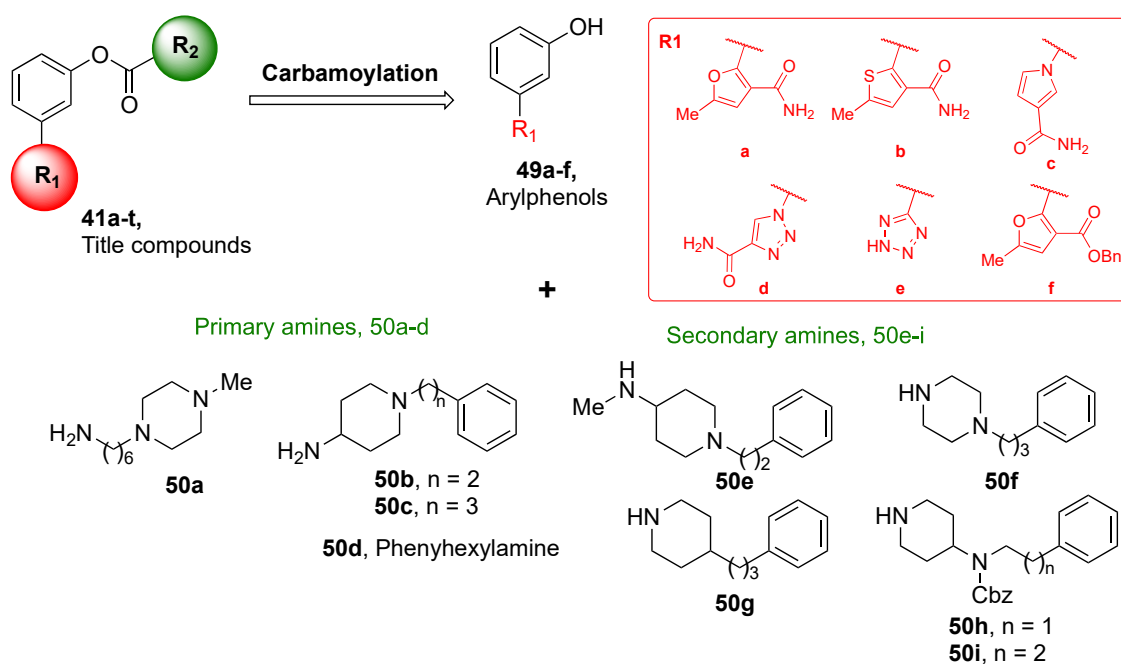
For the obtainment of the well know phenyl pyrrole scaffold **49c**, a new synthetic approach was necessary since that a key reagent was not available anymore. The new synthetic route depicted in the **Scheme 1**, starts from the 3-hydroxybenzenaminium **51** chloride which reacted under Clauson-Kass conditions in presence of *N,N*-diethylnicotinamide, generating phenylpyrrole **52**.
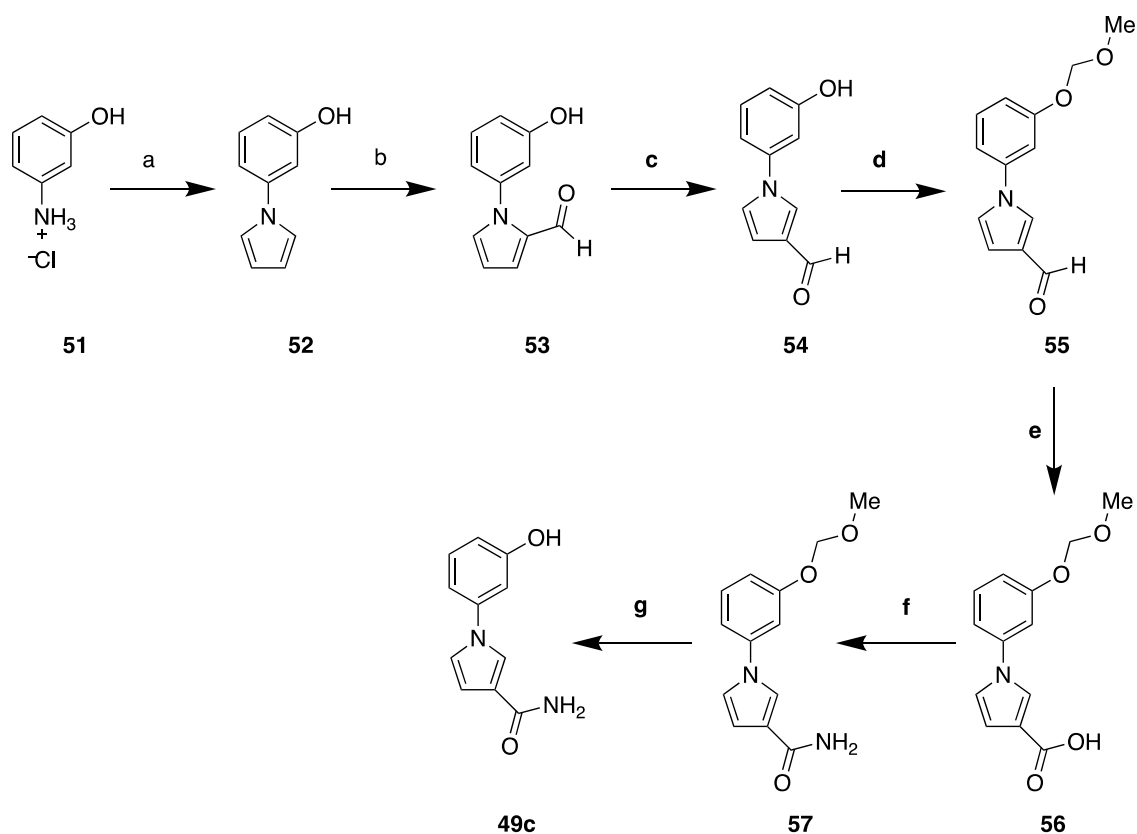
Scheme 1. Synthesis of phenols **49c**.
Reagents and conditions. a) 2,5-dimethoxytetrahydrofuran, *N,N*-diethylnicotinamide, 1,4-dioxane, 102 °C, 2 h, 79%; b) oxalyl chloride, DMF solution in dry DCM, dry DCM, 0 °C to 40 °C, 3 h, then 1N NaOH, 25 °C, 16 h, 70%; c) triflic acid, dry DCE, 85 °C, 6 h, 60%; d) MOM-Cl, DIPEA, dry DCM, 0 °C, 1 h 96%; e) NaClO$_2$ saturated solution, NaH$_2$PO$_4$ 98%; f) NH$_4$OH, EDC-HCl, HOBt, DIPEA, dry DCM, 0 °C to 25 °C, 16 h, 75%; g) 1N HCl/MeOH, MeOH, 25 °C, 16 h, 97%.

A Vilsmeier-Haack reaction on compound **52** by using oxalyl chloride and DMF led to a mixture of isomers **53** and **54** in 90 :10 ratio. Isomer **54** was obtained starting from compound **53** by means triflic acid-assisted α- to β-migration of the formyl group. The

treatment of phenol **54** with MOM-Cl led to derivative **55,** which was oxidized at the corresponding carboxylic acid **56**. Finally, acid **56** was converted in the carboxamide **57** and deprotected under acidic condition leading to phenol **49c**.

The synthesis of phenols **49e,f** is depicted in **Scheme 2**. Compound **49e** was obtained by a cycloaddition reaction involving the 3-cyanophenol **58** and sodium azide in the presence of triethylammonium chloride. For compound **49f**, the methoxy functionality of compound **59** was demethylated using boron tribromide to give the phenol intermediate **60** that was protected as benzyl ester.
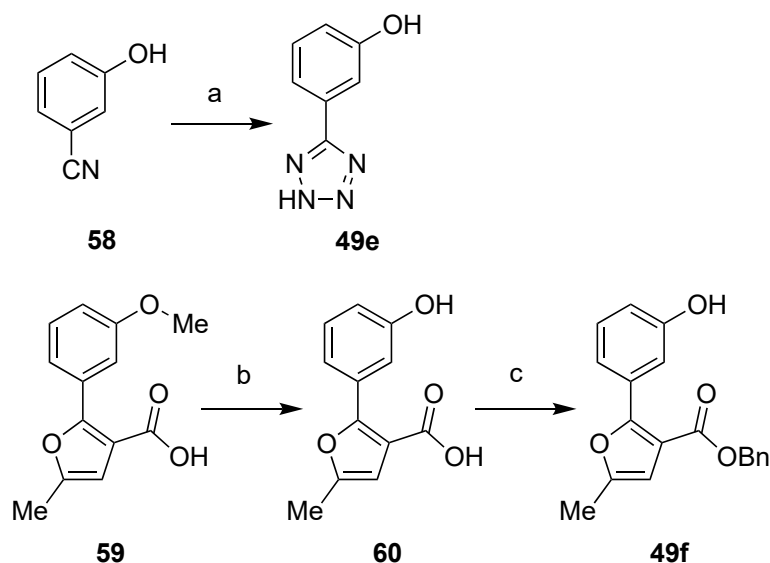
Scheme 2. Synthesis of phenols **5e** and **5f**.
Reagents and conditions. A) triethylamine (TEA) hydrochloride, sodium azide, dry toluene, 110 °C, 20 h, 45%; b) BBr$_3$, dry DCM, from -78 °C to 25 °C, 2 h, 99%; c) benzyl bromide, NaHCO$_3$, dry DMF, 40 °C, 12 h, 70%.

The synthesis of the primary amines **50a-c** is reported in **Scheme 3**. Alkylation of 1-methylpiperazine **61** using 5-bromovaleronitrile gave intermediate **62** which was reduced by LiAlH$_4$ leading to amine **50a**. Alkylation of 4-*N*-Boc-aminopiperidine **63** with 2-(bromoethyl)benzene gave the derivative **64**, which was then deprotected in the presence of TFA to obtain the amine **50b**. To obtain the amine **50c**, 4-amino-*N*-Boc-piperidine **65** was previously protected as benzyl carbamate **66** and then subjected to a selective Boc

deprotection, furnishing **67**. This latter was treated with aldehyde **69** to obtain *N*-alkyl

derivative **70** that generated the amine **50c** after Cbz removal. The synthesis of the needed

aldehyde **69** started from 3-phenylpropanol **68** which underwent a (2,2,6,6-

tetramethylpiperidin-1-yl)oxidanyl (TEMPO)-catalyzed oxidation that employs

trichloroisocyanuric acid (TCICA) to obtain the aldehyde in a quantitative yield.
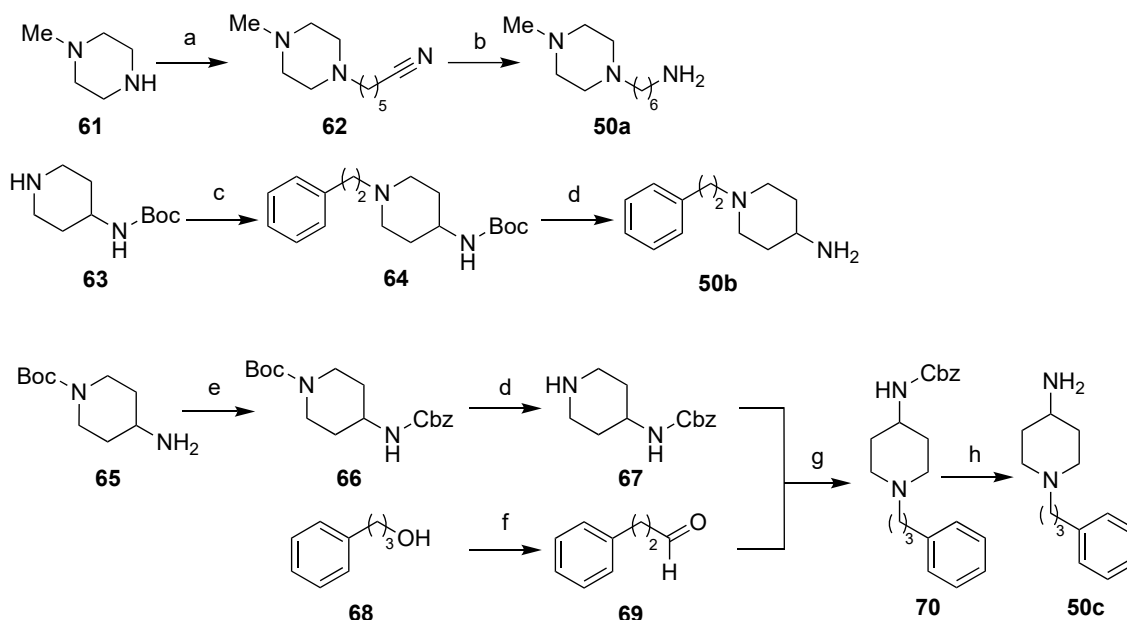
Scheme 3. Synthesis of primary amines **50 a-c**.
Reagents and conditions: a) 5-bromovaleroonitrile, Na$_2$CO$_3$, EtOH, 25 °C, 12 h, 25%; b)
LiAlH$_4$, dry THF, 0 °C to 25 °C 1 h, 95%; c) 2-bromo ethylbenzene, TEA, dry THF, 70
°C, 12 h, 88%; d) TFA, dry DCM, from 0 °C to 25 °C 2 h, 95-99%; e) benzyl
chloroformate, NaHCO$_3$, dry THF, 0 °C to 25 °C, 12 h, 80%; f) TEMPO, TCICA, dry
DCM, 0 °C, 15 min, 99%; g) NaBH(OAc)$_3$, dry DCM, 25 °C, 12 h, 66%; h) H$_2$, Pd on
carbon, MeOH, 25 °C, 2 h, 75%.

Secondary amines **50e-g** were synthesized according to **Scheme 4**. The treatment

of compound **64** with LiALH$_4$ furnished the *N*-methyl derivative **50e**. The 1-(3-

phenylpropyl)piperazine **50f** was obtained by a conversion of the commercially available

3-phenyl-1-propanol **68** in the corresponding bromoderivative **71**. The nucleophilic

substitution of 1-Boc-piperazine with **71** gave compound **72**, which was then subjected

to a Boc deprotection. The Wittig reaction between the triphenyl(3-

phenylpropyl)phosphonium bromide **75**, in turn obtained from the bromoderivative **71**,

and benzyl piperidone **74**, in turn obtained from *N*-alkylation of **73**, led to the unsaturated product **76**. Catalytic hydrogenation of the olefin furnished amine **50g**.

For the orthogonally Cbz-protected secondary amines **50h,i**, we applied the synthesis reported in **Scheme 5**. Under reductive amination conditions, the phenylethylamine, *N*-Boc-piperidone **77** and NaBH(OAc)$_3$ provided compound **78** which was then treated with benzyl chloroformate to obtain derivative **79**. Orthogonal deprotection of the Boc group under acidic conditions led to amine **50h**. To obtain **50i**, 4-amino-*N*-Boc-piperidine **80** was subjected to a reductive amination protocol in the presence of the aldehyde **69** affording derivative **81**. Introduction of the Cbz protecting group gave the intermediate **82** which after Boc deprotection provided the desired amine **50i**.
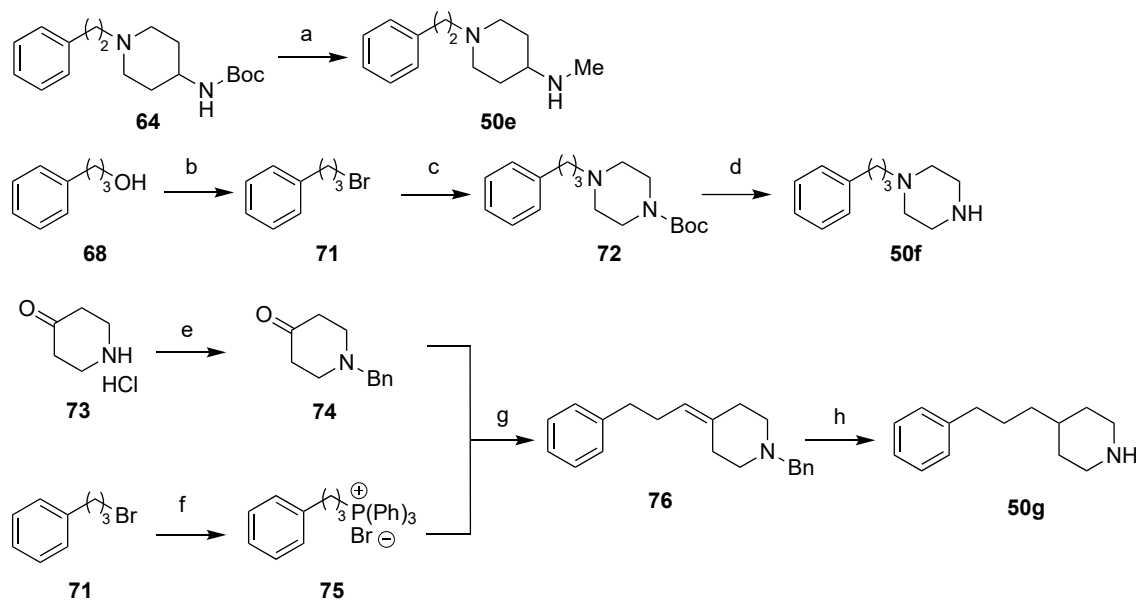
Scheme 4. Synthesis of secondary amines **50e-g**.
Reagents and conditions: a) LiAlH$_4$, dry THF, 0 °C to 70 °C 18 h, 63%; b) PPh$_3$, CBr$_4$, 1*H*-imidazole, dry DCM 25 °C, 12 h 95%; c) *N*-Boc-piperazine, K$_2$CO$_3$, KI, dry acetonitrile, 25 °C, 12 h, 93%; d) TFA, dry DCM, from 0 °C to 25 °C 2 h, 99%; e) benzyl bromide, K$_2$CO$_3$, dry DMF, 75 °C, 12 h, 70%; f) PPh$_3$, dry toluene, 110 °C, 24 h, 26%; g) *n*-butyllithium (1.6 M in hexane), dry THF, from 0 °C to 25 °C, 12 h, 28%; h) Pd on carbon, H$_2$, MeOH, 25 °C, 2 h, 82%.
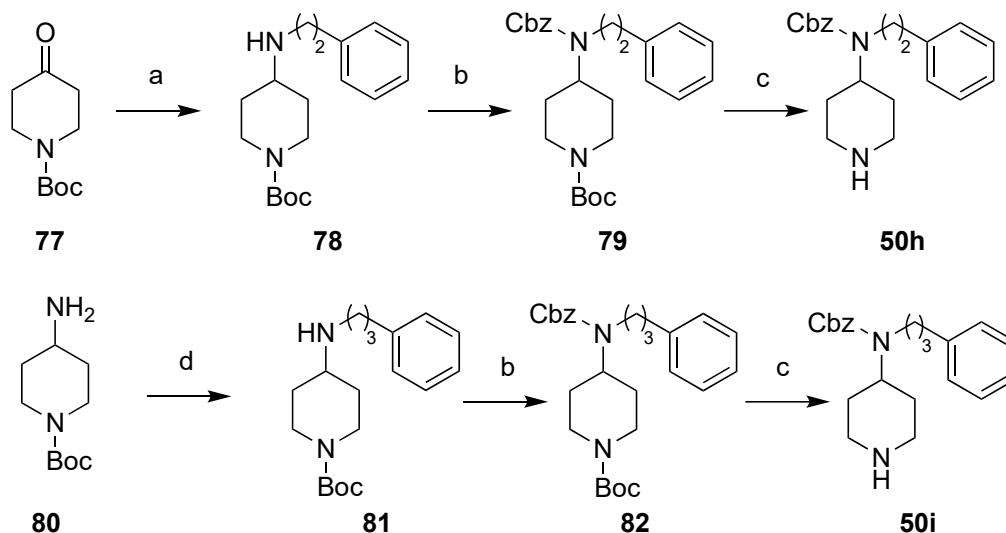
Scheme 5. Synthesis of secondary amines **46h,i**.
Reagents and conditions: a) NaBH(OAc)$_3$, phenylethylamine, dry DCM, 25 °C 12 h, 62%;
b) benzyl chloroformate, NaHCO$_3$, THF, from 0 °C to 25 °C, 12 h, 99-88%; c) TFA, dry
DCM, 0 °C to 25 °C 2 h, 87-99%%; d) NaBH(OAc)$_3$, aldehyde **69** dry DCM, 25 °C, 12
h, 60%.
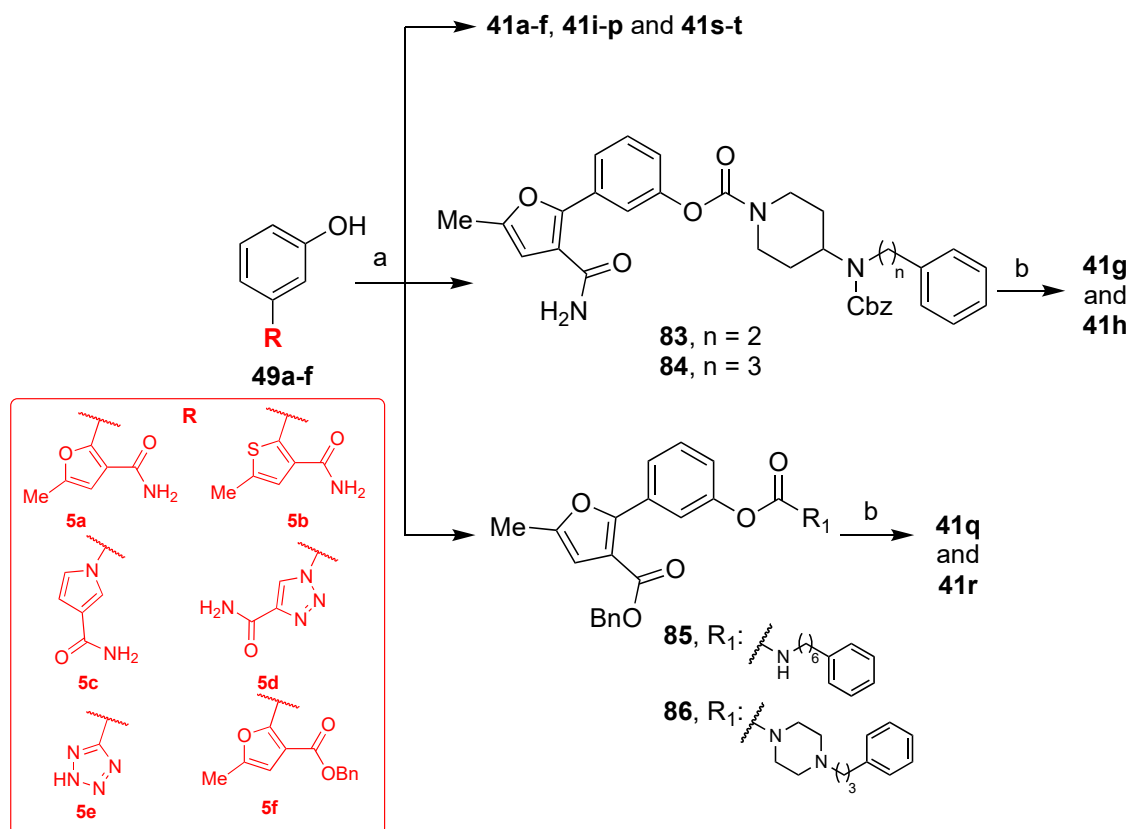
Scheme 6. Synthesis of compounds **41a-t**. Reagents and conditions: a) 4-nitrophenyl
chloroformate, TEA, dry DCM, 0 °C to 25 °C, 4 h, and suitable amine,17-64%; b) H$_2$, Pd
on carbon, MeOH/EtOAc, 25 °C, 2 h, 13-74%.

The final steps for the synthesis of compounds **41a-t** are depicted in **Scheme 6**. The phenols **49a-c**, **49d** and the new phenol derivatives **49e,f** (**Scheme 1**) were combined with the corresponding amines to form secondary o tertiary carbamates in the presence of *p*-nitrophenyl chloroformate (**Scheme 6**). By choosing the appropriate combination of phenol derivative and amine the final compounds were obtained. Briefly, the phenol **49a** was combined with amines **50a-c** and **50e-g** to obtain carbamates **41a-c** and **41d-f** respectively. **49a** was also reacted with amines **50h,i** to obtain the intermediate protected compounds **83** and **84**. From these latter Cbz deprotection provided the target compounds **41g,h**. Phenols **49b,c** were combined with amines **50b**, **50e** and **50f** to obtain compounds **41i-k** and **41l-n** respectively. Phenols **49d,e** were combined with phenylhexyl amine **50d** and amine **50f** to obtain derivatives **41o,p** and **41s,t** respectively. Phenol **49f** was combined with phenylhexyl amine **50d** and amine **50f** to obtain intermediates **85** and **86** that gave **41q,r** following a palladium catalysed hydrogenation for removing of the benzyl group

Table 1. Inhibitory activity towards *human* FAAH and *human* MAGL (expressed as IC$_{50}$ nM) for title compounds **44a–t**, and reference compounds **23** and **b**.

Cmpds	Structure	IC$_{50}$ (nM) *h*FAAH[a]	IC$_{50}$ (nM) *h*MAGL[a]
41a		1044 ± 73	>10000
41b		188 ± 11	>10000
41c		407 ± 32	>10000
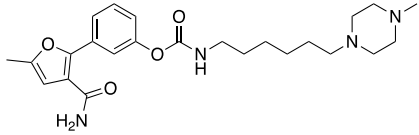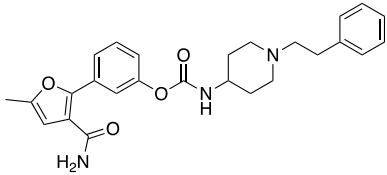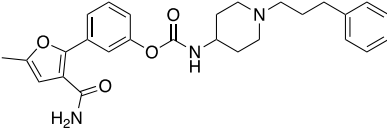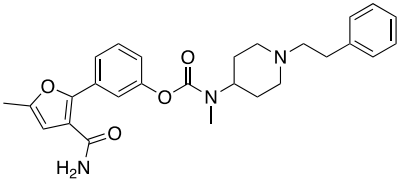
41d		6556 ± 412	>10000
41e		8.29 ± 0.58	5061 ± 387
41f		11.7 ± 0.8	4116 ± 314
41g		26 ± 2	>10000
41h		165 ± 12	9878 ± 677
41i		194 ± 13	>10000
41j		8450 ± 523	>10000
41k		15.6 ± 0.9	>10000
41l		315 ± 19	>10000
41m		>10000	>10000
41n		10.1 ± 0.6	>10000
41o		15.8 ± 1.1	479 ± 28
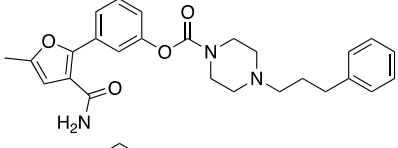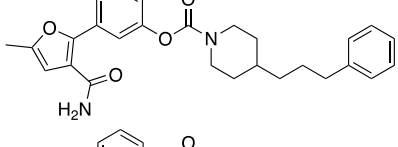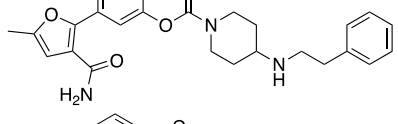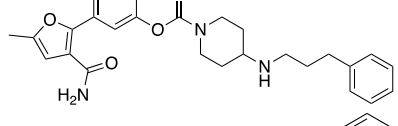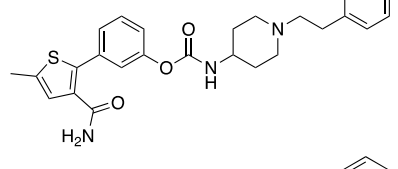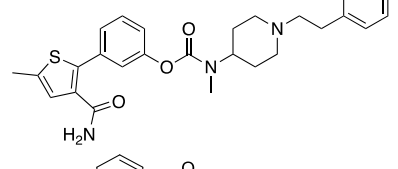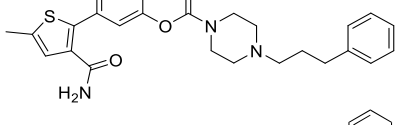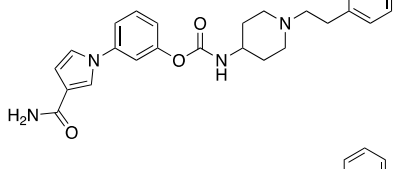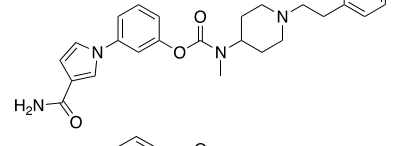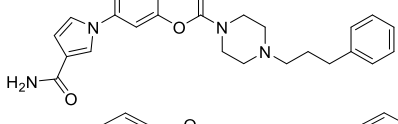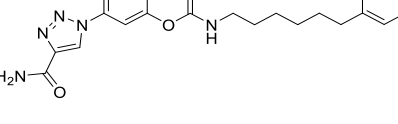
41p		47 ± 3	2899 ± 193
41q		10.5 ± 0.8	2437 ± 178
41r		128 ± 9	>10000
41s		7.54 ± 0.51	8396 ± 621
41t		253 ± 13	>10000
23		3.72 ± 0.21	-[114]
47		102 ± 9 [114]	-[114]

[a]Each value is the mean of at least three experiments; FAAH and MAGL inhibition was measured after 30 min of pre-incubation; [b]NT not tested; [c]NC not calculable.

3.4. SAR of the newly developed FAAH inhibitors

The goal of our investigation was the identification of compounds with balanced potency on FAAH, solubility, chemical stability and lack of activity on MAGL. Substitution of the terminal phenyl substituent of arylfuran **47** with a 4-methylpiperazine group (compound **41a**) resulted in a 10-fold decrease in the inhibitory potency. The loss in activity was less prominent when a 4-phenylalkylpiperidine was introduced at the nitrogen atom as in the case of **41b** and **41c**, displaying IC_{50} values of 188 and 407 nM, respectively. Tertiarization of the carbamate group of **41b** had a different impact on inhibitory potency, with direct methylation of the nitrogen dramatically reducing activity (**41d**, IC_{50} = 6556 nM), and its inclusion in a piperazine ring leading to a single digit nanomolar compound (**41e**, IC_{50} = 8.3 nM). Compound **41e** thus emerged as key inhibitor deserving further investigations, considering our multiparametric optimization aimed at finding inhibitors with good potency and balanced physico-chemical properties. Replacement of the 4-(3-phenylpropyl)piperazine of **41e** with a 4-(3-phenylpropyl)piperidine substituent, avoiding a basic center, was well tolerated by FAAH with **41f** having an IC_{50} value (11.7 nM) approaching that of **41e**. A loss in the inhibitory potency was observed when the 4-(3-phenylpropyl)piperazine moiety of **41e** was replaced by, likely more basic, 4-(phenylalkylamino)piperidine chains of **41g** and **41h**, displaying IC_{50} values of 26 and 165 nM, respectively. This trend suggests that FAAH preferentially recognizes the neutral form of tested inhibitors, and that an increment in the pK_a of the substituent incorporating the nitrogen atom of the carbamate hampers inhibitory potency by reducing the availability of the neutral species.

Our SAR exploration continued investigating the importance of the peripheral 5-methylfuran-3-carboxamide on FAAH inhibitory potency by replacing it with different substituted heterocycles: *i.* 5-methylthiophene-3-carboxamide (compounds **41i-k**), *ii.* 1*H*-

pyrrole-3-carboxamide (**44l-n**) and *iii.* 1*H*-1,2,3-triazole-4-carboxamide (**41o,p**). Gathered data suggest that all these substitutions were essentially bioisosteric replacements, as indicated by the activity of 4-(3-phenylpropyl)piperazine derivatives **41e, 41k, 41n**, and **41p**, displaying IC_{50} values in the medium-low nanomolar range (8.3-47 nM).

As a final step of our SAR investigation, we evaluated the impact of inserting an acid group on the aryl substituent at the oxygen atom on inhibitory potency. In the cases of arylfuran derivatives **47** and **41e**, replacement of the 3-carbamoyl with a 3-carboxylic acid had an opposite effect. In the first case, a significant improvement of the inhibitory potency was observed, with compound **41q** displaying an IC_{50} value of 10.5 nM, 10-fold lower than that of parent compound **47**. In the second one, a significant drop in the inhibitory potency was observed, with compound **41r** displaying an IC_{50} value 15-fold higher than that of parent compound **41e**. When the 1H-pyrrole-3-carboxamide fragment of **47** and **41n** was replaced by a *2H*-tetrazol-5-yl group, a loss of inhibitory potency was observed in both cases. While for **41s** the unfavorable effect on the IC_{50} was moderate, in the case of **41t** it was considerable. We speculate that the detrimental impact on inhibitory potency of introducing an acid group on compounds already having a basic center (as for **41r** and **41t**) may generate zwitterionic species with low affinity for FAAH active site.

The present exploration thus allowed us to identify several candidates with fair potency ($IC_{50} < 100$ nM) potentially endowed with higher solubility and/or enhanced chemical stability compared to reference inhibitors **47** and **23**, and devoid of significant activity on MAGL.

3.5. Computational studies

Docking studies conducted on the key inhibitor compound **41e** was performed to determine the binding mode of this derivative. Considering its basic moiety in the lateral chain, derivative **41e** was docked in the neutral and protonated forms in the FAAH binding pocket. Both these forms of compound **41e** proposed a binding mode comparable with our previously reported FAAH inhibitors, with the electrophilic carbon of the carbamate placed at nearly 3.0 Å from Ser241 hydroxyl oxygen, a distance consistent with a nucleophilic attack, the 3-(3-carbamoyl-5-methylfuran-2-yl)phenoxy group harbored in the solvent exposed CA channel, and the 4-(3-phenylpropyl)piperazine moiety accommodated in the ACB pocket (see **Figure 25**).
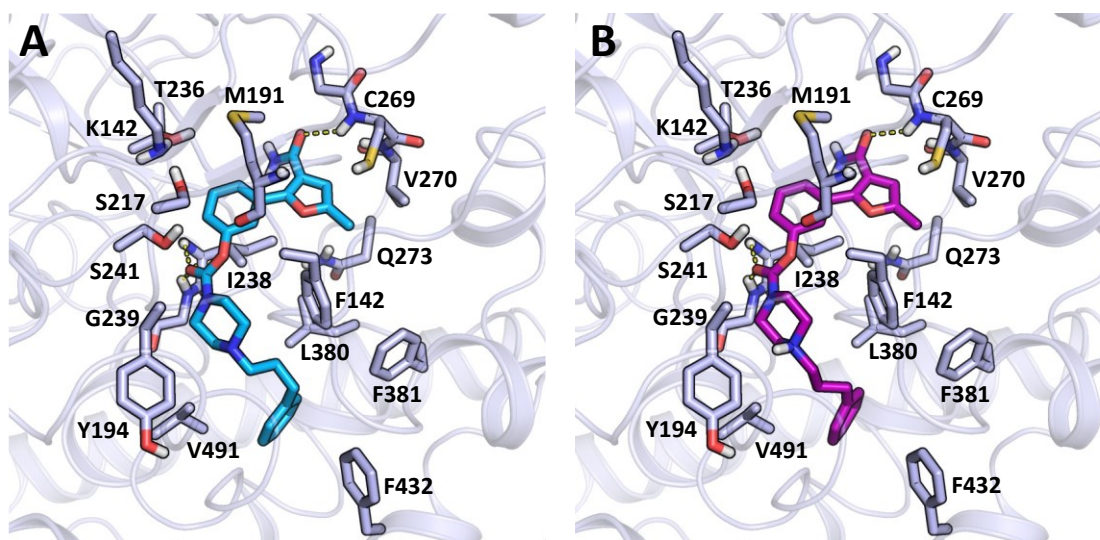
Figure 25. Best pose for compound **41e** docked into FAAH (light violet carbon atoms) in neutral (cyan carbon atoms, panel A) or protonated form (purple carbon atoms, panel B).

Moreover, terminal 3-CONH$_2$ substituent emerging from the furan ring formed H-bonds with CA channel residues (Cys269, Val270 NH groups), the phenylpropylpiperazine fragment did not undertake any polar interaction with the ACB pocket, being this region mostly composed by hydrophobic residues. However, the 100 ns-long MD simulations showed that **41e** maintained an arrangement consistent with the docked pose only when

modelled in the neutral form. The presence of a protonated piperazine in the ACB pocket increased the mobility of **41e** already in the early phases of MD simulations, pushing the carbamate group away from both the oxyanion hole and the nucleophile, stabilizing a disposition not compatible with Ser241 carbamoylation. This data suggests that FAAH preferentially recognizes the neutral form of tested inhibitors, and that an increment in the pK_a of the substituent incorporating the nitrogen atom of the carbamate hampers inhibitory potency by reducing the availability of the neutral species.

Compounds **41k**, **41n** and **41p** which show the same lateral chain of **41e** were docked in the FAAH binding pocket in the neutral form. All these derivatives reproposed the same binding mode previously described, in line with their low nanomolar inhibition potency (see **Figure 26**).
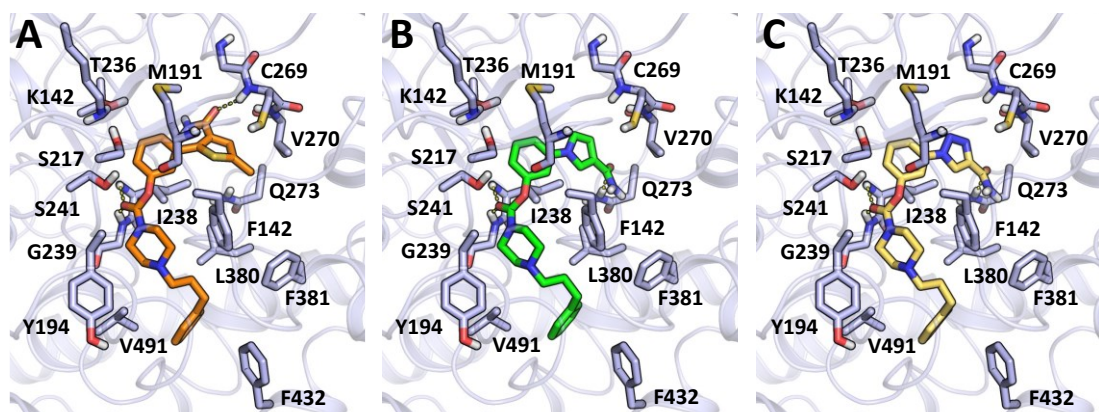
Figure 26. Best poses for compound **44k** (orange carbon atoms, panel A), **44n** (green carbon atoms, panel B) and **44p** (yellow carbon atoms, panel C) docked into FAAH (light violet carbon atoms) in neutral form.

3.6. Mechanism of action of carbamate-based FAAH inhibitors 41e, and 41g

To investigate the inhibition mechanism of two of the most interesting compounds, **41e** and **41g**, rapid dilution assays were performed. The compounds were incubated at two different concentrations (10 and 100 nM) in the presence of a 50-fold higher amount of FAAH than in standard conditions. After a 50-fold dilution, the

substrate was added, and the enzymatic activity was evaluated. In the case of reversible inhibitors, rapid dilution disrupts the equilibrium between the inhibitor and the enzyme, resulting in enzymatic activity recovery. In contrast, dilution of the assay mixture containing the enzyme and an irreversible inhibitor would not lead to the recovery of enzymatic activity. After rapid dilution, a virtually complete recovery of FAAH activity was observed for both compounds **41e** (**Figure 27 A**) and **4g** (**Figure 27 B**) when compared to standard incubation conditions. These results suggest that derivatives **41e** and **41g** inhibit FAAH through a reversible mechanism.
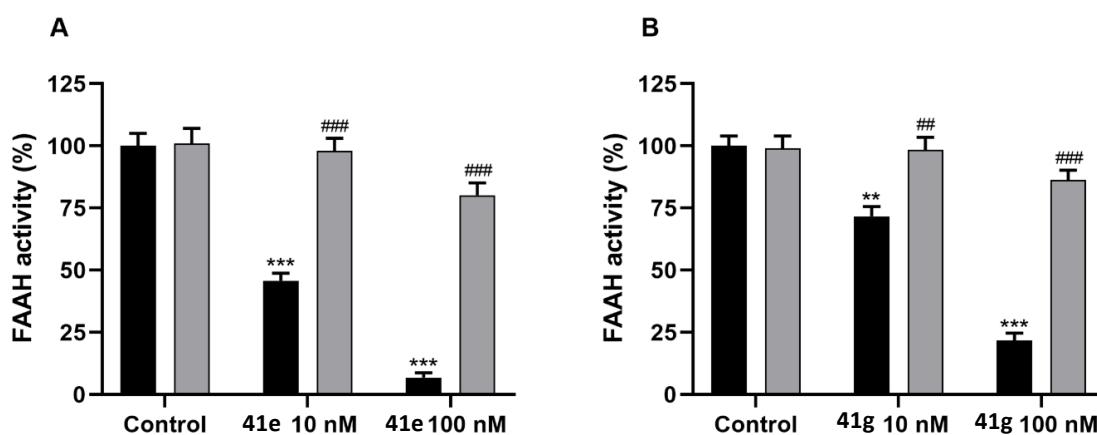
Figure 27. Reversibility of FAAH inhibition by compounds **41e** (A) and **41g** (B).

3.7. Evaluation of chemical stability and solubility profile.

For the optimization of the drug-like properties of the novel FAAH inhibitors, we inserted specific basic lateral chains or acidic moieties in the byarilic scaffolds to study their effects on water solubility and chemical stability. These data were evaluated by using HPLC method at pH 3 and pH 7.4 for selected compounds **41b,e,g,h,n-t** and are summarized in **Table 2**.

Table 2. Chemical stability and solubility of compounds **44b,e,g,h,n-t**.

Cmpd	Structure	Stability% pH 3, 24 h	Stability% pH 7.4, 24 h	Solubility pH 3, 24 h (µM)	Solubility pH 7.4, 24 h (µM)
41b		96.6	>99	282.5	67.4
41e		97.8	>99	167.6	<1
41g		>99	>99	277.1	205.5
41h		>99	>99	353.26	322.4
41n		>99	>99	228.2	41.5
41o		63.2	78.8	ND[a]	ND[a]
41p		>99	>99	297.5	38.4
41q		<1	92.7	ND[a]	172.4
41r		>99	96.8	249.1	259.0
41s		<1	>99	ND[a]	107.7
41t		>99	>99	268.1	272.2
23	-	32.4	38.3	2.7	3.4
47	-	31.4	9.3	<1[b]	<1[b]

[a]ND = Not determined; [b] the data was evaluated after 12 h.

In general, all the tested derivatives showed an excellent chemical stability at both pH values. The improved chemical stability of most of the new compounds might be due to distinct effects that disadvantage aqueous hydrolysis of the new carbamates as compared to **23** and **47**. These effects could be due to the increased steric hindrance in proximity of the carbamate that was obtained either by tertiarization of carbon proximal to the carbamate nitrogen (see **41b** vs **47**, **Table 2**), or the tertiarization of carbamate nitrogen (see **41e** vs **47**, **Table 2**). On the other hand, the introduction of an acid group

on leaving group as in **41q** and **41s** (see **41q** vs **47**, and **41s** vs **47**, **Table 2**) stabilized the carbamate possibly due to the presence of a negatively charged group that could disadvantage expulsion of the phenate. The poor stability, at pH 3, of compounds **41s** and **41q** is perfectly in line with this analysis.

Improved solubility at physiological pH was obtained after insertion of a 4-aminopiperidine or a piperazine in the lateral chain of the carbamates (see **41b**, **41n**, and **41p** vs **47 Table 2**). The notable solubility of the "inverted" 4-aminopiperidine derivatives **41g** and **41h** confirmed that the nitrogen tertiarization represents a key point for enhancing the drug disposition proprieties of our FAAH inhibitors particularly when associated with a secondary amine in the lateral chain that strongly increased the water solubility at pH = 7.4 up to 205.5 or 322.4 µM respectively (**Table 2**). The effects of acidic moieties in the byarilic portion of the inhibitors were also evaluated. The presence of a carboxylic group in the phenylhexyl derivative **41q** (**Table 2**) remarkably improved the water solubility at pH = 7.4 compared to the carboxamide analogue **47**. The replacement of the carboxamido five membered heterocycle of **47** and **47** with a tetrazole ring, as in derivative **44s** (Table 2), allowed us to noticeably improve water solubility at pH = 7.4. We also explored the combination of a piperazine basic lateral chain with the tetrazole or with the furane carboxylic acid moiety in compounds **41t** and **41r** that led to compounds bearing both an acidic and a basic moiety which were characterized by excellent water solubility.

3.8. Selectivity and toxicity profile

For the most promising compounds, the selectivity profile against CBR_1 and CBR_2 was evaluated, and the potential cytotoxicity was investigated in *murine* fibroblast cell lines NIH3T3 and in *human* astrocytes cell lines 1321N1. None of the selected analogues

showed off-target effects for either CBRs subtypes. Moreover, selected analogues displayed notable safety profile at all tested concentrations in both the assessed cell lines.

To evaluate the cardiotoxic potential of the new developed FAAH inhibitors, the activity of compound **41n** was evaluated on cardiac mechanical function and electrocardiogram (ECG) in Langendorff-isolated rat hearts. In this *ex vivo* toxicity assay, only at the at the maximum concentration tested, which was three orders of magnitude higher than that effective in FAAH inhibition, **41n** exhibited negative inotropic and chronotropic activity and prolonged the cardiac cycle length as well as the atrioventricular conduction time.

3.9. Evaluation of the anti-inflammatory profile

Although neurodegenerative diseases display different aetiology and pathogenesis, the main hallmark of these pathological conditions is represented by neuroinflammatory processes, which determine the activation of several biological mechanisms such as OS and glia responses. Glia cells, including astrocytes, are involved in the maintenance of CNS homeostasis exacerbating inflammatory reactions or promoting tissue repair. In this context ECS catabolic enzyme pharmacologic or genetic inhibition led to reduce both neuroinflammatory and neurodegenerative states in different animal models. On these bases, we investigated the role of our new developed FAAH inhibitors in the reduction of OS in 1321N1 *human* astrocytes cell line and determined the protective effects of our selected analogues in inflammation-induced neurodegeneration *ex vivo* cultures of rat hippocampal explants.

3.9.1.   Effect of selected compound on TBHP-induced ROS production

When administered to 1321N1 astrocytes, FAAH inhibitors **41e**, **41n**, and **41s** resulted

effective in the prevention of TBHP-induced ROS production as shown in **Figure 28**. **41e**

and **41s** significantly reduced ROS production starting from the 10 nM concentration,

while compound **41n** from the 100 nM concentration. All the tested compounds at 1 μM

exerted an effect similar to that of 2 mM *N*-acetylcysteine (NAC), used as a reference

antioxidant compound (**Figure 28**).
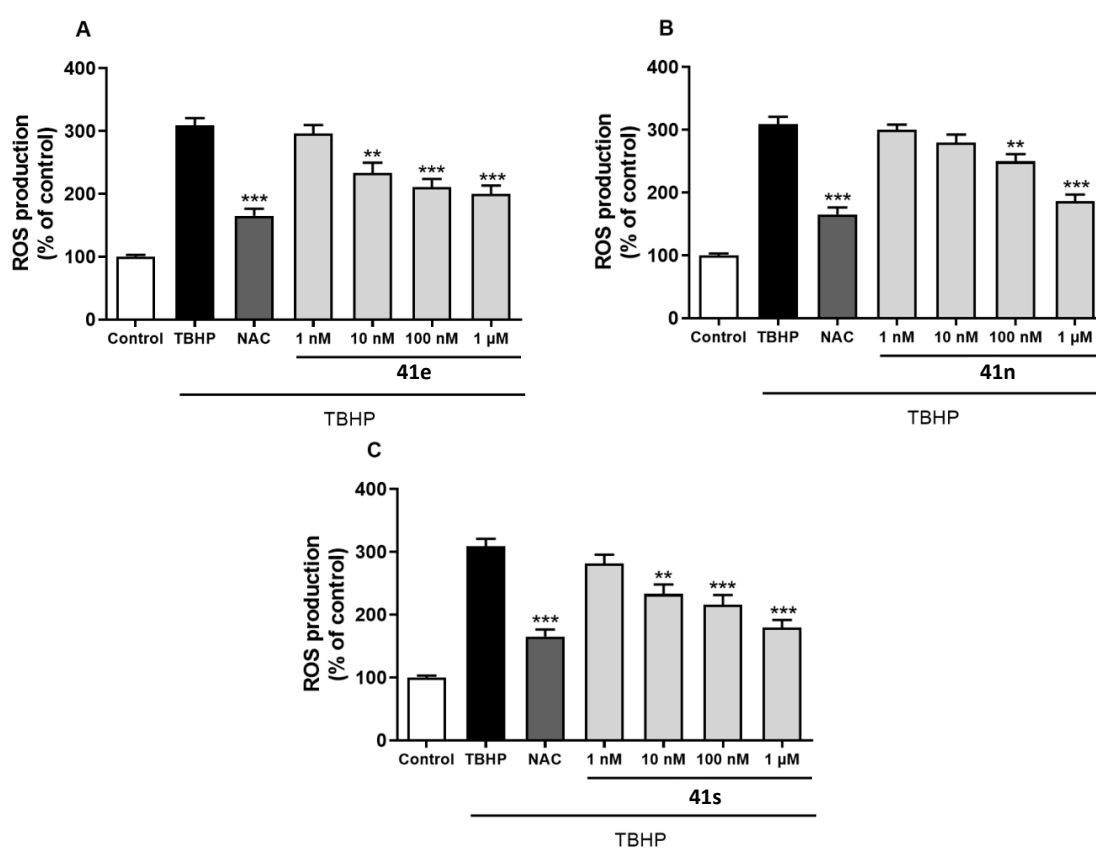
Figure 28. Effect of novel FAAH inhibitors **41e**, **41n** and **41s** on *tert*-butyl hydroperoxide
(TBHP)-induced ROS production in 1321N1 astrocytes in comparison to NAC.

3.9.2.   Protective effect against inflammation-induced neurodegeneration in ex vivo cultures of rat hippocampal explants

To study the neuroprotective actions of FAAH inhibitors on neuroinflammatory damage,

organotypic explants were exposed to a combined application of 10 μg/mL LPS and

recombinant 100 ng/mL IFN-gamma for 96 h, and cell death was assessed with propidium

iodide (PI) staining.
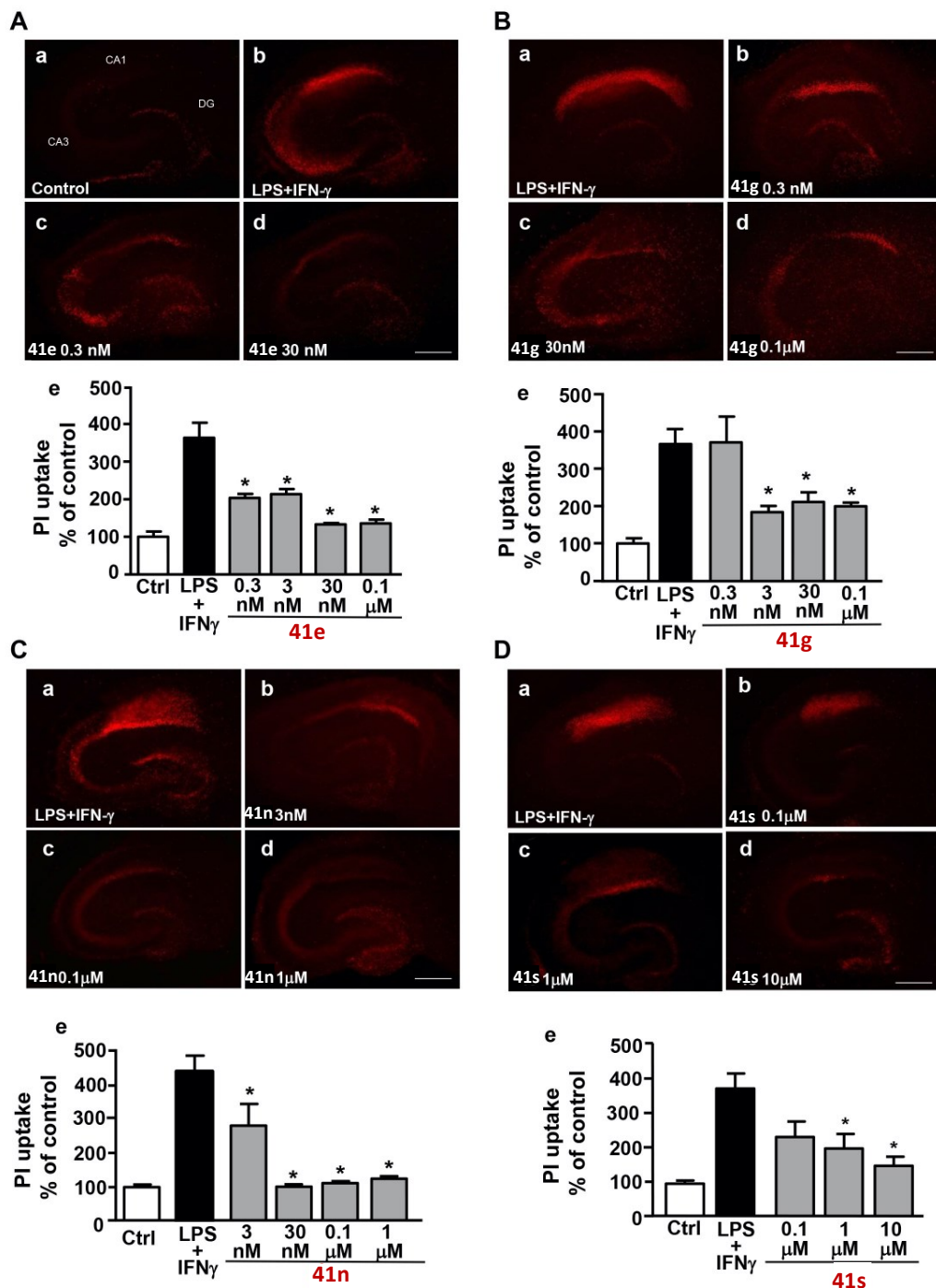
Figure 29. Effects of FAAH inhibitors against LPS+IFN-γ-induced inflammatory damage in hippocampal organotypic cultures. A–D, a-d; PI fluorescence staining patterns observed in representative hippocampal organotypic slices under control conditions (A, a) and following 96 h of LPS + IFN-γ-exposure in the absence of drug exposure (A, b; B-D, a) or in the presence of 0.3 nM – 30 nM **41e** (A, c-d); 0.3 nM – 0.1 μM **41g** (B, b-d); 3 nM – 1 μM **41n** (C, b-d); 0.1 μM – 10 μM **41s** (D, b-d).

Densitometric analysis of PI uptake revealed that when hippocampal explants were exposed to the inflammatory injury, cell death selectively occurred after 96 h in the CA1 pyramidal cell layer. The presence of **41e** (0.3 nM – 0.1 μM), **41g** (0.3 nM– 0.1 μM)**, 41n** (3 nM – 1 μM) and **41s** (0.1–10 μM) in the incubation media significantly prevented the increase in PI uptake occurring in the CA1 region 96 hours after LPS+IFN-γ exposure (**Figure 29 A-D**). All the tested compounds showed a dose-dependent anti-neuroinflammatory effect.

4. Synthesis of new MAGL inhibitors

4.1. Background

The lead role played by the MAGL in the regulation of 2-AG levels and the huge number of physiological functions and pathologies in which this endocannabinoid is involved, encouraged the research activity of our group in the development of selective MAGL inhibitors [115]. Triazole based MAGL inhibitors such as **32** (**SAR629)** or **34** (**JJKK048)** adopt a "Y shape" conformation in the enzyme banding pocket. The steric hindrance of their biphenyl portion guarantees selectivity by interacting with hydrophobic residues whilst the carbonyl group (electrophilic center) sits in proximity to the catalytic triad [103,116,117]. These compounds represented the early prototypes of irreversible MAGL inhibitors, and they were deeply studied as pharmacological tools to clarify the role of the MAGL enzyme in different pathophysiological conditions, establishing a starting point for the design of new potent inhibitors. In this context, in our group was recently proposed a new series of azetidinone-based compounds typified by compound **36** [68] . This high potent and selective MAGL inhibitors challenged the Y shape of the diphenylmethane derivatives **32** and **34**. The β-lactam core of **36** supports the substituted aromatic groups respectively inserted in *trans* configuration the position 3 and 4 of the azetidine-2-one nucleolus. As showed in **Figure 30** (panel B), the *trans* configuration of the β-lactam substituents lead to the formation of a dihedral angle of 119.4 °C. This spatial orientation guarantees a distance of ~7Å between the centroids of the aromatic system needed to maximize the hydrophobic interaction in the MAGL catalytic site. The diphenylmethane **34**, shows a similar pharmacophoric model (**Figure 30**, panel A), but with a decreased distance between the aromatic groups (5-6Å) which results in a low potency against the target when compared with our MAGL inhibitor **36**.

Moreover, in compound **36**, the piperidinic spacer directly connected to electrophilic centre accommodate the triazole-based ureidic moiety close to the catalytic tread (**Figure 30**).
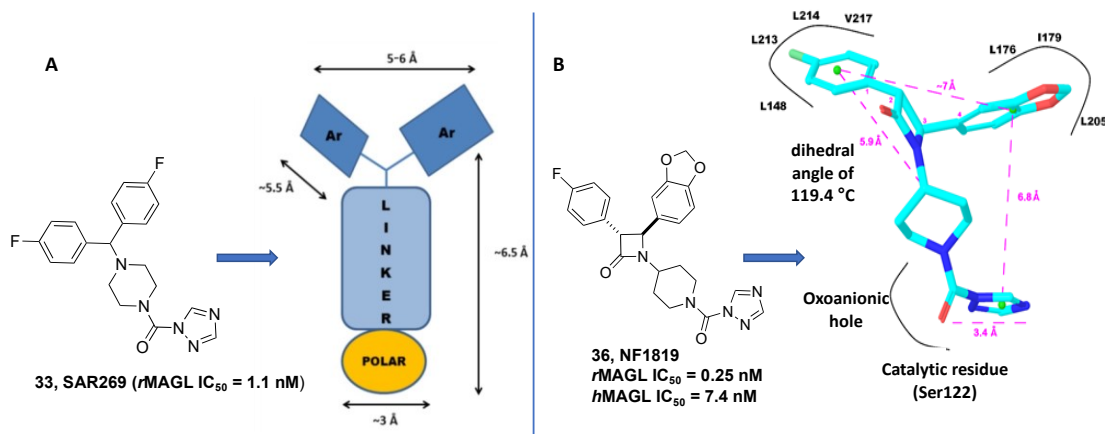
Figure 30. A) Pharmacophoric model of the diphenylmethane-based MAGL inhibitors **33**; **B)** pharmacophore distances and spatial arrangement of the key structural elements of **36**.

Both the enantiomers of **36** (*3R-4S* and *3S-4R*) were tested toward MAGL enzyme. **36** *3R-4S* resulted the eutomer derivative (IC$_{50}$ = 4.6 nM), 7 time more potent than the corresponding distomer (*3S-4R,* IC$_{50}$ = 31.2 nM). This difference in the activity could be ascribable at a more comfortable accommodation of the aromatic portion in the enzyme binding pocket. By using mass spectrometry experiments the irreversible mechanism of action of **36** was demonstrated, determining that Ser122 performs a nucleophilic attack on the carbonylic group of the inhibitors with the formation of carbamylated enzyme. Moreover **36** resulted effective in reducing the clinical severity of EAE and produced analgesic effects in two different murine model of acute inflammatory pain [68].

4.2. Developed of compounds 42e and 42f as potential MAGL inhibitors

The modern medicinal chemistry led to the identification of privileged molecular moieties which can confer at different compounds the ability to interact with distinctive receptors. These privileged molecular frameworks represent a valid opportunity in the rational design of therapeutic agents, combining the possibility to explore the efficacy of new scaffolds in innovative therapeutic opportunities [118]. Concerning that, spirocycles are included in the panel of privileged moieties, offering innate three-dimensional peculiarities, combined with an increased structure complexity and rigidity, which can enhance the target-ligand complementarity [118,119]. Moreover, further advantages deriving from the use of spirocyclic-based compounds are measurable also in terms of target selectivity, physiochemical proprieties, and pharmacokinetic (PK) profile, counterbalancing the increased synthetic efforts needed to obtain spiro-derivatives [120]. In this context our group developed spiroindolne-based compounds as selective histone deacetylase 6 (HDAC6) inhibitors [121]. Also the benzodiazepine core deserves to be mentioned among the privileged scaffolds. This nucleus, deeply studied over the years, shows a high pharmacogenic structure endowed with low toxicity profile combined to a wide spectrum of neuropharmacological activity correlated to high blood brain barrier penetration, but also antibacterial, and anticancer properties [122]. The β-lactam moiety also can be considered as a privileged medicinal chemistry moiety since its first application as antibiotics [123]. Inspired from our previous work on the β-lactam based MAGL inhibitors, we decided to explore the chemical space of MAGL inhibition, developing new inhibitors by maintaining the piperidine-azole urea moiety as a key motif for MAGL inhibition, combined with the opportunely modified above mentioned privileged spiroindoline, β- lactam and benzodiazepine scaffolds (**Figure 31**).
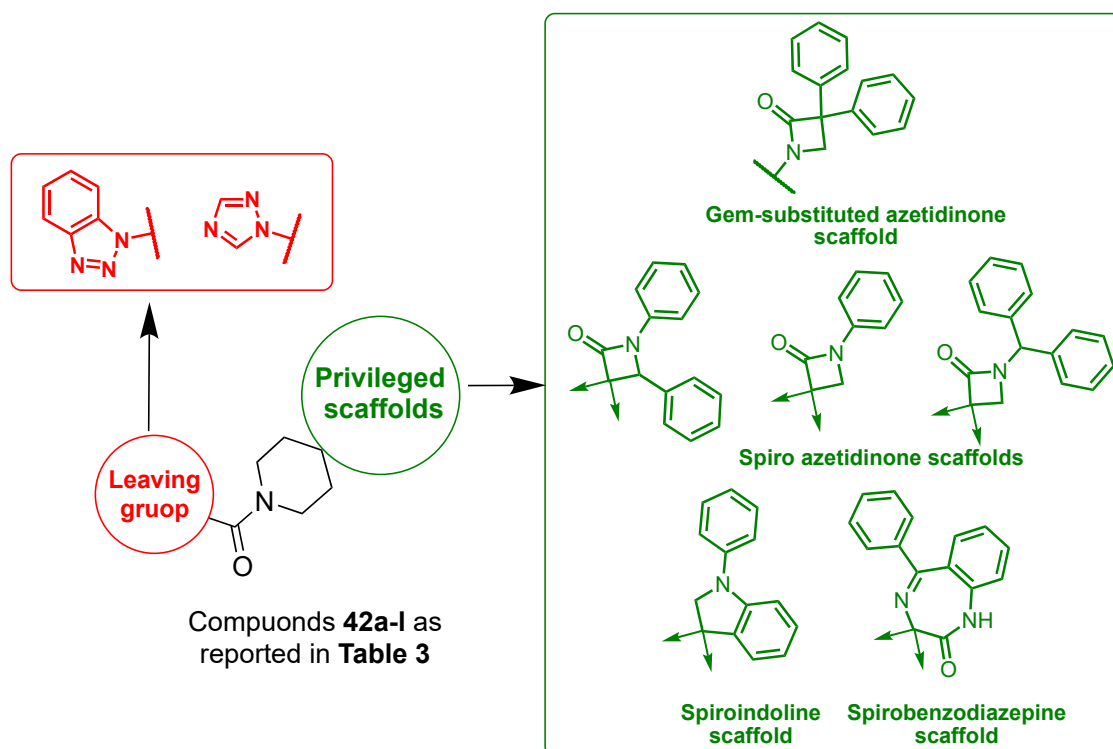
Figure 31. Newly developed MAGL inhibitors.

A library of 12 new MAGL inhibitors was synthesized (compounds **42a-l**, **Figure 22** and **Table 6**) as a result of our scaffolds investigation, leading to develop of: i) two gem- β-lactams compounds **42a,b** (**Table 6**); ii) six spiro-β-lactams, compounds **42c-h** (**Table 6**); iii) two spiroindoline-based inhibitors, **42i,j** (**Table 6**); iv) two benzodiazepine-based derivatives, **42k,l** (**Table 6**).

In this context my contribution was relative to the preparation of two spiro-β-lactams derivatives, compounds **42e-f**, to complete the SAR study and to better characterize our scaffolds exploration. For the most interesting compound of the series, we are currently evaluating their neuroinflammatory properties in hippocampal rat explants.

4.3. Synthesis of the compounds 42e-f

The synthesis of the spiro-β-lactam **42e-f** is represented in the **Scheme 7**. α alkylation of ester **87** in presence of LDA and ethyl chloroformate furnished the di-ester **88**. Mono

hydrolysis of this latter, led to the carboxylic acid **89** which reacted in coupling condition with aniline to obtain intermediates **90**. After treatment with NaBH$_4$ in ethanol, esters **90** were reduced to the corresponding alcohols **91**. Intramolecular Mitsunobu reaction led to the formation of the spiro-β-lactam **92**. Treatment with TFA allowed to obtain the free amine **93** which reacted with carbonyl-ditriazole furnishing compounds **42e**, or with 1*H*-benzotriazole and phosgene leading to compounds **42f**.
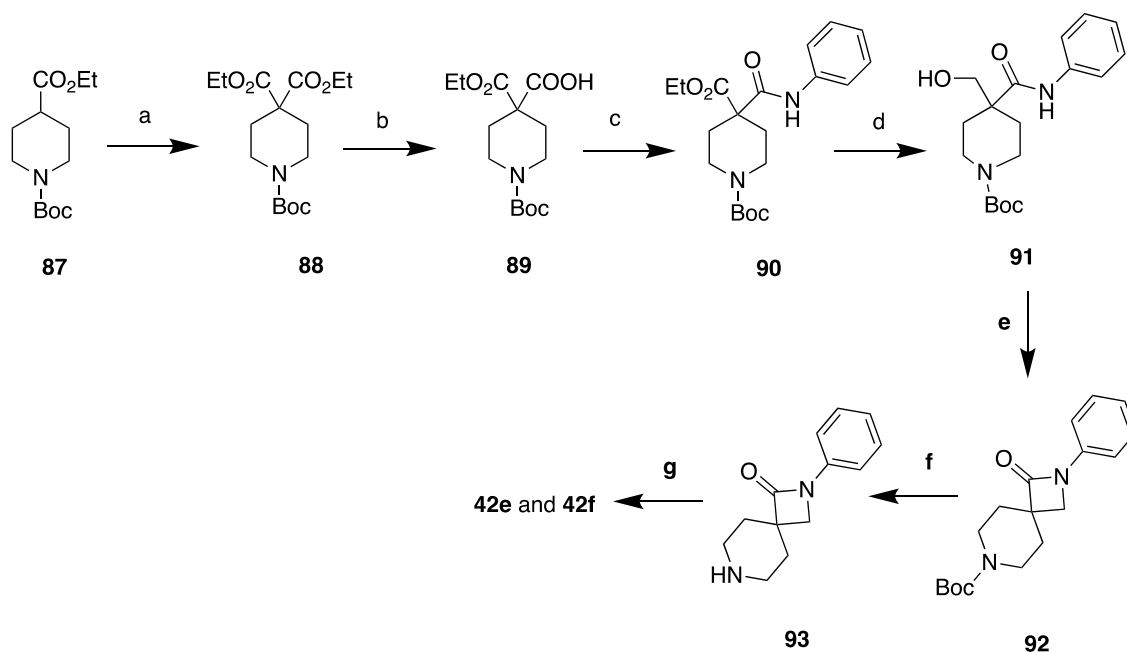
Scheme 7. Synthesis of compounds **42 e-f.**
Reagents and conditions. a) *n*-BuLi (2.5M in hexane), DIPA, **87**, ethyl chloroformate, dry THF, -78 °C, 3h, 99%; b) LiOH (0.5 M), ethanol, 25 °C, 12 h, 50%; c) PPh$_3$, hexachloroacetone, aniline, dry DCM, -10 °C, 45 min, 91%; d) NaBH$_4$, ethanol, 25 °C, 1 h; e) PPh$_3$, DIAD, dry THF, 25 °C, 2 h, 68%; f) TFA, dry DCM, 25 °C, 2 h, 89%: g) CDT, dry DCM, 25 °C, 12 h 44% for **42e**,; or 1*H*-benzotriazole, phosgene (20% in toluene) DMAP, dry DCM, 25 °C, 12 h, 42%for **4f**.

Table 3. Inhibitory activity towards *human* MAGL and *human* FAAH (expressed as IC$_{50}$ nM) for title compounds **42a–l**.

Cmpd	Leaving group	Privileged scaffold	IC$_{50}$ *h*MAGL (nM)	IC$_{50}$ *h*FAAH (nM)
42a			1.55 ± 0.12	829 ± 61
42b			5.76 ± 0.37	639 ± 38
42c			21 ± 2	792 ± 58
42d			368 ± 31	782 ± 44
42e			89 ± 6	63 ± 4
42f			466 ± 38	325 ± 26
42g			1.95 ± 0.12	212 ± 13
42h			36 ± 2	166 ± 11
42i			1.86 ± 0.12	13.9 ± 1.1
42j			252 ± 18	351 ± 23
42k			21 ± 1	9380 ± 458
42l			1652 ± 109	>10000
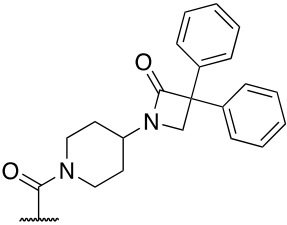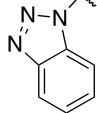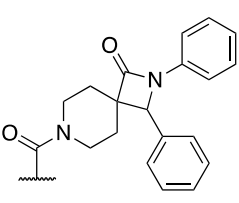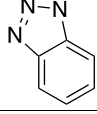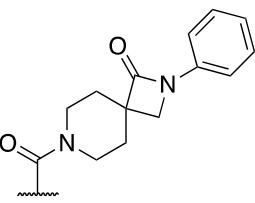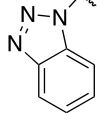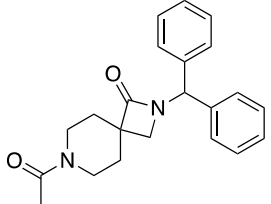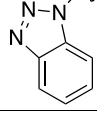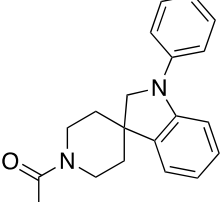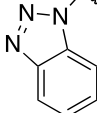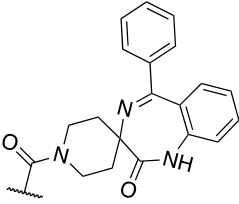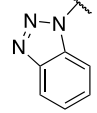
Values are means of three experiments and all SD are within 10%

5. Development of dual FAAH/MAGL inhibitors

5.1. Background

The development of dual FAAH/MAGL inhibitors represents an important task for our research activity. After accurate SAR and molecular modeling studies performed in our research group, we could identify the structural requirements for dual FAAH/MAGL inhibition. These studies resulted in the development of a small set of multitarget compounds characterized by a pyrroloquinoxaline scaffold (compounds **94a-d**, **Table 4**) [124].

Table 4. IC_{50} values on FAAH and MAGL enzyme for pyrroloquioxaline-based dual inhibitors.
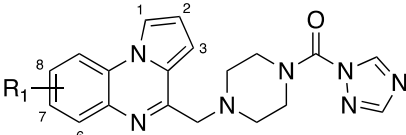
Cpds	R₁	MAGL IC_{50} (nM)	FAAH IC_{50} (nM)
94a	H	37.0	44.7
94b	7-F	10.7	49.9
94c	7-Cl	32.4	95.5
94d	7,8-diMe	32.4	80.1

The appropriate combination between pyrrloquinoxaline-based scaffold and the piperazine carboxamide/carbamate moiety was explored to identify compounds characterized by suitable size and geometrical shape for fitting FAAH and MAGL binding pocket. Developed compounds showed IC_{50} values in the nanomolar range against both enzymes and these biological data were supported by detailed docking studies performed on the lead compound **94a** [124].

5.2. Development and biological characterization of compounds 43a-l as potential dual FAAH/MAGL inhibitors

In this context, part of my PhD work was also focused on the development of new dual FAAH/MAGL inhibitors. The design of these polypharmacological compounds started taking account the chemical structure of our MAGL inhibitor **36** [68]. From this high potent and selective β-lactam-based derivatives we applied a scaffold simplification strategy, merging all the key pharmacophoric elements needed for the simultaneous inhibition of both the ECS catabolic enzymes. Our first approach consisted in the elimination of the chiral centers because of the replacement of the β-lactam core with an azetidine moiety. This modification allowed to obtain a more flexible structure which could be better accommodate in both the enzymes binding pockets.
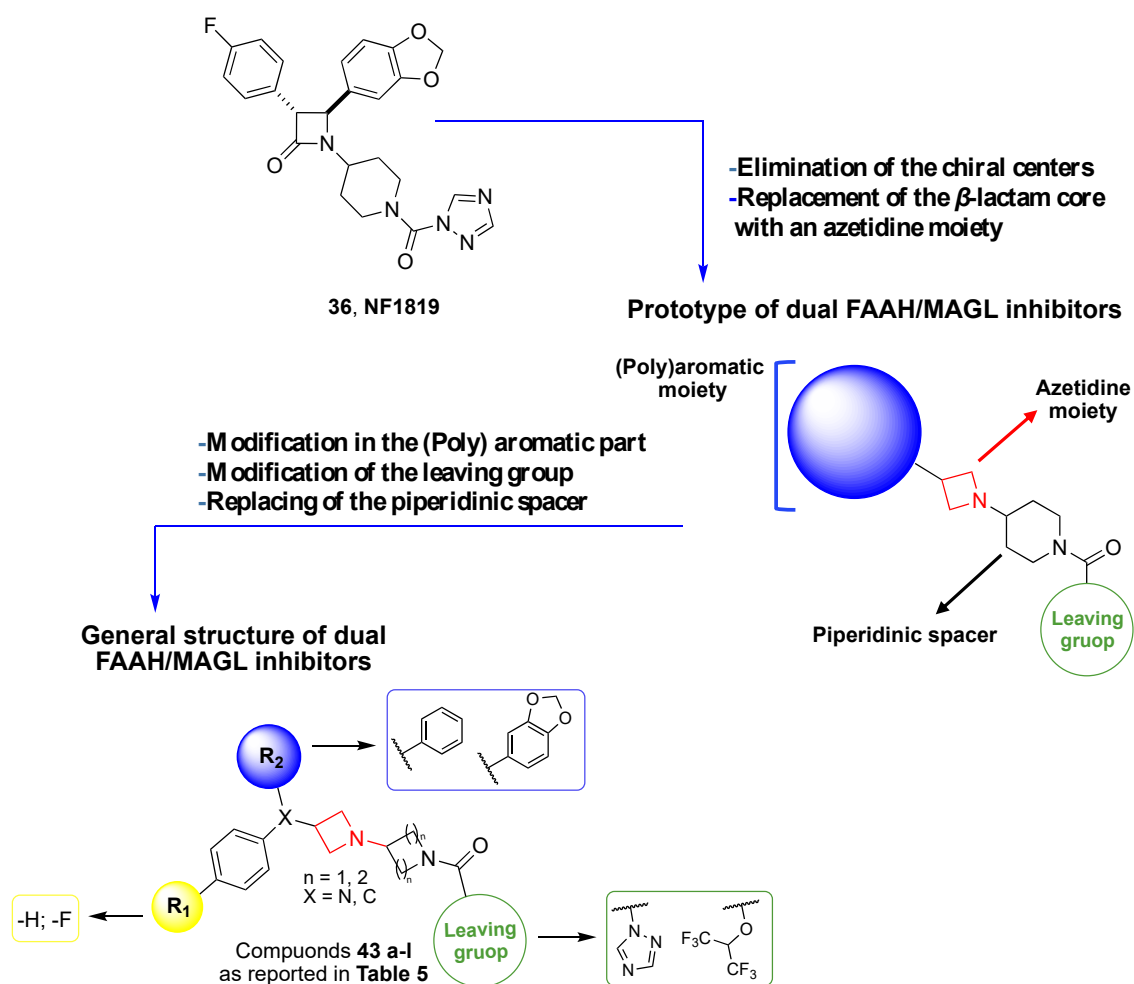
Figure 32. Design of dual FAAH/MAGL inhibitors.

In this way obtained a prototype structure of our dual FAAH/MAGL inhibitors (see **Figure 32**) in which is possible identify the key elements such as: i) a (poly) aromatic part, which could be characterized by different lipophilic level; ii) an azetidine core; iii) a piperidinic spacer; iv) a leaving group. In this prototype structure we decide to keep the piperidinic spacer because it is a crucial element for the MAGL inhibition but resulted useful also for some of our previously reported FAAH inhibitors (see **Table 1**, compounds **41f** and **41g**). However, the key point for the simultaneous FAAH and MAGL inhibition is represented by the electrophilic moiety, which direct interacts with the catalytic serine of both the targets. Several studies outlined triazole heterocycles as the best performing moiety to engage FAAH and MAGL enzymes since their conjugate acids pK_a values guarantee effective interaction with the catalytic serine of both targets. For selectively engaging the MAGL enzyme, the pK_a of the leaving group should be between 8 and 10. These data are in line with the IC_{50} values of compounds such as **32** and **35** where the pK_a values of the leaving groups of the triazole and hexafluoroisopropanol (HFIP) are 9.3 and 10.0, respectively. However, diverse leaving groups are tolerated by the FAAH enzyme. With the aim to obtain an exhaustive library of hybrid FAAH/MAGL inhibitors we suitably modified our prototype structure at different levels. The aromatic part was modified introducing mono or diphenilmethane moieties, where we also inserted an instauration. The replacement of the piperidinic spacer with a ciclobuthylamine linker was also assessed, to reduce the steric hindrance in proximity of the electrophilic center. For few analogues, we also evaluated the effect of the triazole or HFIP as leaving group. Following this approach, a library of novel 12 dual FAAH/MAGL inhibitors (compounds **43a-l**) was synthetized, and a large number of the new derivatives showed activity in the nanomolar range against both the targets. These inhibitory activities were evaluated together with a selectivity profile, for a sub-set of selected analogues, towards CBRs.

Moreover, I also performed solubility and chemical stability studies on the most interesting analogues. Finally for three derivatives **43h**, **43i** and **43k** the anti-neuroinflammatory effect was evaluated on rat hippocampal slice cultures.

5.3. Chemistry of the dual FAAH/MAGL inhibitors

The synthesis of derivatives **43a-e** is reported in the **Scheme 8**

95a, R$_1$ = H
95b, R$_1$ = F

96a, R$_1$ = H
96b, R$_1$ = F

97a, R$_1$ = H; R$_2$ = H
97b, R$_1$ = F; R$_2$ = 3-4-O-CH$_2$-O

98a, R$_1$ = H; R$_2$ = H
98b, R$_1$ = F; R$_2$ = 3-4-O-CH$_2$-O

100a, R$_1$ = H; R$_2$ = H
100b, R$_1$ = F; R$_2$ = 3-4-O-CH$_2$-O

99a, R$_1$ = H; R$_2$ = H
99b, R$_1$ = F; R$_2$ = 3-4-O-CH$_2$-O
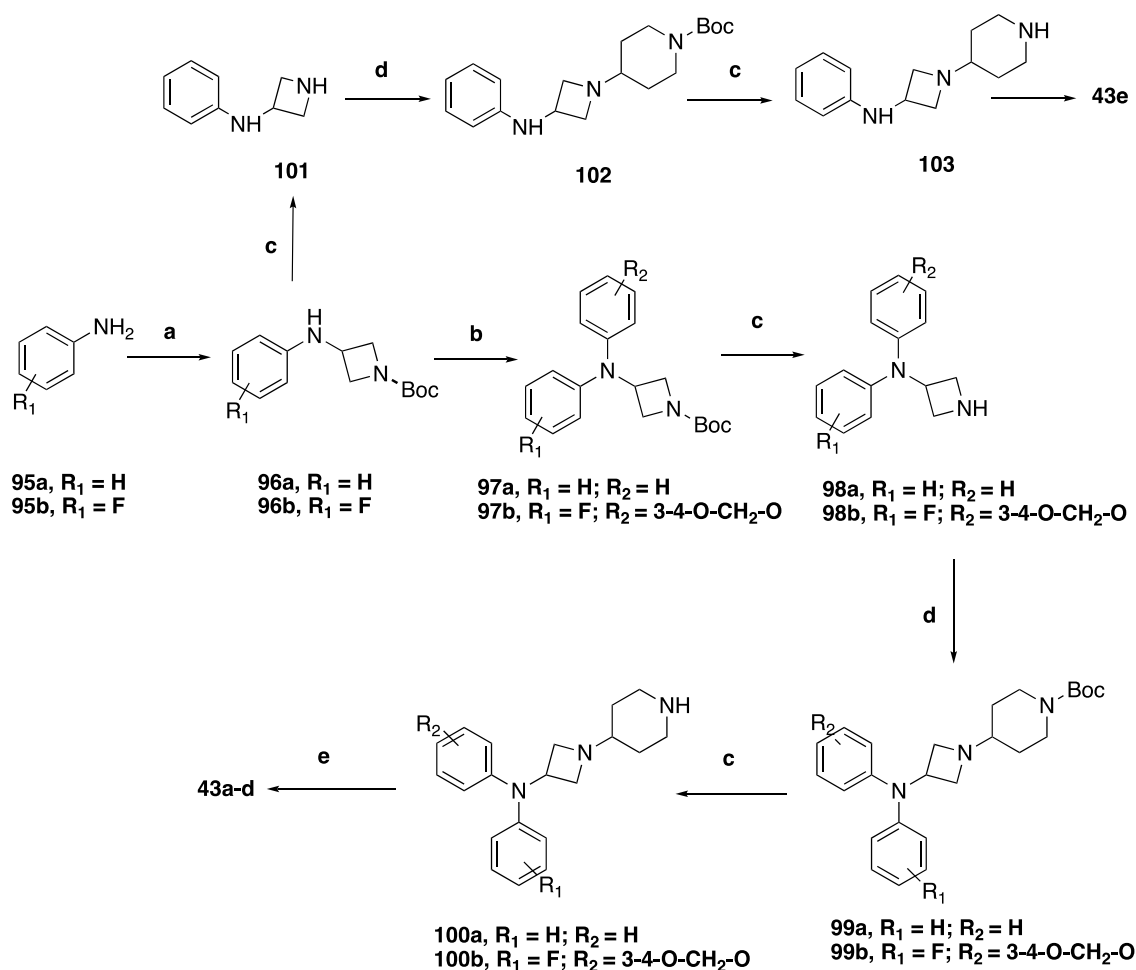
Scheme 8. Synthesis of compounds **43a-e**.
Reagent and conditions. a) 1-Boc-3-azetidinone, AcOH, DCE, NaBH$_3$CN, 12 h, 25 °C, 80-82%; b) bromobenzene (for compound **97a**) or 5-Iodo-1,3-benzodioxole (for compound **97b**), NaO-*t*-But, Pd(OAc)$_2$, *t*-Bu$_3$P, toluene, 25 °C, 12 h, 84-97%; c) HCl, MeOH, 40 °C, 40 min, 99%; d)1-Boc-piperidone, AcOH, NaBH$_3$CN, EtOH, 25 °C, 12 h, 74-98%; e) CDT, DCM 12 h, 25 °C (for compounds **43a, 43c, 43e**) 20-57%; hexafluoro-2-propanol, triphosgene, DIPEA, dry DCM, 0 °C to 25 °C, 12 h (for compounds **43b** and **43d**), 20-37%.

Aniline **95a** and 4-fluroaniline **95b** reacted in the presence of 1-Boc-azetidinone under reductive amination conditions to obtain intermediate **96a-b**. The Buchkwald reaction performed on compounds **96a-b** by using bromobenzene or 5-iodo-1,3-benzodioxole furnished derivatives **97a-b** which, after Boc-deprotection, led to the free amines **98a-b**. From these latter, by applying a reductive amination protocol, in the presence of 1-Boc-piperidone, we obtained intermediates **99a-b**. Finally, after Boc-deprotection, amines **100a-b** reacted in presence of carbonyl-di-triazole or triphosgene and hexafluoro-2-propanol, furnishing ureas **43a,c** and carbamates **43b,d**. The same synthetic approach furnished amine **103** starting from compound **96a** passing thought intermediates **101**, and **102**. Reaction of derivative **103** in the presence of carbonyl-di-triazole gave compound **43e**.

In **Scheme 9** the synthesis of compounds **43f-g** is reported. The Wittig salt **105,** obtained from bromoderivative **104** and P(Ph)₃, reacted in presence of potassium bis(trimethylsilyl)amide and 1-Boc-3-azetidinone furnished the olefine **106**. A palladium-catalyzed reduction of this latter led to the saturated product **107** which, after Boc-deprotection (**108**) and reductive amination, led to compound **109**. Removal of the Boc-protecting group give intermediate **110**. From compound **106** after the elimination of Boc we obtained intermediate **111** which was then *N*-alkylated in presence of 4-iodo-*N*-Boc-piperidone, obtaining compound **112**. Finally, Boc-deprotection of **112** furnished compound **113** which reacted as for intermediated **110** under coupling conditions to give compounds **43f-g**.
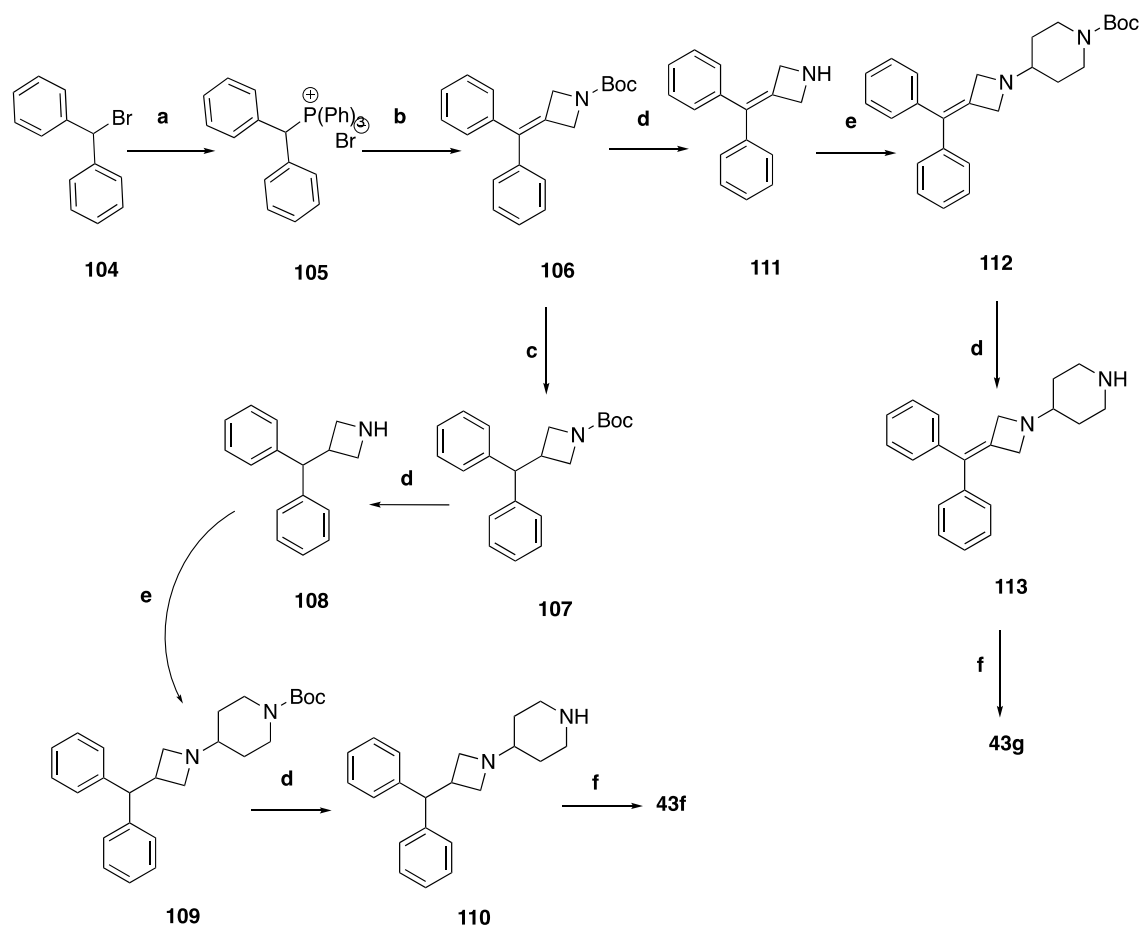
Scheme 9. Synthesis of derivatives of compounds **43f-g**.
Reagent and conditions. a) P(Ph)3, dry toluene, 110 °C, 12 h, 83%; b) 1-Boc-3-azetidinone, Potassium bis(trimethylsilyl)amide solution 0.5M in toluene, THF, 0 °C to 70 °C, 12h, 58%; c) H_2, 10% Pd on carbon, MeOH, 25 °C, 2 h, 91%; d) HCl, MeOH, 40 °C, 40 min, 89-97%; e) N-Boc-piperidone, AcOH, NaBH₃CN, DCE, 25 °C, 12 h, 44-48%-; f) CDT, DCM, 25 °C, 12 h, 63-70%.

The synthesis of compounds **43h-j** is depicted in **Scheme 10**. The reaction between the P(Ph)₃ and bromine **114** furnished Wittig-salt **115**, which reacted with the 1-Boc-3-azetidinone leading to intermediate **116**. The well-established sequence of Boc-deprotection (**117**) and reductive amination led to compound **118**. Reduction of olefine **118** to intermediated **119** and its subsequent Boc-deprotection allowed us to obtain amine **120**. At the same time, deprotection of **118** furnished the free amine **121**. Intermediate **120** and **121** reacted in presence of carbonyl-di-triazole or triphosgene and hexafluoro-2-propanol, furnishing ureas **43g-h** and carbamate **43i**.
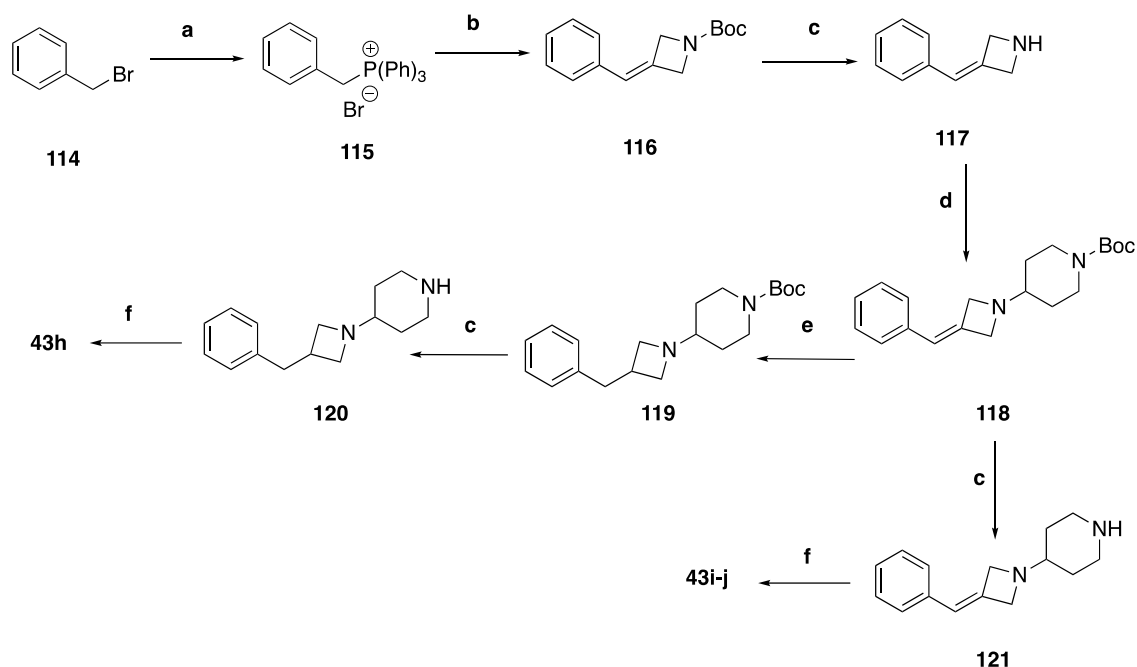
Scheme 10. Synthesis of derivatives of compounds **43h-j**.
Reagent and conditions. a) P(Ph)3, dry toluene, 110 °C, 12 h, 84%; b) 1-Boc-3-azetidinone, *n*-buthyl lithium solution 2.5M in THF, dry THF, 0 °C to 25 °C, 12 h, 96%; c) HCl, MeOH, 40 °C, 40 min, 99%; d) 1-Boc-piperidone, AcOH, NaBH$_3$CN, EtOH, 25 °C, 12 h, 78%; e) H$_2$, 10% Pd on carbon, MeOH, 25 °C, 2 h, 97%; c) HCl, MeOH, 40 °C, 40 min; f) CDT, DCM, 25 °C ,12 h, 30-47% (for compounds **43h** and **43i**); hexafluoro-2-propanol, triphosgene, DIPEA, dry DCM, 0 °C to 25 °C, 12 h, 30% (for compound **43j**).

The synthesis of derivatives **43k-l** is depicted in the **Scheme 11**. The reductive amination between intermediate **98a** and the 1-Boc-3-azetidinone led to **122**, which was then Boc-deprotected furnishing amine **123**. *N*-alkylation of **111** in presence of 3-iodine-*N*-Boc-azetidine allowed us to obtain **124**, which was deprotected leading to ammine **125**. From this latter and amine **123**, following the same procedure previously described, was possible to obtain ureas **43k-l**.
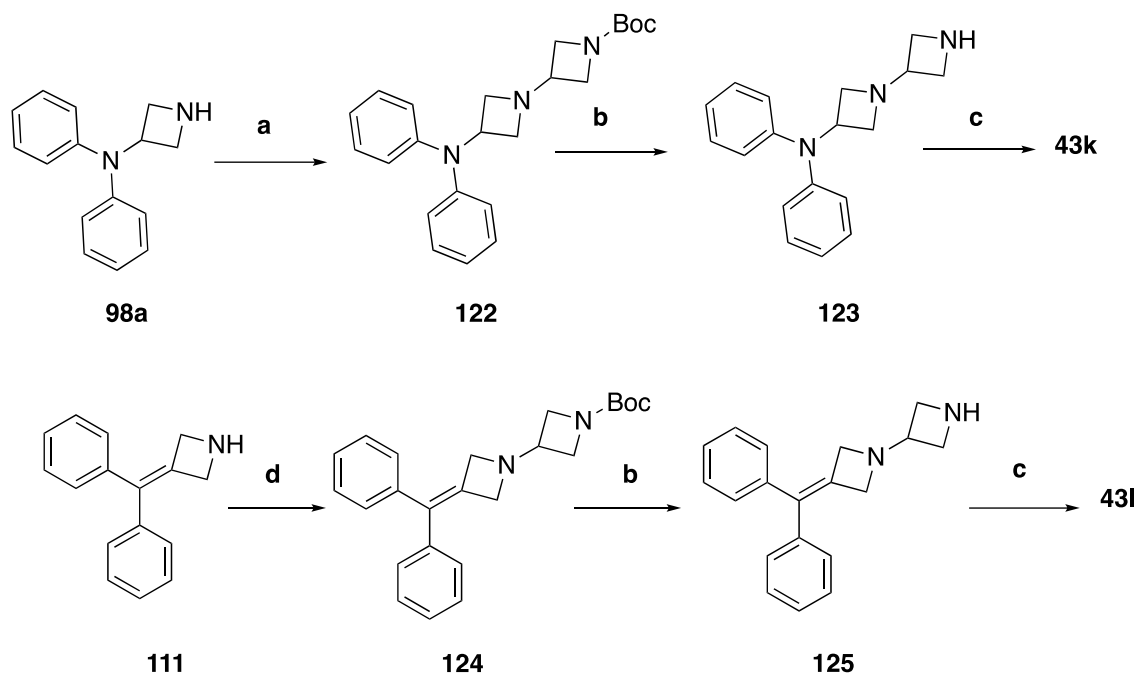
Scheme 11. Synthesis of derivatives of compounds **43k-l**.
Reagent and conditions. a) 1-Boc-3-azetidinone, AcOH, NaBH$_3$CN, EtOH, 25 °C, 12 h, 54%; b) HCl, MeOH, 40 °C, 40 min, 99%; c) CDT, DCM 12 h, 25 °C, 30-67%; d) 1-Boc-3-Iodoazetidine, K$_2$CO$_3$, dry DMF, 25 °C, 12 h, 40%.

Table 5. Inhibitory activity towards *human* MAGL and *human* FAAH (expressed as IC$_{50}$ nM) for title compounds **43a-l**
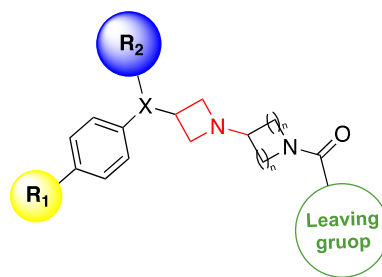
Cmps	R$_1$	R$_2$	X	n	Leaving group	IC$_{50}$ nM hFAAH	IC$_{50}$ nM hMAGL
43a	-H	-Phe	-N	2	(triazole)	163 ± 9	10.2 ± 0.7
43b	-H	-Phe	-N	2	(hexafluoroisopropyl)	3115 ± 214	39 ± 3
43c	-F	-benzo[*d*][1,3]dioxole	-N	2	(triazole)	82 ± 5	5.5 ± 0.3
43d	-F	-benzo[*d*][1,3]dioxole	-N	2	(hexafluoroisopropyl)	2362 ± 17	126 ± 9
43e	-H	-H	-N	2	(triazole)	77 ± 5	86 ± 4
43f	-H	-Phe	-CH	2	(triazole)	64 ± 4	6.7 ± 3
43g	-H	-Phe	-C	2	(triazole)	36 ± 2	1.6 ± 0.1
43h	-H	-Phe	-CH$_2$	2	(triazole)	18.3 ± 1.2	37 ± 2
43i	-H	-Phe	-CH	2	(triazole)	17.7 ± 1	10.7 ± 0.8
43j	-H	-Phe	-CH	2	(hexafluoroisopropyl)	2275 ± 116	22 ± 2
43k	-H	-Phe	-N	1	(triazole)	32 ± 2	5.25 ± 0.3
43l	-H	-Phe	-C	1	(triazole)	23 ± 2	3.3 ± 0.2

5.4. SAR discussion

The aim of our work was the identification of compounds characterized by balanced potency against FAAH and MAGL enzymes. Our SAR investigation started from the diphenylamino derivatives **43a-d**. Compounds **43a** (hFAAH IC$_{50}$ = 163 nM, hMAGL IC$_{50}$ = 10 nM) and its analogues fluorine/dioxole-substituted analogue **43c** (hFAAH IC$_{50}$ = 82 nM, hMAGL IC$_{50}$ = 5.5 nM) show an activity against MAGL 10-fold major compared to FAAH. As expected, the activity of the corresponding derivative bearing the HFIP moiety, **43b** (hFAAH IC$_{50}$ = 3115 nM, hMAGL IC$_{50}$ = 39 nM) and **43d** (hFAAH IC$_{50}$ = 2362 nM, hMAGL IC$_{50}$ = 126 nM), resulted much more unbalanced versus MAGL. By removing a phenyl group from compound **43a**, the aniline-based derivative **43e** was obtained, which show a balanced activity with IC$_{50}$ values of 77 nM and 84 nM against hFAAH and hMAGL respectively. Switching from the diphenylamino system of **43a** to the diphenylmetane group of **43f** (hFAAH IC$_{50}$ = 64 nM, hMAGL IC$_{50}$ = 6 nM) an increased inhibition potency against both the targets can be observed. Moreover, the unsaturated analogue **43g** (hFAAH IC$_{50}$ = 36 nM, hMAGL IC$_{50}$ = 1 nM) benefits from increased molecular rigidity. An analogue behaviour can be observed with the benzyl derivative **43h** (hFAAH IC$_{50}$ = 18 nM, hMAGL IC$_{50}$ = 37 nM) and its unsaturated analogues **43i**, where this latter shows IC$_{50}$ values of 17 nM and 10 nM against FAAH and MAGL respectively. Combining the vinylic scaffold of **43i** with the HFIP moiety we obtained an MAGL selective inhibitor (hFAAH IC$_{50}$ = 2275 nM, hMAGL IC$_{50}$ = 22 nM). Finally, we investigated the replacement of the piperidine system with the smaller ciclobuthylamino group in both the diphenylmethane and diphenylamine scaffold. This structural modification led to compounds **43k** (hFAAH IC$_{50}$ = 32 nM, hMAGL IC$_{50}$ = 5 nM) and **43j** (hFAAH IC$_{50}$ = 23 nM, hMAGL IC$_{50}$ = 3 nM) which also can be considered balanced dual FAAH/MAGL inhibitors.

5.5. Selectivity profile and evaluation of the drug-like proprieties

The selectivity profile against CBR_1 and CBR_2 was evaluated for the most interesting compounds **92a,b,d,f,g,i,j,l**. All the tested did not show relevant activity towards CBRs. Moreover, the solubility and the chemical stability data experimentally determined at pH = 3 and pH =7.4, are reported in **Table 6** for compounds **43g,h,I,k**. All the compounds show a god solubility profile combined with a good chemical stability at both the pH values.

Table 6. Chemical stability and solubility of compounds **85g,h,I,k.**

Cmpd	Stability% pH 3, 12 h	Stability% pH 7.4, 12 h	Solubility pH 3, 12 h (μM)	Solubility pH 7.4, 12 h (μM)
43g	85	>99	156	93
43h	88	89	219	153
43i	97	93	197	121
43k	>99	>99	247	166

the data was evaluated after 12 h.

5.6. Anti-neuroinflammatory activity of dual FAAH/MAGL inhibitors

To evaluate the anti-neuroinflammatory and neuroprotective activity of the new developed dual FAAH/MAGL inhibitors, organotypic rat hippocampal explants were exposed to 10 μg/mL LPS and recombinant 100 ng/mL IFN-γ for 96 h. Cell death was assessed with propidium iodide (PI) staining. Densitometric analysis of PI uptake revealed that when hippocampal explants were exposed to the inflammatory injury, cell death selectively occurred after 96 h in the CA1 pyramidal cell layer. The treatment of hippocampal explants with compounds **43h** (3 nM – 0.1 μM), **43i** (0.1 nM – 0.1 μM) and **43k** (3 nM – 1 μM) significantly prevented the increase in PI uptake occurring in the CA1 region 96 h after LPS+IFN-gamma exposure (**Figure 33 A-C**).
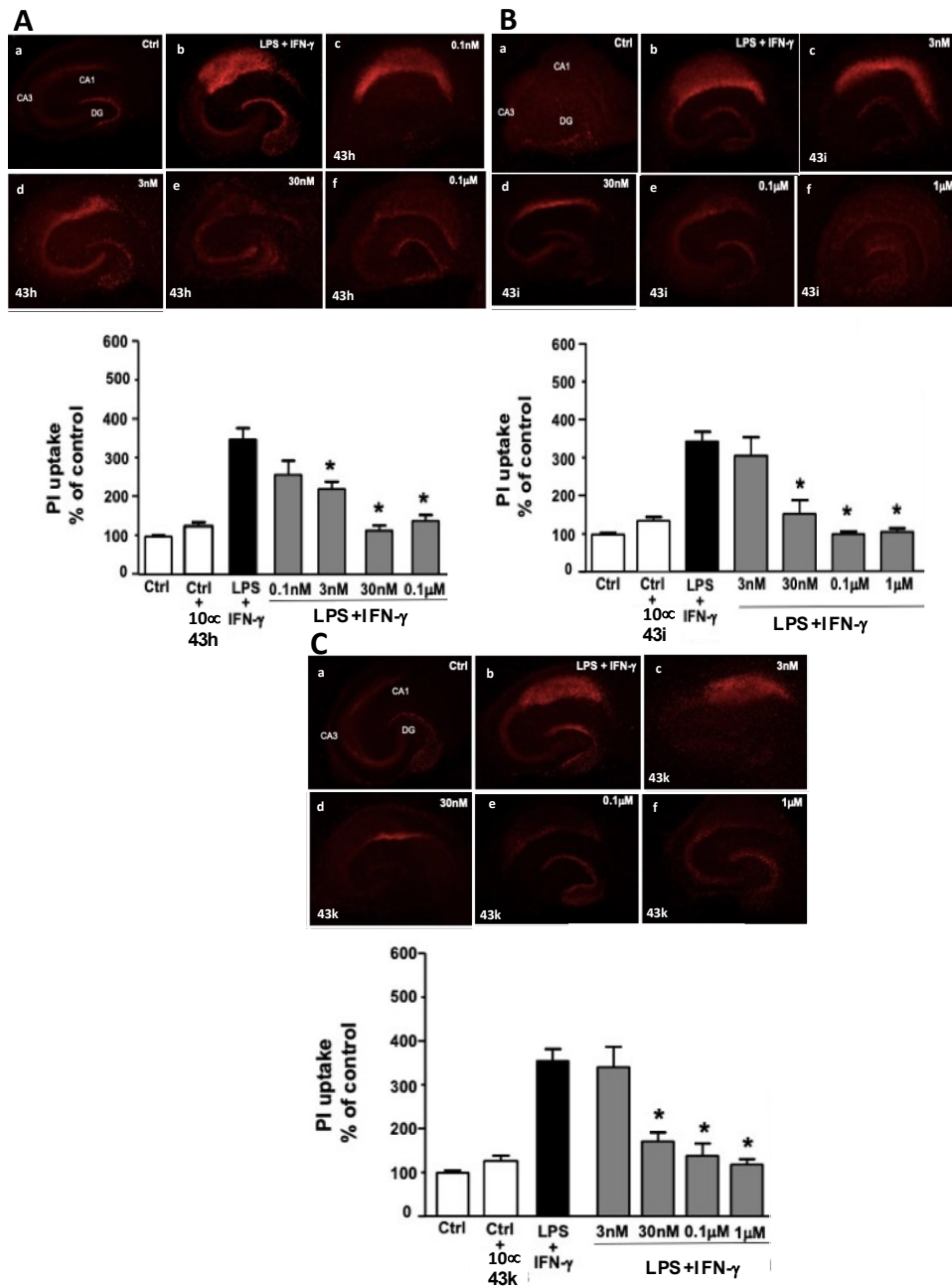
Figure 33. Effects of dual FAAH/MAGL inhibitors against LPS+IFN-γ-induced inflammatory damage in hippocampal organotypic cultures. PI fluorescence staining patterns observed in representative hippocampal organotypic slices under control conditions and following 96 h of LPS + IFN-γ-exposure in the absence of drug exposure or in the presence of 3 nM – 0.1 μM M **43h** (A, c-f); 0.1 nM – 0.1 μM **43** (B, c-f); 3 nM – 1 μM **43k** (C, c-f). Scale bars in a-d: 500 μm. A-D, e; Quantification of cell damage in the CA1 subfield evaluated by densitometric analysis of PI fluorescence and normalized to that recorded in the CA1 subregion of untreated hippocampal slices. *$p < 0.05$ versus LPS+IFN-γ.

6. Development of dual FAAH/Histone Deacetylase 6 (HDAC6) inhibitors

6.1. Background

Neurodegenerative diseases (NDs) are complex and multifactorial pathological conditions which includes a wide range of diseases such as AD, PD, HD, and ALS. NDs are due to a protein-encoding gene mutations (e.g. tau, amyloid-β, α-synuclein) and scientific evidence of the last 30 years suggests that these genetic mutations are connected to alterations in the protein homeostasis, also called "proteostasis" [125]. This latter is maintained by the activity of protein homeostasis network, which include several pathways involved in the protein synthesis, folding, trafficking, aggregation, and degradation [126]. Dysregulation in the proteostasis, together with environment stress and aging, strongly contribute with the NDs amplification [126,127]. It has been recently demonstrated that dysregulation in the histone deacetylase (HDAC) enzymes activity is involved in several NDs[128] [129]. The superfamily of HDACs play an important physiological role in the regulation of gene expression. In the eukaryotic cells, DNA is curled up in a compact structure, stabilized by histones and other protein, called chromatin. Histones are basic and positively charged proteins, due to the presence of amino acids (lysine and arginine) which are involved in electrostatic interactions with the phosphate groups of the DNA [130]. The histones *N*-terminal tail is protruding outside the nucleosome. Chromatin structure depends on histones tails enzymatic modifications which can include methylation and acetylation processes. Histone acetyltransferases (HATs) acetylates the lysine residues on the *N*-terminal of the histones which will lose their basic nature and will bind the DNA less firmly [131]. This process allows the deconstruction of chromatin and promote the gene transcription. The opposite process of

deacetylation of lysine residues is operated by HDAC enzymes which favor the chromatin compaction, preventing gene transcription [132]. These histonic modifications represent one of the epigenetic mechanisms used by cells to modulate the transcriptional processes. Currently, 18 HDAC isoforms have been recognized in mammalian cells and on the base of the sequence homology in the catalytic site they can be classified into 4 groups: class I includes HDAC 1, 2, 3, 8; class II: HDAC 4, 5, 6, 7, 9, 10; class III: Sirtuine 1-7; class IV: HDAC 11. Class I, II, IV are Zn^{+2} dependent enzymes while the sirtuine family belongs to the class III which are nicotinamide adenine dinucleoside (NAD^+) dependent enzymes. [130][133]. HDAC6 represent one of the most studied enzymatic isoforms. This enzyme is involved in several biological pathways including, protein degradation, cell proliferation and regulation of the cytoskeleton. HDAC6 interacts with several cytoplasmatic proteins (as reported in **Table 7**) and for this reason it cannot be considered as an epigenetic modulator. Moreover, its predominant cytoplasmatic localization makes HDAC6 a privileged pharmacological target in the family of HDAC enzymes [133].

Table 7. HDAC6 substrates and related biological functions.

Protein	Type of interaction	Biological function
α-tubulin	substrate	Regulation on microtubule stability and function
contactin	substrate	Development of nervous system
HSP90	substrate	Chaperone expression
β-catenin	substrate	Cell proliferation
peroxiredoxins	substrate	Redox regulation
ubiquitin	protein-protein	Protein degradation regulation
tau	protein-protein	Tau sequestration and degradation
EGFR	protein-protein	EGFR trafficking and degradation

Several evidences indicate that HDAC6 can be as promising target also for the treatment of ND. In fact, the alteration of HDAC6 activity is linked to impairment in the mitochondrial transport and in the degradation of proteins aggregates [134]. In AD clearance of the tau protein is increased by reduction of HDAC6 activity. Moreover, selective HDAC6 inhibition reduced the deficits in the mitochondrial transports due to amyloid-β toxicity [135]. Genetic deletion of *Hdac6* decreased the progression of ALS in mice, also determining an increased survival of mutants[136].These evidences point out the use of HDAC6 inhibitors as promising therapeutics tools for the treatment of neurodegenerative conditions.

In the structure of HDAC6 it is possible to identify two catalytic domains named DD1 and DD2 involved in the deacetylation of α-tubulin, HSP90, cortactin and β-catenin. Whilst the zing finger motif characterized by conserved cysteine and histidine residues is responsible of the catalytic process.

The relevant role of HDAC6 in several diseases including NDs and cancer opened the way at the discovery of selective HDAC6 inhibitors [133]. The structural elements required for the zinc-dependent HDAC inhibition are three: i) a bulky CAP group for the superficial recognition; ii) a zinc binding group (ZBG) which interacts with the Zn^{2+} in the enzyme binding pocket; iii) a linker moiety which connects the CAP group with the ZBG. The CAP group is responsible of isoforms selectivity while modifications in the ZBG led to a change in potency towards the HDAC enzymes [130]. Currently, four HDAC inhibitors are available on the market as anti-cancer drugs: romidepsin (**126**, **Figure 34**), vorinostat (**127**, **Figure 34**), belinostat (**128**, **Figure 34**) and panobinostat (**129**, **Figure 34**). Compounds **127**, **128** and **129** are hydroxamic acid derivative. This moiety is responsible of Zn^{+2} chelation [130] [137].

Romidepsin, 126

Vorinostat, 127

Belinostat, 128
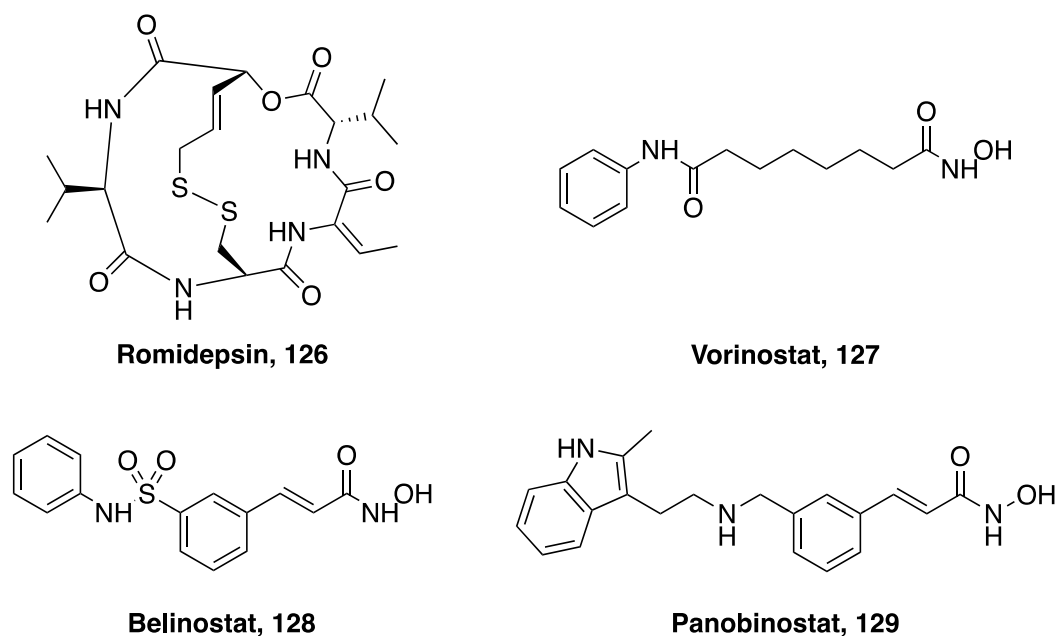
Panobinostat, 129

Figure 34. Chemical structure of HDACs inhibitors romidepsin (**126**), vorinostat (**127**), belinostat (**128**) and panobinostat (**129**).

All these compounds are not isoform selective HDAC inhibitors. This lack of selectivity is often associated with several unwanted effects such as nausea, vomiting, and thrombocytopenia [138]. Consequently, research efforts are focused on the development of isoform-selective HDAC inhibitors.

Since many years, our research group is involved in the development of potent and selective HDAC6 inhibitors as potential pharmacological tools for the treatment of idiopathic pulmonary fibrosis (IPF) and leukemias [121,139–141]. Different structural classes of HDAC6 inhibitors were identified, including phenylpyrrole, spiroindoline and indoline derivatives respectively typified by compounds **130** [139], **131** [140] and **132** [121] in **Figure 35**. These compounds show a nanomolar activity against the target combined with a good selectivity profile versus the other HDAC isoforms.

Phenylpyrrole-based HDAC6 inhibitor   **Quinolone-based HDAC6 inhibitor**   **Indoline-based HDAC6 inhibitor**

130, IC$_{50}$ HDAC6 = 36 nM   131, IC$_{50}$ HDAC6 = 6.9 nM   132, IC$_{50}$ HDAC6 = 48.5 nM
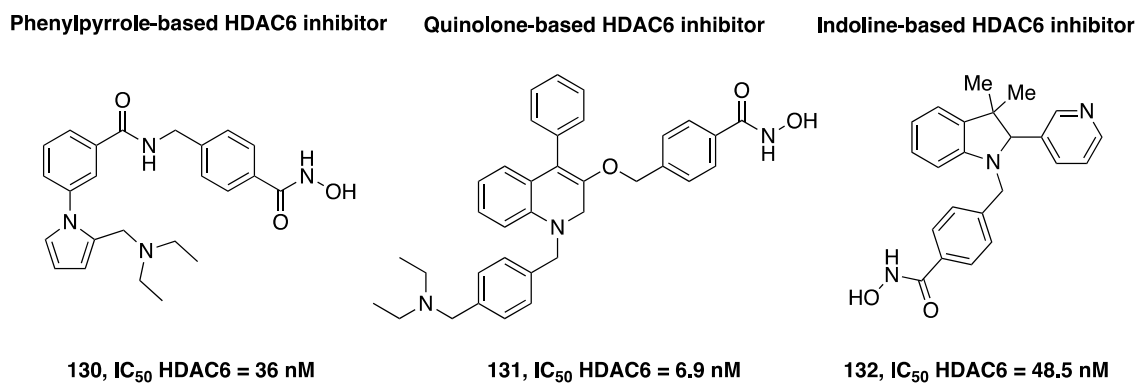
Figure 35. Chemical structure of phenylpyrrole **130**, spiroindoline **131** and indoline **132** selective HDAC6 inhibitors.

6.2. Synthesis and preliminary evaluation data of potential dual FAAH/HDAC6 inhibitors

Considering the beneficial effects deriving from the ECS stimulation in the NDs and the emergent role of HDAC6 inhibitors in the same pathological context, we decided to explore an innovative poly-pharmacological approach, designing and synthetizing a small library of dual FAAH/HDAC6 inhibitors. To this end, after analising of the chemical structure of the carbamate-based FAAH inhibitors and HDAC6 inhibitors previously synthetized in our research group, we merged the key pharmacophoric elements needed for a simultaneous enzymatic inhibition. As above mentioned, HDAC6 inhibition requires three elements: a CAP group, a ZBG and a linker moiety. HDAC6 inhibitors synthetized in our group show an hydroxamic acid as ZBG. From our analysis we observed that the chemical structure of the FAAH inhibitors **23** [97], **133** (**Figure 25**) [111] and **41n** [113] (**Table 1**) could be the starting points for our pharmacophoric merging. We selected these compounds for their common structural features such as the lateral chains and the phenylpyrrole scaffold, which can mime a linker moiety or a cap group of an HDAC6 inhibitor. Hence, to engage the HDC6 we decided to embed a zinc-banding hydroxamic acid group in the scaffold of our carbamate based FAAH inhibitor **23**, **41n** and **133** (see **Figure 36**). The ZBG was inserted in the phenylpyrrole scaffold or anchored to the phenyl

ring or at the end of the lateral chain of the selected FAAH inhibitors, to evaluate which one of the two positions resulted better tolerated by HDAC6 enzyme.
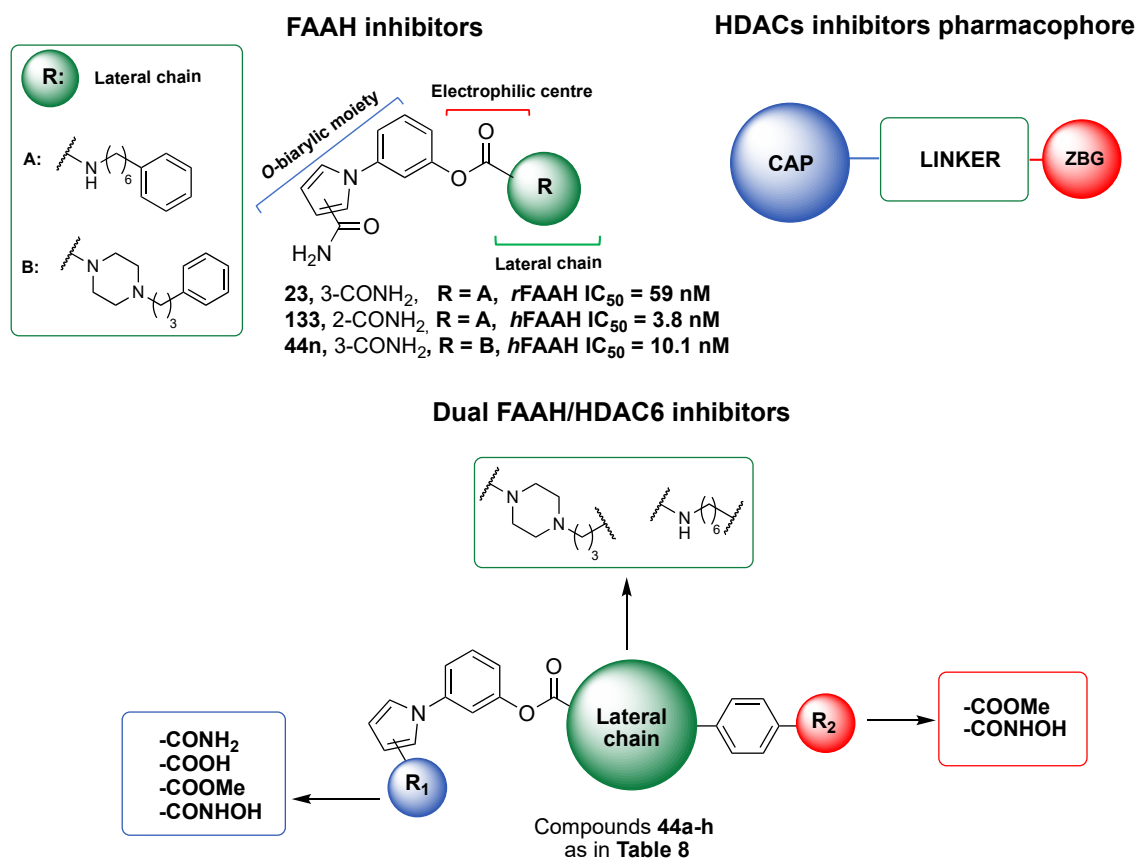
Figure 36. Structure of FAAH inhibitors **23**, **133** and **41n**, representation of HDACs pharmacophore and general structure of dual FAAH/HDAC6 inhibitors (compounds **44a-h**).

6.3. Chemistry of the dual FAAH/HAD6 inhibitors

For the synthesis of the carbamate based FAAH/HDAC6 we took advantage from the same convergent approach previously described for the FAAH inhibitors (**41a-t**). According with our retrosynthetic analysis (**Figure 37**), the reported *O*-biaryl synthon **49c** and the new derivatives **134a-d** were suitably combined with amine **135a-b** and the described intermediates **50d,f** to obtain the carbamate derivatives. Where needed, a last step of debenzylation led to compounds **44a-h**
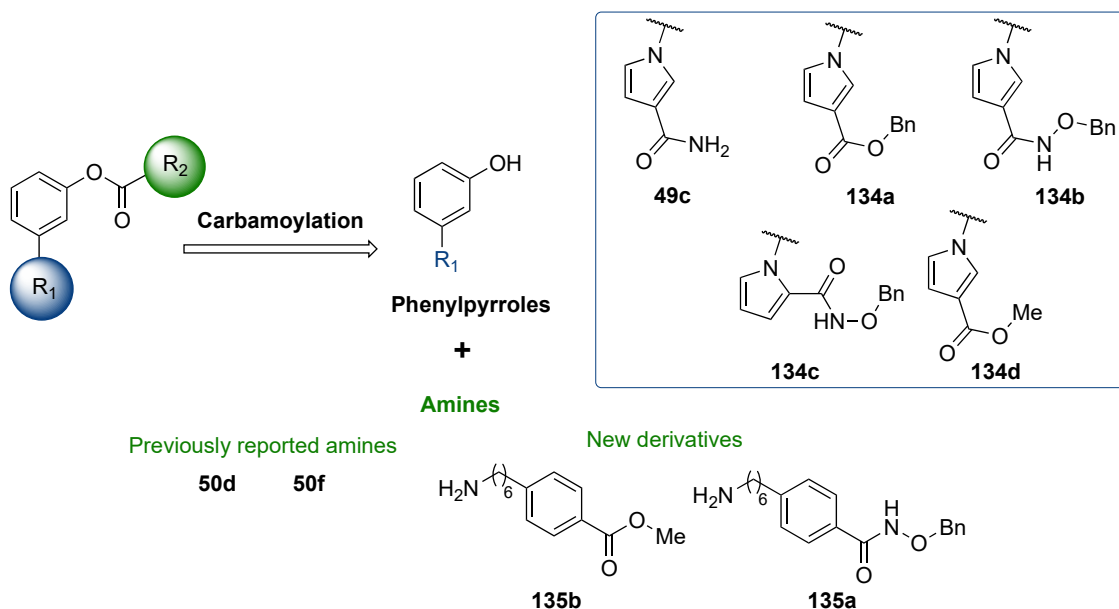
Figure 37. Retrosynthetic analysis of the new dual FAAH/HDAC6 inhibitors

In **Scheme 12** the synthesis of phenylpyrroles **134a-d** is reported. Intermediate **134a** was obtained from the oxidation of the 1*H*-pyrrole-3-carbaldehyde **54** in the corresponding carboxylic acid **136**, which was then protected as benzyl ester. To obtain synthons **134b,c** aldehyde **53** was protected at the level of phenolic group as MOM-ether **137**. Further, the Pinnick oxidation protocol was applied to **137** for obtaining intermediate **138**. This latter together with the previously reported carboxylic acid **56** were simultaneously converted in the corresponding protected hydroxamic acids **139a-b** by using BOP-Cl and *O*-benzyl hydroxylamine hydrochloride. Final MOM deprotection furnished phenols **134b-c**. Methylation of the carboxylic acid **56** in the presence of iodomethane led to ester **140**, which, after treatment with 1N HCl, allowed us to obtain intermediate **134d**.
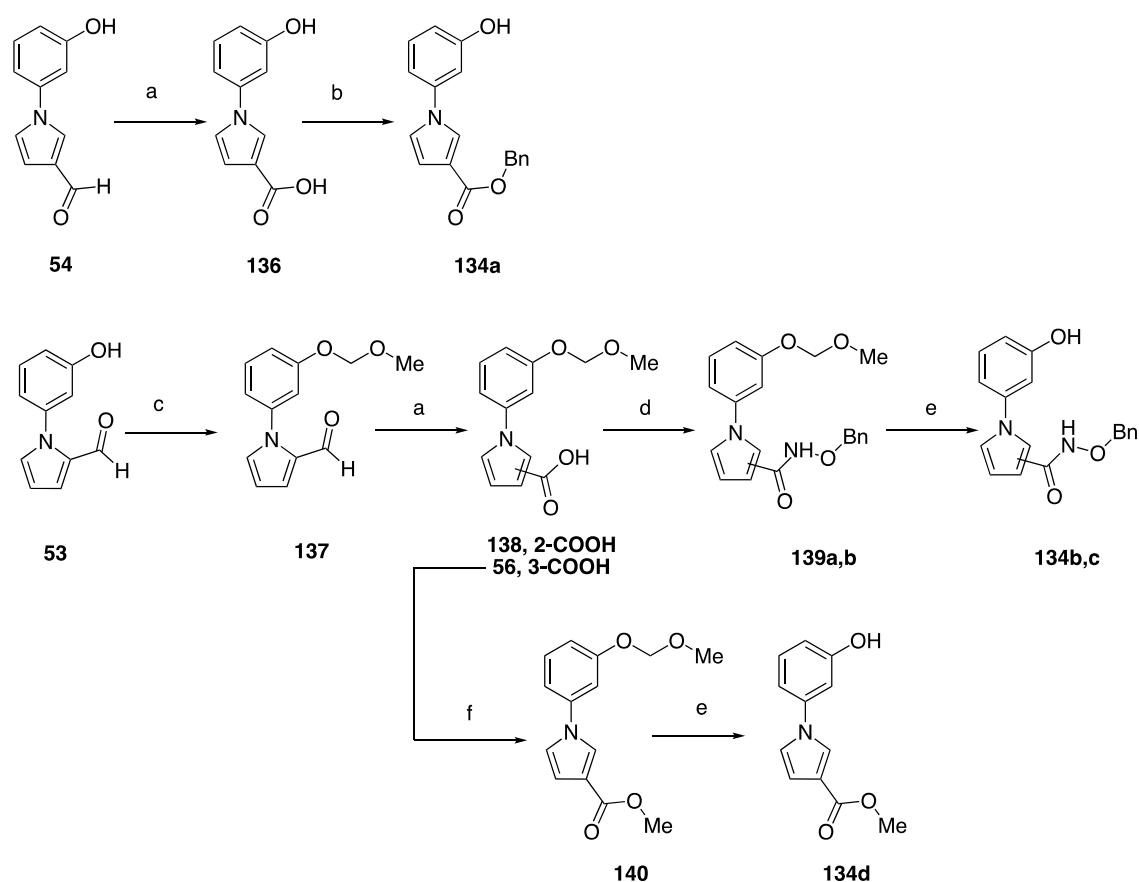
Scheme 12. Synthesis of phenolic derivatives **134a-d**.
Reagent and conditions. a) NaClO$_2$ saturated solution, NaH$_2$PO$_4$ saturated solution, 2-methyl-2-butene, t-BuOH, 25 °C, 16 h, 99%; b) BnBr, NaHCO$_3$, dry DMF, 40 °C, 16 h, 36%; c) MOM-Cl, DIPEA, dry DCM, 0 °C, 1 h, 91-96%; d) O-benzylhydroxylamine hydrochloride, BOP-Cl, TEA, dry THF, 25 °C, 16 h, 55-78%; e) 1N HCl/MeOH, MeOH, 25 °C, 16 h; f) MeI, K$_2$CO$_3$, dry DMF, 25 °C, 16 h, 44-54%.

In **Scheme 13** the synthesis of amines **135a-b** is depicted. 4-(Bromomethyl)benzoate **141** was refluxed in toluene and P(Ph)$_3$ to obtain the Wittig salt **142**. The commercially available 5-aminopentan-1-ol **143** was protected as phthalimido derivative **144** and subsequently oxidized in the corresponding aldehyde **145** in a TEMPO-catalyzed reaction. This latter reacted with the Wittig salt **142** in presence of KHMDS to afford olefine **146**. Palladium-catalyzed hydrogenation furnished intermediate **147**, which was then hydrolyzed in the carboxylic acid **148**. Treatment of this latter with thionyl chloride and subsequent reaction with O-benzylhydroxylamine hydrochloride generated the key protected hydroxamic acid **149**. Final phthalimide deprotection, by means hydrazine monohydrate, on compounds **147** and **149** furnished amines **135a-b**.
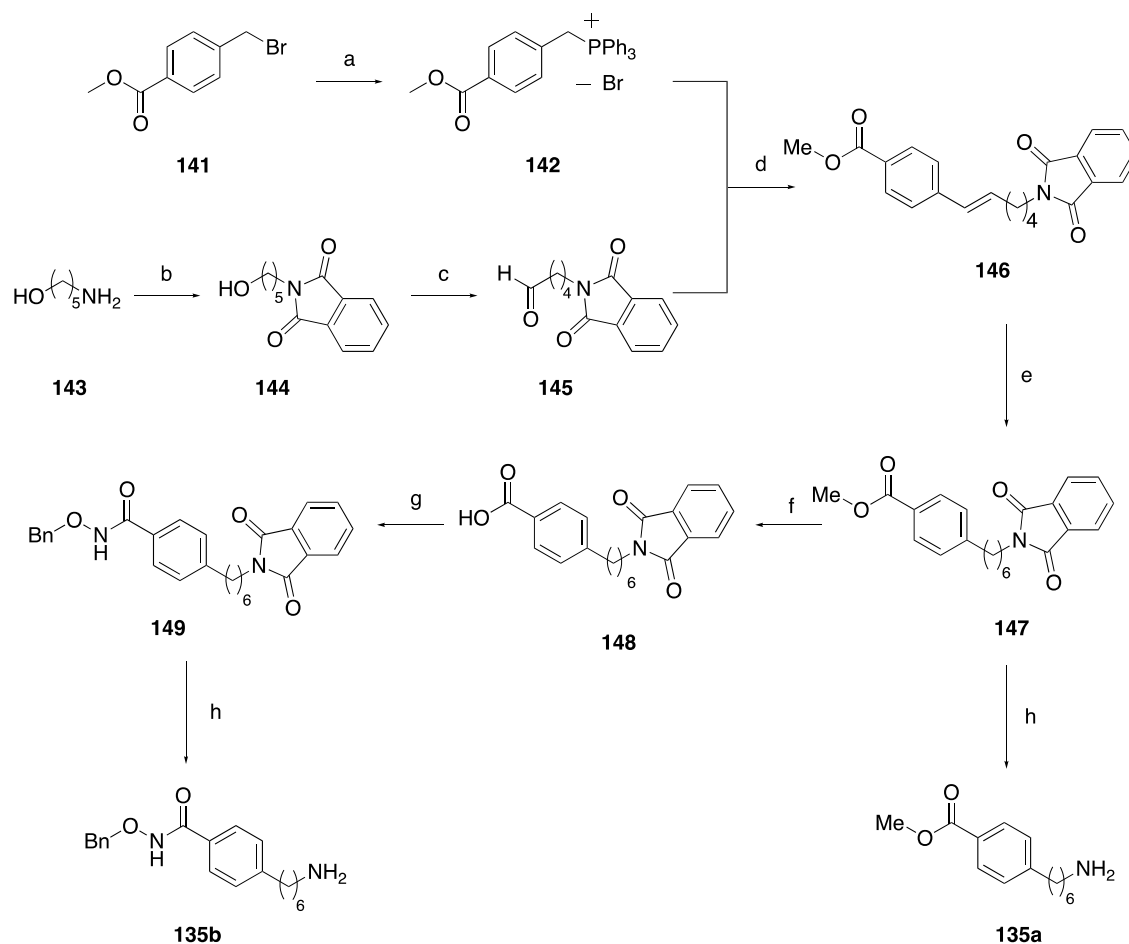
Scheme 13. Synthesis of amines **135a-b**.
Reagents and conditions, a) PPh₃, dry toluene, 110 °C, 16 h, 99%; b) phthalic anhydride, dry toluene, 110 °C, 24 h 80%; c) TEMPO, TCICA, dry DCM, 0 °C, 15 min, 99%; d) KHMDS, dry THF, 0 °C to 25 °C, 16 h, 80%; e) H₂ Pd/C, EtOAc/MeOH, 25 °C, 1 h, 90; f) NaOH solution, dry THF, 25 °C, 16 h, 99%; g) SOCl₂, dry THF, 70 °C, 2 h, *O*-benzylhydroxylamine hydrochloride, DIPEA, dry DCM, 25 °C, 16 h, 29%; h) hydrazine monohydrate, EtOH, 78 °C, 1h 72-99%.

The final steps for the synthesis of compounds **44a-h** are reported in **Scheme 14**. Phenols **49c** and **134a-d** were combined with the corresponding amines (**50d**, **50f**, **135a-b**) in presence of *p*-nitrophenyl chloroformate to obtain carbamates derivatives. Briefly, the phenol **134a** was combined with amines **50d** and **50f** to obtain carbamates **150** and **151**. From these latter benzyl deprotection provided the target compounds **44a-b**. Phenols **134b** reacted with amine **50d,f** to form derivatives **152** and **153**. Phenols **134c** was combined with amine **50f** furnishing compound **154**. Final palladium-catalyzed hydrogenation on compound **152**, **153** and **154** lead to the corresponding hydroxamic acid

derivatives **44c,d,f**. From the combination of phenol **134d** with amine **50d** and phenol **49c** with amine **135a**, compounds **44e,h** were obtained. Finally, phenol **49c** was combined with amine **135b** obtaining intermediate **155**, which was deprotected furnishing compound **44g**.
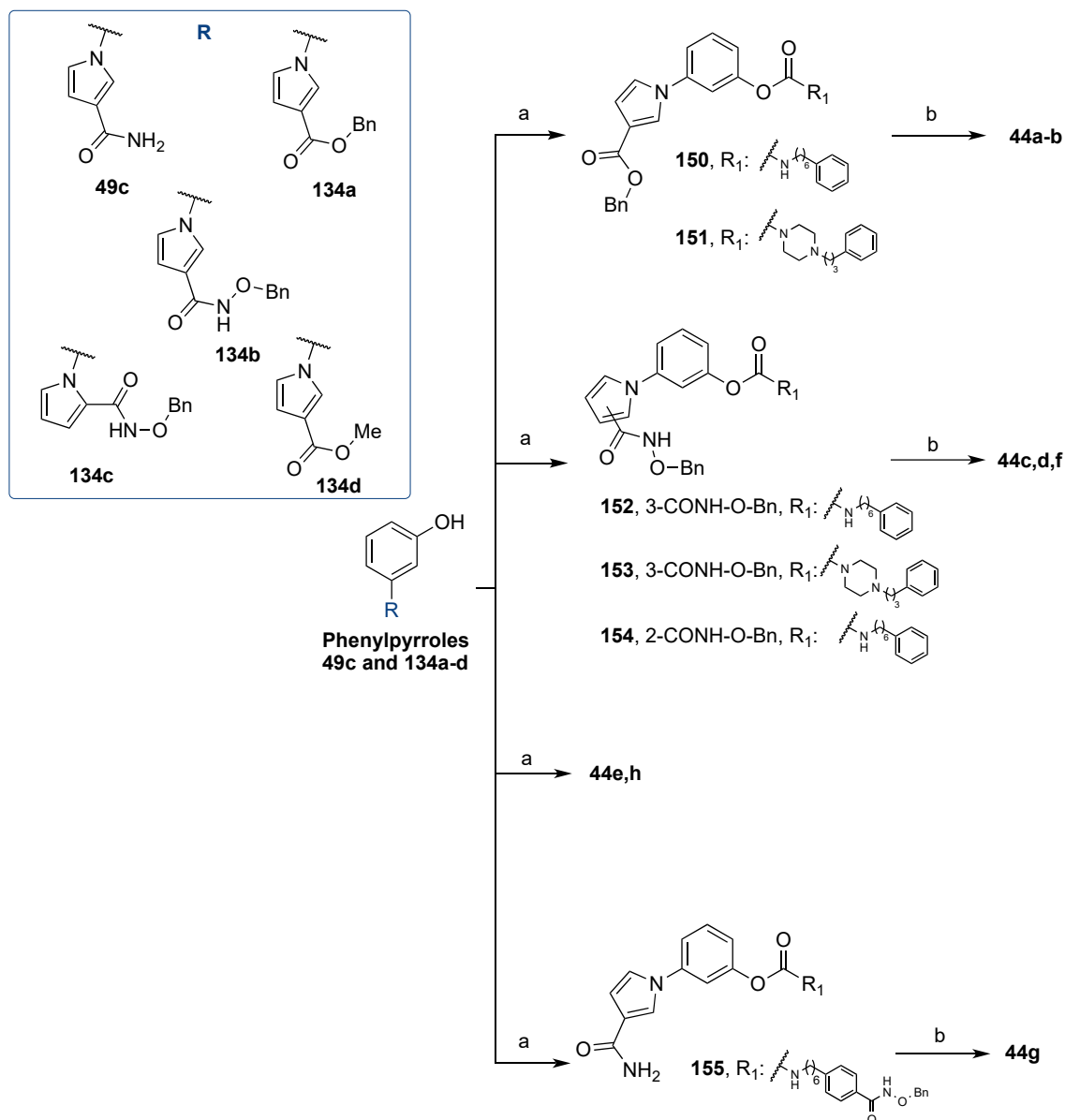
Scheme 14. Synthesis target compounds **44a-h**.
Reagents and conditions: a) 4-nitrophenyl chloroformate, TEA, dry DCM, 0 °C to 25 °C, 4 h, and suitable amine,24-80%; b) H_2, Pd on carbon, MeOH/EtOAc, 25 °C, 2 h, 12-69%.

Table 8. Inhibitory activity towards *human* FAAH and *human* HDAC6 (expressed as IC_{50} nM) for title compounds **44a-h**.
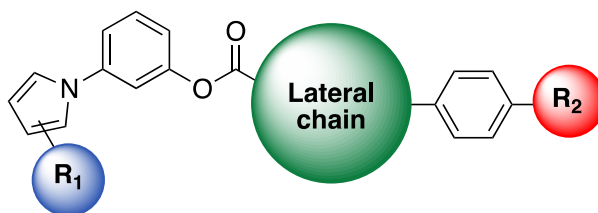
Cmps	R_1	Lateral chain	R_2	IC_{50} nM *h*FAAH	IC_{50} nM *h*HDAC6
44a	-3-COOH		-H	28 ± 2	>1000(8%)
44b	-3-COOH		-H	1817 ± 154	>1000(3%)
44c	-3-CONHOH		-H	15.9 ± 1.2	3999 ± 312
44d	-3-CONHOH		-H	36 ± 3	1387 ± 108
44e	$-3-CO_2Me$		-H	6.75 ± 0.47	>1000(1%)
44f	-2-CONHOH		-H	66 ± 5	>1000(6%)
44g	$-3-CONH_2$		-CONHOH	**297 ±17**	**370 ±23**
44h	$-3-CONH_2$		$-CO_2Me$	31 ± 2	>1000(1%)

Each value is the mean of at least three experiments

6.4. SAR analysis of dual FAAH/HDAC6 inhibitors

With the aim to explore which structural decoration on our phenylpyrrole-based FAAH inhibitors resulted efficacious also for the engagement of the HDAC6 enzyme, a small library of 8 potential dual compounds **44a-h** was synthetized. The applied structural modifications can be lists as:

i) insertion of the ZBG in the biarylic core or at the extremity of the phenylhexyl lateral chain;

ii) replacement of the hydroxamic acid with a carboxylic acid. Despite carboxylic acids lead to weak HDAC inhibition, some HDAC inhibitors showed this moiety (butyric acid, valproic acid and phenylbutyric acid), this could constitute a worthwhile modification able also to improve the water solubility of the newly developed compounds;

iii) development of methyl ester derivatives as "proof of concept" for HDAC6 inhibition. Among the carboxylic acid derivatives **44a-b**, only **44a** resulted a FAAH inhibitor of nanomolar potency (hFAAH IC$_{50}$ = 28 nM, **Table 12**) and as expected, both **44a** and **44b** resulted inactive against HDAC6. Converting the carboxylic acid moiety of **44a-b** in an hydroxamate functionality **44c-d** interesting results were obtained. Both the compounds combined a high inhibition potency of the FAAH enzyme (**44c** hFAAH IC$_{50}$ = 15 nM, **44d** hFAAH IC$_{50}$ = 36 nM) with an activity in the micromolar range against HDCA6 (**44c** hHDAC6 IC$_{50}$ = 3999 nM, **44d** hHDAC6 IC$_{50}$ = 1378 nM). These data suggest that the hydroxamate moiety can interact in the FAAH binding pocket similarly to the carboxamide group present in the parent compound (e.g. **NF1245**). However, the low activity of these compounds against HDAC6 could be due to the fact that the ZBG moiety on the pyrrole ring cannot perfectly reach the bottom of the enzyme binding pocket to chelate the Zn^{+2}. As proof of concept, we synthetized the 3-methyl ester derivatives **44e** which completely lost activity against HDAC6, resulting a highly potent FAAH inhibitors

(hFAAH IC$_{50}$ = 6 nM). Inserting the hydroxamic acid in position 2 in the pyrrole ring, as in compound **44f**, a good FAAH inhibition profile (hFAAH IC$_{50}$ = 66 nM) was maintained while HDAC6 inhibition was lost. This result is in line with the FAAH inhibition activity of the 2-carboxamide derivatives **132**. When the ZBG was placed at the end of the phenylhexyl lateral chain, the obtained derivative **44g** resulted the most interesting compound of the series and behaves as a dual FAAH/HDAC6 inhibitor (hFAAH IC$_{50}$ = 297 nM, hHDAC6 IC$_{50}$ = 370 nM). With compound **44g** a three-digit nM inhibition potency for HDAC6 was obtained at the expenses of FAAH inhibition. Finally, the replacement of the ZBG of **44g** with a methyl ester led to compound **44h** which was inactive against HDAC6. With respect to these modifications, we can speculate that the lower activity toward FAAH of the hydroxamate **44g** compared to the corresponding methyl ester **44h** (IC$_{50}$ = 31 nM) could be ascribable to the acidic nature of the hydroxamic group.

7. Design and synthesis of dual MAGL/Histaminergic 3 receptor (H3R) ligands

7.1. Background

Histamine (HA) is an endogenous amine widely distributed through the body. It works as major mediator of inflammation and allergic reactions, as a physiological regulator of gastric acid secretion, as a neurotransmitter in the CNS and may also have a role in tissue growth and repair [142]. HA biosynthesis consists of one enzymatic step in which the precursor *L*-Histidine is converted in HA by *L*-Histidine decarboxylase. In the CNS, HA catabolism is operated by Histamine *N*-methyl transferase which transfers a methyl group to form the *N*-methylimidazole. This latter will be further transformed by the combined activity monoamino oxidase B (MAO-B) and aldehyde dehydrogenase (ALDH) in the *N*-methylimidazole acetate [143]. In the peripheral tissues the HA inactivation is catalyzed by diamine oxidase (DAO) to form the imidazole acetaldehyde, which is converted in imidazole acetate by ALDH (see **Figure 38**) [144]. In the CNS, the histaminergic neuron bodies are localized in the tuberomammillary nucleus of the hypothalamus from where their afferent projections are widely distributed in the brain areas, including infralimbic cortex, lateral septum and preoptical nucleus [145]. Moreover, HA is also produced in the mast cells in the pia mater, thalamus and hypothalamus and the rate of HA synthesis, release and metabolism in mast cells is much slower than that in histaminergic neurons [146]. The neuronal histaminergic system is involved in several functions, such as the sleep–wake cycle, energy and endocrine homeostasis, sensory and motor functions, cognition, and attention. These physiological functions are explicated by the interaction of HA with four subtypes of histaminergic receptor ($H_{1-4}R$), all of which belong to the GPCRs family (see **Table 9**) [147].
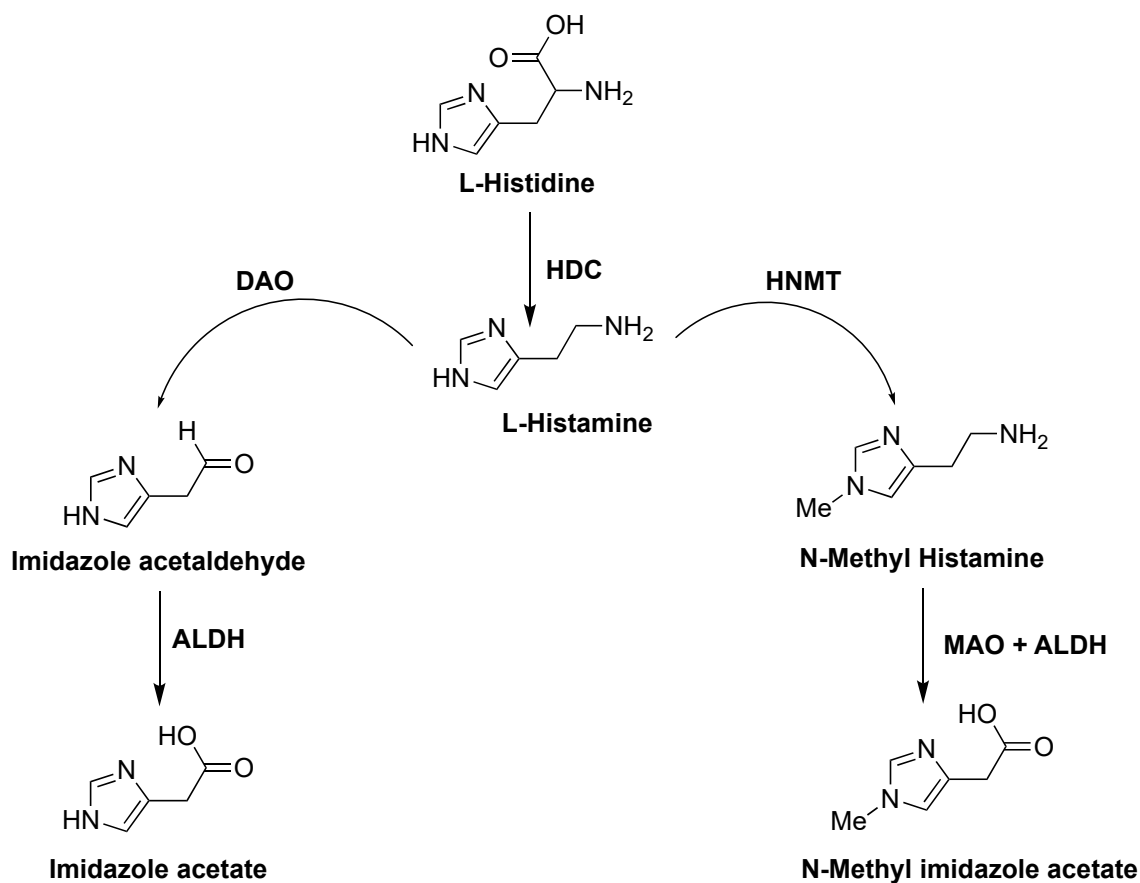
Figure 38. Schematic representation of histamine biosynthetic and catabolic pathways

Histamine H_{1-2} receptors (H_1R and H_2R) are widely distributed in the CNS especially in the ganglia, hippocampus, amygdala, and cerebral cortex. They are mainly involved in the regulation of arousal state and sleep-wakefulness. H_1R stimulation favor the release of NO and increase the activity of phospholipase A2 (PLA2), which induces arachidonic acid formation [148,149]. H_2R activation has an opposite physiological role, determining the inhibition of PLA2. It is also localized in the gastric parietal cells where regulates gastric secretion [150,151]. The HA H_4 receptor (H_4R) has recently been identified as a new member of the histaminergic system. It is expressed in the mast cells, eosinophils, and dendritic cells. The physiological role of the H_4R is not completely know but it seems to be involved in the inflammatory process [147].

Table 9 Characteristics of histamine receptor subtypes

Characteristics	H₁R	H₂R	H₃R	H₄R
Receptor proteins in humans	487 amino acids	359 amino acids	445 amino acids	390 amino acids
K_d	≈10 µmol/L	≈30 µmol/L	≈10 nmol/L	≈20-40 nmol/L
Receptor expression	Widespread, including neurons and smooth muscle (e.g., airways, vascular)	Widespread, including gastric mucosa parietal cells, smooth-muscle, heart	Highly expressed in histaminergic neurons, low expressed elsewhere	Highly expressed in bone marrow and peripheral hematopoietic cells, low expressed elsewhere
G-protein coupling	$G_{\alpha q/11}$	$G_{\alpha s}$	$G_{i/0}$	$G_{i/0}$
Principal signaling effectors	$Ca^{2+}\uparrow$, cAMP cGMP, NF-κB, PLC↑, PLA2, PLD, NOS	cAMP↑, $Ca^{2+}\uparrow$, PKC, PLC	$Ca^{2+}\uparrow$, MAP kinase↑, inhibition of cAMP↓	$Ca^{2+}\uparrow$, MAP kinase↑, inhibition of cAMP↓

Abbreviations: cAMP cyclic adenosine monophosphate, cGMP cyclic guanosine monophosphate, NF-κB nuclear factor κ-B, PLC phospholipase C, PLA2 phospholipase A2, PLD phospholipase D, MAP mitogen-activated protein, PKC protein kinase C

The HA H₃ receptor (H₃R) is expressed in the CNS at the level of cortex, hippocampus caudate nucleus, amygdala cerebellum and thalamus. The H₃R is a presynaptic auto-receptor localized on histaminergic neurons where it modulates the release of HA [147,152]. Moreover, it can be found also on non-histaminergic neurons regulating the release of other neurotransmitters such as dopamine, glutamate, GABA, and acetylcholine [147,153]. H₃R structure consists of 7-loop transmembrane coupled with a $G_{i/0}$ protein. Its crystal structure is not yet available but by means mutation studies and homologies model was possible to clarify the binding mode of HA in the enzyme binding pocket. The electrostatic interaction between the Asp114, in the transmembrane helix 3 (TM3), with the imidazole nitrogen of HA is a key point to form the agonist-protein complex, as reported in **Figure 39** [154]. However, this amino acid is highly conserved

in all the receptor subtypes, hence the affinity for the HA and the H₃R is guaranteed by an H-bond between the imidazole group of HA end the Glu206 in TM5 [154].
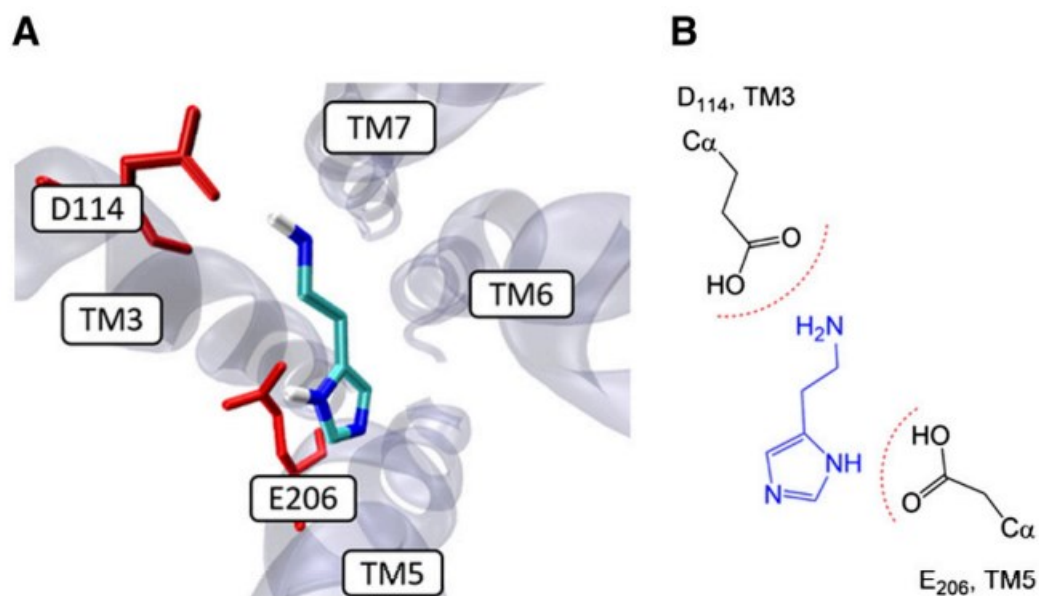
Figure 39. (A) Docking pose of HA in the H₃R active site. (B) View of the HA keys interactions in *h*H₃R active site.

The agonist activity mediated by HA on the H₃R reduces the release of several neurotransmitters in the CNS. Accordingly, H₃R antagonism can be considered an available option to indirectly enhance the HA and other neurotransmitter levels. In the last years several H₃R antagonists were developed, and these compounds can be classified into imidazole-based antagonists and non-imidazole-based antagonists. The lack of selectivity of imidazole-based derivatives always determined a greater interest about the non-imidazole-based compounds which today represent the most widely studied H₃R antagonists. In the non-imidazole derivatives, the imidazole group responsible of the engagement of the H₃R has been replaced by secondary or tertiary cyclic amines which interact with at level of the TM3 [155]. Pitolisant (**156**, **Figure 40**), can be considered the prototype of the H₃R antagonists, in which presence of the 3- piperidinopropiloxy (PiProp) moiety remarkably increased the activity against the target [156]. A basic

benzoazepine scaffold was explored by GSK leading to the high potent and selective compound **GSK-239512** (**157**, **Figure 40**). The increased molecular rigidity as in compound **ABT-288** (**158**, **Figure 40**) also resulted effective to generate antagonists/reverse agonists of the H_3R. The research group of the professor Stark, where I performed the time abroad of my PhD work, is also involved in the development of H_3R antagonists. The Stark's research group recently developed a library of piperazine-based compounds typified by compound **159** (**Figure 40**) [157]. In the context of the piperazine-based inhibitors, the high affinity of the H_3R antagonist **GSK-835726** (**160**, **Figure 40**) demonstrated that the *N*-1-acylation with an aromatic group together with the introduction of bulky substituents in *N*-4, is well tolerated by the target [158].

156, Pitolisant, Ki = 5.3 nM   **157, GSK-239512, Ki = 0.2 nM**   **158, ABT-288, Ki = 0.45 nM**

159, Ki = 0.45 nM   **160, Ki = 1.26nM**
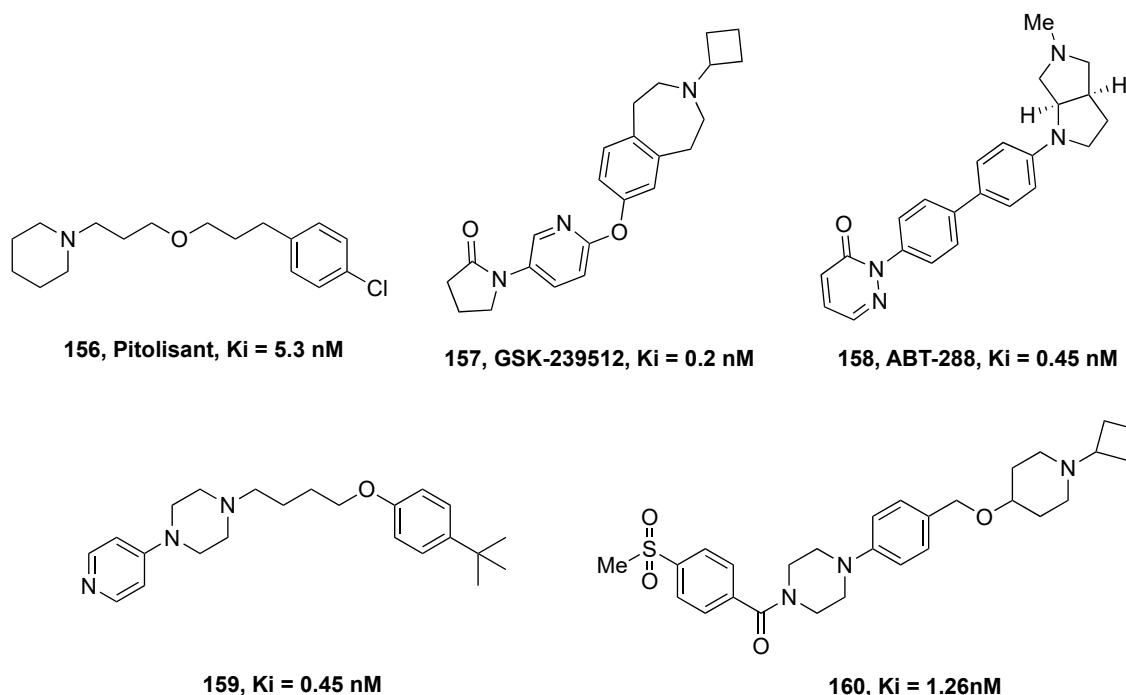
Figure 40. Chemical structure of H_3R antagonists.

The neuronal histaminergic system regulates several physiological functions such as cognition, attention, sleep–wake cycle, endocrine homeostasis which are all severely affected in neuropsychiatric disorders, such as PD, AD, HD, depression, and narcolepsy. In this context, it is widely accepted that the activity of the H_3R is crucial in the

modulation of neurodegenerative and neurological processes. In this frame, Pitolisant was firstly approved by FDA and EMA for treatment of narcolepsy [147], and furthermore completed the phase III (NCT01036139) of clinical trials for treatment of PD. Both the derivatives **157** and **158** completed the phase II of the clinical trials for AD treatment (NCT01009255 and NCT01018875).

Interestingly, dysregulated levels of HA were detected in the cerebrospinal fluid of MS patients and H_3R resulted overexpressed in demyelinated areas [159–161]

7.2. Development and biological characterization of compounds 45a-d and 46 a-d as potential MAGL/H3 dual acting compounds

During the three months period that I spent at the Heinrich Heine University (HHU) as Erasmus Plus student in Düsseldorf under the supervision of Professor Holger Stark, I continued my on the synthesis of new multitarget compounds able to simultaneously modulate the activity of the ECS and the histaminergic systems. This collaborative project started from the common high interest of our, and Professor Stark's research group in the development of new pharmacological tools for the treatment of neurodegenerative conditions. We focused our efforts on the design of new potential dual $MAGL/H_3R$ ligands since the clear enrollment of these targets in NDs. This innovative polypharmacological approach which combines the inhibition of a serine hydrolase enzyme and a GPCR antagonism, emerged from high adaptability of H_3R pharmacophore. Our first approach in this field took inspiration from a recent work by Szczepańska *et al*. which encompasses a series of piperazine-based scaffolds needed for the interaction with the H_3R [158]. Among these, one the reported general structure (reported in figure **41**) allowed us to merge all the pharmacophoric elements for the simultaneous MAGL and H_3R engagement deriving from the piperazine based H_3R

antagonists developed in the Stark's group and the well know MAGL inhibitors **32** or **34** (see **figure 41**). In these compounds, the basic piperazine *N*-4 should guarantee the interaction with the TM3 of the H₃R. An amino group close to the aromatic part was inserted to replace the phenolic ether generally showed in the H₃R. This moiety allowed us to confer at the new developed derivatives the classical Y shaped required for the inhibition of MAGL. Moreover, an appropriate alkyl spacer, composed by 3 or 4 carbons units, works as support for a bulky aromatic moiety which could be well tolerated by H₃R and could confer selectivity versus MAGL enzyme. The *N*-1-acylation with an aromatic small group, such a triazole moiety guarantees the presence of the electrophilic center essential for the interaction with the catalytic Ser241 of MAGL. A first explorative set of derivatives (called Set A, compounds **45a-d**, as in **Figure 41**) reported in **Table 10** was designed and synthetized following this approach.
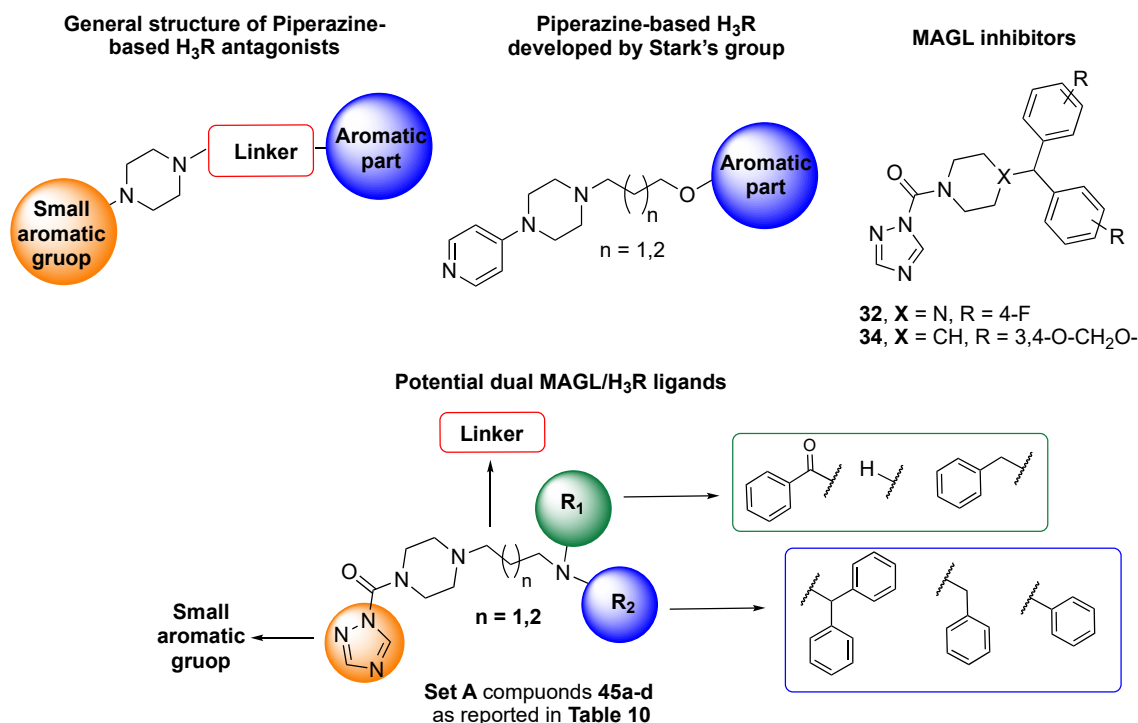
Figure 41. Design of dual MAGL/H₃R ligands belonging to the Set A (compounds **45a-d**).

At the same time, we focused our efforts on the design of another approach aimed to obtain hybrid MAGL/H₃R ligands. In this case, based on the structure of the well know

H$_3$R antagonist **156**, we explored the introduction of the PiProp moiety in piperazine and piperidine Y-shaped scaffolds, taking inspiration from high potent MAGL inhibitors **32** and **34**. In the general structure of this Set B of potential dual MAGL/H$_3$R ligands (reported in **Figure 42** and in **Table 11**) is possible to identify the key elements for the simultaneous interactions with both the selected targets. The piperdin/piperazine triazole ureidic part guarantees the engagement of the Ser122 of MAGL. This portion is connected to the terminal branched nitrogen containing moiety by a carbonyl- or propyl-based linker. As previously mentioned, the PiProp moiety is responsible of H$_3$R engagement. To this end we anchored the PiProp group in the -*para* position on the bifurcated aromatic portion. Combining these structural elements, a small library of potential dual MAGL/H$_3$R ligands was synthetized.
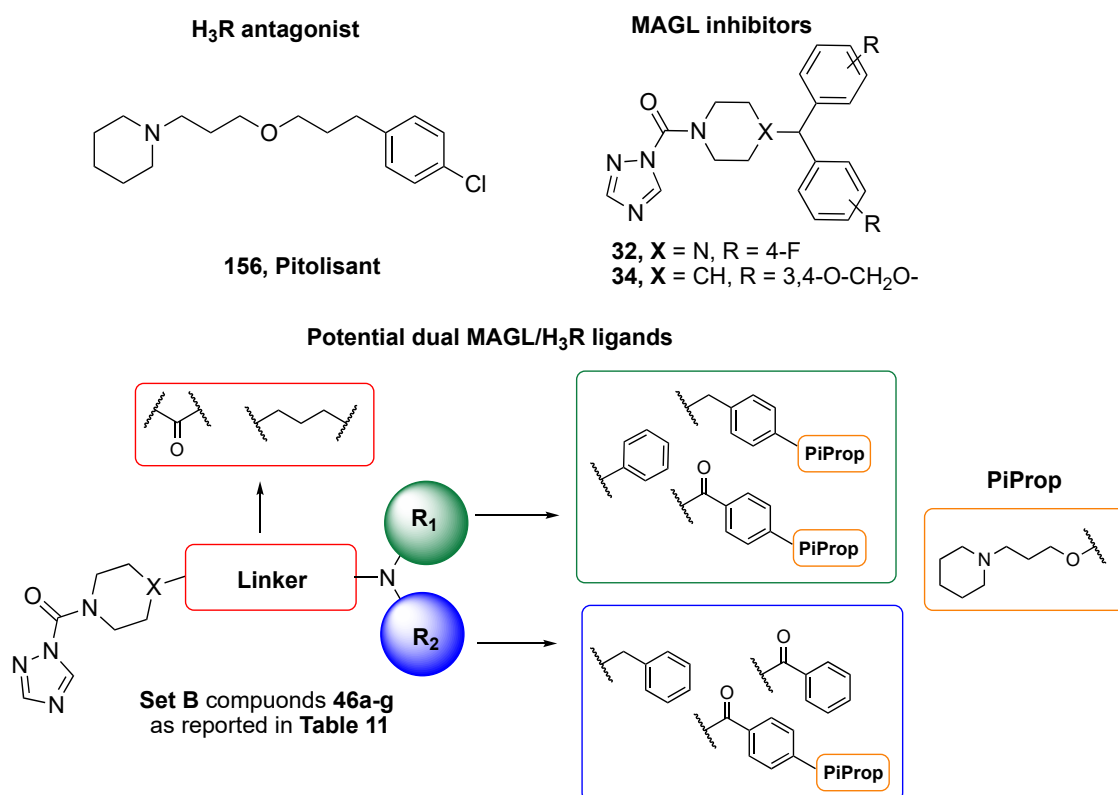
Figure 42. Design of Set B potential dual MAGL/H$_3$R ligands, **46a-g**

7.3. Synthesis of the Set-A compounds

In **Scheme 15** the synthesis of the derivatives **45a-b** is depicted. Benzophenone **160** reacted, under reductive amination conditions, in the presence of 3-aminopropan-1-ol or 4-aminobutan-1-ol and a catalytic amount of *p*-Ts-OH in toluene by using the Dean Stark apparatus. These strong conditions allowed us to obtain intermediate **1601a-b** which were converted in the corresponding Cbz-protected intermediates **162a-b**. Activation of compound **162a** as bromine derivate **163** and its use as alkylating agent of Boc-piperazine led to intermediate **165a**. Whereas compound **165b** was obtained after the conversion of the intermediate **162b** in the corresponding mesylate **164** needed for the Boc-piperazine alkylation. Selective Boc-deprotection of **165a-b**, furnished the free amines **166a-b**. These latter reacted with carbonylditriazole to form the ureas **167a-b**. The final palladium catalyzed hydrogenation allowed us to obtain compounds **45a-b**.
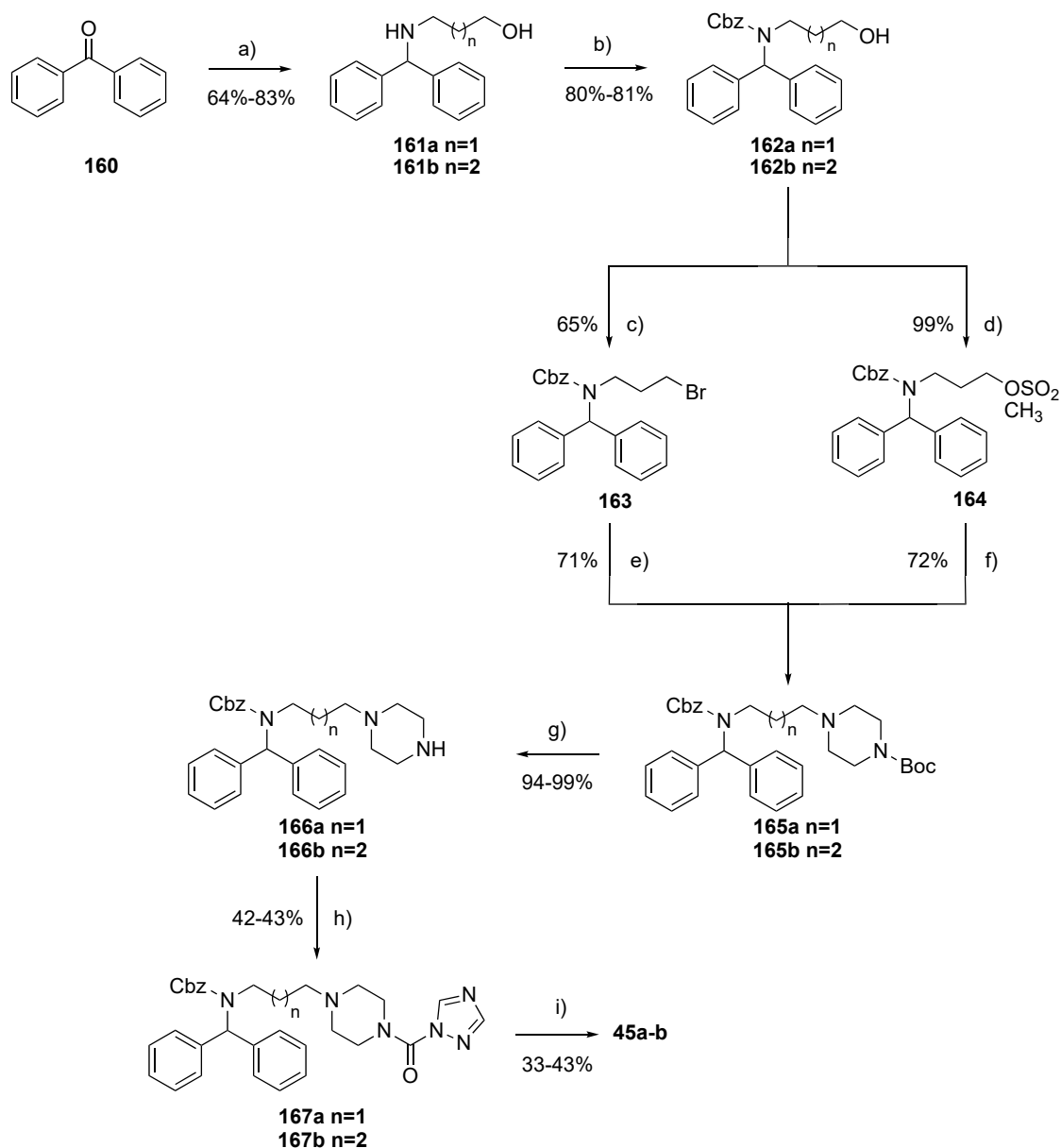
Scheme 15. Synthesis target compounds **45a-b**.
Reagents and conditions. a) 3-aminopropan-1-ol or 4-aminobutan-1-ol, p- TsOH, dry toluene, 150 °C, 48 h, NaBH4, MeOH, 0 °C to 25 °C, 30 min, 64-83%; b) Cbz-Cl, NaHCO3 solution, THF, 0 °C to 25 °C, 12 h, 80%; c) CBr4, PPh3, 1-H-imidazole, dry DCM, 25 °C, 12 h, 65%; d) MsCl, TEA, dry DCM, 0 °C to 25 °C, 30 min, 99%; e) 1-Boc piperazine, TEA, dry THF, 75 °C, 12 h, 71%; f) 1-Boc piperazine, K_2CO_3, dry MeCN, 85 °C, 12 h, 72%; g) 1N HCl/MeOH, MeOH, 40 °C, 1 h, 94-99%; h) CDT, dry DCM, 25 °C, 12 h,42-43% i) H2 Pd/C, EtOAC/MeOH, 25 °C, 1 h, 33-43%.

7.4. Synthesis of target compounds 45c-d

The synthesis of derivatives **45c-d** is reported in the **Scheme 16**. Alkylation of N-Boc-piperazine **168** with 3-bromopropan-1-ol generated intermediate **169**. Activation of

alcohol **169** led to the mesylate **170** which reacted with an excess of dibenzylamine to obtain the alkylated product **171**. Final Boc-deprotection furnished amine **172**. At the same time, alcohol **169** was converted in the corresponding bromine **173**. This latter reacted in presence of aniline, leading to the secondary amine **174**. The reaction of this latter with the benzoyl chloride gave the intermediate **175** which was then Boc-deprotected to obtain the amine **176**. Intermediates **172** and **176** reacted with carbonylditriazole to obtain compounds **45c-d**.
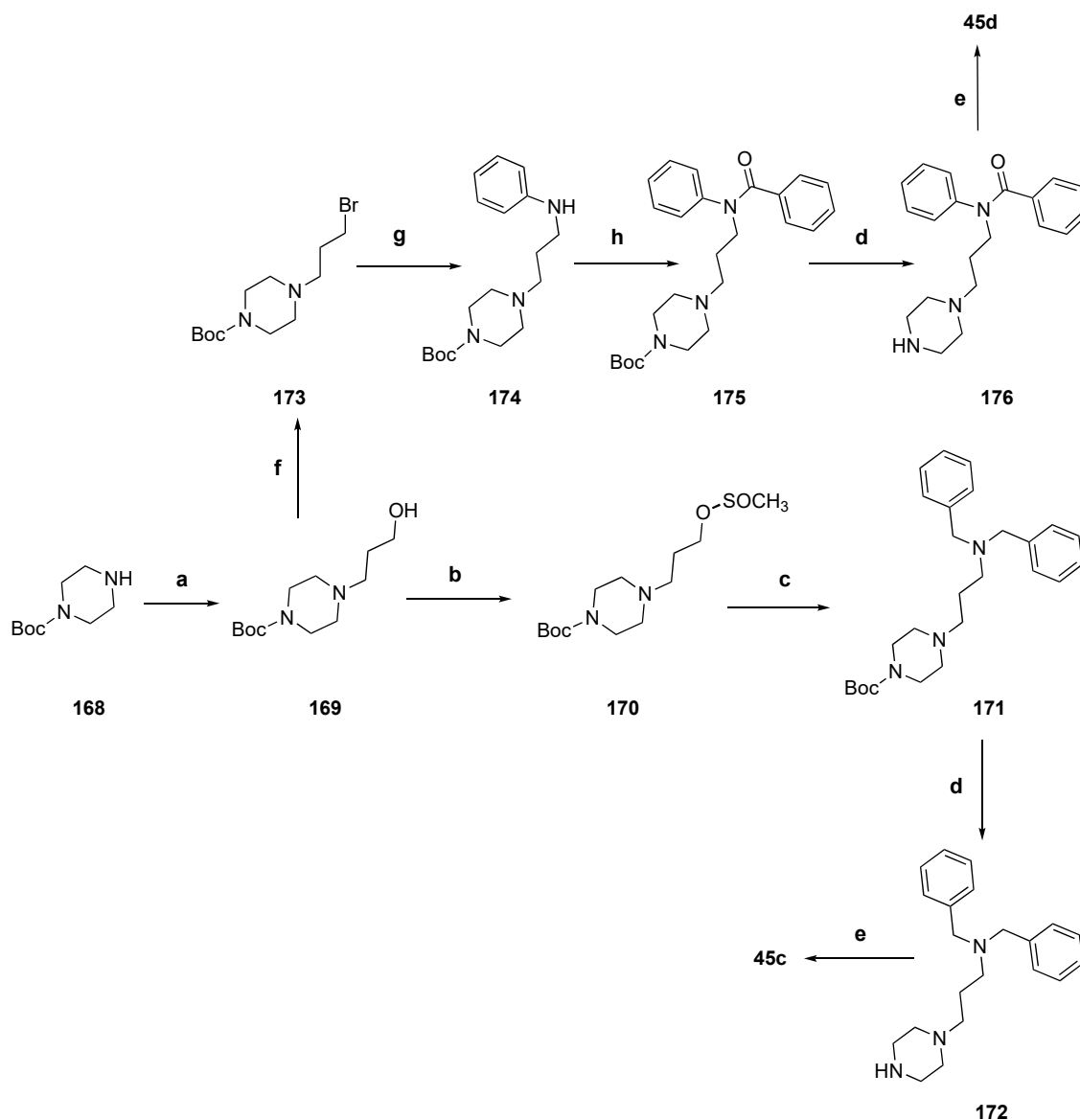
Scheme 16. Synthesis target compounds **45c-d**.
Reagents and conditions. a) 3-bromopropan-1-ol, TEA, dry THF, 75 °C, 12 h, 94%; b) MsCl, TEA, dry DCM, 0 °C to 25 °C, 30 min, 99%; c) Dibenzylamine, K$_2$CO$_3$, dry MeCN, 85 °C, 12 h, 57%; d) 1 N HCl/MeOH, MeOH, 40 °C, 1 h, 79-95%; e) CDT, dry

DCM, 25 °C, 12 h, 20-53%; f) CBr$_4$, PPh$_3$, 1-H-imidazole, dry DCM, 25 °C, 12 h, 21-47 %; g) Aniline, K$_2$CO$_3$, dry DMF, 0 °C to 60 °C, 12 h, 70%; h) Benzoyl chloride, TEA, dry dioxane, 0 °C to 75 °C, 12 h, 56 %.

7.5. Synthesis of Set B compounds

Compound **46a-b** (see **Table 11**) represent the first derivatives belonging to the Set B, which were synthetized in the Professor's Stark laboratories in the first part of this collaborative project. During my period of 3 moths at the HHU I continued with the synthesis of the Set B compounds, focusing my efforts on the obtainment of the derivatives **46c-d** (see **Table 11**).

For the obtainment of the Set B compounds my synthetic approach initially consisted in the synthesis of PiProp containing moieties, which were subsequently attached to the piperazine/piperdine scaffolds.

The synthesis of the PiProp containing moieties in depicted in the **Scheme 17**. Starting from the commercially available piperidine **177** and the 3-chlroniepropan-1-ol intermediate **178** was obtained by using a Finkelstein alkylation protocol. Alcohol **178** was then converted in the salt **179** in presence of an excess of thionyl chloride. This latter represents the key intermediate for the synthesis of all the PiProp containing derivatives. Alkylation of the 4-hydroxybenzaldhayde with compound **179** furnished intermediate **180**. At the same time Boc-protection of the 4-hydroxy benzylamine **181** gave phenol **182** which was then *O*-alkylated in presence of intermediate **179**, obtaining compound **183**. Final Boc-deprotection furnished amine **184**. By using a similar approach carboxylic acid **188** was obtained. 4-hydroxybenzoic acid **185** was converted in the corresponding benzyl ester **186**, which after reaction with salt **179** furnished the phenolic ether **187**. Final palladium catalyzed hydrogenation led to intermediate **188**.
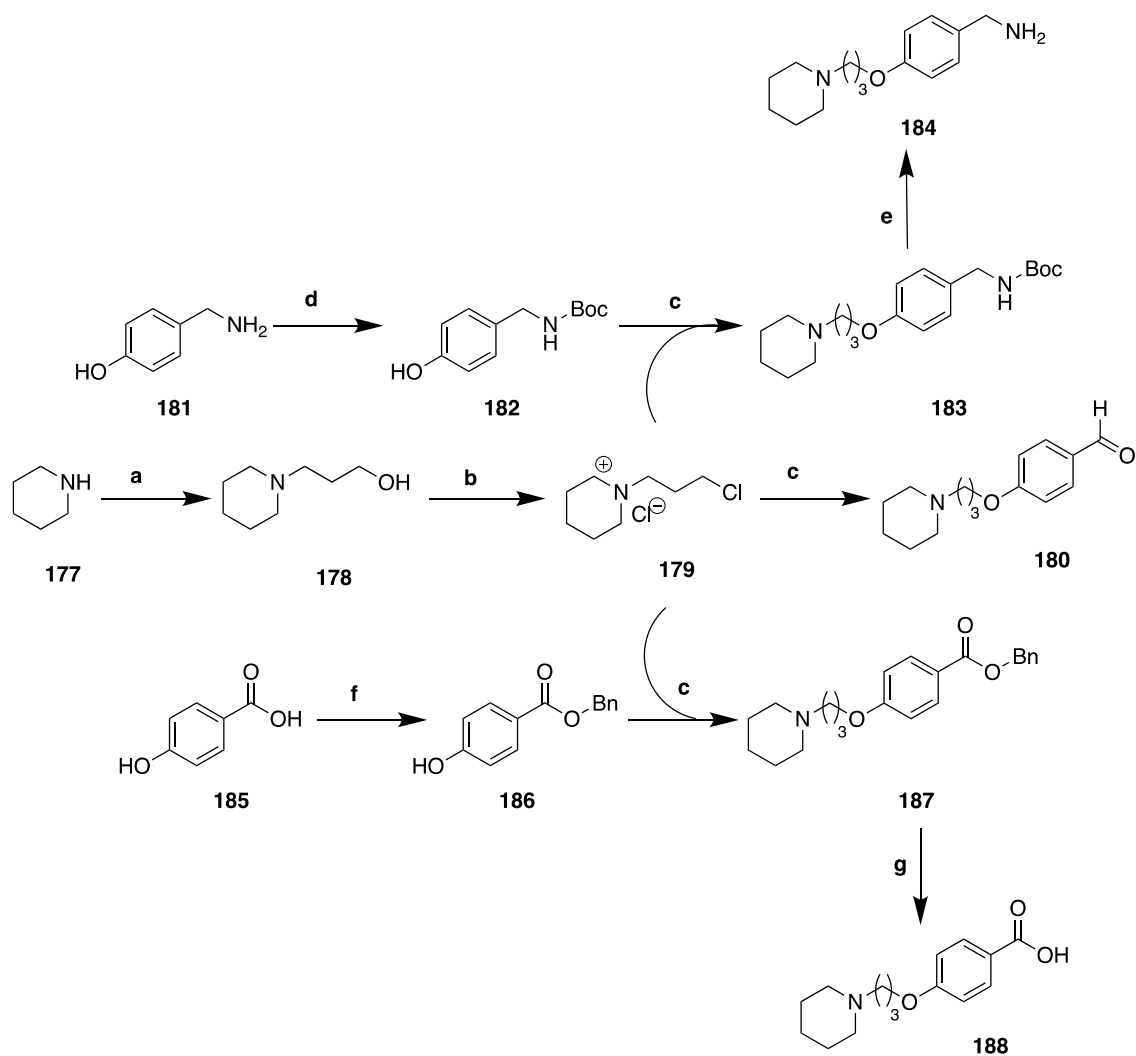
Scheme 17. Synthesis compounds **180**, **184** and **188**.
Reagents and conditions. a) 3-chloropropan-1-ol, KI, K_2CO_3, acetone, 65 °C, 48 h, 65%; b) $SOCl_2$, THF, 0 °C to 60 °C, 2 h, 95%; c) 4-hydroxy benzaldehyde, or compound **182**, or compound **186**, K_2CO_3, MeCN, 85 °C, 2 d, 52%; d) Boc-anhydride, TEA, DCM, 12 h, 0 °C to 25 °C, 52-70%; e) 1N HCl/MeOH, MeOH, 40 °C, 99%; f) Benzyl bromide, TEA, dry DMF, 25 °C, 12 h, 84%; g) H_2, 5 % Pd on carbon, MeOH, 25 °C, 4 h, 99%.

The synthesis of compound **46c** is reported in the **Scheme 18**. Acidic derivative **188** was activated at the corresponding chlorine which reacted with amine **174** to form amide **189**. Boc deprotection of this latter lead to amine **190**, which in presence of carbonylditriazole allowed us to obtain derivative **46c**
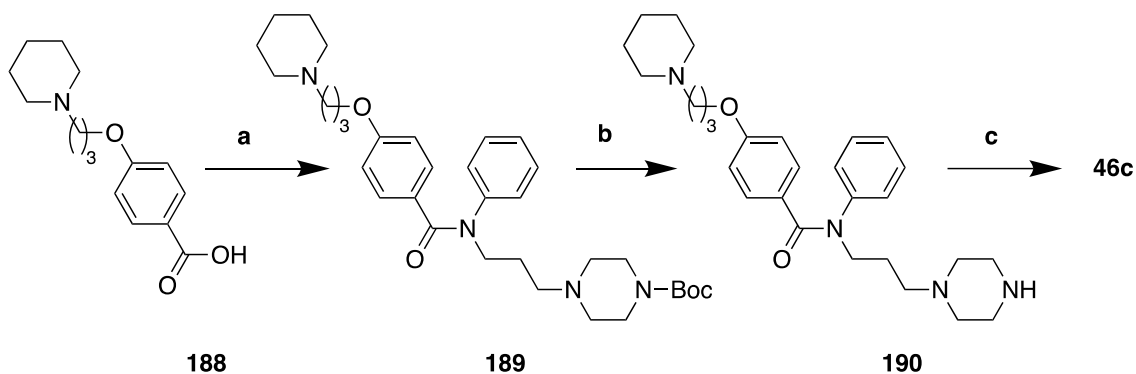
Scheme 18. Synthesis of compound **46b-c.**
Reagents and conditions. a) SOCl$_2$, THF, 70 °C, 1 h, then amine **174**, DIPEA, DCM, 25 °C, 1 h, 21%; b) 1N HCl/MeOH, MeOH, 40 °C, 1 h, 99%; c) CDT, DCM, dry DCM, 25 °C, 12 h, 40%.

In the **Scheme 19** the synthesis of compounds **46d-f** is reported. Under reductive amination protocol, amine **184** reacted with the *N*-Boc-piperidone furnishing intermediate **191**. This latter reacted with the benzoyl chloride to form amide **192**. Its isomer **196** was instead obtained starting from *N*-Boc-piperidone **194** which in presence of benzylamine gave amine **195** under reductive amination conditions. This latter reacted with acidic derivative **188** opportunely activated as benzoyl chloride. At the same time aldehyde **180** reacted with benzyl amine to form intermediate **198**. This latter was coupled with the commercially available *N*-Boc-piperidine-4-carboxylic acid obtaining amide **199**. Compounds **192**, **196** and **199** followed the same synthetic route consistent of a Boc-deprotection, (that furnished amine **193, 197** and **200)**, and final coupling reactions in presence of CDT, to obtain targets compounds **46c-d** respectively.
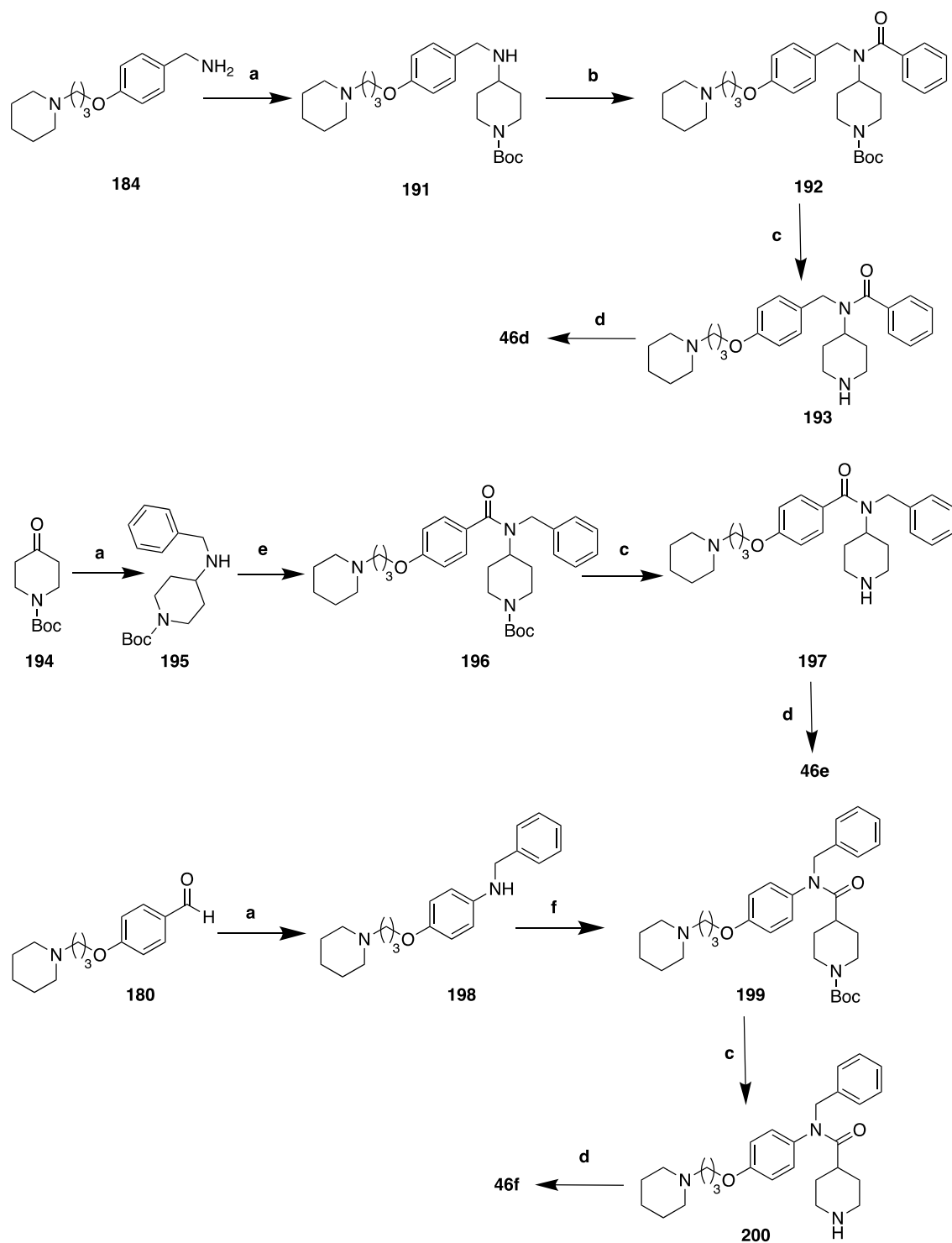
Scheme 19. Synthesis of compounds **46d-f**

Reagents and conditions. a) Boc-piperidone **(**for compound **191),** benzylamine (for compounds **195** and **198**), EtOH, 82 °C, 2 h; NaBH4, MeOH, 0 °C to 25 °C, 12 h, 21-61%; b) Benzoyl chloride , DIPEA, DCM, 25 °C, 1 h, 41%; c) 1N HCl/MeOH, MeOH, 40 °C, 1 h, 81-99%; d) CDT, DCM, 25 °C, 12 h, 41-58%; e) SOCl₂, THF, 70 °C, 1 h, then, Amine **195**, DIPEA, DCM, 25 °C, 1 h, 21%; f) 1-(*tert*-butoxycarbonyl)piperidine-4-carboxylic acid, HBTU, DIPEA, dry DCM, 25 °C, 12 h, 98%.

In the **Scheme 20** the synthesis of compound **46g** is reported. Starting from amine **198** and *N*-Boc-piperazine, urea **201** was obtained in presence of triphosgene. Also in this case, Boc elimination of intermediate **201** gave amine **202** which reacted with CDT furnishing compound **46g**.
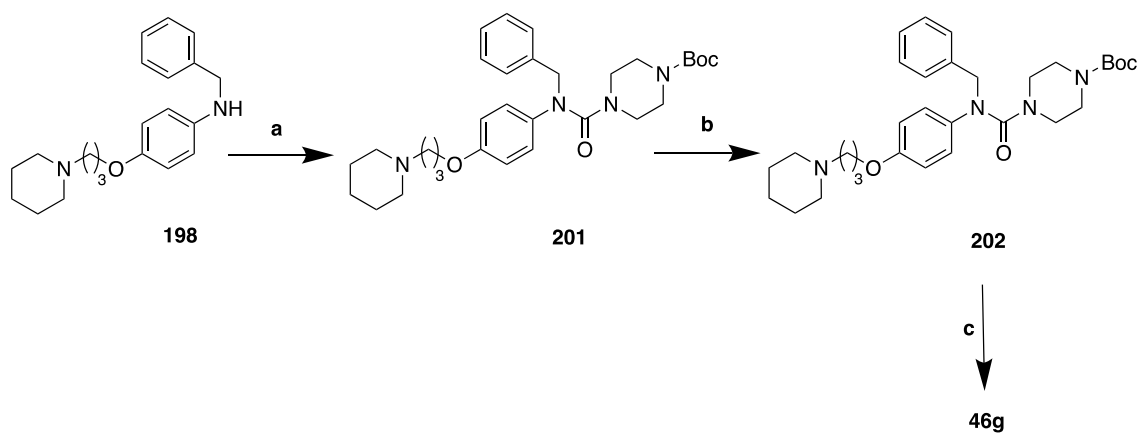
Scheme 20. Synthesis of compound **46g.**
Reagents and conditions. a) *N*-Boc-piperazine, triphosgene, DIPEA, DCM, 0 °C to 25 °C, 12 h, 70%; b) 1N HCl/MeOH, MeOH, 40 °C, 1 h, 99%; c) CDT, DCM, 25 °C, 12 h, 45%.

7.6. SAR analysis of the dual MAGL/H₃R ligands

In **Table 10** the activies of Set A compounds (**45a-d**) towards *human* FAAH/MAGL and *human* H$_{1-3}$R are reported. With these derivatives we performed an initial scaffold exploration, investigating the potentiality of our piperazine-based compounds as hybrid MAGL/H₃R ligands

Table 10. Inhibitory activity towards *human* FAAH/MAGL (expressed as IC$_{50}$ nM) and *human* H$_{1-3}$R (expressed as Ki nM) for the Set A compounds **45a-d**.

Cmps	n	R$_1$	R$_2$	IC$_{50}$ nM hFAAH	IC$_{50}$ nM hMAGL	Ki nM H$_3$R	Ki nM H$_1$R
45a	1	-H	(diphenylmethyl)	64 ± 4	32 ± 2	11397	8956.25
45b	2	-H	(diphenylmethyl)	24 ± 2	13.1 ± 0.9	8887	8956.25
45c	1	(benzyl)	(benzyl)	27 ± 2	2.02 ± 0.16	8360	1146.94
45d	1	(phenyl)	(benzoyl)	207 ± 15	3.83 ± 0.27	18890	9752.26
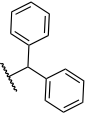
Each value is the mean of at least three experiments

For these analogues the selectivity profile was evaluated against FAAH and the H$_1$R. Piperazine N-4 could interact with the Glu206 leading to an H₃R antagonism. Moreover, modifications in the N-containing bifurcated aromatic portion were applied to explore how the effect of the basicity could influence the activity against the targets. The first synthetized analogues **45a** and **45b** are characterized by a diphenyl methane aromatic

moiety and a propyl- or butyl-based linkers respectively. Both compounds can be considered as dual FAAH/MAGL (for compound **45a** hFAAH IC$_{50}$ = 64 nM, hMAGL IC$_{50}$ = 32 nM, for compound **45b**, hFAAH IC$_{50}$ = 24 nM, hMAGL IC$_{50}$ = 13 nM) inhibitors although they are characterized by a Y-shaped moiety. Probably the dual inhibition of the ECS catabolic enzyme is explained by the fact that the bifurcate moiety is too distant to the piperazinc group to guarantee the selectivity against MAGL. The same situation can be also observed in the di-benzylic derivatives **45c** (hFAAH IC$_{50}$ = 27 nM, hMAGL IC$_{50}$ = 2 nM). Introduction of an amide bomd as in derivative **45d** (hFAAH IC$_{50}$ = 207 nM, hMAGL IC$_{50}$ = 3.8 nM) led to a major potency against MAGL.,All the compounds of the Set A show a micromolar activity against the H$_3$R together with a good potency profile against the H$_1$R. These results highlight that the pharmacophoric merging should include elements that could better direct activity towards the H$_3$R that was performed with compounds of the Set B.

Table 11. Inhibitory activity towards *human* FAAH/MAGL (expressed as IC$_{50}$ nM) and *human* H$_{1\text{-}3}$R (expressed as Ki nM) for the Set B compounds **46a-g**.

Cmps	Structure	IC$_{50}$ nM hFAAH	IC$_{50}$ nM hMAGL	Ki nM H$_3$R	Ki nM H$_1$R
46a		164 ± 10	54 ± 3	23.1	114777
46b		16.9 ± 1.1	46 ± 3	t.b.d	t.b.d.
46c		t.b.d	t.b.d	t.b.d	t.b.d
46d		t.b.d	t.b.d	t.b.d	t.b.d
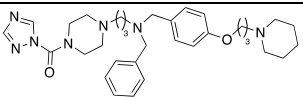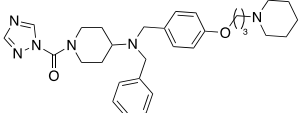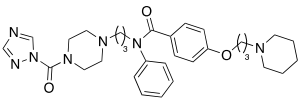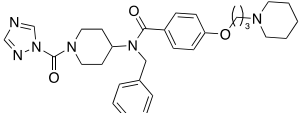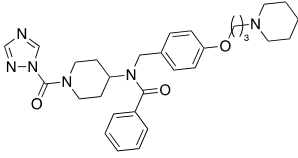
46e		t.b.d	t.b.d	t.b.d	t.b.d
46f		t.b.d	t.b.d	t.b.d	t.b.d
46g		t.b.d	t.b.d	t.b.d	t.b.d
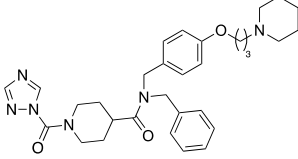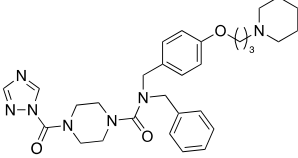
Each value is the mean of at least three experiments**;T.d.b. = to be detetcted**

In the **Table 11** the structures of the Set B derivatives are reported. To date we have only preliminary data regarding the activity of compounds **46a** and **46b**. In these two derivatives we inserted the PiProp moiety respectively in the aromatic portion of the piperazine and the piperdidine portions. Compound **46a** (hFAAH IC$_{50}$ = 164 nM, hMAGL IC$_{50}$ = 53 nM), despite the Y-shape, shows a dual FAAH/MAGL inhibitory profile. Probably, the high molecular flexibility may allow the compound to properly adapt to both enzymatic clefts. However, this compound also shows an excellent activity against the H$_3$R (Ki = 23 nM) combined with a good selectivity toward H$_1$R. In the same way, derivative **46b** is dual FAAH/MAGL inhibitor (hFAAH IC$_{50}$ = 16 nM, hMAGL IC$_{50}$ = 46 nM). The evaluation of the inhibitory activity of this compound toward H1-3R is currently in progress but, must probably it should show a similar profile to compound **46a**. With compound **46a** we succeeded in the identification of a hybrid FAAH/MAGL and H$_3$R ligand characterized by a nanomolar activity against all the targets. However, other derivatives (compounds **46c-g** as in **Table 11**) were synthetized with the aim to improve the selectivity toward MAGL, keeping the activity against H$_3$R. To achieve this aim, introduced amide or ureidic substructures at the level of the branched nitrogen moiety of compounds **46a-b**. Taking inspiration from compound **45d** in the Set A, which shows

the better inhibitory FAAH/MAGL profile, we synthetized the amide **46c**. The increased rigidity and the presence of the PiProp group could ameliorate the selectivity profile against MAGL and H_3R for this derivative.

In a similar way, starting from compound **46b** we tried to constrict the branched nitrogen containing moiety, inserting an amido or an ureidic group. Following this approach derivatives **46d-g** were obtained. The evaluation of the activity of these newly developed derivatives **46b-g** is currently in progress at the University of Ferrara (for the activity against FAAH and MAGL enzyme) and in the Professor Stark' laboratories (for the activity towards the $H_{1-3}R$).

8. Conclusions

The pharmacological treatment of complex and multifactorial pathologies, characterized by pathogenic mechanisms involving numerous different pathways and neurotransmission systems, is still a paramount challenge. The ECS is emerging as a particularly attractive therapeutic target in CNS disorders and NDs diseases including AD, PD, ALS and MS. In this field, the increase of the endocannabinoid tone, by using FAAH and MAGL inhibitors, represents an innovative therapeutic option plentifully investigated in the neurodegenerative context. Taking into account the intensive activity of our research group in the discovery of ECS catabolic enzyme inhibitors, during my PhD work I focused my efforts on the development of selective FAAH or MAGL inhibitors and of multitarget compounds able to engage these ECS enzymes and other relevant targets for the treatment of NDs. The cross-link between neuroinflammation and neurodegeneration is a common feature of several complex CNS diseases in which the ECS play a central role in the management of the neuroinflammatory conditions. In this context, a first part of my work was devoted to the synthesis of new selective carbamate based FAAH inhibitors. The newly developed compounds were obtained introducing ionizable functions and exploring the tertiarization of the carbamate moieties, starting from our lead FAAH inhibitors. These structural modifications, finalized to an improvement in the drug-like properties, lead to identify novel high potent FAAH inhibitors characterized by an excellent selectivity profile evaluated towards MAGL and the CBRs. For a sub-set of derivatives, the solubility and the chemical stability were evaluated together with their lack of toxicity in murine fibroblast and human astrocytes. For the most interesting analogues, the anti-inflammatory profile was successfully evaluated in cellular and in *ex vivo* assays. All the collected data suggest the potential use

of these FAAH inhibitors as pharmacological tools for the treatment of CNS inflammatory disorders.

With the aim to identify new selective MAGL inhibitors we embarked in a scaffolds exploration directed at the investigation of the MAGL chemical space. Inspired from our previous work on the β-lactam based MAGL inhibitors we developed new inhibitors by maintaining the piperidine-azole urea moiety as a key motif for MAGL inhibition, combined with the opportunely modified above discussed privileged scaffolds. My contribution to this scaffolds exploration consisted of the synthesis of two spiro-β-lactams derivatives to complete and better characterized our SAR study. Currently the anti-neuroinflammatory activity of the most interesting compounds of this series is under evaluation on hippocampal slice cultures.

Another part of my PhD work was focused on the exploration of innovative multitarget strategies in which the ECS catabolic enzymes are involved. Accordingly, I developed dual FAAH/MAGL inhibitors by applying a scaffold simplification strategy started from our previously reported β- lactam based MAGL inhibitors. These compounds showed an activity in the low nanomolar range towards the targets of interests combined with a good selectivity profile evaluated against the CBRs. For a sub-set of analogues, the anti-inflammatory and neuroprotective effects were demonstrated in *ex vivo* assays. Additional studies are currently in progress to evaluate the efficacy of our derivatives.

Our polypharmacaological exploration continued with the purpose to develop potential dual FAAH/HDAC6 inhibitors as innovative tools for the treatment of NDs. To this end, the key structural elements needed for FAAH inhibition, such as the presence of an electrophilic center, a lipophilic lateral chain and a byarilic moiety, were opportunely modified to combine also the pharmacophoric elements for the HDAC6 engagement (a bulky cap group, a ZBG and a linker moiety) into the same general structure. Of the small

library of the new developed compounds, one derivative shows an activity in the sub-micromolar range against both the selected target. Following these interesting preliminary data, our SAR investigation, finalized at the synthesis of new potent derivatives, is currently ongoing.

Finally, during the time abroad of my PhD performed at the HHU in Dusseldorf, we set-up a collaborative project aimed to the obtainment of dual MAGL/H_3R ligands as multitarget compounds for the treatment of NDs. One of our approaches consisted of the introduction of the Piprop moiety (responsible for the engagement of the H_3R) in the aromatic portion of piperazine and piperidine Y-shaped scaffolds needed for the MAGL inhibition. This strategy resulted in the identification of the first hybrid MAGL/H_3R ligand, although the new developed compound shows nanomolar activity towards the selected target and FAAH enzyme as well. To direct the activity preferentially against MAGL and H_3R we embarked in a structural optimization, synthetizing new derivatives. For these new compounds the evaluation of the activity against FAAH/MAGL and H_{1-3}R is currently ongoing.

9. Experimental section

Reagents were purchased from Aldrich and were used as received. Reaction progress was monitored by TLC using Merck silica gel 60 F254 (0.040-0.063 mm) with detection by UV. Merck silica gel 60 (0.040-0.063 mm) was used for column chromatography.1H NMR and 13C NMR spectra were recorded on Varian 300 MHz or Bruker 400MHz spectrometer with TMS as internal standard. Splitting patterns are described as singlet (s), doublet (d), triplet (t), quartet (q), and broad (br); the value of chemical shifts (d) are given in ppm and coupling constants (J) in Hertz (Hz). ES-MS spectra were performed by an Agilent 1100 Series LC/MSD spectrometer. Yields refer to purified products and are not optimised. All moisture-sensitive reactions were performed under argon atmosphere using oven-dried glassware and anhydrous solvents.

9.1. Experimental section of the FAAH inhibitors 41a-t

3-(1H-Pyrrol-1-yl)phenol (52). To a solution of **51** (667 mg, 4.58 mmol) in 1,4-dioxane (79 mL), 2,5-dimethoxytetrahydrofuran (956 μL, 7.38 mmol) and *N,N*-diethylnicotinamide (1209 μL, 7.19 mmol) were added. Reaction mixture was refluxed for 2 h, under N_2 atmosphere. After cooling to 25 °C, the solvent was removed under vacuum. Solid residue was dissolved in water and extracted with DCM (3 x 10 mL). Organic phase was dried over sodium sulphate, filtered and concentrated. The crude was purified by column chromatography on silica gel (PE/EtOAc from 4:1 to 2:1) to afford the title compound as an amorphous brown solid (79% yield). **^{1}H NMR** (300 MHz, $(CD_3)_2CO$) δ 8.66 (s, 1H), 7.34 – 7.22 (m, 1H), 7.20 – 7.14 (m, 2H), 7.03 – 6.94 (m, 2H), 6.77 – 6.71 (m, 1H), 6.28 – 6.21 (m, 2H).

*1-(3-Hydroxyphenyl)-1H-pyrrole-2-carbaldehyde (53).*To a solution of oxalyl chloride (348 μL, 4.05 mmol) in dry DCM (22.5 mL), under N_2 atmosphere, a solution of *N,N*-dimethylformamide (314 μL, 4.05 mmol) in dry DCM (2.0 mL) was added dropwise, at 0 °C. Reaction mixture was stirred for 30 minutes, under N_2 atmosphere, at 0 °C. Then, a solution of **52** (461 mg, 2.90 mmol) in dry DCM (2.4 mL) was added at once. Reaction mixture was refluxed for 3 h. Then, solvent was removed. The crude was dissolved in 1N NaOH (10.5 mL) and stirred at 25 °C for 16 h. Reaction mixture was quenched with 1N HCl up to pH 5 and diluted with EtOAc. It was then extracted with EtOAc (3 x 10 mL). Organic phase was dried over sodium sulphate, filtered and concentrated. The crude was purified by column chromatography on silica gel (PE/EtOAc from 10:1 to 3:1) to afford the title compound as a yellow solid (62% yield). ^{1}H NMR (300 MHz, $(CD_3)_2CO$) δ 9.59

– 9.57 (m, 1H), 8.84 (s, 1H), 7.35 – 7.28 (m, 1H), 7.28 – 7.23 (m, 1H), 7.17 – 7.09 (m, 1H), 6.97 – 6.93 (m, 1H), 6.93 – 6.86 (m, 2H), 6.44 – 6.38 (m, 1H).

1-(3-Hydroxyphenyl)-1H-pyrrole-3-carbaldehyde (54). To a solution of **53** (206 mg, 1.10 mmol) in dry 1,2-dichloroethane (9.8 mL), triflic acid (389 μL, 4.40 mmol) was added and reaction mixture was refluxed for 6 h, under N_2 atmosphere. After cooling to 25 °C, the mixture was neutralized by means of saturated solution of $NaHCO_3$, diluted with DCM and extracted with DCM (3 x 10 mL). Organic phase was dried over sodium sulphate, filtered and concentrated. The crude was purified by column chromatography on silica gel (PE/EtOAc from 10:1 to 2:1) to afford the title compound as a yellow solid (46% yield). ^{1}H NMR (300 MHz, $(CD_3)_2CO$) δ 9.84 (s, 1H), 8.87 (s, 1H), 8.07 – 7.91 (m, 1H), 7.41 – 7.23 (m, 2H), 7.16 – 7.03 (m, 2H), 6.91 – 6.80 (m, 1H), 6.73 – 6.66 (m, 1H).

1-(3-(Methoxymethoxy)phenyl)-1H-pyrrole-3-carbaldehyde (55). To a solution of **54** (95 mg, 0.51 mmol) in dry DCM cooled at 0 °C, MOM-Cl (116 μL, 1.52 mmol) and DIPEA (264 μL, 1.52 mmol) were added. The resulting mixture was stirred at 0 °C for 1 h. NH4Cl saturated solution was added, and the mixture was extracted with DCM (3 x 30 mL). Organic phase was dried over sodium sulphate, filtered and concentrated. The crude was purified by column chromatography on silica gel (PE/EtOAc from 6:1 to 3:1) to afford the title compound as an amorphous pale-yellow solid (84% yield). ^{1}H NMR (300 MHz, $(CD_3)_2CO$) δ 9.85 (s, 1H), 8.07 – 8.03 (m, 1H), 7.50 – 7.41 (m, 1H), 7.40 – 7.37 (m, 1H), 7.32 – 7.24 (m, 2H), 7.09 – 7.03 (m, 1H), 6.72 (dd, J = 3.1, 1.6 Hz, 1H), 5.30 (s, 2H), 3.46 (s, 3H).

1-(3-(Methoxymethoxy)phenyl)-1H-pyrrole-3-carboxylic acid (56). To a solution of **55** (146 mg, 0.78 mmol) and 2-methyl-2-butene (1.08 ml, 10.14 mmol) in *tert*-butanol (12 mL), saturated solutions of $NaClO_2$ (0.51 mL, 4.37 mmol) and NaH_2PO_4 (0.82 mL, 5.85 mmol) were added. The reaction mixture was stirred for 16 h at 25 °C. Then, it was quenched with a saturated solution of NH4Cl and extracted with EtOAc (3 x 10 mL). Organic phase was dried over sodium sulphate, filtered and concentrated. The crude was purified by column chromatography on silica gel (PE/EtOAc from 4:1 to 1:1) to afford the title compound as a colorless oil (96% yield). ^{1}H NMR (300 MHz, $(CD_3)_2CO$) δ 10.00-9.66 (br, 1H), 7.86 – 7.81 (m, 1H), 7.43 (t, J = 8.1 Hz, 1H), 7.32 – 7.22 (m, 3H), 7.05 – 6.99 (m, 1H), 6.69 (dd, J = 3.0, 1.6 Hz, 1H), 5.30 (s, 2H), 3.46 (s, 3H).

1-(3-(Methoxymethoxy)phenyl)-1H-pyrrole-3-carboxamide (57). To a solution of **56** (72 mg, 0.29 mmol) in dry DCM (4 mL) at 0 °C, DIPEA (151 μL, 0.87 mmol), EDC-HCl (84 mg, 10.44 mmol) and HOBt (15 mg, 0.11 mmol) were added. The reaction mixture was stirred at 0 °C for 10 minutes. Then, a 28% aqueous solution of NH4OH (55 μL, 0.44 mmol) was added. The reaction mixture was stirred at 0 °C for 30 minutes, then it was allowed to reach 25 °C and stirred for 16 h under N_2 atmosphere. A saturated solution of NH4Cl was then added dropwise and the mixture was extracted with DCM (3 x 10 mL). Organic phase was dried over sodium sulphate, filtered and concentrated. The crude was purified by column chromatography on silica gel (from 1:1 PE/EtOAc to EtOAc only) to afford the title compound as an off-white solid (96% yield). ^{1}H NMR (300 MHz, $(CD_3)_2CO$) δ 7.92 – 7.88 (m, 1H), 7.39 (t, J = 8.1 Hz, 1H), 7.29 – 7.22 (m, 2H), 7.20 (d, J = 8.0 Hz, 1H), 6.98 (dd, J = 8.2, 1.5 Hz, 1H), 6.81 – 6.75 (m, 1H), 6.75 – 6.53 (br, 2H), 5.28 (s, 2H), 3.44 (s, 3H).

1-(3-Hydroxyphenyl)-1H-pyrrole-3-carboxamide (49c). To a solution of **57** (69 mg, 0.28 mmol) in methanol (10.0 mL), a solution of 1N HCl/MeOH (1.25 mL, 1.25 mmol) was added. The reaction mixture was stirred for 12 h at 25 °C. A saturated solution of $NaHCO_3$ was added and solvent was removed under vacuum. The solid residue was suspended in water and extracted with EtOAc (3 x 10 mL). Organic phase was dried over sodium sulphate, filtered and concentrated. Compound was used in the next step without any further purification (yellow oil, 97% yield). ^{1}H NMR (300 MHz, $(CD_3)_2CO$) δ 9.38 (s, 1H), 7.87 (t, *J* = 2.0 Hz, 1H), 7.29 (t, *J* = 8.1 Hz, 1H), 7.24 – 7.19 (m, 1H), 7.05 (t, *J* = 2.1 Hz, 1H), 7.00 (dd, *J* = 8.0, 1.4 Hz, 1H), 6.86 – 6.80 (m, 1H), 6.78 (dd, *J* = 3.0, 1.7 Hz, 1H), 6.76 – 6.60 (br, 2H).

3-(2H-Tetrazol-5-yl)phenol (49e). 3-Hydroxybenzonitrile **58** (200.0 mg, 1.68 mmol,), TEA hydrochloride (463.0 mg, 3.36 mmol) and sodium azide (218 mg, 3.36 mmol) were refluxed in dry toluene (17.0 mL) for 20 h. The mixture was cooled to 25 °C, diluted with water and EtOAc, and extracted with water (20.0 mL). The aqueous phase was acidified by a dropwise addition of 32% HCl until a white solid precipitated. The precipitate was filtered, washed with water and dried to give **49e** as a white solid (122 mg, 45% yield). ^{1}H NMR (300 MHz, MeOD) δ 7.44 (ddt, *J* = 5.3, 2.9, 1.6 Hz, 2H), 7.37 (t, *J* = 8.0 Hz, 1H), 7.01 – 6.95 (m, 1H). ESI-MS *m/z* 161 [*M* -H]⁻.

2-(3-Hydroxyphenyl)-5-methylfuran-3-carboxylic acid (60). To a cooled suspension of **59** (85.0 mg, 0.18 mmol) in dry DCM (3.0 mL) at -78 °C, boron tribromide, (1 M solution in DCM) (1.17 mmol, 1.10 mL) was added. The reaction was allowed to reach to 25 °C and stirred for 2 h. A saturated solution of sodium bicarbonate was added, and the mixture was extracted with DCM. The water phase was treated with 1 N HCl and extracted with EtOAc (3 x 10 mL). The combined organic layers were dried over anhydrous sodium sulfate, filtered, and concentrated *in vacuo*. Title compound **60** was obtained as a white solid and used in the next step without any further purification (85.0 mg, 99% yield). ^{1}H NMR (300 MHz, MeOD) δ 7.43 – 7.37 (m, 2H), 7.20 (dd, *J* = 8.2, 7.5, 1H), 6.82 – 6.76 (m, 1H), 6.42 (s, 1H), 2.33 (s, 3H). ESI-MS *m/z* 217 [*M* -H]⁻.

Benzyl 2-(3-hydroxyphenyl)-5-methylfuran-3-carboxylate (49f). To a solution of **60** (46.0 mg, 0.36 mmol) in dry DMF (2mL), sodium bicarbonate (38.0 mg, 0.45 mmol) and benzyl bromide (0.56 mmol, 73 µL) were added. The reaction was allowed to reach 40 °C and was stirred for 12 h. Saturated ammonium chloride was added, and the mixture was extracted with EtOAc. The organic layer was washed two times with saturated ammonium chloride and then with brine. The organic layer was dried over anhydrous sodium sulfate, filtered, and concentrated. The crude was purified by column chromatography on silica gel (PE/EtOAc from 5:1 to 3:1) to afford the title compound as colorless oil (77.0 mg, yield 70%). ^{1}H NMR (300 MHz, $CDCl_3$) δ 7.57 – 7.45 (m, 2H), 7.42 – 7.29 (m, 5H), 7.31 – 7.18 (m, 1H), 6.86 (dd, *J* = 8.1, 2.5, 1H), 6.46 (s, 1H), 5.27 (s, 2H), 2.33 (s, 3H). ESI-MS *m/z* 307 [*M* -H]⁻.

6-(4-Methylpiperazin-1-yl)hexanenitrile (62). To a solution of 1-methylpiperazine **61** (300.0 mg, 3.0 mmol) in EtOH (5.0 mL), sodium carbonate (476.0 mg, 4.5 mmol) and 6-bromohexanenitrile (1.3 mL, 3.6 mmol) were added. The resulting mixture was stirred for 12 h at 25 °C. Then, the solvent was evaporated and the crude was purified by column chromatography on silica gel (DCM/MeOH/NH$_4$OH 10:1:0.1) to afford the title compound as a yellow oil (144.0 mg, 25% yield) ^{1}H NMR (300 MHz, $CDCl_3$) δ 2.76 (dd,

J = 15.8, 10.6 Hz, 8H), 2.43 (s, 3H), 2.28 (t, J = 7.0 Hz, 2H), 1.65 – 1.45 (m, 4H), 1.45 – 1.32 (m, 4H). ESI-MS m/z 218 $[M + \text{Na}]^+$.

6-(4-Methylpiperazin-1-yl)hexan-1-amine (50a). To a solution of **62** (144.0 mg, 0.74 mmol) in dry THF cooled at 0 °C a solution of lithium aluminum hydride 1 M in THF (184.0 μL, 1.84 mmol) was added dropwise. The reaction mixture was allowed to reach 25 °C and stirred for 1 h. A solution of 1 N sodium hydroxide was added, and the resulting mixture was filtered through a Celite® pad. The aqueous phase was extracted with EtOAc (3 x 10 mL), and the combined organic layers were dried over anhydrous sodium sulfate, filtered, and concentrated *in vacuo.* The crude was purified by column chromatography on silica gel (DCM/MeOH/NH₄OH 10:1:0.) to afford the title compound as a yellow oil (139.0 mg, 94% yield). ¹H NMR (300 MHz, CDCl₃) δ 2.53 (t, J = 6.8 Hz, 2H), 2.44 – 2.23 (m, 8H), 2.24 – 2.16 (m, 2H), 2.14 (s, 3H), 1.46 – 1.25 (m, 4H), 1.24 – 1.09 (m, 4H). ESI-MS m/z 200 $[M + \text{H}]^+$, 241 $[M + \text{Na}]^+$.

4.1.6. tert-Butyl (1-phenethylpiperidin-4-yl)carbamate (64). To a solution of 4-Boc-amino piperidine **63** (500.0 mg, 2.50 mmol) in dry THF (10.0 mL), 2-bromo ethylbenzene (405 μL, 3.0 mmol) and TEA (1.045 mL, 7.50 mmol) were added. The reaction mixture was heated at 70 °C for 12 h. A saturated solution of sodium bicarbonate was added, and the mixture was extracted with EtOAc (3 x 10 mL). The combined organic layers were dried over sodium sulfate, filtered and concentrated. The crude was purified by column chromatography on silica gel (PE/EtOAc from 3:1 to 1:1) to afford the title compound as an amorphous yellow solid (676 mg, 88% yield). ¹H NMR (300 MHz, CDCl₃) δ 7.31 – 7.23 (m, 2H), 7.22 – 7.14 (m, 3H), 3.59 – 3.38 (m, 1H), 2.99 – 2.86 (m, 4H), 2.85 – 2.72 (m, 2H), 2.62 – 2.51 (m, 2H), 2.20 – 2.06 (m, 2H), 2.01 – 1.88 (m, 2H), 1.44 (s, 9H). ESI-MS m/z 305 $[M + \text{H}]^+$, 327 $[M + \text{Na}]^+$.

1-Phenethylpiperidin-4-amine (50b). To a solution of **64** (484.0 mg, 1.5 mmol) in dry DCM (38.0 mL) cooled to 0 °C, TFA (1.3 mL) was added dropwise. The reaction mixture was allowed to reach 25 °C and stirred for 2 h under N₂ atmosphere. A saturated solution of sodium bicarbonate was added, and the mixture was extracted with DCM (3 x 10 mL). The combined organic layers were washed with brine, dried over anhydrous sodium sulfate, filtered and concentrated. Title compound was used in the next step without any further purification (yellow oil, 290.0 mg, 95% yield). ¹H NMR (300 MHz CDCl₃) δ 7.31 – 7.23 (m, 2H), 7.21 – 7.14 (m, 3H), 2.98-2.92 (m, 2H), 2.84 – 2.75 (m, 3H), 2.63 – 2.55 (m, 2H), 2.54 – 2.42 (m, 2H), 2.14 – 2.03 (m, 2H), 1.90 – 1.78 (brs, 2H), 1.52 – 1.37 (m, 2H). ESI-MS m/z 227 $[M + \text{Na}]^+$.

tert-Butyl 4-(((benzyloxy)carbonyl)amino)piperidine-1-carboxylate (66). To a mixture of compound **65** (200.0 mg, 0.98 mmol) in THF (2.5 mL) and water (1.0 mL) cooled at 0 °C sodium bicarbonate (252.0 mg, 2.97 mmol) and benzyl chloroformate (1.17 mmol, 185 μL) were added. The resulting mixture was allowed to reach 25 °C and stirred for 12 h. Water was added, and the mixture was extracted with EtOAc (3 x 10 mL). The combined organic layers were dried over sodium sulfate, filtered and concentrated. The crude was purified by column chromatography on silica gel (DCM/MeOH from 40:1 to 20:1) to afford the title compound as a colorless oil (266 mg, 80% yield) ¹H NMR (300 MHz, CDCl₃) δ 7.42 – 7.28 (m, 5H), 5.08 (s, 2H), 4.79 (brs, 1H), 3.99 (d, J = 13.6 Hz, 2H), 3.71 – 3.57 (m, 1H), 2.90 – 2.77 (m, 2H), 1.95 – 1.85 (m, 2H), 1.44 (s, 9H), 1.33 – 1.25 (m, 2H). ESI-MS m/z 335 $[M + \text{H}]^+$; 357 $[M + \text{Na}]^+$.

Benzyl piperidin-4-ylcarbamate (67). The title compound was obtained following the procedure described for the compound **50b**, starting from compound **66** (226.0 mg, 0.68 mmol), TFA (600 μL), in dry DCM (17.0 mL). Compound **67** was obtained as a yellow oil (156.0 mg, 99% yield). ^{1}H NMR (300 MHz, CDCl$_3$) δ 7.41 – 7.14 (m, 5H), 5.03 (s, 2H), 3.70 – 3.38 (m, 1H), 3.03 – 2.94 (m, 2H), 2.72 – 2.45 (m, 2H), 1.87 (d, J = 9.8 Hz, 2H), 1.40 – 1.09 (m, 2H). ESI-MS m/z 235 $[M + H]^+$; 257 $[M + Na]^+$.

3-Phenylpropanal (69). To a solution of 3-phenylpropan-1-ol **68** (100.0 mg, 0.73 mmol, 100 μL), in dry DCM cooled to 0 °C, TCICA (180.0 mg, 0.77 mmol) and TEMPO (1.0 mg, 0.0074 mmol) were added. The reaction was stirred for 10 minutes at 0 °C, then the mixture was filtered through a Celite® pad and washed with DCM. The filtrate was then washed with sodium bicarbonate (saturated solution) and then with 1 N HCl. The organic layer was dried over anhydrous sodium sulfate, filtered, and concentrated *in vacuo*. Title compound was obtained as a colorless oil, and it was used in the next step without any further purification. (156.0 mg, 99% yield). ^{1}H NMR (300 MHz, (Acetone-d_6) δ 9.77 (s, 1H), 7.35 – 7.14 (m, 5H), 2.93 (t, J = 7.2 Hz, 2H), 2.77 (t, J = 7.8 Hz, 2H).

Benzyl (1-(3-phenylpropyl)piperidin-4-yl)carbamate (70). To a solution of **67** (32.0 mg, 0.14 mmol) and aldehyde **69** (17.0 mg, 0.12 mmol) in dry DCM cooled at 0 °C, NaBH(OAc)$_3$ (39.5 mg, 0.19 mmol) was added. The reaction was allowed to reach 25 °C and stirred for 12 h. A saturated solution of sodium bicarbonate was added, and the mixture was extracted with DCM (3 x 10 mL). The combined organic layers were dried over anhydrous sodium sulfate, filtered, and concentrated *in vacuo*. The crude was purified by column chromatography on silica gel (DCM/MeOH from 40:1 to 20:1) to afford the title compound as a colorless oil (28.0 mg, 66% yield). ^{1}H NMR (300 MHz, CDCl$_3$) δ 7.45 – 7.07 (m, 10H), 5.08 (s, 2H), 4.72 (d, J = 8.1 Hz, 1H), 3.67 – 3.43 (m, 1H), 2.96 – 2.75 (m, 2H), 2.62 (t, J = 7.7 Hz, 2H), 2.46 – 2.30 (m, 2H), 2.10 (t, J = 11.4 Hz, 2H), 2.02 – 1.89 (m, 2H), 1.83 – 1.78 (m, 2H), 1.62 – 1.38 (m, 2H). ESI-MS m/z 375 $[M + Na]^+$.

1-(3-Phenylpropyl)piperidin-4-amine (50c). To a solution of compound **70** (28.0 mg, 0.08 mmol) in a mixture of EtOAc (1.5 mL) and MeOH (1.5 mL) a catalytic amount of 10% Pd on carbon was added. The resulting mixture was stirred for 2 h under H$_2$ atmosphere. Thereafter, the mixture was filtered and evaporated. The title compound, obtained as a yellow oil, was used in the next step without any further purification (12.0 mg, 75% yield). ^{1}H NMR (300 MHz, CDCl$_3$) δ 7.51 – 6.93 (m, 5H), 2.86 – 2.80 (m, 2H), 2.75 – 2.49 (m, 5H), 2.41 – 2.26 (m, 2H), 1.98 (t, J = 10.4 Hz, 2H), 1.89 – 1.70 (m, 4H), 1.53 – 1.32 (m, 2H). ESI-MS m/z 241 $[M + Na]^+$.

N-Methyl-1-phenethylpiperidin-4-amine (50e). To a suspension of LiAlH$_4$ (67.0 mg, 1.76 mmol) in dry THF (1.0 mL) 0 °C, a solution of compound **64** (0.32 mmol in 1 mL of dry THF) was added. The mixture was heated at 70 °C for 18 h under N$_2$ atmosphere. A 2 N solution of NaOH was added, and the mixture was filtered through a Celite® pad and washed with EtOAc. The separated organic layer was dried over sodium sulfate, filtered and concentrated. The crude was purified by column chromatography on silica gel (DCM/MeOH from 20:1 to 10:1) to afford the title compound as a yellow oil (113 mg, 63% yield). ^{1}H NMR (300 MHz, CDCl$_3$) δ 7.26 (dd, J = 8.9, 5.6 Hz, 2H), 7.22 – 7.11 (m, 3H), 3.02 – 2.87 (m, 2H), 2.84 – 2.72 (m, 2H), 2.71 – 2.62 (m, 1H), 2.61 – 2.49 (m, 2H), 2.12 – 1.95 (m, 2H), 1.93 (s, 3H), 1.89 – 1.76 (m, 2H), 1.55 – 1.29 (m, 2H). ESI-MS m/z 241 $[M + Na]^+$.

3-Bromopropyl)benzene (71). To a solution of **68** (500.0 mg, 3.80 mmol) in dry DCM, PPh$_3$ (1.600 g, 6.08 mmol), 1-*H*-imidazole (387.0 mg, 5.7 mmol) and CBr$_4$ (1.380 g, 4.18 mmol) were added. The mixture was stirred for 12 h at 25 °C. After this time water was added and the reaction was extracted with DCM (3 x 20 mL), dried over sodium sulfate, filtered and concentrated *in vacuo*. The crude was purified by column chromatography on silica gel (PE/EtOAc from 20:1 to 10:1) to afford the title compound as a colorless oil (750.0 mg, 95% yield).^{1}H NMR (300 MHz, CDCl$_3$) δ 7.35 – 7.24 (m, 2H), 7.23 – 7.15 (m, 3H), 3.40 (t, *J* = 6.6 Hz, 2H), 2.78 (t, *J* = 7.4 Hz, 2H), 2.28 – 2.09 (m, 2H).

tert-Butyl 4-(3-phenylpropyl)piperazine-1-carboxylate (72). To a solution to 1-Boc-piperazine (61.0 mg, 0.33 mmol) in acetonitrile (1.5 mL) potassium carbonate (115.0 mg, 0.83 mmol), a solution of **71** (100.0 mg, 0.50 mmol) in acetonitrile (1.5 mL) and potassium iodide (cat.) were added. The reaction was stirred at 25 °C for 5 h. Then the solvent was removed, the solid residue was taken up with water and then extracted with EtOAc (3 x 20 mL). The combined organic layers were dried over sodium sulfate, filtered and concentrated *in vacuo*. The crude was purified by column chromatography on silica gel (PE/EtOAc from 2:1 to 1:1) to afford the title compound as a yellow oil (94.0 mg, 93% yield).^{1}H NMR (300 MHz, CDCl$_3$) ^{1}H NMR δ 7.31 – 7.21 (m, 2H), 7.20 – 7.13 (m, 3H), 3.50 – 3.35 (m, 4H), 2.62 (t, *J* = 7.7 Hz, 2H), 2.43 – 2.30 (m, 6H), 1.89 – 1.73 (m, 2H), 1.45 (s, 9H). ESI-MS *m/z* 327 [*M* + Na]$^+$.

1-(3-Phenylpropyl)piperazine (50f). The title compound was obtained according with the procedure previously described for compound **50b**, starting from **72** (50.0 mg, 0.16 mmol) and TFA (114 μL) in dry DCM (4.0 mL). **50f** was used in the next step without any further purification (yellow oil, 28.0 mg, 99% yield). ^{1}H NMR (300 MHz, CDCl$_3$) δ 7.27 (dd, *J* = 8.6, 6.0 Hz, 2H), 7.20 – 7.13 (m, 3H), 2.90 (t, *J* = 4.9 Hz, 2H), 2.81 – 2.71 (brs, 1H), 2.62 (t, *J* = 7.7 Hz, 2H), 2.47 – 2.31 (m, 8H), 1.81 (p, *J* = 7.7, 7.3 Hz, 2H). ESI-MS *m/z* 205 [*M* +H]$^+$ 227 [*M* +Na]$^+$.

1-Benzylpiperidin-4-one (74). To a solution of **73** (1.000 g, 5.8 mmol) in dry DMF (10.0 mL), potassium carbonate (2.400 g, 17.4 mmol) and benzyl bromide (7.0 mmol, 835 μL) were added. The reaction was heated at 75 °C for 12 h. Then, the reaction was allowed to reach 25 °C and a saturated solution of ammonium chloride was added. The mixture was extracted with EtOAc (2 x 20 mL) and the combined organic layers were washed with ammonium chloride saturated solution (2 x 10 mL) and with brine (2 x 10 mL). The organic phase was dried over anhydrous sodium sulfate, filtered, and concentrated *in vacuo*. The crude was purified by column chromatography on silica gel (PE/EtOAc 5:1) to afford the title compound as a yellow oil (773.0 mg, 70% yield). ^{1}H NMR (300 MHz, CDCl$_3$) δ 7.36 – 7.09 (m, 5H), 3.50 (s, 2H), 2.61 (t, *J* = 6.1 Hz, 4H), 2.32 (t, *J* = 6.1 Hz, 4H). ESI-MS *m/z* 212 [*M* +Na]$^+$.

Triphenyl(3-phenylpropyl)phosphonium bromide (75). To a solution of compound **71** (412.0 mg, 2.07 mmol) in dry toluene (4.0 mL), triphenylphosphine (545.0 mg, 2.07 mmol) was added. The reaction mixture was heated at 110 °C and was stirred for 48 h at this temperature. The mixture was allowed to reach 25 °C then, it was filtered, and the obtained white solid was washed several times with toluene. The solvent residue was removed *in vacuo*. Title compound was obtained as a white solid and used in the next step without any further purification (241.0 mg, 26% yield). ^{1}H NMR (300 MHz, CDCl$_3$) δ

7.92 – 7.55 (m, 15H), 7.35 – 7.01 (m, 5H), 3.93 – 3.48 (m, 2H), 2.96 (t, J = 7.2 Hz, 2H), 1.90 (p, J = 7.6 Hz, 2H).

1-Benzyl-4-(3-phenylpropylidene)piperidine (76). To a solution of the Wittig salt **75** (245.0 mg, 0.53 mmol) in dry THF (2.0 mL) cooled at 0 °C, a solution of *n*-butyl lithium (1.6 M in hexane, 280 µL, 0.44 mmol) was added and the resulting mixture was stirred for 2 h at this temperature. Then a solution of ketone **74** in dry THF (1.0 mL) was added dropwise at 0 °C. The reaction was allowed to reach 25 °C and it was stirred for 12 h. A saturated solution of ammonium chloride was added, and the mixture was extracted with EtOAc (3 x 10 mL). The combined organic layers were dried over anhydrous sodium sulfate, filtered, and concentrated *in vacuo*. The crude was purified by column chromatography on silica gel (PE/EtOAc 5:1) to afford the title compound as a colorless oil (43.0 mg, 28% yield). ^{1}H NMR (300 MHz, CDCl$_3$) δ 7.37 – 7.20 (m, 7H), 7.21 – 7.10 (m, 3H), 5.20 – 5.13 (m, 1H), 3.50 (s, 2H), 2.69 – 2.57 (m, 2H), 2.40 (t, J = 5.7 Hz, 2H), 2.34 – 2.24 (m, 4H), 2.22 – 2.14 (m, 4H). ESI-MS *m/z* 314 [M +Na]$^+$.

4-(3-Phenylpropyl)piperidine (50g)
The title compound was obtained following the procedure described for compound **50c**, starting from amine **76** (18.0 mg, 0.06 mmol) in a mixture of EtOAc (1.0 mL) and MeOH (1.0 mL). The title compound was obtained as a yellow oil and was used in the next step without any further purification (10 mg, 82% yield). ^{1}H NMR (300 MHz, CDCl$_3$) δ 7.73 – 7.38 (m, 2H), 7.37 – 6.83 (m, 3H), 5.71 – 5.07 (brs, 1H), 3.28 (d, J = 11.8 Hz, 2H), 2.81 – 2.44 (m, 4H), 1.97 – 1.52 (m, 4H), 1.48 – 1.12 (m, 5H). ESI-MS *m/z* 226 [M +H]$^+$.

tert-Butyl 4-(phenethylamino)piperidine-1-carboxylate (78). The title compound was obtained following the procedure described for compound **70**, starting from **77** (300.0 mg, 1.51 mmol), phenylethylamine (208.63 µL, 1.66 mmol) and NaBH(OAc)$_3$ (478.0 mg, 2.26 mmol) in dry DCM (22.0 mL). The crude was purified by column chromatography on silica gel (DCM/MeOH from 40:1 to 20:1) to afford the title compound as a colorless oil (287 mg, 62% yield). ^{1}H NMR (300 MHz, CDCl$_3$) δ 7.30 – 7.10 (m, 5H), 3.98 (s, 2H), 2.91 – 2.81 (m, 2H), 2.80 – 2.67 (m, 4H), 2.56 (m, 1H), 1.83 – 1.71 (m, 2H), 1.41 (s, 9H), 1.31 – 1.09 (m, 3H). ESI-MS *m/z* 327 [M + Na]$^+$.

tert-Butyl 4-(((benzyloxy)carbonyl)(phenethyl)amino)piperidine-1-carboxylate (79). The title compound was obtained following the procedure described for compound **66**, starting from **78** (286.0 mg, 0.94 mmol), benzyl chloroformate (174.0 µL, 1.2 mmol) and sodium bicarbonate (237.0 mg, 2.8 mmol) in THF (2.5 mL) and water (1.0 mL).The crude was purified by column chromatography on silica gel (PE/EtOAc from 5:1 to 3:1) to afford the title compound as a colorless oil (410.0 mg, 99% yield).^{1}H NMR (300 MHz, CDCl$_3$) δ 7.59 – 6.94 (m, 10H), 5.18 (s, 2H), 4.28 – 4.05 (m, 3H), 3.46 – 3.21 (m, 2H), 2.99 – 2.60 (m, 4H), 1.77 – 1.50 (m, 4H), 1.48 (s, 9H). ESI-MS *m/z* 461 [M + Na]$^+$.

Benzyl phenethyl(piperidin-4-yl)carbamate (50h). The title compound was obtained follow the procedure described for the compound **50b**, starting from **79** (410.0 mg, 0.94 mmol) and TFA (300 µL), in dry DCM (30.0 mL). Compound **50h** was obtained as a yellow oil (276.0 mg, 87% yield). ^{1}H NMR (300 MHz, CD$_3$OD) δ 7.74 – 6.64 (m, 10H), 4.91 (s, 2H), 3.96 – 3.90 (m, 1H), 3.52 – 3.33 (m, 4H), 3.00 (t, J = 12.6 Hz, 2H), 2.90 – 2.76 (m, 2H), 2.34 – 1.92 (m, 2H), 1.77 (d, J = 13.6 Hz, 2H). ESI-MS m/z 361 [M + Na]$^+$.

tert-Butyl 4-((3-phenylpropyl)amino)piperidine-1-carboxylate (81). The title compound was obtained following the procedure described for compound **70**, starting from **80** (153.0 mg, 0.76 mmol), aldehyde **69** (93.0 mg, 0.69 mmol) and NaBH(OAc)$_3$ (220.0 mg, 1.0 mmol) in dry DCM (10.0 mL). The crude was purified by column chromatography on silica gel (DCM/MeOH from 40:1 to 20:1) to afford the title compound as a yellow oil (131.0 mg, 60% yield). ^{1}H NMR (300 MHz, CDCl$_3$) δ 7.31 – 7.09 (m, 5H), 4.05-3.93 (m, 2H), 2.88 – 2.45 (m, 7H), 1.93 – 1.71 (m, 4H), 1.42 (s, 9H), 1.32 – 1.11 (m, 2H). ESI-MS *m/z* [M + Na]$^+$ 341.

tert-Butyl 4-(((benzyloxy)carbonyl)(3-phenylpropyl)amino)piperidine-1-carboxylate (82). Title compound was obtained following the procedure described for compound **66**, starting from **81** (131.0 mg, 0.41 mmol), benzyl chloroformate (91.2 mg, 0.54 mmol) and sodium bicarbonate (91.3 mg, 0.54 mmol) in THF (1.0 mL) and water (500 µL). The crude was purified by column chromatography on silica gel (PE/EtOAc from 5:1 to 3:1) to afford the title compound as a colorless oil (165.0 mg, 88% yield). ^{1}H NMR (300 MHz, CDCl$_3$) δ 7.47 – 7.03 (m, 10H), 5.14 (s, 2H), 4.33 – 4.02 (m, 3H), 3.34 – 3.02 (m, 2H), 2.86 – 2.44 (m, 4H), 1.99 – 1.75 (m, 2H), 1.72 – 1.51 (m, 4H), 1.48 (s, 9H). ESI-MS *m/z* [M + Na]$^+$ 475.

Benzyl (3-phenylpropyl)(piperidin-4-yl)carbamate (50i). The title compound was obtained following the procedure described for the compound **6b,** starting from **82** (165 mg, 0.37 mmol) and TFA (330 µL) in dry DCM (9.0 mL). After purification, compound **50i** was obtained as a yellow oil (130.0 mg, 99% yield). ^{1}H NMR (300 MHz, CDCl$_3$) δ 7.55 – 7.00 (m, 10H), 5.13 (s, 2H), 4.16 – 3.92 (brs, 1H), 3.33 – 2.96 (m, 4H), 2.74 – 2.48 (m, 4H), 2.46 – 2.37 (m, 1H), 1.96 – 1.79 (m, 2H), 1.75 – 1.50 (m, 4H). ESI-MS *m/z* 375 [M + Na]$^+$.

3-(3-Carbamoyl-5-methylfuran-2-yl)phenyl-(((benzyloxy)carbonyl)(phenethyl)amino)piperidine-1-carboxylate (83). To a solution of **49a** (18.0 mg, 0.083 mmol) in dry DCM (4.0 mL) under N$_2$ atmosphere cooled to 0 °C, TEA (34 µL, 0.25 mmol) and 4-nitrophenyl chloroformate (25.0 mg, 0.12 mmol) were added. The mixture was kept for 2 h at 0 °C. After this time, a solution of the amine **50h** (41.0 mg, 0.12 mmol) in dry DCM (1.5 mL) was added. The reaction was allowed to reach 25 °C and was stirred for 2 h. Water was added, and the mixture was extracted with DCM (3 x 10 mL). The combined organic layers were dried over sodium sulfate, filtered and concentrated. The crude was purified by column chromatography on silica gel (DCM/MeOH from 90:1 to 70:1) to afford the title compound as a colorless oil (31.0 mg, 64% yield). ^{1}H NMR (300 MHz, CDCl$_3$) δ 7.67 (dd, J = 7.8, 1.7, Hz, 1H), 7.62 – 7.55 (m, 1H), 7.49 – 7.24 (m, 5H), 7.31 – 7.15 (m, 4H), 7.16 – 7.04 (m, 3H), 6.31 (s, 1H), 5.79 (brs, 2H), 5.19 (s, 2H), 4.48 – 4.27 (m, 2H), 4.22 – 4.17 (m, 1H), 3.43 – 3.30 (m, 2H), 3.14 – 2.77 (m, 4H), 2.33 (s, 3H), 1.82 – 1.62 (m, 4H). ESI-MS *m/z* 604 [M + Na]$^+$.

3-(3-Carbamoyl-5-methylfuran-2-yl)phenyl 4-(((benzyloxy)carbonyl)(3-phenylpropyl)amino)piperidine-1-carboxylate (84). The title compound was prepared according with the procedure described for **83**, starting from **49a** (15.0 mg, 0.07 mmol), 4-nitrophenyl chloroformate (21.0 mg, 0.10 mmol), TEA (30.0 µL, 0.21 mmol) amine **50i** (36.5 mg, 0.10 mmol) in dry DCM (6.0 mL). The crude was purified by column chromatography on silica gel (DCM/MeOH from 70:1 to 60:1) to afford the title compound as an amorphous white solid (21.0 mg, 51% yield). ^{1}H NMR (300 MHz, CDCl$_3$) δ 7.76 – 7.53 (m, 2 H), 7.49 – 7.02 (m, 12 H), 6.32 (s, 1H), 5.76 – 5.59 (brs, 2H),

5.15 (s, 2H), 4.35 (t, J = 15.0 Hz, 2H), 4.23 – 4.04 (m, 1H), 3.34 – 3.08 (m, 2H), 3.06 – 2.80 (m, 2H), 2.68 – 2.46 (m, 2H), 2.34 (s, 3H), 2.00 – 1.60 (m, 6H). ESI-MS m/z 596 [M + H]$^+$; 618 [M + Na]$^+$.

Benzyl 5-methyl-2-(3-((((6-phenylhexyl)carbamoyl)oxy)phenyl)furan-3-carboxylate (85)
The title compound was prepared according to the procedure described for **83a**, starting from **49f** (77.0 mg, 0.25 mmol), 4-nitrophenyl chloroformate (74.0 mg, 0.37 mmol), TEA (104 µL, 0.75 mmol) and amine **50d** (65.0 mg, 0.37 mmol) in dry DCM (9.0 mL). The crude was purified by column chromatography on alumina gel (PE/EtOAc 8:1 to 5:1) to afford the title compound as an amorphous white solid (21.0 mg, 16% yield). ^{1}H NMR (300 MHz, CDCl$_3$) δ 7.92 – 7.76 (m, 1H), 7.54 – 7.47 (m, 1H), 7.41 – 7.10 (m, 11H), 6.89 – 6.77 (m, 1H), 6.46 (s, 1H), 5.27 (s, 2H), 5.03 (t, J = 5.8 Hz, 1H), 3.31 – 3.20 (m, 2H), 2.65 – 2.56 (m, 2H), 2.33 (s, 3H), 1.71 – 1.49 (m, 4H), 1.43 – 1.34 (m, 4H). ESI-MS m/z 534 [M + Na]$^+$.

3-(3-((Benzyloxy)carbonyl)-5-methylfuran-2-yl)phenyl 4-(3-phenylpropyl)piperazine-1-carboxylate (86). The title compound was prepared according to the procedure described for **83**, starting from **49f** (42.0 mg, 0.13 mmol), 4-nitrophenyl chloroformate (40.0 mg, 0.20 mmol), TEA (57 µL, 0.40 mmol) and amine **50f** (42.0 mg, 0.20 mmol) in dry DCM (6.0 mL). The crude was purified by column chromatography on alumina gel (PE/EtOAc 4:1 to 2:1) to afford the title compound as an amorphous white solid (21.0 mg, 64% yield). ^{1}H NMR (300 MHz, CDCl$_3$) δ 7.88 (dd, J = 7.9, 1.3 Hz, 1H), 7.77 (t, J = 2.0 Hz, 1H), 7.45 – 7.08 (m, 12H), 6.46 (d, J = 1.3 Hz, 1H), 5.28 (s, 2H), 3.67 (d, J = 28.6 Hz, 4H), 2.68 (t, J = 7.7 Hz, 2H), 2.58 – 2.40 (m, 6H), 2.33 (s, 3H), 1.94 – 1.81 (m, 2H).

3-(3-carbamoyl-5-methylfuran-2-yl)phenyl (6-(4-methylpiperazin-1-yl)hexyl)carbamate (41a). The title compound was prepared according to the procedure described for **83**, starting from **49a** (15.0 mg, 0.07 mmol), 4-nitrophenyl chloroformate (20.0 mg, 0.10 mmol), TEA (30 µL, 0.46 mmol) and amine **50a** (20.0 mg, 0.10 mmol) in dry DCM (4.0 mL). The crude was purified by column chromatography on silica gel (EtOAc/MeOH/TEA 8:1:0.1) to afford the title compound as a colorless oil (5.2 mg, 17% yield). ^{1}H NMR (300 MHz, CDCl$_3$) δ 7.73 – 7.68 (m, 1H), 7.65 (t, J = 2.0 Hz, 1H), 7.39 (t, J = 8.0 Hz, 1H), 7.10 – 7.04 (m, 1H), 6.39 (s, 1H), 3.19 (t, J = 6.8 Hz, 2H), 3.04 – 2.79 (m, 8H), 2.77 – 2.65 (m, 2H), 2.54 (s, 3H), 2.36 (s, 3H), 1.69 – 1.51 (m, 4H), 1.47 – 1.35 (m, 4H). ^{13}C NMR (75 MHz, CDCl$_3$) 165.7, 154.5, 151.9, 151.7, 151.0, 131.0, 129.6, 122.1, 121.1, 117.8, 108.3, 108.1, 58.7, 54.8, 52.9, 45.9, 45.7, 41.1, 29.7, 27.0, 26.5, 13.5. ESI-MS m/z 442 [M +H]$^+$.

3-(3-Carbamoyl-5-methylfuran-2-yl)phenyl (1-phenethylpiperidin-4-yl)carbamate (41b). The title compound was prepared according to the procedure described for **83**, starting from **49a** (40.0 mg, 0.17 mmol), 4-nitrophenyl chloroformate (51.0 mg, 0.25 mmol), TEA (71 µL, 0.51 mmol) and amine **50b** (51.0 mg, 0.25 mmol) in dry DCM (14.0 mL). The crude was purified by column chromatography on silica gel (EtOAc/MeOH from 20:1 to 10:1) to afford the title compound as an amorphous white solid (38.7 mg, 51% yield). ^{1}H NMR (300 MHz, DMSO-d_6) δ 7.76 (dd, J = 20.2, 7.9 Hz, 2H), 7.67 (d, J = 8.3 Hz, 2H), 7.38 (t, J = 8.0 Hz, 1H), 7.31 – 7.14 (m, 5H), 7.06 (d, J = 8.1 Hz, 1H), 6.49 (s, 1H), 4.04 (s, 1H), 2.89 (d, J = 11.0 Hz, 2H), 2.74 – 2.66 (m, 2H), 2.32 (s, 3H), 2.07 – 1.89 (m, 3H), 1.84 – 1.72 (m, 2H), 1.54 – 1.40 (m, 4H). ^{13}C NMR (75 MHz, DMSO-d_6) 165.4, 153.9, 151.3, 151.2, 150.5, 141.0, 131.6, 129.5, 129.1, 128.7, 126.2, 123.5, 122.0, 120.3, 119.7,

109.0, 60.1, 52.3, 48.8, 33.4, 32.1, 29.5, 29.1, 22.5. ESI-MS *m/z* 448 [*M* +H]$^+$, 470 [*M* + Na]$^+$. HRMS(ESI)

3-(3-Carbamoyl-5-methylfuran-2-yl)phenyl (1-(3-phenylpropyl)piperidin-4-yl)carbamate (41c). The title compound was prepared according to the procedure described for **83**, starting from **49a** (8.0 mg, 0.04 mmol), 4-nitrophenyl chloroformate (11.0 mg, 0.06 mmol), TEA (20 μL, 0.15 mmol) and amine **50c** (12.0 mg, 0.06 mmol) in dry DCM (2.0 mL). The crude was purified by column chromatography on silica gel (18.0 mg, 66% yield). ^{1}H NMR (300 MHz, CD$_3$OD) δ 7.71 (dd, *J* = 7.9, 1.7, Hz, 1H), 7.67 - 7.63 (m, 1H), 7.39 (t, *J* = 8.0 Hz, 1H), 7.32 – 7.13 (m, 5H), 7.07 – 7.03 (m, 1H), 6.39 (s, 1H), 3.72 – 3.52 (m, 1H), 3.27 – 3.16 (m, 2H), 2.81 – 2.48 (m, 6H), 2.35 (s, 3H), 2.16 – 2.01 (m, 2H), 1.98 – 1.85 (m, 2H), 1.83 – 1.63 (m, 2H). ^{13}C NMR (75 MHz, CD$_3$OD) δ 167.7, 154.9, 151.7, 151.2, 151.0, 140.9, 131.4, 128.8, 128.1, 128.0, 125.8, 123.6, 121.4, 120.0, 118.0, 107.7, 107.6, 56.8, 51.4, 32.7, 29.8, 26.8, 11.8, 11.8. ESI-MS *m/z* 484 [*M* + Na]$^+$. HRMS(ESI) *m/z* [*M* + H]$^+$ calcd for [C$_{27}$H$_{32}$N$_3$O$_4$]$^+$ 462.2387, found 462.2374.

3-(3-Carbamoyl-5-methylfuran-2-yl)phenylmethyl-1-phenethylpiperidin-4-amine carbamate (41d). The title compound was prepared according to the procedure described for **83**, starting from **49a** (25.0 mg, 0.11 mmol), 4-nitrophenyl chloroformate (33.0 mg, 0.16 mmol), TEA (0.33 mmol, 45 μL) and amine **50e** (32.0 mg, 0.15 mmol) in dry DCM (5.0 mL). The crude was purified by column chromatography on silica gel (EtOAc/MeOH from 50:1 to 20:1) to afford the title compound as an amorphous white solid (18.7 mg, 37% yield). ^{1}H NMR (300 MHz, CD$_3$OD) δ 7.74 (d, *J* = 7.9 Hz, 1H), 7.67 (s, 1H), 7.40 (t, *J* = 8.0 Hz, 1H), 7.32 – 7.14 (m, 5H), 7.12 – 7.01 (m, 1H), 6.39 (s, 1H), 4.06 (d, *J* = 18.2 Hz, 1H), 3.15 (d, *J* = 11.4 Hz, 2H), 3.02 (s, 3H), 2.94 – 2.72 (m, 2H), 2.63 (dd, *J* = 10.8, 5.7 Hz, 2H), 2.35 (s, 3H), 2.20 (s, 2H), 2.04 – 1.66 (m, 4H). ^{13}C NMR (75 MHz, CD$_3$OD) δ 168.6, 154.9, 151.3, 141.1, 139.7, 139.6, 134.5, 132.7, 129.1, 128.2, 128.1, 126.6, 126.54, 125.8, 125.7, 121.9, 121.3, 59.8, 52.5, 32.8, 28.2, 13.5. ESI-MS *m/z* 484 [*M* + Na]$^+$.

3-(3-Carbamoyl-5-methylfuran-2-yl)phenyl 4-(3-phenylpropyl)piperazine-1-carboxylate (41e). The title compound was prepared according to the procedure described for **83**, starting from **49a** (10.0 mg, 0.04 mmol), 4-nitrophenyl chloroformate (12.0 mg, 0.06 mmol), TEA (20 μL, 0.15 mmol) amine **50f** (13.0 mg, 0.06 mmol) in dry DCM (3.0 mL). The crude was purified by column chromatography on silica gel (EtOAc/MeOH 100:1) to afford the title compound as an amorphous white solid (11.8 mg, 66% yield). ^{1}H NMR (300 MHz, CDCl$_3$) δ 7.65 (dd, *J* = 7.8, Hz, 1H), 7.56 (t, *J* = 1.9 Hz, 1H), 7.39 (t, *J* = 8.0 Hz, 1H), 7.32 – 7.23 (m, 2H), 7.22 – 7.14 (m, 3H), 7.13 – 7.06 (m, 1H), 6.32 (s, 1H), 5.92 – 5.45 (brs, 2H), 3.63 (d, *J* = 31.5 Hz, 4H), 2.66 (t, *J* = 7.7 Hz, 2H), 2.53 – 2.37 (m, 6H), 2.33 (d, *J* = 1.0 Hz, 3H), 1.84 (p, *J* = 7.6, 7.2 Hz, 2H). ^{13}C NMR (75 MHz, CDCl$_3$) δ 165.2, 154.4, 152.5, 151.4, 150.6, 141.9, 131.8, 130.3, 128.4, 128.3, 126.3, 124.5, 122.9, 121.1, 118.4, 108.2, 57.8, 52.2, 44.9, 43.4, 35.6, 29.0, 16.4. ESI-MS *m/z* 470 [*M* + Na]$^+$. HRMS(ESI) *m/z* [*M* + H]$^+$ calcd for [C$_{26}$H$_{30}$N$_3$O$_4$]$^+$ 448.2231 found 448.2231, [*M* + Na]$^+$ calcd for [C$_{26}$H$_{29}$N$_3$NaO$_4$]$^+$ 470.2050, found 470.2041.

3-(3-Carbamoyl-5-methylfuran-2-yl)phenyl 4-(3-phenylpropyl)piperidine-1-carboxylate (41f). The title compound was prepared according to the procedure described for **83**, starting from **49a** (7.0 mg, 0.26 mmol), 4-nitrophenyl chloroformate (8.0 mg, 0.23 mmol), TEA (10 μL, 0.46 mmol) and amine **50g** (9.0 mg, 0.04 mmol) in dry DCM (2.0 mL). The crude was purified by column chromatography on silica gel (DCM/acetone 8:1) to afford

the title compound as a colorless oil (4.5 mg, 40% yield). ^{1}H NMR (300 MHz, CDCl$_3$) δ 7.63 (d, J = 7.5 Hz, 1H), 7.54 (d, J = 3.0 Hz, 1H), 7.50 – 7.36 (m, 2H), 7.27 (d, J = 8.3 Hz, 3H), 7.22 – 7.05 (m, 2H), 6.34 (s, 1H), 5.89 – 5.45 (brs, 2H), 4.24 (t, J = 18.4 Hz, 2H), 3.02 – 2.74 (m, 2H), 2.62 (t, J = 7.7 Hz, 2H), 2.34 (s, 3H), 1.79 – 1.59 (m, 7H), 1.33–1.21 (m, 2H). ^{13}C NMR (75 MHz, CDCl$_3$) δ 165.6, 153.5, 151.9, 151.6, 151.2, 142.4, 130.9, 129.5, 128.4, 128.3, 125.7, 124.4, 122.3, 121.7, 121.8, 108.3, 108.2, 44.9, 44.5, 36.0, 35.8, 32.2, 31.8, 29.7, 28.5. ESI-MS m/z 447 [M +H]$^+$. HRMS(ESI) m/z [M + H]$^+$ calcd for [C$_{27}$H$_{31}$N$_2$O$_4$]$^+$ 447.2278, found 447.2264; [M + Na]$^+$; calcd for [C$_{27}$H$_{30}$N$_2$NaO$_4$]$^+$ 469.2098, found 469.2079.

3-(3-Carbamoyl-5-methylfuran-2-yl)phenyl 4-(phenethylamino)piperidine-1-carboxylate (41g). The title compound was obtained according to the procedure described for compound **50c**, starting from **83** (31.0 mg, 0.06 mmol) in a mixture of EtOAc (1.0 mL) and MeOH (2.0 mL). The crude was purified by column chromatography on silica gel (DCM/MeOH/NH$_4$OH 10:1:0.1) to afford the title compound as an amorphous white solid (12.0 mg, 54% yield). ^{1}H NMR (300 MHz, CDCl$_3$) δ 7.67 – 7.62 (m, 1H), 7.56 (d, J = 1.8 Hz, 1H), 7.42 – 7.35 (m, 1H), 7.34 – 7.25 (m, 2H), 7.25 – 7.18 (m, 3H), 7.08 (dd, J = 8.2, 2.5 Hz, 1H), 6.31 (s, 1H), 5.95 – 5.78 (brs, 2H), 4.28 – 4.09 (m, 2H), 3.06 (t, J = 12.5 Hz, 1H), 3.00 – 2.90 (m, 4H), 2.89 – 2.81 (m, 2H), 2.81 – 2.71 (m, 1H), 2.32 (s, 3H), 2.00 – 1.88 (m, 2H), 1.42 (d, J = 11.7 Hz, 2H). ^{13}C NMR (75 MHz, CDCl$_3$) δ 165.8, 153.5, 151.9, 151.5, 151.2, 139.4, 131.0, 129.5, 128.7, 128.6, 126.4, 124.4, 122.1, 121.1, 117.8, 108.2, 54.6, 47.8, 43.3, 43.0, 36.0, 32.0, 31.6, 13.4. ESI-MS m/z 470 [M + Na]$^+$. HRMS(ESI) m/z [M + H]$^+$ calcd for [C$_{26}$H$_{30}$N$_3$O$_4$]$^+$ 448.2231, found 448.2213.

3-(3-Carbamoyl-5-methylfuran-2-yl)phenyl 4-((3-phenylpropyl)amino)piperidine-1-carboxylate (41h). The title compound was obtained according to the procedure described for compound **50c**, starting from **84** (21.0 mg, 0.035 mmol) in a mixture of EtOAc (1.5 mL) and MeOH (1.5 mL). The crude was purified by column chromatography on silica gel (DCM/MeOH/NH$_4$OH 10:1:0.1) to afford the title compound as an amorphous white solid (12.0 mg, 74% yield). ^{1}H NMR (300 MHz, CDCl$_3$) δ 7.63 (dd, J = 7.8, 1.7, 1H), 7.58 (dd, J = 2.3, 1.6 Hz, 1H), 7.38 (t, J = 8.0 Hz, 1H), 7.28 – 7.22 (m, 2H), 7.21 – 7.14 (m, 3H), 7.10 – 7.04 (m, 1H), 6.30 (s, 1H), 6.14 – 5.93 (m, 2H), 4.31 – 4.13 (m, 1H), 3.07 – 2.84 (m, 4H), 2.83 – 2.76 (m, 2H), 2.67 (t, J = 7.6 Hz, 2H), 2.32 (s, 3H), 2.07 – 1.93 (m, 5H), 1.62-158 (m, 2H). ^{13}C NMR (75 MHz, CDCl$_3$) δ 166.0, 153.5, 151.9, 151.4, 151.2, 141.0, 131.1, 129.5, 128.5, 128.3, 126.1, 124.3, 122.1, 120.9, 117.8, 108.2, 54.8, 45.3, 43.2, 42.9, 33.2, 30.7, 30.2, 29.9, 13.4. ESI-MS m/z 484 [M + Na]$^+$. HRMS(ESI) m/z [M + H]$^+$ calcd for [C$_{27}$H$_{32}$N$_3$O$_4$]$^+$ 462.2387, found 462.2372.

3-(3-Carbamoyl-5-methylthiophen-2-yl)phenyl (1-phenethylpiperidin-4-yl)carbamate (41i). The title compound was prepared according to the procedure described for **83**, starting from **49b** (37.0 mg, 0.16 mmol), 4-nitrophenyl chloroformate (47.0 mg, 0.23 mmol), TEA (70 μL, 0.51 mmol) and amine **50b** (46.0 mg, 0.23 mmol) in dry DCM (12.0 mL). The crude was purified by column chromatography on silica gel (EtOAc/MeOH 30:1) to afford the title compound as an amorphous white solid (28.0 mg, 38% yield). ^{1}H NMR (300 MHz, DMSO-d_6) δ 7.81 (d, J = 7.7 Hz, 1H), 7.60 (s, 1H), 7.36 (t, J = 8.0 Hz, 1H), 7.30 – 7.13 (m, 7H), 7.10 – 7.02 (m, 1H), 6.94 (s, 1H), 2.89 (d, J = 11.1 Hz, 2H), 2.70 (t, J = 7.8 Hz, 2H), 2.43 (s, 3H), 2.33 – 2.29 (m, 1H), 2.06 – 1.95 (m, 3H), 1.79 (d, J = 12.4 Hz, 2H), 1.53 – 1.38 (m, 4H). ^{13}C NMR (75 MHz, DMSO-d_6) δ 166.7, 153.8, 141.0, 139.6, 139.0, 134.9, 134.7, 129.8, 129.1, 128.7, 127.7, 126.2, 125.3, 125.2, 121.6,

60.1, 52.3, 48.8, 33.4, 32.1, 31.6, 29.5, 22.5. ESI-MS m/z 486 $[M + \text{Na}]^+$. HRMS(ESI) m/z $[M + \text{H}]+$ calcd for $[\text{C}_{26}\text{H}_{30}\text{N}_3\text{O}_3\text{S}]^+$ 464.2002, found 464.1990.

3-(3-Carbamoyl-5-methylthiophen-2-yl)phenylmethyl(1-phenethylpiperidin-4-yl)carbamate (41j). The title compound was prepared according to the procedure described for **83**, starting from **49b** (40.0 mg, 0.17 mmol), 4-nitrophenyl chloroformate (51.0 mg, 0.25 mmol), TEA (71 μL, 0.51 mmol) and amine **50e** (54.5 mg, 0.25 mmol) in dry DCM (10.0 mL). The crude was purified by column chromatography on silica gel (EtOAc/MeOH from 50:1 to 20:1) to afford the title compound as an amorphous white solid (48.6 mg, 60% yield). ^{1}H NMR (300 MHz, CD$_3$OD) δ 7.44 – 7.32 (m, 2H), 7.31 – 7.14 (m, 6H), 7.13 – 7.07 (m, 1H), 6.99 – 6.95 (m, 1H), 4.18 – 3.94 (m, 1H), 3.16 (d, J = 11.5 Hz, 2H), 3.04 – 2.89 (m, 3H), 2.82 (dd, J = 10.6, 5.7 Hz, 2H), 2.68 – 2.60 (m, 2H), 2.48 – 2.45 (m, 3H), 2.28 – 2.13 (m, 2H), 2.02 – 1.71 (m, 4H). ^{13}C NMR (75 MHz, CD$_3$OD) δ 168.6, 154.9, 151.4, 141.1, 139.7, 139.6, 134.5, 132.7, 129.1, 128.2, 128.1, 126.6, 126.5, 125.8, 125.7, 121.9, 121.3, 59.9, 52.5, 32.8, 28.2, 13.5. ESI-MS m/z 500 $[M + \text{Na}]^+$.

3-(3-Carbamoyl-5-methylthiophen-2-yl)phenyl-4-(3-phenylpropyl)piperazine-1-carboxylate (41k). The title compound was prepared according to the procedure described for **83**, starting from **49b** (10.0 mg, 0.04 mmol), 4-nitrophenyl chloroformate (12.0 mg, 0.06 mmol), TEA (20 μL, 0.15 mmol) amine **50f** (12.0 mg, 0.06 mmol) in dry DCM (3.0 mL). The crude was purified by column chromatography on silica gel (EtOAc/MeOH from 100:1 to 80:1) to afford the title compound as an amorphous yellow solid (14.2 mg, 77% yield) ^{1}H NMR (300 MHz, CDCl$_3$) 7.40 (t, J = 7.8 Hz, 1H), 7.36 – 7.21 (m, 5H), 7.24 – 7.12 (m, 3H), 7.12 (t, J = 2.3 Hz, 1H), 5.57 – 5.47 (brs, 2H), 3.66 (d, J = 30.5 Hz, 4H), 2.67 (t, J = 7.6 Hz, 2H), 2.59 – 2.46 (m, 6H), 2.46 (s, 3H), 1.97 – 1.78 (m, 2H).^{13}C NMR (75 MHz, CDCl$_3$) δ 166.8, 153.2, 151.4, 141.7,141.4, 139.3, 134.1, 132.4, 129.7, 128.4, 127.7, 126.9, 125.9, 123.1, 122.2, 57.7, 52.7, 52.6, 44.7, 43.7, 33.5, 29.7, 28.1. ESI-MS m/z 486 $[M + \text{Na}]^+$. HRMS(ESI) m/z $[M + \text{H}]^+$ calcd for $[\text{C}_{26}\text{H}_{30}\text{N}_3\text{O}_3\text{S}]^+$ 464.2002, found 464.1996, $[M + \text{Na}]^+$; calcd for $[\text{C}_{26}\text{H}_{29}\text{N}_3\text{O}_3\text{NaS}]^+$ 486.1822, found 486.1815.

3-(3-Carbamoyl-1H-pyrrol-1-yl)phenyl (1-phenethylpiperidin-4-yl)carbamate (41l)
The title compound was prepared according to the procedure described for compound **83**, starting from **49c** (40.0 mg, 0.20 mmol), 4-nitrophenyl chloroformate (60.0 mg, 0.30 mmol), TEA (83 μL, 0.60 mmol) and amine **50b** (61.0 mg, 0.30 mmol) in dry DCM (14.0 mL). The crude was purified by column chromatography on silica gel (EtOAc/MeOH from 20:1 to 10:1) to afford the title compound as an amorphous white solid (14.7 mg, 17% yield). ^{1}H NMR (300 MHz, DMSO-d_6) δ 7.97 – 7.83 (m, 1H), 7.52 – 7.34 (m, 5H), 7.32 – 7.11 (m, 4H), 7.08 – 6.97 (m, 1H), 6.96 – 6.81 (m, 2H), 6.64 (s, 1H), 3.49 (s, 1H), 2.91 (d, J = 11.0 Hz, 2H), 2.71 (t, J = 7.8 Hz, 2H), 2.56 – 2.50 (m, 2H), 2.14 – 1.97 (m, 3H), 1.84 – 1.72 (m, 2H), 1.56 – 1.38 (m, 2H). ^{13}C NMR (75 MHz, DMSO-d_6) δ 165.5, 153.7, 152.5, 140.9, 140.5, 130.9, 129.1, 128.7, 126.3, 122.7, 121.8, 120.4, 119.9, 116.4, 113.8, 110.9, 60.1, 52.3, 48.8, 33.4, 32.0, 31.2. ESI-MS m/z 433 $[M + \text{H}]^+$, 456 $[M + \text{Na}]^+$. HRMS(ESI) m/z $[M + \text{H}]^+$ calcd for $[\text{C}_{25}\text{H}_{29}\text{N}_4\text{O}_3]^+$ 433.2234, found 433.2216.

3-(3-Carbamoyl-1H-pyrrol-1-yl)phenylmethyl-1-phenethylpiperidin-4-yl)carboxylate (41m). The title compound was prepared according to the procedure described for **83**, starting from **49c** (20.0 mg, 0.10 mmol), 4-nitrophenyl chloroformate (30.0 mg, 0.15 mmol), TEA (41 μL, 0.30 mmol) and amine **50e** (33.0 mg, 0.15 mmol) in dry DCM (6.0

mL). The crude was purified by column chromatography on silica gel (EtOAc/MeOH from 50:1 to 20:1) to afford the title compound as an amorphous white solid (13.8 mg, 31% yield). ^{1}H NMR (300 MHz, CD$_3$OD) δ 7.81 (s, 1H), 7.49 (t, J = 8.1 Hz, 1H), 7.42 – 7.31 (m, 3H), 7.30 – 7.14 (m, 5H), 7.12 – 7.06 (m, 1H), 6.73 (s, 1H), 4.21 – 3.98 (m, 1H), 3.19 (d, J = 11.5 Hz, 2H), 3.03 (s, 3H), 2.89 – 2.76 (m, 2H), 2.73 – 2.59 (m, 2H), 2.24 (d, J = 12.3 Hz, 2H), 2.05 – 1.71 (m, 4H). ^{13}C NMR (75 MHz, CD$_3$OD) δ 172.2, 158.5, 156.31, 144.6, 143.7, 134.2, 132.2, 132.1, 129.8, 126.0, 124.8, 124.2, 123.6, 120.9, 118.0, 114.0, 63.7, 56.4, 36.6, 32.5, 32.2, 31.8. ESI-MS m/z 469 [M + Na]$^+$

3-(3-Carbamoyl-1H-pyrrol-1-yl)phenyl 4-(3-phenylpropyl)piperazine-1-carboxylate (41n). The title compound was prepared according to the procedure described for **83**, starting from **49c** (10.0 mg, 0.05 mmol), 4-nitrophenyl chloroformate (15.0 mg, 0.075 mmol), TEA (20 µL, 0.15 mmol) and amine **50f** (15.0 mg, 0.075 mmol) in dry DCM (6.0 mL). The crude was purified by column chromatography on silica gel (EtOAc/MeOH 30:1) to afford the title compound as an amorphous yellow solid (10.8 mg, 50% yield). ^{1}HNMR (300 MHz, CDCl$_3$) δ 7.67 (d, J = 2.0 Hz, 1H), 7.45 (t, J = 8.1 Hz, 1H), 7.37 – 7.26 (m, 4H), 7.27 – 7.18 (m, 3H), 7.11 (dd, J = 8.1, 2.2 Hz, 1H), 7.06 (s, 1H), 6.58 (s, 1H), 5.82 – 5.52 (brs, 2H), 3.67 (dd, J = 28.5, 6.1 Hz, 4H), 2.70 (t, J = 7.7 Hz, 2H), 2.58 – 2.50 (m, 4H), 2.46 (t, J = 7.5 Hz, 2H), 1.88 (p, J = 7.5 Hz, 2H). ^{13}CNMR (75 MHz, CDCl$_3$) δ 166.2, 153.1, 152.3, 142.0, 140.6, 130.3, 128.4, 128.3, 125.8, 122.56, 120.8, 120.5, 120.0, 117.5, 114.8, 109.6, 57.8, 52.9, 52.7, 44.6, 44.1, 33.5, 28.4. ESI-MS m/z 433 [M + H]$^+$. HRMS(ESI) m/z [M + H]$^+$ calcd for [C$_{25}$H$_{29}$N$_4$O$_3$]$^+$ 433.2234, found 433.2221.

3-(4-Carbamoyl-1H-1,2,3-triazol-1-yl)phenyl (6-phenylhexyl)carbamate (41o). The title compound was prepared according to the procedure described for **83**, starting from **49d** (20.0 mg, 0.10 mmol), 4-nitrophenyl chloroformate (30.0 mg, 0.15 mmol), TEA (41 µL, 0.30 mmol) amine **50d** (26.0 mg, 0.15 mmol) in dry DCM (7.0 mL). The crude was purified by column chromatography on silica gel (DCM/MeOH 100:1) to afford the title compound as a white solid (17.0 mg, 23% yield). ^{1}H NMR (300 MHz, DMSO-d_6) δ 9.27 (s, 1H), 8.02 (s, 1H), 7.91 (t, J = 5.6 Hz, 1H), 7.86 – 7.71 (m, 2H), 7.66 – 7.53 (m, 2H), 7.41 – 7.08 (m, 5H), 4.41 (t, J = 5.2 Hz, 1H), 3.05 (q, J = 6.7 Hz, 2H), 2.62 – 2.51 (m, 2H), 1.67 – 1.38 (m, 4H), 1.39 – 1.25 (m, 4H). ^{13}C NMR (75 MHz, DMSO-d_6) δ 163.6, 161.6, 154.3, 152.3, 144.3, 142.7, 137.3, 131.1, 128.8, 128.7 (2C), 128.2, 126.0, 122.9, 35.5, 31.4, 29.5, 28.8, 26.5. ESI-MS m/z 408 [M + H]$^+$. HRMS(ESI) m/z [M + H]$^+$ calcd for [C$_{22}$H$_{26}$N$_5$O$_3$]$^+$ 408.2030, found 408.2024, [M + Na]$^+$ calcd for [C$_{22}$H$_{25}$N$_5$NaO$_3$]$^+$ 430.1850 found 430.1843.

3-(4-Carbamoyl-1H-1,2,3-triazol-1-yl)phenyl 4-(3-phenylpropyl)piperazine-1-carboxylate (41p). The title compound was prepared according to the procedure described for **83**, starting from **49d** (20.0 mg, 0.10 mmol), 4-nitrophenyl chloroformate (30.0 mg, 0.30 mmol), TEA (41 µL, 0.15 mmol) and a solution of the amine **50f** (26.0 mg, 0.15 mmol) in dry DCM (12.0 mL). The crude was purified by column chromatography on silica gel (DCM/MeOH from 70:1 to 10:1) to afford the title compound as an amorphous white solid (14.0 mg, 38% yield). ^{1}H NMR (300 MHz, DMSO-d_6) δ 9.25 (s, 1H), 8.06 – 7.95 (m, 2H), 7.84 – 7.75 (m, 2H), 7.65 – 7.52 (m, 2H), 7.34 – 7.08 (m, 5H), 3.63 – 3.36 (m, 4H), 2.58 (t, J = 7.7 Hz, 2H), 2.44 – 2.35 (m, 4H), 2.30 (t, J = 7.2 Hz, 2H), 1.72 (p, J = 7.6 Hz, 2H). ^{13}C NMR (75 MHz, DMSO-d_6) δ 161.6, 152.8, 152.4, 144.7, 142.4, 137.3, 131.1, 128.8, 128.7, 126.1, 125.4, 123.0, 117.4, 114.7, 57.5, 52.8, 44.6, 44.2, 33.3, 28.5. ESI-MS m/z 408 [M + H]$^+$. HRMS(ESI) m/z [M + H]$^+$ calcd for [C$_{23}$H$_{27}$N$_6$O$_3$]$^+$ 435.2139, found 435.2126.

*5-Methyl-2-(3-(((6-phenylhexyl)carbamoyl)oxy)phenyl)furan-3-carboxylic acid (**41q**)*
The title compound was obtained according to the procedure described for compound
50c, starting from **85** (21.0 mg, 0.04 mmol) in methanol (30.0 mL). The crude was
purified by column chromatography on silica gel (PE/EtOAc 2:1 to 1:1) to afford the title
compound as a brown solid (5.17 mg, 13% yield). ^{1}H NMR (300 MHz, CDCl$_3$) δ 7.88 –
7.79 (m, 1H), 7.79 – 7.72 (m, 1H), 7.39 (t, J = 8.0 Hz, 1H), 7.33 – 7.21 (m, 3H), 7.22 –
7.10 (m, 3H), 6.46 (s, 1H), 5.14 – 5.05 (brs, 1H), 3.25 (q, J = 6.7 Hz, 2H), 2.60 (t, J = 7.7
Hz, 2H), 2.34 (s, 3H), 1.70 – 1.50 (m, 4H), 1.37– 1.20 (m, 4H). ^{13}C NMR (75 MHz,
CDCl$_3$) δ 167.8, 156.1, 154.4, 151.6, 150.8, 142.6, 130.9, 128.9, 128.4, 128.7, 125.6,
125.2, 122.5, 121.4, 113.8, 109.2, 41.2, 35.8, 31.3, 29.7, 28.9, 26.6, 13.3. ESI-MS m/z
422[M + H]$^+$. HRMS(ESI) m/z [M + Na]$^+$; calcd for [C$_{25}$H$_{27}$NNaO$_5$]$^+$ 444.1781, found
444.1774

5-Methyl-2-(3-((4-(3-phenylpropyl)piperazine-1-carbonyl)oxy)phenyl)furan-3-
*carboxylic acid (**41r**).* The title compound was obtained according to the procedure
described for compound **50c**, starting from **86** (21.0 mg, 0.04 mmol) in methanol (30.0
mL). The crude was purified by column chromatography on silica gel (DCM/MeOH from
60:1 to 40:1) to afford the title compound as a brown solid (15.3 mg, 39%yield). ^{1}H NMR
(300 MHz, CDCl$_3$) δ 9.39 – 8.33 (brs, 1H), 7.82 (s, 1H), 7.73 – 7.65 (m, 1H), 7.37 (t, J =
8.0 Hz, 1H), 7.31 – 7.21 (m, 2H), 7.20 – 7.04 (m, 4H), 6.44 (t, J = 1.0 Hz, 1H), 3.95 –
3.58 (m, 4H), 2.82 – 2.68 (m, 4H), 2.66 – 2.54 (m, 4H), 2.33 (s, 3H), 1.97 – 1.85 (m, 2H).
^{13}C NMR (75 MHz, CDCl$_3$) δ 162.2, 148.5, 148.0, 146.0, 145.4, 135.7, 126.6, 123.7,
123.3, 123.2, 123.1, 120.9, 119.6, 116.8, 116.5, 111.7, 104.4, 51.9, 46.6, 46.4, 37.8, 37.2,
28.1, 21.1. ESI-MS m/z 449 [M + H]$^+$, 472 [M + Na]$^+$. HRMS(ESI) m/z [M + H]$^+$ calcd
for [C$_{26}$H$_{29}$N$_2$O$_5$]$^+$ 449.2071, found 449.2062.

*3-(2H-Tetrazol-5-yl)phenyl (6-phenylhexyl)carbamate (**41s**).* The title compound was
prepared according to the procedure described for **83**, starting from **49e** (15.0 mg, 0.10
mmol), 4-nitrophenyl chloroformate (28.0 mg, 0.15 mmol), TEA (41 μL, 0.27 mmol) and
amine **50d** (26.0 mg, 0.15 mmol) in dry DCM (3.0 mL). The crude was purified by
column chromatography on silica gel (DCM/MeOH/formic acid 30:1:0.1) to afford the
title compound as a white solid (yield 17.3 mg, 52%). ^{1}H NMR (300 MHz, CD$_3$OD) δ
7.91 – 7.82 (m, 1H), 7.80 – 7.77 (m, 1H), 7.57 (t, J = 8.0 Hz, 1H), 7.36-7.31 (m, 1H),
7.26 – 7.07 (m, 5H), 3.24 – 3.13 (m, 2H), 2.60 (t, J = 8.5, 6.8 Hz, 2H), 1.70 – 1.51 (m,
4H), 1.47 – 1.32 (m, 4H). ^{13}C NMR (75 MHz, CD$_3$OD) δ 155.9, 155.2, 152.0, 142.5,
130.1, 128.0, 127.8, 125.6, 125.2, 124.5, 123.4, 120.2, 40.6, 35.4, 31.7, 29.6, 28.6, 26.3.
ESI-MS m/z 366 [M + H]$^+$. HRMS(ESI) m/z [M + H]$^+$ calcd for [C$_{20}$H$_{24}$N$_5$O$_2$]$^+$ 366.1925,
found 366.1921, [M + Na]$^+$ calcd for [C$_{20}$H$_{23}$N$_5$NaO$_2$]$^+$ 388.1744, found 388.1734.

*3-(2H-Tetrazol-5-yl)phenyl 4-(3-phenylpropyl)piperazine-1-carboxylate(**41t**).* The title
compound was prepared according to the procedure described for **83**, starting from **49e**
(25.0 mg, 0,154 mmol), 4-nitrophenyl chloroformate (47.0 mg, 0.23 mmol), TEA (65 μL,
0.46 mmol) and amine **50f** (47.0 mg 0.23 mmol) in dry DCM (10.0 mL). The crude was
purified by column chromatography on silica gel (DCM/MeOH/formic acid 30:1:0.1) to
afford the title compound as an amorphous white solid (yield 32.0 mg, 53%). ^{1}H NMR
(300 MHz, CD$_3$OD) δ 8.14 (s, 1H), 7.91 (dt, J = 7.8, 1.3 Hz, 1H), 7.82 (t, J = 1.9 Hz, 1H),
7.51 (t, J = 8.0 Hz, 1H), 7.32 – 7.09 (m, 5H), 4.04 – 3.66 (m, 4H), 3.40 – 3.23 (m, 4H),
3.18 – 3.01 (m, 2H), 2.68 (t, J = 7.4 Hz, 2H), 2.17 – 1.95 (m, 2H). ^{13}C NMR (75 MHz,
CD$_3$OD) δ 160.6, 154.4, 152.9, 141.4, 131.2, 130.5, 129.7, 129.4, 127.4, 125.1, 124.1,

121.2, 57.8, 52.7, 42.9, 42.3, 33.45, 26.91. ESI-MS *m/z* 393 [*M* + H]$^+$, 415 [*M* + Na]$^+$. HRMS(ESI) *m/z* [*M* + H]$^+$ calcd for [C$_{21}$H$_{25}$N$_6$O$_2$]$^+$ 393.2034, found 393.2028.

9.2. Experimental section of the MAGL inhibitors 42e and 42f

1-(tert-Butyl)4,4-diethyl piperidine-1,4,4-tricarboxylate (88). A solution n-BuLi 2.5 M in hexane (1.8 mL, 4.66 mmol,) was added to a solution of DIPA (653.0 µL, 4.66 mol,) in dry THF (4.0 mL) cooled at -78 °C. The mixture was stirred for 45 min at -78 °C, then a solution of **87** (200.0 mg, 0.78 mmol) in dry THF (4.0 mL) was added dropwise and the resulting mixture was stirred for 1 h at -78°C. Thereafter, a solution of ethyl chloroformate (745.0 µL, 7.8 mmol) in dry THF (2.0 mL) was added and the reaction mixture was stirred at -78 °C for 3 h. The reaction was allowed to reach 25 °C and NH_4Cl *s.s.* (10 mL) was added. The mixture was extracted with EtOAc (3 x 10 mL) and the combined organic layers were dried over anhydrous sodium sulfate, filtered, and concentrated *in vacuo*. Title compound was obtained as a yellow oil and used in the next step without any further purification (256.0 mg, 99% yield). ^{1}H NMR (300 MHz, CDCl$_3$) δ 4.20 (q, J = 7.1 Hz, 4H), 3.49 – 3.37 (m, 4H), 2.10 – 1.97 (m, 4H), 1.44 (s, 9H), 1.25 (t, J = 7.1 Hz, 6H).

1-(tert-Butoxycarbonyl)-4-(ethoxycarbonyl)piperidine-4-carboxylic acid (89). To a solution of **88** 100.0 mg, 0.3 mmol) in ethanol (1.0 mL), a solution of 0.5N LiOH in water (300 µL, 0.30 mmol) wad added. The reaction mixture was stirred 12 h at 25 °C. Ethanol was removed and water was extracted with Et$_2$O (2 x 10 mL). Water phase was treated with 1N HCl until pH = 5 and extracted with Et$_2$O (3 x 10 mL). The combined organic layers were dried over anhydrous sodium sulfate, filtered, and concentrated *in vacuo*. Title compound was obtained as a yellow oil and used in the next step without any further purification (45.0 mg, 50% yield). ^{1}H NMR (300 MHz, CDCl$_3$) δ 7.08 – 6.01 (br, 1H), 4.22 (q, J = 7.1 Hz, 2H), 3.55 – 3.33 (m, 4H), 2.15 – 1.97 (m, 4H), 1.44 (s, 9H), 1.27 (t, J = 7.0 Hz, 3H).

1-(tert-Butyl) 4-ethyl 4-(phenylcarbamoyl)piperidine-1,4-dicarboxylate (90). To a stirred solution of **89** (135.0 mg, 0.45 mmol) and PPh$_3$ (35.0 mg, 0.90 mmol) in dry DCM (8.0 mL) cooled at -10 °C, hexachlroacetone (35.0 µL, 0.225 mmol) was added and the resulting mixture was stirred for 15 min at -10 °C. Thereafter, a solution of aniline (41.0 µL, 0.45 mmol), in dry DCM (4.0 mL) was added and the reaction was stirred for 30 min at -10 °C. NH_4Cl *s.s.* (10 mL) was added and the mixture was extracted with DCM (3 x 10 mL). The combined organic layers were dried over anhydrous sodium sulfate, filtered, and concentrated *in vacuo*. The crude was purified by column chromatography on silica gel (1:3 EtOAc/PE) affording title compound as a yellow oil (156.0 mg, 91% yield). ^{1}H NMR (300 MHz, CDCl$_3$) δ 7.96 (s, 1H), 7.45 (d, J = 8.0 Hz, 2H), 7.28 (t, J = 8.1 Hz, 2H), 7.14 – 7.03 (m, 1H), 4.31 – 4.18 (m, 2H), 3.80 (d, J = 13.8 Hz, 2H), 3.10 (t, J = 11.9 Hz, 2H), 2.28 – 1.96 (m, 4H), 1.42 (d, J = 1.7 Hz, 9H), 1.32 – 1.21 (m, 3H). ESI-MS *m/z*: 398.9 [M+Na]$^+$

tert-Butyl 4-(hydroxymethyl)-4-(phenylcarbamoyl)piperidine-1-carboxylate (91). To a solution of **90** (156.0 mg, 0.41 mmol) in in ethanol (4.5 mL), NaBH$_4$ (47.0 mg, 1.23 mmol) was added. The mixture was stirred at 25 °C for 1 h. Ethanol was removed, then water was added, and the mixture was extracted with Et$_2$O (3 x 10 mL). The combined organic layers were dried over anhydrous sodium sulfate, filtered, and concentrated *in vacuo*. Title compound was obtained as an amorphous white solid and was used in the next step without any further purification. (94.0 mg, 68% yield). ^{1}H NMR (300 MHz, CDCl$_3$) δ 8.85 (s, 1H), 7.45 (d, J = 7.9 Hz, 2H), 7.27 (t, J = 7.8 Hz, 2H), 7.11 – 7.02 (m,

1H), 4.26 – 4.03 (m, 1H), 3.61 (s, 2H), 3.57 (d, J = 6.7 Hz, 2H), 3.35 (d, J = 13.3 Hz, 2H), 2.03 (dd, J = 13.7, 4.9 Hz, 4H), 1.43 (s, 9H). ESI-MS m/z: 357.3[M+Na]$^+$

*tert-Butyl 1-oxo-2-phenyl-2,7-diazaspiro[3.5]nonane-7-carboxylate (**92**).* To a solution of **91** (94.0 mg, 0.28 mmol) in dry THF (6.0 mL), PPh3 (147.0 mg, 0.56 mmol) and DIAD (110 µL, 0.56 mmol) were added. The mixture was stirred at 25 °C for 2 h. Solvent was removed under reduced pressure, and the crude was purified by column chromatography on silica gel (1:2 EtOAc/PE) affording title compound as a yellow oil (55.0 mg, 62% yield).^{1}H NMR (300 MHz, CDCl3) δ 7.37 – 7.27 (m, 5H), 3.82 – 3.69 (m, 2H), 3.46 (s, 2H), 3.44 – 3.32 (m, 2H), 2.05 – 1.92 (m, 2H), 1.84 – 1.73 (m, 2H), 1.45 (s, 9H). ESI-MS *m/z*: 339.4 [M+Na]$^+$.

*2-Phenyl-2,7-diazaspiro[3.5]nonan-1-one (**93**).* To a solution of **92** (55.0 mg, 0.17 mmol) in dry DCM (3.5 mL), TFA (600.0 µL) was added dropwise at 0 °C. The reaction mixture was stirred for 2 h at 25 °C. Thereafter, NaHCO3 *s.s.* was added and the resulting mixture was extracted with DCM (3 x 5 mL). The combined organic layers were dried over anhydrous sodium sulfate, filtered, and concentrated *in vacuo*. Title compound was obtained as a yellow pail oil and used in the next step without any further purification (3.0 mg, 89 %yield). ^{1}H NMR (300 MHz, CDCl3) δ 7.39 – 7.26 (m, 4H), 7.17 – 6.96 (m, 1H), 3.45 (s, 2H), 3.24 – 3.08 (m, 2H), 2.94 – 2.73 (m, 2H), 2.67 – 2.45 (br, 1H), 2.06 – 1.93 (m, 2H), 1.90 – 1.74 (m, 2H). ESI-MS *m/z*: 217.2 [M+H]$^+$

*Phenyl-7-(1H-1,2,4-triazole-1-carbonyl)-2,7-diazaspiro[3.5]nonan-1-one (**42e**).* To a solution of **93** (44.0 mg, 0.02 mmol) in dry DCM (14.0 mL), CDT (28.0 mg, 0.17 mmol) was added. The reaction mixture was stirred at 25 °C for 12 h. Solvent was removed *in vacuo*, and the crude was purified by column chromatography on silica gel (1:2 EtOAc/PE) affording title compound as an amorphous white solid (23.3 mg, 44% yield). ^{1}H NMR (300 MHz, CDCl3) δ 8.79 (s, 1H), 8.00 (s, 1H), 7.45 – 7.27 (m, 4H), 7.19 – 7.05 (m, 1H), 4.30 – 3.87 (m, 4H), 3.52 (s, 2H), 2.21 (dd, J = 14.0, 4.5 Hz, 2H), 2.10 – 1.97 (m, 2H). ESI-MS *m/z*: 312.3 [M+H]$^+$

*7-(1H-benzo[d][1,2,3]triazole-1-carbonyl)-2-phenyl-2,7-diazaspiro[3.5]nonan-1-one(**42f**).* To a solution of 1*H* benzotriazole (38.0 mg, 0.32 mmol) in dry DCM (5.0 mL), DMAP (50.0 mg, 0.64 mmol) and a solution of phosgene 20% in toluene (160.0 µL, 0.32 mmol) were added. The reaction was stirred for 30 min, then a solution of **93** (35.0 mg, 0.16 mmol) in dry DCM (1.0 mL) was added dropwise. The resulting mixture was stirred for at 25 °C for 12 h. The solvent was removed under reduced pressure, and the crude was purified by column chromatography on silica gel (1:3 EtOAc/PE) affording title compound as a yellow oil (20.5 mg, 42% yield). ^{1}H NMR (300 MHz, CDCl3) δ 8.10 (d, J = 8.2 Hz, 1H), 7.99 (d, J = 8.3 Hz, 1H), 7.66 – 7.58 (m, 1H), 7.51 – 7.42 (m, 1H), 7.40 – 7.32 (m, 4H), 7.18 – 7.07 (m, 1H), 4.24 – 4.01 (m, 4H), 3.57 (s, 2H), 2.35 – 2.11 (m, 4H). ESI-MS *m/z*: 451.9 [M+H]$^+$.

9.3. Experimental section of the dual FAAH/MAGL inhibitors 43a-l

tert-butyl 3-(phenylamino)azetidine-1-carboxylate (96a). To a solution of aniline **95a** (1.56 mmol, 142 µL) in DCE (7.0 mL) 1-Boc-3-azetidinone (2.34 mmol, 400.0 mg) and acetic acid (3.12 mmol, 180 µL) were added. The mixture was heated to 50 °C and was stirred for 12h at this temperature. The reaction was allowed to reach 25 °C, then NaBH$_3$CN (1.56 mmol, 100.0 mg) was added, and the mixture was stirred for 3h at this temperature. A saturated solution of sodium bicarbonate was added, and the mixture was extracted with DCM (3 x 10 mL). The combined organic layers were dried over anhydrous sodium sulfate, filtered and concentrated *in vacuo*. The crude was purified by column chromatography on silica gel (PE/EtOAc from 8:1 to 4:1) to afford the title compound as a colourless oil (82 % yield). ^{1}H NMR (300 MHz, CDCl$_3$) δ 7.24 – 7.14 (m, 2H), 6.82 – 6.70 (m, 1H), 6.56 – 6.46 (m, 2H), 4.33 – 4.23 (m, 2H), 4.22 – 4.09 (m, 1H), 3.73 (dd, *J* = 9.0, 4.5 Hz, 2H), 1.46 (s, 9H). ESI-MS *m/z* 271 [M + Na]$^+$.

tert-butyl 3-((4-fluorophenyl)amino)azetidine-1-carboxylate(96b). Title compound was obtain following the procedure described for compound **96a**, starting from 4-fluroaniline **95b** (200.0 mg, 1.8 mmol), 1-Boc-3-azetidinone (464.0 mg, 2.7 mmol), acetic acid (205 µL 3.6 mmol), and NaBH$_3$CN (1.8 mmol, 112.0 mg) in dry DCE (8.0mL). The crude was purified by column chromatography on silica gel (PE/EtOAc 3:1) to afford the title compound as yellow oil. 383.0 mg, yield 80 %).^{1}H NMR (300 MHz, CDCl$_3$) δ 6.96 – 6.79 (m, 2H), 6.66 – 6.55 (m, 1H), 6.48 – 6.38 (m, 2H), 4.32 – 4.21 (m, 2H), 4.16 – 4.04 (m, 1H), 3.76 – 3.64 (m, 2H), 1.44 (s, 9H). ESI-MS *m/z* 249 [M + Na]$^+$.

tert-butyl 3-(diphenylamino)azetidine-1-carboxylate (97a). To a solution of **96a** (1.07 mmol 266.0 mg,) in toluene (6 mL) were added Pd(OAc)$_2$ (0.02 mmol, 9.0 mg) and bromobenzene (1.07 mmol, 168.0 mg) and the mixture was stirred for 30 min at 25 °C. Then, sodium *tert*-butoxide (1.33 mmol, 128.0 mg) and tri-*tert*-butylphosphine (0.16 mmol, 39 µL) were added. The reaction was heated to 110 °C and stirred for 12h. Solvent was removed, and the crude was purified by column chromatography on silica gel (PE/EtOAc from 8:1 to 5:1) to afford the title compound as a colourless oil (84 % yield).^{1}H NMR **(**300 MHz, CDCl$_3$) δ 7.41 – 7.18 (m, 4H), 7.14 – 6.97 (m, 2H), 6.94 – 6.75 (m, 4H), 4.68 – 4.50 (m, 1H), 4.15 (dd, *J* = 9.0, 7.3 Hz, 2H), 3.85 (dd, *J* = 9.1, 5.7 Hz, 2H), 1.43 (s,9H). ESI-MS *m/z* 347 [M + Na]$^+$.

tert-butyl 3-(benzo[d][1,3]dioxol-5-yl(4-fluorophenyl)amino)azetidine-1-carboxylate (97b). Title compound was obtain following the procedure described for compound **96a**, starting from **96b** (50.0 mg, 0.20 mmol), 5-Iodo-1,3-benzodioxole (28.0 µL, 0.20 mmol), Pd(OAc)$_2$ (1.7 mg, 0.008 mmol), sodium *tert*-butoxide (23.0 mg, 0.24) and tri-*tert*-butylphosphine (7.0 µL, 0.03 mmol) in dry Toluene (1.5 mL). The crude was purified by column chromatography on silica gel (PE/EtOAc 8:1) to afford the title compound as yellow oil. (71.0 mg, 97 % yield). ^{1}H NMR (300 MHz, Chloroform-*d*) δ 7.01 – 6.86 (m, 2H), 6.76 (dd, *J* = 7.9, 0.7 Hz, 1H), 6.75 – 6.56 (m, 2H), 6.49 – 6.35 (m, 2H), 5.95 (s, 2H), 4.53 – 4.27 (m, 1H), 4.20 – 3.95 (m, 2H), 3.87 – 3.61 (m, 2H), 1.41 (s, 9H). ESI-MS *m/z* 409 [M + Na]$^+$.

N-diphenylazetidin-3-amine (98a). To a solution of **97a** (0.9 mmol, 293.0 mg) in MeOH (10 mL) a solution of 1N HCl in MeOH was dropwise added (3 mL). The solvent was removed *in vacuo* and this procedure was repeated for 3 times. The crude was diluted

with DCM and a saturated solution of sodium bicarbonate was added. The mixture was extracted with DCM (3 x 10 mL), the combined organic layers were dried over anhydrous sodium sulfate, filtered and concentrated *in vacuo*. Title compound was obtained as un yellow oil without any further purification (200 mg, 99% yield). ^{1}H NMR (300 MHz, MeOD) δ 7.38 – 7.20 (m, 4H), 7.08 (t, *J* = 7.3 Hz, 2H), 6.93 – 6.79 (m, 4H), 4.95 (q, *J* = 7.3 Hz, 1H), 4.30 (t, *J* = 9.0 Hz, 2H), 3.94 (t, *J* = 8.4 Hz, 2H). ESI-MS *m/z* 225 [M + H]$^+$.

N-(benzo(1,3)dioxol-5-yl)-N-(4-fluorophenyl)azetidin-3-amine **(98b)**. Title compound was obtained according to the procedure described for **98a** starting from **97b** (71.0 mg, 0.18 mmol) in methanol (5.0 mL) and a solution of 1N HCl in methanol (3.0 mL). Title compound was used in the next step without any further purification (45.0 mg, 87 % yield). **^{1}H NMR** (300 MHz, CDCl$_3$) δ 6.92 (t, *J* = 8.6 Hz, 2H), 6.75 (d, *J* = 8.1 Hz, 1H), 6.65 (dd, *J* = 8.9, 4.6 Hz, 2H), 6.45 – 6.35 (m, 2H), 5.94 (s, 2H), 4.62 – 4.52 (m, 1H), 3.73 – 3.52 (m, 4H), 2.53 – 2.37 (m, 1H). ESI-MS *m/z* 309 [M + Na]$^+$

tert-butyl 4-(3-(diphenylamino)azetidin-1-yl)piperidine-1-carboxylate **(99a)**. To a solution of **98a** (0.57 mmol, 125.0 mg) in EtOH (4.0 mL) were added 1-Boc-4-piperidone (0.83 mmol, 165.0 mg) and AcOH (38 μL). The mixture was stirred at 25 °C for 12h. After this time, NaBH$_3$CN (0.57 mmol 37.0 mg) and the reaction was stirred for further 3h. Water and a saturated solution of sodium bicarbonate were added and then EtOH was removed *in vacuo*. The water phase was extracted with DCM (3x 10 mL) the combined organic layers were dried over anhydrous sodium sulfate, filtered and concentrated *in vacuo*. The crude was purified by column chromatography on silica gel (DCM/MeOH from 70:1 to 50:1) to afford the title compound as a colorless oil (173.0 mg, 74 % yield). ^{1}H NMR (300 MHz, Methanol-*d*$_4$) δ 7.32 – 7.18 (m, 4H), 7.09 – 6.93 (m, 2H), 6.87 – 6.73 (m, 4H), 4.89 (s, 1H), 4.41 (p, *J* = 7.0 Hz, 1H), 4.01 – 3.86 (m, 2H), 3.66 (td, *J* = 6.4, 1.9 Hz, 2H), 2.85 (t, *J* = 7.6 Hz, 2H), 2.17 – 1.99 (m, 2H), 1.60 (dd, *J* = 13.5, 3.5 Hz, 2H), 1.42 (s, 9H), 1.17 – 0.95 (m, 2H).

tert-butyl 4-(3-(benzo(1,3)dioxol-5-yl(4-fluorophenyl)amino)azetidin-1-yl)piperidine-1-carboxylate **(99b)**. Title compound was obtained according to the procedure described for **99a** starting from **98b** (45.0 mg, 0.19 mmol) in ethanol (1.0 mL), 1-Boc-4-piperidonone (45.0 mg, 0.23 mmol), acetic acid (10 μL), and NaBH$_3$CN (9.0 mg, 0.15 mmol). The crude was purified by column chromatography on silica gel (DCM/MeOH from 70:1 to 50:1) to afford the title compound as a yellow oil (74.0 mg, 98 % yield). ^{1}H NMR (300 MHz, CDCl$_3$) δ 6.97 – 6.83 (m, 2H), 6.75 (d, *J* = 8.1 Hz, 1H), 6.70 – 6.58 (m, 2H), 6.45 – 6.34 (m, 2H), 5.94 (s, 2H), 4.31 (p, *J* = 6.9 Hz, 1H), 3.89 (d, *J* = 13.2 Hz, 2H), 3.70 – 3.59 (m, 2H), 2.89 – 2.71 (m, 4H), 2.14 – 2.01 (m, 1H), 1.66 – 1.52 (m, 2H), 1.42 (s, 9H), 1.20 – 1.12 (m, 2H). ESI-MS *m/z* 492 [M + Na]$^+$.

N,N-diphenyl-1-(piperidin-4-yl)azetidin-3-amine **(100a)**. Title compound was obtained according to the procedure described for **97a** starting **99a** (173.0 mg, 0,42 mmol) in methanol (5.0 mL) and a solution of 1 N HCl in methanol (3.0 mL). Title compound was used in the next step without any further purification. ^{1}HNMR (300 MHz, Methanol-*d*$_4$) δ 7.34 (t, *J* = 7.6 Hz, 4H), 7.11 (t, *J* = 7.4 Hz, 2H), 6.95 (dd, *J* = 11.9, 7.9 Hz, 4H), 4.96 – 4.72 (m, 1H), 4.54 (q, *J* = 9.7, 8.2 Hz, 2H), 4.06 (q, *J* = 11.1, 9.4 Hz, 2H), 3.88 – 3.64

(m, 1H), 3.53 (t, J = 13.3 Hz, 2H), 3.16 – 2.91 (m, 2H), 2.38 – 2.05 (m, 2H), 1.80 (d, J = 11.8 Hz, 2H). ESI-MS m/z 308 [M + H]$^+$.

N-(benzo(1,3)dioxol-5-yl)-N-(4-fluorophenyl)-1-(piperidin-4-yl)azetidin-3-amine (100b). Title compound was obtained according to the procedure described for **97a** starting from **98b** (74.0 mg, 0.18 mmol) in methanol (5.0 mL) and a solution of 1N HCl in methanol (7.0 mL). Title compound was used in the next step without any further purification (45.0 mg, yield 87 %). ^{1}H NMR (300 MHz, CDCl$_3$) δ 6.95 – 6.84 (m, 2H), 6.74 (d, J = 8.1 Hz, 1H), 6.68 – 6.60 (m, 2H), 6.44 – 6.34 (m, 2H), 5.93 (s, 2H), 4.30 (p, J = 6.9 Hz, 1H), 3.66 – 3.57 (m, 2H), 3.08 – 2.98 (m, 2H), 2.79 – 2.69 (m, 2H), 2.52 (td, J = 12.0, 2.7 Hz, 2H), 2.37 – 2.29 (m, 1H), 2.04 – 1.92 (m, 1H), 1.71 – 1.58 (m, 2H), 1.20 – 1.01 (m, 2H). ESI-MS m/z 370 [M + H] $^+$.

N-phenylazetidin-3-amine (101). Title compound was obtained according to the procedure described for **97a** starting **96a** (103.0 mg, 0,44 mmol) in methanol (10.0 mL) and a solution of 1 N HCl in methanol (3.0 mL). Title was used in the next step without any further purification. (74mg, 99%yield). ^{1}HNMR (300 MHz, Methanol-d_4) δ 7.53 – 7.27 (m, 5H), 4.77 (p, J = 7.3 Hz, 1H), 4.56 – 4.35 (m, 4H). ESI-MS m/z [M + Na]$^+$ 171.

tert-butyl   4-(3-(phenylamino)azetidin-1-yl)piperidine-1-carboxylate   (102).   Title compound was obtained according to the procedure described for **99a** starting from **101** (78.0 mg, 0.52 mmol), 1-Boc-4-piperidone (155.0 mg, 0.78 mmol), acetic acid (1.04 mmol, 60 μL), and NaBH$_3$CN (0.52 mmol, 32.0 mg) in dry DCE (7.0 mL). The crude was purified by column chromatography on silica gel (DCM/MeOH from 50:1 to 20:1) to afford the title compound as a colorless oil (80.0 mg, 46 % yield). ^{1}H NMR (300 MHz, Methanol-d_4) δ 7.17 – 7.06 (m, 2H), 6.66 (t, J = 7.3 Hz, 2H), 6.61 – 6.53 (m, 1H), 4.20 – 4.00 (m, 3H), 3.95 (t, J = 7.0, 1.7 Hz, 2H), 3.26 – 3.16 (m, 2H), 2.88 – 2.66 (m, 2H), 2.62 – 2.51 (m, 1H), 1.81 (d, J = 12.8 Hz, 2H), 1.45 (s, 9H), 1.25 – 1.08 (m, 2H). ESI-MS m/z 354 [M + Na]$^+$.

N-phenyl-1-(piperidin-4-yl)azetidin-3-amine   (103). Title compound was obtained according to the procedure described for **97a** starting from **102** (40.0 mg, 0,12 mmol) in methanol (5.0 mL) and a solution of 1 N HCl in methanol (5.0 mL). Title compound was used in the next step without any further purification. (Yield 27.0 mg, 99%). ^{1}H NMR (300 MHz, CDCl$_3$) δ 7.23 – 7.11 (m, 2H), 6.74 (t, J = 7.4 Hz, 1H), 6.55 (d, J = 8.0 Hz, 2H), 4.19 – 4.01 (m, 1H), 4.01 – 3.82 (m, 1H), 3.79 – 3.58 (m, 2H), 3.21 – 3.05 (m, 2H), 2.86 (d, J = 6.7 Hz, 2H), 2.67 (d, J = 11.0 Hz, 2H), 2.24 – 2.09 (m, 2H), 1.81 – 1.65 (m, 2H). ESI-MS m/z 254 [M + Na]$^+$.

Benzhydryltriphenylphosphonium bromide (105). A solution of bromomethyl benzene (**104**) (2.6 g, 15.25 mmol) and triphenylphosphine (4.0 g, 15.25 mmol) in toluene (30.0 mL) was stirred for 12h at 110 °C. The reaction was allowed to reach 25 °C then was filtered and the solid residue was washed with toluene. Title compound, obtained as a white solid (83% yield), was used in the next step without any further purification. ^{1}H NMR (300 MHz, DMSO-d_6): δ 7.95−7.83 (m, 3H), 7.79−7.61 (m, 12H), 7.39−7.26 (m, 11H)

tert-butyl 3-(diphenylmethylene)azetidine-1-carboxylate (106). To a solution of witting salt **105** (886.0 mg, 1.74 mmol) in dry THF (7.0 mL) cooled at 0 °C a solution of Potassium bis(trimethylsilyl)amide solution 0.5M in toluene (3.40 mL, 1.74 mmol) was added. The mixture was stirred for 30 minutes at 0 °C, then 1-Boc-3-azetidinone (150.0 mg, 0.87 mmol) was added. The reaction was allowed to reach 70 °C and stirred for 12h. Ammonium chloride was added, and the mixture was extracted with EtOAc (3 x 10 mL), the combined organic layers were dried over anhydrous sodium sulfate, filtered and concentrated *in vacuo*. The crude was purified by column chromatography on silica gel (PE/EtOAc from 20:1 to 10:1) to afford the title compound as a colorless oil (162.0 mg, 58 % yield). ^{1}H NMR (300 MHz, CDCl$_3$) δ 7.45 – 7.21 (m, 6H), 7.21 – 7.05 (m, 4H), 4.66 (s, 4H), 1.44 (s, 9H). ESI-MS *m/z* 344 [M + Na]$^+$.

tert-butyl 3-benzhydrylazetidine-1-carboxylate (107). To a solution of **106** (68.0 mg, 0.21 mmol) in methanol (7.0 mL), 10% Pd on carbon was added (2.2 mg, 0.021 mmol). The reaction was stirred under H$_2$ atmosphere for 2h. The mixture was filtered, and the solvent was then removed *in vacuo*. Title compound was used in the next step without any further purification. (62.0 mg, 91%). ^{1}H NMR (300 MHz, CDCl$_3$) δ 7.40 – 7.10 (m, 10H), 4.13 (d, *J* = 11.8 Hz, 1H), 4.00 (t, *J* = 8.4 Hz, 2H), 3.65 (dd, *J* = 8.8, 5.6 Hz, 2H), 3.40 – 3.24 (m, 1H), 1.44 (s, 9H). ESI-MS *m/z* 324 [M + H]$^+$.

3-benzhydrylazetidine (108). Title compound was obtained according to the procedure described for **97a** starting from **107** (62.0 mg, 0.2 mmol) in methanol (5.0 mL) and a solution of 1 N HCl in methanol (3.0 mL). Title compound was used in the next step without any further purification (50.0 mg, 96 %). ^{1}H NMR (300 MHz, CDCl$_3$) δ 7.39 – 7.07 (m, 10H), 4.24 (d, *J* = 10.5 Hz, 1H), 3.76 – 3.30 (m, 5H), 2.49 – 2.27 (br, 1H). ESI-MS *m/z* 224 [M + H]$^+$.

tert-butyl 4-(3-benzhydrylazetidin-1-yl)piperidine-1-carboxylate (109). Title compound was obtained according to the procedure described for **98a** starting from **108** (50.0 mg, 0.2 mmol) in ethanol (3.0 mL), 1-Boc-4-piperidonone (56.0 mg, 0.3 mmol), acetic acid (20 μL), and NaBH$_3$CN (12.0 mg, 0.2 mmol). The crude was purified by column chromatography on silica gel (DCM/MeOH from 70:1 to 50:1) to afford the title compound as a colorless oil (31.0 mg, 40 % yield). ^{1}H NMR (300 MHz, CDCl$_3$) δ 7.34 – 7.12 (m, 10H), 4.08 (d, *J* = 11.4 Hz, 1H), 4.02 – 3.86 (m, 2H), 3.43 (t, *J* = 7.2 Hz, 2H), 3.35 – 3.17 (m, 1H), 2.89 – 2.71 (m, 4H), 2.21 – 2.08 (m, 1H), 1.68 – 1.53 (m, 4H), 1.44 (s, 9H). ESI-MS *m/z* 429 [M + Na]$^+$.

4-(3-benzhydrylazetidin-1-yl)piperidine (110). Title compound was obtained according to the procedure described for **97a** starting from **109** (31.0 mg, 0.07 mmol) in methanol (5.0 mL) and a solution of 1 N HCl in methanol (3.0 mL). Title compound was used in the next step without any further purification (21.0 mg, 99 %). ^{1}H NMR (300 MHz, MeOD) δ 7.42 – 6.99 (m, 10H), 4.46 – 4.26 (m, 1H), 4.24 – 4.01 (m, 3H), 3.96 – 3.60 (m, 3H), 3.53 (d, *J* = 9.2 Hz, 2H), 3.18 – 2.98 (m, 2H), 2.23 (d, *J* = 12.8 Hz, 2H), 1.78 (s, 2H). ESI-MS *m/z* 307 [M + H]$^+$.

3-(diphenylmethylene)azetidine (111). Title compound was obtained according to the procedure described for **97a** starting from **106** (94.0 mg, 0.29 mmol) in methanol (5.0 mL) and a solution of 1 N HCl in methanol (3.0 mL). Title compound was used in the

next step without any further purification. (61.0 mg, 95% yield). ^{1}H NMR (300 MHz, CDCl$_3$) δ 7.53 – 6.95 (m, 10H), 4.49 (s, 4H), 2.71 (s, 1H). ESI-MS *m/z* 344 [M + Na]$^+$.

tert-butyl 4-(3-(diphenylmethylene)azetidin-1-yl)piperidine-1-carboxylate(112). To a solution of **111** (0.27 mmol, 61.0 mg) in dry acetonitrile (1.5 mL) potassium carbonate (0.41 mmol, 93.0 mg), a solution of 1-Boc-4-iodo-piperidine (0.41 mmol, 126.0 mg) in acetonitrile (1.5 mL) and potassium iodine (0.01 %) were added. The reaction was stirred for 12h at 25 °C. Water was added, then acetonitrile was removed *in vacuo*. The water phase was extracted with DCM (3 x 10 mL), the combined organic layers were dried over anhydrous sodium sulfate, filtered, and concentrated *in vacuo*. The crude was purified by column chromatography on silica gel (DCM/MeOH 80:1 to 40:1) to afford the title compound as a yellow oil (51.0 mg, 46% yield). ^{1}H NMR (300 MHz, CDCl$_3$) δ 7.51 – 7.17 (m, 6H), 7.18 – 6.96 (m, 4H), 5.15 (d, *J* = 11.7 Hz, 2H), 4.70 (d, *J* = 14.3 Hz, 2H), 4.40 – 4.16 (m, 2H), 3.38 – 3.21 (m, 1H), 2.81 – 2.61 (m, 2H), 1.95 (d, *J* = 12.4 Hz, 2H), 1.59 (d, *J* = 29.9 Hz, 2H), 1.44 (s, 9H). ESI-MS *m/z* 405 [M + H]$^+$.

4-(3-(diphenylmethylene)azetidin-1-yl)piperidine (113). Title compound was obtained according to the procedure described for **97a** starting from **113** (25.0 mg, 0.061 mmol) in methanol (5.0 mL) and a solution of 1 N HCl in methanol (3.0 mL). Title compound was used in the next step without any further purification (18.0 mg, 99 %). ^{1}H NMR (300 MHz, MeOD) δ 7.67 – 6.96 (m, 10H), 5.13 (d, *J* = 21.5 Hz, 2H), 3.99 – 3.68 (m, 1H), 3.60 (d, *J* = 21.6 Hz, 2H), 3.22 – 3.02 (m, 2H), 2.35 (d, *J* = 12.5 Hz, 2H), 1.96 – 1.72 (m, 2H*)*. ESI-MS *m/z* 405 [M + H]$^+$, 427 [M + Na]$^+$.

Benzyltriphenylphosphonium bromide(115). Title compound was obtained according to the procedure described for compound **105** starting from bromomethyl benzene **114** (2.6 g, 15.25 mmol) and triphenylphosphine (4.0 g, 15.25) in toluene (30.0 mL). Title compound, obtained as a white solid, was used in the next step without any further purification (84% yield). ^{1}H NMR (300 MHz, DMSO-d_6): δ 7.97−7.85 (m, 3H), 7.81−7.63 (m, 12H), 7.35−7.25 (m, 1H), 7.26− 7.18 (m, 2H), 6.99 (d, *J* = 7.1 Hz, 2H), 5.25 (d, *J* = 15.7 Hz, 2H)

tert-butyl 3-benzylideneazetidine-1-carboxylate (116). To a solution of witting salt **115** (1.0 g, 2.45 mmol) in dry THF (7.0 mL) cooled at 0 °C a solution of *n*-buthyl lithium solution 2.5M in THF (460.0 μL, 1.16 mmol) was dropwise added. The mixture was stirred for 30 minutes at 0 °C, then 1-Boc-3-azetidinone (200.0 mg, 1.16 mmol) was added and the reaction was stirred for 12h. Ammonium chloride was added, and the mixture was extracted with EtOAc (3 x 10 mL), the combined organic layers were dried over anhydrous sodium sulfate, filtered and concentrated *in vacuo*. The crude was purified by column chromatography on silica gel (PE/EtOAc from 6:1 to 5:1) to afford the title compound as a colorless oil (236.0 mg, 96% yield). ^{1}HNMR (300 MHz, CDCl$_3$) δ 7.37 – 7.00 (m, 5H), 6.22 (s, 1H), 4.80 (s, 2H), 4.62 (s, 2H), 1.48 (s, 9H). ESI-MS *m/z* 268 [M + Na]$^+$.

3-benzylideneazetidine (117). Title compound was obtained according to the procedure described for **97a** starting from **116** (236.0 mg, 0.96 mmol) in methanol (5.0 mL) and a solution of 1N HCl in methanol (5.0 mL). Title compound was used in the next step without any further purification. (128.0 mg, yield 99%). ^{1}HNMR (300 MHz, CDCl$_3$) δ

7.32 – 7.00 (m, 5H), 6.08 (s, 1H), 4.56 (s, 2H), 4.38 (s, 2H), 3.32 – 3.23 (m, 1H). ESI-MS *m/z* 168 [M + Na]$^+$.

tert-butyl 4-(3-benzylideneazetidin-1-yl)piperidine-1-carboxylate (118). Title compound was obtained according to the procedure described for **98a**, starting from **117** (128.0 mg, 0.88 mmol) in ethanol (6.0 mL), 1-Boc-4-piperidonone (263.0 mg, 1.32 mmol), acetic acid (60 µL), and NaBH$_3$CN (55.0 mg, 0.88 mmol). The crude was purified by column chromatography on silica gel (DCM/MeOH from 70:1 to 50:1) to afford the title compound as a yellow oil (220.0 mg, 75% yield). ^{1}H NMR (300 MHz, CDCl$_3$) δ 7.35 – 6.93 (m, 5H), 6.13 (s, 1H), 4.13 (s, 2H), 3.98 – 3.50 (m, 4H), 3.02 – 2.76 (m, 2H), 2.40 – 2.27 (m, 1H), 1.84 – 1.58 (m, 2H), 1.40 (s, 9H), 1.30 – 1.06 (m, 2H). ESI-MS *m/z* 351 [M + Na]$^+$.

tert-butyl 4-(3-benzylazetidin-1-yl)piperidine-1-carboxylate (119). Title compound was obtained according to the procedure described for **107** starting from **118** (98.0 mg, 0.30 mmol) in EtOAc (10.0mL) and palladium on carbon (5.0 mg, 0.03mmol). Title compuond was used in the next step without any further purification (97% yield). ^{1}H NMR (300 MHz, Methanol-*d*$_4$) δ 7.26 (h, *J* = 7.3 Hz, 5H), 4.37 – 4.13 (m, 2H), 4.13 – 3.91 (m, 2H), 3.81 – 3.45 (m, 3H), 3.22 – 2.85 (m, 4H), 2.25 (d, *J* = 13.1 Hz, 2H), 1.82 (d, *J* = 15.6 Hz, 2H). ESI-MS *m/z* 353 [M + Na]$^+$.

4-(3-benzylazetidin-1-yl)piperidine (120). Title compound was obtained according to the procedure described for **97a** starting from **119** (75.0 mg, 0.23 mmol) in methanol (5.0 mL) and a solution of 1N HCl in methanol (3.0 mL). Title compound was used in the next step without any further purification (53.0 mg, yield 99 %). ^{1}H NMR (300 MHz, Methanol-*d*$_4$) δ 7.26 (h, *J* = 7.3 Hz, 5H), 4.37 – 4.13 (m, 2H), 4.13 – 3.91 (m, 2H), 3.81 – 3.45 (m, 3H), 3.22 – 2.85 (m, 4H), 2.25 (d, *J* = 13.1 Hz, 2H), 1.82 (d, *J* = 15.6 Hz, 2H). ESI-MS *m/z* 253 [M + Na]$^+$.

4-(3-benzylideneazetidin-1-yl)piperidine (121). Title compound was obtained according to the procedure described for **97a** starting from **118** (75.0 mg, 0.23 mmol) in methanol (5.0 mL) and a solution of 1N HCl in methanol (3.0 mL). Title compound was used in the next step without any further purification (53.0 mg, yield 99 %). ^{1}H NMR (300 MHz, CDCl$_3$) δ 7.42 – 6.92 (m, 5H), 6.16 (s, 1H), 4.15 (s, 2H), 3.95 (s, 2H), 3.22 – 3.00 (m, 2H), 2.60 (ddd, *J* = 12.5, 11.0, 2.7 Hz, 2H), 2.35 – 2.22 (m, 1H), 2.20 – 2.11 (br, 1H), 1.81 – 1.69 (m, 2H), 1.30 – 1.13 (m, 2H). ESI-MS *m/z* 229 [M + H]$^+$.

tert-butyl 3-(diphenylamino)-[1,3'-biazetidine]-1'-carboxylate (122). Title compound was obtained according to the procedure described for **98a** starting from **98a** (65.0 mg, 0.29 mmol) in ethanol (2.0 mL), 1-Boc-3-azetidinone (74.0 mg, 0.43 mmol), acetic acid (20 µL), and NaBH$_3$CN (18.0 mg, 0.28 mmol). The crude was purified by column chromatography on silica gel (DCM/MeOH from 70:1 to 50:1) to afford the title compound as a colorless oil (59.0 mg, 54 % yield). ^{1}HNMR (300 MHz, Methanol-*d*$_4$) δ 7.32 – 7.21 (m, 4H), 7.07 – 6.96 (m, 2H), 6.87 – 6.78 (m, 4H), 4.48 (p, *J* = 7.0 Hz, 1H), 3.86 (t, *J* = 8.1 Hz, 2H), 3.71 – 3.52 (m, 4H), 3.37 – 3.13 (m, 1H), 3.01 – 2.89 (m, 1H), 1.40 (s, 9H). ESI-MS *m/z* 380 [*M* + Na]$^+$.

N,N-diphenyl-[1,3'-biazetidin]-3-amine(123). Title compound was obtained according to the procedure described for **97a** starting from **122** (59.0 mg, 0,15 mmol) in methanol (5.0 mL) and a solution of 1 N HCl in methanol (5.0 mL). Title compound was used in the next step without any further purification. (Yield 42.0 mg, 99%). ^{1}HNMR AP75 (300 MHz, Methanol-d_4) δ 7.42 – 7.25 (m, 4H), 7.11 (t, J = 7.3 Hz, 2H), 6.99 – 6.88 (m, 4H), 4.99 – 4.84 (m, 1H), 4.58 (s, 2H), 4.49 – 4.28 (m, 4H), 4.14 (s, 2H). ESI-MS *m/z* 280 [M + Na]$^+$.

tert-butyl 3-(diphenylmethylene)-(1,3'-biazetidine)-1'-carboxylate(124). To a solution of compound **111** (50.0 mg, 0.15mmol) in dry DMF (1 mL), potassium carbonate (62.0 mg, 0.45 mmol) and a solution of 1-Boc-3-Iodoazetidine (53.0 mg, 0.19mmol) in dry DMF (1 mL) were added. The mixture was allowed to reach 75 °C and was stirred for 12h. A solution of ammonium chloride was added, and the water phase was extracted with EtOAc (2 x 10 mL). The combined organic layers were washed 2 times with a solution ammonium chloride, dried over anhydrous sodium sulfate, filtered, and concentrated *in vacuo.* The crude was purified by column chromatography on silica gel (PE/EtOAc 4:1 to 2:1) to afford the title compound as a yellow oil (22.0 mg, 40% yield). ^{1}HNMR (300 MHz, CDCl$_3$) δ 7.40 – 7.24 (m, 6H), 7.21 – 7.02 (m, 4H), 5.18 – 5.04 (m, 1H), 4.78 (s, 4H), 4.28 – 4.13 (m, 2H), 3.94 – 3.82 (m, 2H), 1.43 (s, 9H). ESI-MS *m/z* 499 [M + Na]$^+$.

3-(diphenylmethylene)-1,3'-biazetidine(125). Title compound was obtained according to the procedure described for **97a** starting from **124** (22.0 mg, 0.06 mmol) in methanol (5.0 mL) and a solution of 1 N HCl in methanol (3.0 mL). Title compound was used in the next step without any further purification (18.0 mg, 99 %).^{1}H NMR (300 MHz, Methanol-d_4) δ 7.40 – 7.25 (m, 6H), 7.19 – 7.09 (m, 4H), 5.31 – 5.18 (m, 1H), 4.87 – 4.70 (m, 4H), 4.39 (dd, J = 12.2, 6.8 Hz, 2H), 4.13 (dd, J = 12.3, 5.2 Hz, 2H). ESI-MS *m/z* 399 [M + Na]$^+$.

*(4-(3-(diphenylamino)azetidin-1-yl)piperidin-1-yl)(1H-1,2,4-triazol-1-yl)methanone (43a).*To a solution of **100a** (7.0 mg, 0.02 mmol) in dry DCM (2.0 mL) CDT (7.22 mg, 0.04 mL) was added. The mixture was stirred overnight at 25 °C. Water was added and the mixture was extracted with DCM (3x 10 mL). The combined organic layers were dried over anhydrous sodium sulfate, filtered and concentrated *in vacuo.* The crude was purified by column chromatography on silica gel (DCM/MeOH from 80:1 to 50:1) to afford the title compound as a colorless oil (5.0 mg, 57 % yield). ^{1}HNMR (300 MHz, Methanol-d_4) δ 8.95 (s, 1H), 8.11 (s, 1H), 7.33 (d, J = 7.7 Hz, 4H), 7.09 (d, J = 7.4 Hz, 2H), 7.04 – 6.96 (m, 1H), 6.90 (d, J = 7.9 Hz, 3H), 4.72 – 4.57 (m, 2H), 4.49 – 4.30 (m, 2H), 4.25 – 4.06 (m, 2H), 3.65 – 3.46 (m, 2H), 3.20 – 3.00 (m, 2H), 2.08 – 1.85 (m, 2H), 1.50 – 1.35 (m, 2H). ESI-MS *m/z* 403 [M + H]$^+$.

1,1,1,3,3,3-hexafluoropropan-2-yl   4-(3-(diphenylamino)azetidin-1-yl)piperidine-1-carboxylate (43b). To a solution of hexafluoro-2-propanol (10 μL, 0.10 mmol) in dry DCM (7.0 mL) cooled at 0 °C, triphosgene (0.05 mmol, 15.0 mg) and DIPEA (26.0 mg, 0.20 mmol) were added. The mixture was stirred for 30 min at this temperature, then a solution of **100a** (30.0mg, 0.1mmol) in DCM (6.0 mL) was dropwise added. The rection was allowed to reach 25 °C and was stirred for 12 h. Solvent was removed *in vacuo*, and the crude was purified by column chromatography on silica gel (PE/EtOAc 2:1) to afford the title compound as colorless oil. (14.0 mg, yield 20%). ^{1}H NMR (300 MHz, CDCl$_3$) δ 7.40 – 7.06 (m, 5H), 6.21 (s, 1H), 5.74 (h, J = 6.3 Hz, 1H), 4.23 (s, 2H), 4.04 (s, 2H), 3.98

– 3.83 (m, 2H), 3.29 – 3.10 (m, 2H), 2.61 – 2.47 (m, 1H), 1.76 (d, J = 10.6 Hz, 2H), 1.52 – 1.35 (m, 2H). ESI-MS m/z 445 [M + Na]$^+$.

(4-(3-(benzo(1,3)dioxol-5-yl(4-fluorophenyl)amino)azetidin-1-yl)piperidin-1-yl)(1H-1,2,4-triazol-1-yl)methanone (43c). Title compound was obtained according to the procedure described for **43a**, starting from **100b** (26.0 mg, 0.11 mmol), and CDT (22.0 mg, 0.13 mmol) in dry DCM (10.0 mL). The crude was purified by column chromatography on silica gel (DCM/MeOH from 80:1 to 20:1) to afford the title compound as a colorless oil (20.0 mg, 36 % yield). ^{1}H NMR (300 MHz, CDCl$_3$) δ 8.75 (s, 1H), 7.98 (s, 1H), 6.97 – 6.85 (m, 1H), 6.76 (d, J = 8.1 Hz, 2H), 6.70 – 6.58 (m, 2H), 6.45 – 6.36 (m, 2H), 5.96 (s, 2H), 4.34 (p, J = 6.8 Hz, 1H), 4.26 – 4.06 (m, 2H), 3.77 – 3.59 (m, 2H), 3.34 (s, 2H), 2.84 (t, J = 7.2 Hz, 2H), 2.34 – 2.23 (m, 1H), 1.75 (d, J = 13.2 Hz, 2H), 1.50 – 1.32 (m, 2H). ESI-MS m/z 487 [M + Na]$^+$.

(4-(3-(benzo(1,3)dioxol-5-yl(4-fluorophenyl)amino)azetidin-1-yl)piperidin-1-yl)(1H-1,2,4-triazol-1-yl)methanone (43d). Title compound was obtained according with the procedure described for compound **43b**, starting from compound **100b** (28.0 mg, 0.1 mmol), hexafluoro-2-propanol (10 µL, 0.10 mmol), triphosgene (15.0 mg, 0.05 mmol) and DIPEA (35.0 mg, 0.20 mmol) in dry DCM (8.0 mL). The crude was purified by column chromatography on silica gel (PE/EtOAc 3:1) to afford the title compound as colorless oil.(14.0 mg, 37%) ^{1}H NMR (300 MHz, CDCl3) δ 6.98 – 6.87 (m, 2H), 6.76 (dd, J = 8.1, 1.3 Hz, 1H), 6.69 – 6.61 (m, 2H), 6.45 – 6.36 (m, 2H), 5.96 (s, 2H), 5.73 (hept, J = 6.2 Hz, 1H), 4.34 (p, J = 6.9 Hz, 1H), 3.91 (dd, J = 13.3, 5.0 Hz, 2H), 3.73 – 3.62 (m, 2H), 3.15 – 2.98 (m, 2H), 2.83 (t, J = 7.1 Hz, 2H), 2.26 – 2.14 (m, 1H), 1.72 – 1.60 (m, 2H), 1.40 – 1.22 (m, 2H). ESI-MS m/z 564 [M + H]$^+$.

(4-(3-(phenylamino)azetidin-1-yl)piperidin-1-yl)(1H-1,2,4-triazol-1-yl)methanone (43e). Title compound was obtained according to the procedure described for **43a**, starting from **103** (27.0 mg, 0.12 mmol), and CDT (0.12 mmol, 18.0 mg) in dry DCM (10.0 ml). The crude was purified by column chromatography on silica gel (DCM/MeOH from 80:1 to 20:1) to afford the title compound as a colorless oil (21.60 mg, 60 % yield). ^{1}H NMR (300 MHz, Methanol-d_4) δ 8.94 (s, 1H), 8.11 (s, 1H), 7.18 – 7.02 (m, 2H), 6.61 (dd, J = 24.6, 7.6 Hz, 3H), 4.32 (d, J = 13.4 Hz, 2H), 4.07 (p, J = 6.6 Hz, 1H), 3.94 – 3.72 (m, 2H), 3.17 (t, J = 12.5 Hz, 2H), 3.09 – 2.86 (m, 2H), 2.54 – 2.35 (m, 1H), 1.87 (d, J = 13.0 Hz, 2H), 1.52 – 1.24 (m, 2H). ^{13}C NMR (75 MHz, Me Methanol-d_4) δ 151.1, 148.6, 147.2, 146.4, 128.8, 117.2, 112.7, 63.8, 59.5, 48.4, 48.16, 47.9, 47.6, 47.3, 47.0, 46.7, 43.5, 28.4. ESI-MS m/z 327 [M + H]$^+$.

(4-(3-benzhydrylazetidin-1-yl)piperidin-1-yl)(1H-1,2,4-triazol-1-yl)methanone (43f). Title compound was obtained according to the procedure described for **43a**, starting from **110** (21.0 mg, 0.07 mmol), and CDT (10.0 mg, 0.14 mmol) in dry DCM (6.0 ml). The crude was purified by column chromatography on silica gel (DCM/MeOH from 80:1 to 20:1) to afford the title compound as a colorless oil (19.0 mg, 70 % yield). ^{1}HNMR (300 MHz, MeOD) δ 8.93 (s, 1H), 8.09 (s, 1H), 7.31 – 7.11 (m, 10H), 4.30 (d, J = 13.3 Hz, 2H), 4.12 (d, J = 11.3 Hz, 1H), 3.47 – 3.39 (m, 2H), 3.36 – 3.24 (m, 1H), 3.12 (t, J = 12.5 Hz, 2H), 2.95 (t, J = 7.1 Hz, 2H), 2.50 – 2.37 (m, 1H), 1.81 (d, J = 12.8 Hz, 2H), 1.37 – 1.21 (m, 2H). ^{13}C NMR (75 MHz, MeOD) δ 151.1, 151.0, 148.6, 146.4, 146.3, 142.8,

128.2, 127.5, 126.1, 63.7, 57.0, 56.9, 55.8, 55.7,42.5, 34.9, 28.2. ESI-MS *m/z* 424 [*M* + Na]$^+$.

(4-(3-(diphenylmethylene)azetidin-1-yl)piperidin-1-yl)(1H-1,2,4-triazol-1-yl)methanone (43g). Title compound was obtained according to the procedure described for **43a**, starting from **113** (18.0 mg, 0.06 mmol), and CDT (0.15 mmol, 15.0 mg) in dry DCM (5 ml). The crude was purified by column chromatography on silica gel (DCM/MeOH from 80:1 to 50:1) to afford the title compound as a colorless oil (15.70 mg, 63 % yield). ^{1}H NMR (300 MHz, Methanol-*d*$_4$) δ 8.94 (s, 1H), 8.10 (s, 1H), 7.49 – 7.19 (m, 7H), 7.20 – 7.05 (m, 3H), 4.31 (d, *J* = 13.4 Hz, 2H), 4.15 (s, 4H), 3.44 – 3.07 (m, 2H), 2.75 – 2.47 (m, 1H), 2.03 – 1.81 (m, 2H), 1.57 – 1.14 (m, 2H). ^{13}C NMR (75 MHz, Methanol-*d*$_4$) δ 150.3, 147.8, 145.6, 145.5, 138.7, 133.0, 128.6, 127.3, 126.1, 62.1, 59.7, 43.7, 27.8. ESI-MS *m/z* 422 [*M* + Na]$^+$.

(4-(3-benzylazetidin-1-yl)piperidin-1-yl)(1H-1,2,4-triazol-1-yl)methanone (43h). Title compound was obtained according to the procedure described for **43a**, starting from **120** (37.0 mg, 0.16 mmol), and CDT (49.0 mg, 0.48 mmol) in dry DCM (14.0 mL). The crude was purified by column chromatography on silica gel (DCM/MeOH from 80:1 to 20:1) to afford the title compound as a colorless oil (25.6 mg, yield 47%). ^{1}H NMR (300 MHz, Methanol-*d*$_4$) δ 8.93 (s, 1H), 8.10 (s, 1H), 7.35 – 7.02 (m, 5H), 4.43 – 4.23 (m, 2H), 3.52 – 3.39 (m, 2H), 3.20 – 3.03 (m, 2H), 3.01 – 2.91 (m, 2H), 2.84 (d, *J* = 8.3 Hz, 2H), 2.80 – 2.64 (m, 1H), 2.49 – 2.34 (m, 1H), 1.84 (d, *J* = 13.0 Hz, 2H), 1.38 – 1.22 (m, 2H). ^{13}C NMR (75 MHz, Methanol-*d*$_4$) δ 155.0, 152.5, 150.3, 143.7, 142.0, 132.0, 132.0, 123.0, 69.0, 67.8, 61.4, 61.7, 48.3, 43.5, 35.6, 35.4, 32.1. ESI-MS *m/z* 346 [*M* + Na]$^+$.

4-(3-benzylideneazetidin-1-yl)piperidin-1-yl)(1H-1,2,4-triazol-1-yl)methanone (43i). Title compound was obtained according to the procedure described for **43a**, starting from **121** (26.0 mg, 0.11 mmol), and CDT (22.0 mg, 0.13 mmol) in dry DCM (10.0 mL). The crude was purified by column chromatography on silica gel (DCM/MeOH from 80:1 to 20:1) to afford the title compound as a colorless oil (10.0 mg, 30 % yield). ^{1}H NMR (300 MHz, CDCl$_3$) δ 8.77 (s, 1H), 7.99 (s, 1H), 7.44 – 7.03 (m, 5H), 6.22 (s, 1H), 4.23 (q, *J* = 2.6 Hz, 4H), 4.04 (s, 2H), 3.61 – 3.38 (m, 2H), 2.69 – 2.56 (m, 1H), 1.94 – 1.79 (m, 2H), 1.63 – 1.47 (m, 2H). ^{13}C NMR (75 MHz, CDCl$_3$) δ 152.0, 151.9, 148.5, 146.5, 136.6, 133.2, 128.6, 127.1, 126.7, 121.0, 62.0, 61.3, 61.2, 42.0, 29.0. ESI-MS *m/z* 346 [*M* + Na]$^+$.

1,1,1,3,3,3-hexafluoropropan-2-yl 4-(3-benzylideneazetidin-1-yl)piperidine-1-carboxylate (43j). Title compound was obtained according with the procedure described for compound **43b**, starting from compound **121** (0.16 mmol, 36.0 mg), hexafluoro-2-propanol (17 μL, 0.16 mmol), triphosgene (0.08 mmol, 24.0 mg) and DIPEA (0.32 mmol, 55.0 mg) in dry DCM (7.0 mL). The crude was purified by column chromatography on silica gel (PE/EtOAc 3:1) to afford the title compound as colorless oil (30% yield). ^{1}H NMR (300 MHz, CDCl$_3$) δ 7.40 – 7.06 (m, 5H), 6.21 (s, 1H), 5.74 (h, *J* = 6.3 Hz, 1H), 4.23 (s, 2H), 4.04 (s, 2H), 3.98 – 3.83 (m, 2H), 3.29 – 3.10 (m, 2H), 2.61 – 2.47 (m, 1H), 1.76 (d, *J* = 10.6 Hz, 2H), 1.52 – 1.35 (m, 2H). ESI-MS *m/z* 445 [*M* + Na]$^+$.

(3-(diphenylamino)-[1,3'-biazetidin]-1'-yl)(1H-1,2,4-triazol-1-yl)methanone (43k). Title compound was obtained according to the procedure described for **43a**, starting from **123** (42.0 mg, 0.15 mmol), and CDT (0.45 mmol, 45.0 mg) in dry DCM (14.0 mL). The crude was purified by column chromatography on silica gel (DCM/MeOH from 80:1 to 20:1)

to afford the title compound as a colorless oil (15.74 mg, 30 % yield). ^{1}H NMR (300 MHz, Methanol-d_4) δ 9.01 (s, 1H), 8.08 (s, 1H), 7.37 – 7.18 (m, 4H), 7.15 – 6.97 (m, 2H), 6.91 – 6.77 (m, 4H), 4.68 – 4.45 (m, 2H), 4.39 – 4.25 (m, 1H), 4.17 (t, J = 8.9 Hz, 1H), 3.91 – 3.81 (m, 1H), 3.72 (t, J = 7.2 Hz, 2H), 3.51 – 3.37 (m, 1H), 3.03 (t, J = 7.5 Hz, 2H). ^{13}C NMR (75 MHz, Methanol-d_4) δ 152.0, 147.7, 146.9, 144.7, 129.4, 129.0, 129.0, 129.0, 128.9, 128.6, 122.6, 122.4, 122.4, 122.7, 122.3, 122.31, 58.13, 56.39, 54.64, 52.31, 49.55. ESI-MS *m/z* 397 [M + Na]$^+$.

(3-(diphenylmethylene)-[1,3'-biazetidin]-1'-yl)(1H-1,2,4-triazol-1-yl)methanone **(43l)**. Title compound was obtained according to the procedure described for **43a**, starting from **125** (16.0 mg, 0.06 mmol), and CDT (10.0 mg, 0.18 mmol) in dry DCM (5.0 ml). The crude was purified by column chromatography on silica gel (DCM/MeOH from 80:1 to 20:1) to afford the title compound as a colorless oil (15.00 mg, 67 % yield). ^{1}HNMR (300 MHz, CDCl$_3$) δ 8.87 (s, 1H), 7.97 (s, 1H), 7.41 – 7.24 (m, 6H), 7.17 – 7.09 (m, 4H), 5.27 – 5.20 (m, 1H), 4.96 (t, J = 8.1 Hz, 1H), 4.80 (s, 4H), 4.66 – 4.46 (m, 2H), 4.25 – 4.12 (m, 1H). ^{13}C NMR (75 MHz, CDCl$_3$) δ 154.8, 152.9, 147.3, 144.7, 138.5, 135.5, 128.6, 128.7, 127.6, 126.0, 65.6, 62.0, 59.1, 58.3, 56.3. ESI-MS *m/z* 394 [M + Na]$^+$.

9.4. Experimental section of the dual FAAH/HDAC6 inhibitors 44a-h

1-(3-Hydroxyphenyl)-1H-pyrrole-3-carboxylic acid (136). To a solution of **54** (146 mg, 0.78 mmol) and 2-methyl-2-butene (1.08 ml, 10.14 mmol) in *tert*-butanol (12 mL), saturated solutions of $NaClO_2$ (0.51 mL, 4.37 mmol) and NaH_2PO_4 (0.82 mL, 5.85 mmol) were added. The reaction mixture was stirred for 16 h at 25 °C. Then, it was quenched with a saturated solution of NH_4Cl and extracted with EtOAc (3 x 10 mL). Organic phase was dried over sodium sulphate, filtered and concentrated. The crude was purified by column chromatography on silica gel (PE/EtOAc from 2:1 to 1:1) to afford the product as a colorless oil (76% yield). ^1H NMR (300 MHz, $(CD_3)_2CO$) δ 9.12 – 8.6 (br, 1H), 7.82 – 7.77 (m, 1H), 7.37 – 7.29 (m, 1H), 7.27 – 7.22 (m, 1H), 7.12 – 7.02 (m, 2H), 6.84 (dd, $J = 8.1, 1.7$ Hz, 1H), 6.71 – 6.66 (m, 1H).

Benzyl 1-(3-hydroxyphenyl)-1H-pyrrole-3-carboxylate (134a). To a solution of **136** (50 mg, 0.45 mmol) in dry DMF (2 mL), $NaHCO_3$ (101 mg, 0.54 mmol) and benzyl bromide (80 μL, 0.68 mmol) were added. The reaction mixture was heated to 40 °C and stirred for 16 h under N_2 atmosphere. A saturated solution of NH_4Cl, was added and the mixture was extracted with EtOAc (3 x 10 mL). The combined organic layers were washed with NH_4Cl (1 x 10 mL) and brine (2 x 10 mL). Organic phase was dried over sodium sulphate, filtered and concentrated. The crude was purified by column chromatography on silica gel (PE/EtOAc from 3:1 to 2:1) to afford the title compound as an amorphous off-white solid (36% yield). ^1H NMR (300 MHz, $(CD_3)_2CO$) δ 8.93 – 8.77 (br, 1H), 7.88 – 7.80 (m, 1H), 7.50 – 7.45 (m, 1H), 7.43 – 7.27 (m, 5H), 7.27 – 7.23 (m, 1H), 7.10 – 7.03 (m, 2H), 6.88 – 6.81 (m, 1H), 6.72 (dd, $J = 2.9, 1.6$ Hz, 1H), 5.29 (s, 2H).

1-(3-(Methoxymethoxy)phenyl)-1H-pyrrole-2-carbaldehyde (137). To a solution of **54** (307 mg, 1.64 mmol) in dry DCM (15.1 mL), DIPEA (851 μL, 4.92 mmol) and MOM-Cl (374 μL, 4.92 mmol) were added. The reaction mixture was stirred at 0 °C, under N_2 atmosphere for 1 h. A saturated solution of $NaHCO_3$ was added and the mixture was extracted with DCM (3 x 10 mL). Organic phase was dried over sodium sulphate, filtered and concentrated. The crude was purified by column chromatography on silica gel (PE/EtOAc from 6:1 to 4:1) to afford the title compound as an amorphous pale-yellow solid (96% yield). ^1H NMR (300 MHz, $(CD_3)_2CO$) δ 9.59 (s, 1H), 7.42 (t, $J = 8.4$ Hz, 1H), 7.30 (s, 1H), 7.19 – 7.10 (m, 3H), 7.10 – 7.04 (m, 1H), 6.43 (s, 1H), 5.27 (s, 2H), 3.45 (s, 3H).

1-(3-(Methoxymethoxy)phenyl)-1H-pyrrole-2-carboxylic acid (138). Compound **138** was prepared according to the procedure used for **136** starting from **137** (361 mg, 1.56 mmol), 2-methyl-2-butene (2.16 ml, 20.29 mmol) and saturated aqueous solutions of $NaClO_2$ (0.69 mL, 5.78 mmol) and NaH_2PO_4 (1.10 mL, 7.81 mmol). The crude was purified by column chromatography on silica gel (PE/EtOAc from 3:1 to EtOAc only) to afford the title compound as a colorless oil (91% yield). ^1H NMR (300 MHz, $(CD_3)_2CO$) δ 7.41 – 7.26 (m, 1H), 7.18 – 7.01 (m, 4H), 7.02 – 6.92 (m, 1H), 6.29 (s, 1H), 5.23 (s, 2H), 3.44 (s, 3H).

N-(Benzyloxy)-1-(3-(methoxymethoxy)phenyl)-1H-pyrrole-2-carboxamide (139a). To a solution of **138** (345 mg, 1.40 mmol) in dry THF (20 mL) at 25 °C, TEA (777 μL, 5.59 mmol) was added. The suspension was stirred for 10 min, then *O*-benzylhydroxylamine hydrochloride (223 mg, 1.40 mmol) and BOP-Cl (391 mg, 1.54 mmol) were added. The reaction mixture was stirred for 16 h under N_2 atmosphere. A saturated solution of NH_4Cl

was added and the reaction mixture was extracted with EtOAc (3 x 10 mL). Then, the combined organic layers were washed with a saturated solution of NaHCO₃. Organic phase was dried over sodium sulphate, filtered and concentrated. The crude was purified by column chromatography on silica gel (PE/EtOAc from 8:1 to 1:1) to afford the title compound as an amorphous off-white solid (78% yield). ^{1}H NMR (300 MHz, (CD₃)₂CO) δ 10.43 (s, 1H), 7.48 – 7.29 (m, 6H), 7.11 – 7.00 (m, 3H), 6.98 – 6.91 (m, 1H), 6.78 – 6.72 (m, 1H), 6.22 (dd, J = 3.7, 2.9 Hz, 1H), 5.24 (s, 2H), 4.93 (s, 2H), 3.45 (s, 3H).

N-(Benzyloxy)-1-(3-(methoxymethoxy)phenyl)-1H-pyrrole-3-carboxamide **(139b)**. Compound 1**39b** was prepared according to the procedure used for **139a** starting from **56** (52 mg, 0.21 mmol), TEA (117 μL, 0.84 mmol), *O*-benzylhydroxylamine hydrochloride (34 mg, 0.21 mmol) and BOP-Cl (59 mg, 0.23 mmol. The crude was purified by column chromatography on silica gel (PE/EtOAc from 3:1 to 1:1) to afford the title compound as an amorphous off-white solid (55% yield). ^{1}H NMR (300 MHz, (CD₃)₂CO) δ 10.37 (s, 1H), 7.82 – 7.78 (m, 1H), 7.52 – 7.32 (m, 6H), 7.30 – 7.26 (m, 1H), 7.25 – 7.15 (m, 2H), 7.05 – 6.96 (m, 1H), 6.70 (dd, J = 3.0, 1.7 Hz, 1H), 5.29 (s, 2H), 4.98 (s, 2H), 3.46 (s, 3H).

N-(Benzyloxy)-1-(3-hydroxyphenyl)-1H-pyrrole-2-carboxamide **(134b)**. To a solution of compound **139a** (100 mg, 0.28 mmol) in MeOH (10 mL), a solution of HCl 1 N in ethanol was added (0.43 mL, 0.43 mmol). The reaction mixture was stirred 12 h at 25 °C. NaHCO3saturated solution was added and MeOH was removed in vacuo. The water phase was extracted with DCM (3 x 20 mL), the combined organic phases dried over sodium sulphate and then concentrated. The crude was purified by column chromatography on silica gel (PE/EtOAc from 3:1 to EtOAc only) to afford the title compound as an amorphous off-white solid (54% yield). ^{1}H NMR (300 MHz, (CD₃)₂CO) δ 10.47 (s, 1H), 8.75 (s, 1H), 7.48 – 7.30 (m, 5H), 7.27 – 7.17 (m, 1H), 7.05 (dd, J = 2.6, 1.7 Hz, 1H), 6.87 – 6.68 (m, 4H), 6.21 (dd, J = 3.7, 2.8 Hz, 1H), 4.92 (s, 2H).

N-(Benzyloxy)-1-(3-hydroxyphenyl)-1H-pyrrole-3-carboxamide **(134c)**. Compound **134c** was prepared according to the procedure used for **134b** starting from **139b** (108 mg, 0.42 mmol) and a solution of 1N HCl/MeOH (460 μL, 0.46 mmol). The crude was purified by column chromatography on silica gel (PE/EtOAc from 4:1 to EtOAc only) to afford the title compound as an amorphous off-white solid (44% yield). ^{1}H NMR (300 MHz, (CD₃)₂CO) δ 10.35 (s, 1H), 8.86 (s, 1H), 7.79 – 7.73 (m, 1H), 7.52 – 7.43 (m, 2H), 7.42 – 7.26 (m, 4H), 7.26 – 7.18 (m, 1H), 7.07 – 6.97 (m, 2H), 6.87 – 6.77 (m, 1H), 6.68 (dd, J = 2.9, 1.7 Hz, 1H), 4.98 (s, 2H).

methyl 1-(3-(methoxymethoxy)phenyl)-1H-pyrrole-3-carboxylate **(140)**. To a solution of **56** (117 mg, 0.47 mmol) and K₂CO₃ (105 mg, 0.76 mmol) in dry DMF (3 mL), iodomethane (47 μL, 0.76 mmol) was added. The reaction mixture was stirred for 16 h at 25 °C Then, the reaction was quenched with a saturated solution of NH₄Cl and extracted with EtOAc (3 x 10 mL). The combined organic layers were washed with a saturated solution of NH₄Cl (1 x 10 mL) and brine (2 x 10 mL). Organic phase was dried over sodium sulphate, filtered and concentrated. Compound was used in the next step without any further purification. (88% yield, colorless oil). ^{1}H NMR (300 MHz, CDCl₃) δ 7.72 – 7.65 (m, 1H), 7.35 (t, J = 8.1 Hz, 1H), 7.11 – 7.07 (m, 1H), 7.07 – 6.96 (m, 3H), 6.73 (dd, J = 2.9, 1.6 Hz, 1H), 5.21 (s, 2H), 3.84 (s, 3H), 3.49 (s, 3H).

Methyl 1-(3-hydroxyphenyl)-1H-pyrrole-3-carboxylate (134d). To a solution of **140** (109 mg, 0.42 mmol) in methanol (10.9 mL), a solution of 1N HCl/MeOH (1.25 mL, 1.25 mmol) was added. The reaction mixture was stirred for 16 h. A saturated solution of NaHCO₃ was added and solvent was removed under vacuum. The solid residue was suspended in water and extracted with EtOAc (3 x 10 mL). Organic phase was dried over sodium sulphate, filtered and concentrated. Compound was used in the next step without any further purification. (89% yield, off-white solid). ^{1}H NMR (300 MHz, CDCl₃) δ 7.68 (s, 1H), 7.34 – 7.22 (m, 1H), 7.03 – 6.88 (m, 3H), 6.88 – 6.79 (m, 1H), 6.72 (dd, J = 2.7, 1.5 Hz, 2H), 3.86 (s, 3H). ESI-MS *m/z*: 216 [M-H]⁻.

(4-(Methoxycarbonyl)benzyl)triphenylphosphonium bromide (142). To a solution of methyl 4-(bromomethyl)benzoate **141** (2000 mg, 8.73 mmol) in dry toluene (17.5 mL), triphenylphosphine (2290 mg, 8.73 mmol) was added. The reaction mixture was refluxed for 16 h. After cooling to 25 °C, the reaction mixture was filtered. The solid residue was washed with toluene and the residual solvent was removed under vacuum. The crude was used in the next step without any further purification (99% yield, white solid).

2-(5-Hydroxypentyl)isoindoline-1,3-dione (144). To a solution of 5-aminopentan-1-ol **143** (1000 mg, 9.69 mmol) in dry toluene (9.7 mL), phthalic anhydride (1436 mg, 9.69 mmol) was added. The reaction mixture was refluxed for 24 h. After cooling to 25 °C, the solvent was removed. The crude was taken up with diethyl ether and filtered. The solution was washed with 1N HCl (3 x 10 mL). Then, the organic layers were dried over sodium sulphate, filtered and concentrated. The crude was used in the next step without any further purification (80% yield, yellow oil). ^{1}H NMR (300 MHz, CDCl₃) δ 7.80 – 7.54 (m, 4H), 3.59 (dt, J = 13.0, 6.8 Hz, 4H), 1.74 – 1.47 (m, 4H), 1.42 – 1.25 (m, 2H).

5-(1,3-Dioxoisoindolin-2-yl)pentanal (145). To a solution of **144** (200 mg, 0.86 mmol) in dry DCM (2.7 mL) at 0 °C, TCICA (209 mg, 0.90 mmol) and TEMPO (1.34 mg, 0.01 mmol) were added. The mixture was stirred at 0 °C for 15 minutes. The reaction mixture was then filtered through celite and washed with DCM. The collected organic layers were washed with a saturated solution of NaHCO₃ and 1N HCl, then dried over sodium sulphate, filtered and concentrated. The crude was used in the next step without any further purification (99% yield, yellow oil). ^{1}H NMR (300 MHz, (CD₃)₂CO) δ 9.72 (s, 1H), 7.83 – 7.75 (m, 4H), 3.70 – 3.57 (m, 2H), 2.55 – 2.46 (m, 2H), 1.80 – 1.55 (m, 4H).

Methyl (E/Z)-4-(6-(1,3-dioxoisoindolin-2-yl)hex-1-en-1-yl)benzoate (146). To a solution of **142** (841 mg, 1.71 mmol) in dry THF (7 mL) at 0 °C, KHMDS (0.5 M solution in toluene, 2568 μL, 1.28 mmol) was added. The reaction mixture was stirred at 0 °C for 30 minutes. Then, a solution of **145** (396 mg, 1.7 mmol) in dry THF (4 mL) was added at 0 °C. The reaction mixture was stirred for 16 h at 25 °C, under N₂ atmosphere. The reaction mixture was quenched with a saturated solution of NH₄Cl and extracted with EtOAc (2 x 10 mL). the collected organic layers were dried over sodium sulphate, filtered and concentrated. The crude was purified by column chromatography on silica gel (PE/EtOAc from 7:1 to 3:1) to afford the title compound as a white solid (83% yield). ^{1}H NMR (300 MHz, CDCl₃) δ 7.93 – 7.81 (m, 2H), 7.78 – 7.69 (m, 2H), 7.65 – 7.58 (m, 2H), 7.32 – 7.16 (m, 2H), 6.39 – 6.17 (m, 2H), 3.82 (d, J = 3.6 Hz, 3H), 3.69 – 3.54 (m, 2H), 2.35 – 2.13 (m, 2H), 1.75 – 1.57 (m, 2H), 1.54 – 1.39 (m, 2H).

Methyl 4-(6-(1,3-dioxoisoindolin-2-yl)hexyl)benzoate (147). To a solution of **146** (515 mg, 1.42 mmol) in EtoAc/MeOH 2:1 (45 mL), palladium on carbon (0.14 mol) was added. The reaction mixture was stirred under H_2 atmosphere for 1 h. The catalyst was removed by filtration and the crude was concentrated under vacuum. The crude was used in the next step without any further purification (90% yield, white solid). ^{1}H NMR (300 MHz, $CDCl_3$) δ 7.91 (d, J = 8.1 Hz, 2H), 7.84 – 7.63 (m, 4H), 7.19 (d, J = 8.1 Hz, 2H), 3.87 (s, 3H), 3.68 – 3.60 (m, 2H), 2.66 – 2.57 (m, 2H), 1.73 – 1.55 (m, 4H), 1.39 – 1.31 (m, 4H).

4-(6-(1,3-Dioxoisoindolin-2-yl)hexyl)benzoic acid (148). To a solution of **147** (313 mg, 0.86 mmol) in dry THF (18 mL), an aqueous solution of NaOH (137 mg, 3.43 mmol, 18 mL) was added. The reaction mixture was stirred for 16 h at 25 °C The reaction mixture was quenched with 6N HCl and extracted with EtOAc (3 x 20 mL). The organic layers were dried over sodium sulphate, filtered and concentrated. The crude was used in the next step without any further purification (99% yield, white solid). ^{1}H NMR (300 MHz, Methanol-d_4) δ 7.96 – 7.88 (m, 3H), 7.61 – 7.46 (m, 2H), 7.42 – 7.36 (m, 1H), 7.29 (d, J = 8.2 Hz, 2H), 3.33 – 3.27 (m, 2H), 2.74 – 2.63 (m, 2H), 1.75 – 1.54 (m, 4H), 1.51 – 1.36 (m, 4H).

N-(Benzyloxy)-4-(6-(1,3-dioxoisoindolin-2-yl)hexyl)benzamide (149). To a solution of **148** (76 mg, 0.22 mmol) in dry THF (3 mL), thionyl chloride (224 µL, 3.07 mmol) was added dropwise. The reaction mixture was refluxed for 2 h under N_2 atmosphere. After cooling to 25 °C, the solvent was removed, the solid residue was suspended in DCM and then, the solvent was removed under vacuum. This procedure was repeated twice. The obtained solid was dissolved in dry DCM (2 mL) and then, DIPEA (79 µL, 0.45 mmol) and *O*-benzylhydroxylamine hydrochloride (27 mg, 0.17 mmol) were added. The reaction mixture was stirred at 25 °C, under N_2 atmosphere for 16 h. A saturated solution of NH_4Cl was added and the mixture was extracted with DCM (3 x 10 mL). The collected organic layers were dried over sodium sulphate, filtered and concentrated The crude was purified by column chromatography on silica gel (PE/EtOAc from 3:1 to 1:1) to afford the title compound as an white solid (29% yield). ^{1}H NMR (300 MHz, $(CD_3)_2CO$) δ 10.73 (s, 1H), 7.84 (s, 4H), 7.76 – 7.65 (m, 2H), 7.48 (dd, J = 7.7, 1.7 Hz, 2H), 7.42 – 7.33 (m, 2H), 7.30 – 7.25 (m, 2H), 5.00 (s, 2H), 3.64 (t, J = 7.1 Hz, 2H), 2.70 – 2.60 (m, 2H), 1.72 – 1.56 (m, 4H), 1.43 – 1.34 (m, 4H).

4-(6-Aminohexyl)-N-(benzyloxy)benzamide (135a). To a solution of **147** (63 mg, 0.17 mmol) in EtOH (2.4 mL), hydrazine monohydrate (63 mg, 0.17 mmol) was added. The solution was refluxed for 1 h until appearance of white precipitate, which was removed by filtration. The filtrate was concentrated under reduced pressure. The crude was taken up with water, treated with 1N HCl and extracted with DCM (3 x 10 mL). The combined aqueous layers were treated with 1 NaOH to reach pH = 8 and extracted with DCM (3 x 5 mL). The organic layer was dried over anhydrous sodium sulphate, filtered and concentrated. The crude was used in the next step without any further purification (72% yield, pale-yellow oil). **^{1}H NMR** (300 MHz, $CDCl_3$) δ 7.96 – 7.90 (m, 2H), 7.24 – 7.18 (m, 2H), 3.88 (s, 3H), 2.94 (br, 2H), 2.78 – 2.67 (m, 2H), 2.67 – 2.58 (m, 2H), 1.69 – 1.54 (m, 2H), 1.54 – 1.41 (m, 2H), 1.38 – 1.28 (m, 4H).

4-(6-Aminohexyl)-N-(benzyloxy)benzamide (135b). Compound **135b** was prepared according to the procedure used for **135a** starting from **149** (74 mg, 0.16 mmol) and hydrazine monohydrate (31 µL, 0.65 mmol). The crude was used in the next step without any further purification (99% yield, pale-yellow oil). ^{1}H NMR (300 MHz, CD_3OD) δ 8.19

(dd, J = 6.0, 3.3 Hz, 1H), 7.78 (dd, J = 6.0, 3.3 Hz, 1H), 7.62 (d, J = 8.2 Hz, 2H), 7.51 – 7.44 (m, 1H), 7.41 – 7.33 (m, 2H), 7.26 (d, J = 8.2 Hz, 2H), 4.96 (s, 2H), 2.85 – 2.77 (m, 2H), 2.70 – 2.61 (m, 2H), 1.71 – 1.47 (m, 4H), 1.47 – 1.28 (m, 4H).

Benzyl 1-(3-(((6-phenylhexyl)carbamoyl)oxy)phenyl)-1H-pyrrole-3-carboxylate (150). To a solution of **134a** (40 mg, 0.14 mmol) in dry DCM (5 mL) under N_2 atmosphere at 0 °C, TEA (57 µL, 0.41 mmol) and 4-nitrophenyl chloroformate (41 mg, 0.21 mmol) were added. Reaction mixture was stirred for 2 h. Subsequently, a solution of the amine **50d** (0.21 mmol, 4.2 mL) in dry DCM was added and the reaction was stirred for 2 h. Reaction mixture was quenched with water and extracted with DCM (3 x 10 mL). The combined organic layers were dried over sodium sulphate, filtered and concentrated. The crude was purified by column chromatography on silica gel (DCM/acetone 100:1) to afford the title compound as a pale-yellow oil (50% yield). ^{1}H NMR (300 MHz, (CD$_3$)$_2$CO) δ 7.95 – 7.88 (m, 1H), 7.53 – 7.07 (m, 14H), 6.91 (t, J = 5.3 Hz, 1H), 6.73 (dd, J = 3.0, 1.6 Hz, 1H), 5.29 (s, 2H), 3.22 (dd, J = 13.0, 6.8 Hz, 2H), 2.65 – 2.56 (m, 2H), 1.70 – 1.52 (m, 4H), 1.46 – 1.31 (m, 4H). ESI-MS *m/z*: 520 [*M*+Na]$^+$.

3-(3-((Benzyloxy)carbonyl)-1H-pyrrol-1-yl)phenyl 4-(3-phenylpropyl)piperazine-1-carboxylate (151). Compound **151** was prepared according to the procedure used for **150** starting from **134a** (28 mg, 0.10 mmol), TEA (40 µL, 0.29 mmol), 4-nitrophenyl chloroformate (29 mg, 0.14 mmol) and a solution of the amine **50f** (0.14 mmol, 2.9 mL) in dry DCM. The crude was purified by column chromatography on silica gel (Hex/EtOAc 3:1 to 1:1) to afford the title compound as a pale-yellow oil (50% yield). ^{1}H NMR (300 MHz, (CD$_3$)$_2$CO) δ 7.95 – 7.90 (m, 1H), 7.53 – 7.11 (m, 15H), 6.73 (dd, J = 3.0, 1.6 Hz, 1H), 5.29 (s, 2H), 3.76 – 3.63 (m, 2H), 3.57 – 3.46 (m, 2H), 2.67 (dd, J = 15.5, 7.8 Hz, 2H), 2.54 – 2.42 (m, 4H), 2.44 – 2.28 (m, 2H), 1.88 – 1.77 (m, 2H). ESI-MS m/z: *525* [*M*+H]$^+$.

3-(3-((Benzyloxy)carbamoyl)-1H-pyrrol-1-yl)phenyl (6-phenylhexyl)carbamate (152). Compound **152** was prepared according to the procedure used for **150** starting from **134b** (20 mg, 0.07 mmol), TEA (29 µL, 0.21 mmol), 4-nitrophenyl chloroformate (21 mg, 0.10 mmol) and a solution of the amine **50d** (0.10 mmol, 2.1 mL) in dry DCM. The crude was purified by column chromatography on silica gel (DCM/acetone 100:1) to afford the title compound as a pale-yellow oil (24 % yield). ^{1}H NMR (300 MHz, CD$_3$OD) δ 7.74 – 7.68 (m, 1H), 7.52 – 7.04 (m, 15H), 6.66 – 6.61 (m, 1H), 4.94 (s, 2H), 3.21 – 3.14 (m, 1H), 3.11 – 3.04 (m, 1H), 2.60 (dd, J = 15.6, 8.0 Hz, 2H), 1.71 – 1.50 (m, 4H), 1.51 – 1.30 (m, 4H).

3-(3-((Benzyloxy)carbamoyl)-1H-pyrrol-1-yl)phenyl 4-(3-phenylpropyl)piperazine-1-carboxylate (153). Compound **153** was prepared according to the procedure used for **150** starting from **134b** (30 mg, 0.10 mmol), TEA (41 µL, 0.29 mmol), 4-nitrophenyl chloroformate (29 mg, 0.15 mmol) and a solution of the amine **50f** (0.15 mmol, 2.9 mL) in dry DCM. The crude was purified by column chromatography on Al$_2$O$_3$ (PE/EtOAc 2:1 to EtOAc/MeOH 100:1) to afford the title compound as a pale-yellow oil (80% yield). ^{1}H NMR (300 MHz, (CD$_3$OD) δ 7.74 – 7.71 (m, 1H), 7.52 – 7.44 (m, 3H), 7.43 – 7.31 (m, 5H), 7.29 – 7.06 (m, 7H), 6.64 (s, 1H), 4.94 (s, 2H), 3.78 – 3.68 (m, 2H), 3.61 – 3.52 (m, 2H), 2.71 – 2.60 (m, 2H), 2.59 – 2.50 (m, 3H), 2.50 – 2.40 (m, 3H), 1.95 – 1.78 (m, 2H).

3-(2-((Benzyloxy)carbamoyl)-1H-pyrrol-1-yl)phenyl (6-phenylhexyl)carbamate (154).
Compound **154** was prepared according to the procedure used for **150** starting from **134c** (47 mg, 0.15 mmol), TEA (63 µL, 0.46 mmol), amine **50d** (0.15 mmol, 2.9 mL) and 4-nitrophenyl chloroformate (46 mg, 0.23 mmol). The crude was purified by column chromatography on silica gel (DCM/MeOH 100:1 to 90:1) to afford the title compound as a pale-yellow oil (54% yield). ^{1}H NMR (300 MHz, (CD$_3$)$_2$CO) δ 10.51 (s, 1H), 7.48 – 7.06 (m, 15H), 6.94 – 6.83 (m, 1H), 6.77 (d, J = 2.2 Hz, 1H), 6.25 – 6.19 (m, 1H), 4.93 (s, 2H), 3.20 (dd, J = 13.1, 6.7 Hz, 2H), 2.59 (dd, J = 14.6, 6.7 Hz, 2H), 1.67 – 1.52 (m, 4H), 1.47 – 1.31 (m, 4H).

3-(3-Carbamoyl-1H-pyrrol-1-yl)phenyl   (6-(4 ((benzyloxy)carbamoyl)phenyl)hexyl)carbamate (155). Compound **155** was prepared according to the procedure used for **150** starting from **49c** (42 mg, 0.11 mmol), TEA (45 µL, 0.32 mmol), 4-nitrophenyl chloroformate (33 mg, 0.16 mmol) and a solution of the amine **135b** (0.16 mmol, 3.3 mL) in dry DCM. The crude was purified by column chromatography on silica gel (DCM/MeOH 100:1 to 90:1) to afford the title compound as a white solid (4% yield).]$^+$. ^{1}H NMR (300 MHz, CDCl$_3$) δ 7.74 – 7.68 (m, 1H), 7.63 – 7.56 (m, 2H), 7.48 – 7.34 (m, 6H), 7.26 (d, J = 1.3 Hz, 2H), 7.25 – 7.16 (m, 3H), 7.11 – 7.04 (m, 1H), 7.03 – 6.99 (m, 1H), 5.03 (s, 2H), 3.24 (dd, J = 13.1, 6.6 Hz, 2H), 2.64 (t, J = 7.5 Hz, 2H), 1.70 – 1.51 (m, 4H), 1.44 – 1.29 (m, 4H). ESI-MS *m/z*: 577 [*M*+H

1-(3-(((6-Phenylhexyl)carbamoyl)oxy)phenyl)-1H-pyrrole-3-carboxylic acid (44a).
Compound **44a** was prepared according to the procedure used for **147** starting from **150** (50 mg, 0.10 mmol) and palladium on carbon (0.01 mol). The crude was purified by column chromatography on silica gel (DCM/MeOH 20:1 to DCM/MeOH/HCOOH 20:1:0.1) to afford the title compound as a pale-yellow oil (69% yield). ^{1}H NMR (300 MHz, (CD$_3$)$_2$CO) δ 7.89 – 7.83 (m, 1H), 7.55 – 7.07 (m, 9H), 6.96 – 6.86 (m, 1H), 6.70 (dd, J = 2.9, 1.6 Hz, 1H), 3.22 (dd, J = 13.1, 6.8 Hz, 2H), 2.66 – 2.57 (m, 2H), 1.71 – 1.52 (m, 4H), 1.49 – 1.33 (m, 4H). ESI-MS *m/z*: 407 [*M*+Na]$^+$.

1-(3-((4-(3-Phenylpropyl)piperazine-1-carbonyl)oxy)phenyl)-1H-pyrrole-3-carboxylic acid (44b). Compound **44b** was prepared according to the procedure used for **147** starting from **151** (21 mg, 0.04 mmol) and palladium on carbon (0.004 mmol) in EtOAc/MeOH 3:1 (4 mL). The crude was purified by column chromatography on silica gel (DCM/MeOH 20:1 to DCM/MeOH/HCOOH 20:1:0.1) to afford the title compound as a pale-yellow oil (40% yield). ^{1}H NMR (300 MHz, (CD$_3$)$_2$CO) δ 7.88 – 7.84 (br, 1H), 7.53 – 7.45 (m, 3H), 7.36 – 7.11 (m, 7H), 6.69 (dd, J = 3.0, 1.6 Hz, 1H), 3.76 – 3.60 (m, 2H), 3.60 – 3.47 (m, 2H), 2.73 – 2.64 (m, 2H), 2.54 – 2.43 (m, 4H), 2.44 – 2.36 (m, 2H), 1.90 – 1.76 (m, 2H). **ESI-MS** *m/z*: 434 [*M*+H]$^+$.

3-(3-(Hydroxycarbamoyl)-1H-pyrrol-1-yl)phenyl (6-phenylhexyl)carbamate (44c).
Compound **44c** was prepared according to the procedure used for **147** starting from **152** (34 mg, 0.07 mmol) and palladium on carbon (0.007 mmol) in EtOAc/MeOH 3:1 (4 mL). The crude was purified by column chromatography on silica gel (DCM/MeOH 30:1 to DCM/MeOH/HCOOH 10:1:0.1) to afford the title compound as an amorphous brown solid (58% yield). ^{1}H NMR (300 MHz, CD$_3$OD) δ 7.81 – 7.64 (m, 1H), 7.52 – 7.01 (m, 10H), 6.65 (s, 1H), 3.23 – 3.09 (m, 2H), 2.61 (t, J = 7.5 Hz, 2H), 1.77 – 1.49 (m, 4H), 1.46 – 1.19 (m, 4H). ^{13}C NMR (75 MHz, CD$_3$OD) δ 164.2, 155.3, 152.3, 142.4, 140.5, 130.1, 128.0, 127.8, 125.2, 121.2, 120.3, 119.5, 118.3, 116.7, 113.9, 109.0, 40.6, 35.4, 31.3, 29.2, 28.6, 26.3.

3-(3-(Hydroxycarbamoyl)-1H-pyrrol-1-yl)phenyl 4-(3-phenylpropyl)piperazine-1-carboxylate (44d). Compound **44d** was prepared according to the procedure used for **147** starting from **153** (42 mg, 0.08 mmol) and palladium on carbon (0.008 mmol) in EtOAc/MeOH 3:1 (4 mL). The crude was purified by column chromatography on silica gel (DCM/MeOH 40:1 to DCM/MeOH/NH$_4$OH 10:1:0.1) to afford the title compound as an amorphous brown solid (61% yield). ^{1}H NMR (300 MHz, (CD$_3$)$_2$CO) δ 10.63 – 10.14 (br, 1H), 8.12 – 7.66 (m, 1H), 7.64 – 7.35 (m, 3H), 7.37 – 7.21 (m, 5H), 7.15 (dd, *J* = 17.9, 6.5 Hz, 2H), 6.71 (s, 1H), 3.62 (d, *J* = 50.4 Hz, 4H), 3.18 – 2.75 (m, 2H), 2.77 – 2.58 (m, 2H), 2.59 – 2.27 (m, 4H), 1.91 – 1.68 (m, 2H).

Methyl 1-(3-(((6-phenylhexyl)carbamoyl)oxy)phenyl)-1H-pyrrole-3-carboxylate (44e). Compound **44e** was prepared according to the procedure used for **150** starting from **134d** (37 mg, 0.17 mmol), TEA (71 µL, 0.51 mmol), 4-nitrophenyl chloroformate (52 mg, 0.26 mmol) and a solution of the amine **50d** (0.26 mmol, 5.2 mL) in dry DCM. The crude was purified by column chromatography on silica gel (PE/EtOAc 1:1) to afford the title compound as a pale-yellow oil (34% yield). ^{1}H NMR (300 MHz, CDCl$_3$) δ 7.70 – 7.65 (m, 1H), 7.42 (t, *J* = 8.3 Hz, 1H), 7.33 – 7.13 (m, 7H), 7.11 – 7.05 (m, 1H), 7.00 (t, *J* = 2.6 Hz, 1H), 6.74 (dd, *J* = 2.9, 1.6 Hz, 1H), 3.84 (s, 3H), 3.26 (dd, *J* = 13.4, 6.7 Hz, 2H), 2.66 – 2.57 (m, 2H), 1.72 – 1.53 (m, 4H), 1.45 – 1.33 (m, 4H).

3-(2-(Hydroxycarbamoyl)-1H-pyrrol-1-yl)phenyl (6-phenylhexyl)carbamate (44f). Compound **44f** was prepared according to the procedure used for **147** starting from **154** (41 mg, 0.08 mmol) and palladium on carbon (0.008 mmol) in EtOAc/MeOH 3:1 (4 mL). The crude was purified by column chromatography on silica gel EtOAc/PE 2:1 to EtOAc only) to afford the title compound as an amorphous brown solid (12% yield). ^{1}H NMR (300 MHz, CD$_3$OD) δ 7.44 – 7.35 (m, 1H), 7.27 – 7.05 (m, 9H), 6.75 – 6.70 (m, 1H), 6.28 – 6.23 (m, 1H), 3.16 (t, *J* = 6.9 Hz, 2H), 2.65 – 2.56 (m, 2H), 1.70 – 1.48 (m, 4H), 1.46 – 1.31 (m, 4H).

3-(3-Carbamoyl-1H-pyrrol-1-yl)phenyl (6-(4-(hydroxycarbamoyl)phenyl)hexyl)carbamate (44g). Compound **44h** was prepared according to the procedure used for **147** starting from **155** (12 mg, 0.02 mmol) and palladium on carbon (0.002 mmol) in EtOAc/MeOH 3:1 (1.6 mL). The crude was purified by column chromatography on silica gel (DCM/MeOH 20:1 to DCM/MeOH/trifluoroacetic acid 10:1:0.1) to afford the title compound as an amorphous brown solid. ^{1}H NMR (300 MHz, Methanol-*d$_4$*) δ 7.80 (s, 1H), 7.65 (d, *J* = 7.9 Hz, 2H), 7.54 – 7.35 (m, 2H), 7.34 – 7.18 (m, 4H), 7.07 (d, *J* = 8.4 Hz, 1H), 6.73 (d, *J* = 2.4 Hz, 1H), 3.17 (t, *J* = 6.5 Hz, 2H), 2.68 (t, *J* = 7.6 Hz, 2H), 1.73 – 1.50 (m, 4H), 1.48 – 1.30 (m, 4H). ESI-MS *m/z*: 465.6 [*M*+H]$^+$.

Methyl 4-(6-(((3-(3-carbamoyl-1H-pyrrol-1-yl)phenoxy)carbonyl)amino)hexyl)benzoate (44h). Compound **44g** was prepared according to the procedure used for **150** starting from **49c** (17 mg, 0.08 mmol), TEA (35 µL, 0.25 mmol), 4-nitrophenyl chloroformate (25 mg, 0.13 mmol) and a solution of the amine **125b** (0.13 mmol, 2 mL) in dry DCM. The crude was purified by column chromatography on silica gel (DCM/MeOH 50:1 to 40:1) to afford the title compound as a white solid (54% yield). ^{1}H NMR (300 MHz, CDCl$_3$) δ 7.93 (d, *J* = 8.0 Hz, 2H), 7.67 – 7.62 (m, 1H), 7.36 (t, *J* = 8.0 Hz, 1H), 7.27 – 7.12 (m, 4H), 7.08 – 7.00 (m, 1H), 7.00 – 6.94 (m, 1H), 6.59 – 6.52 (m, 1H), 6.12 – 5.84 (br, 2H), 5.39 (t, *J* = 5.8 Hz, 1H), 3.88 (s, 2H), 3.24 (dd, *J* = 13.3, 6.7 Hz, 2H), 2.69 – 2.59 (m, 2H), 1.70 – 1.48 (m, 4H), 1.45 – 1.30 (m, 4H). ^{13}C NMR (75 MHz, CD$_3$OD) δ 163.3, 163.0,

150.2, 148.0, 144.2, 136.4, 126.5, 125.7, 124.5, 123.7, 119.3, 116.9, 116.1, 115.7, 113.5, 110.6, 105.9, 48.1, 37.3, 31.9, 27.0, 25.7, 24.9, 22.6.

9.5. Experimental section of the dual MAGL/H₃R ligands 45a-d and 46c-g

3-(Benzhydrylamino)propan-1-ol (161a). To a solution of benzophenone **160** (200 mg, 1.10 mmol) in dry toluene (10 mL) *p*-toluenesulfonic acid (19 mg, 0.11 mmol) and 3-aminopropan-1-ol (85µL, 1.10 mmol) were added. Temperature was increased to 150 °C and reaction mixture was stirred for 2 d under N_2 atmosphere with a Dean-Stark apparatus. After that, a solution 1N of NaOH was added and the mixture was extracted with toluene (3 x 10 mL). Organic phase was dried with NaSO₄, filtered and solvent was removed under vacuum. The residue was dissolved in MeOH (2 mL) and sodium borohydride (83 mg, 2.20 mmol) was added at 0°C. Reaction mixture was stirred for 30 minutes. After that, temperature was allowed to reach 25 °C, a solution 1N of NaOH was added and solvent was removed under vacuum. The aqueous phase was extracted with DCM (3 x 10 mL). Organic phase was dried with NaSO₄, filtered and concentrated under vacuum. The crude was used in the following step without any further purification (yellow oil) (83% yield). ¹H NMR (300 MHz, CDCl₃) δ 7.36 – 7.15 (m, 10H), 4.97 (s, 1H), 3.79 – 3.73 (m, 2H), 2.81 – 2.75 (m, 2H), 1.74 – 1.65 (m, 2H).

4-(Benzhydrylamino)butanol-1-ol (161b). Compound **161b** was prepared according to procedure used for compound **161a** starting from benzophenone **160** (200 mg, 1.10 mmol), p-toluenesulfonic acid (21 mg, 0.11 mmol) and 4-aminobutan-1-ol (102 µL, 1.10 mmol) in dry toluene (10 mL) for the first step, then NaBH₄ (83 mg, 2.20 mmol) in MeOH (2 mL) was used in the second step. The crude was purified by column chromatography on silica gel (PE/EtOAc starting from 6:1 to EtOAc) to afford the title compound as a yellowish oil (64% yield). ¹H NMR (300 MHz, CDCl₃) δ 7.52 – 7.21 (m, 10H), 4.90 (s, 1H), 3.68 (t, *J* = 5.2 Hz, 2H), 2.68 (t, *J* = 5.6 Hz, 2H), 1.75 – 1.64 (m, 4H).

Benzyl benzhydryl(3-hydroxypropyl)carbamate (162a). To a solution of compound **161a** (216 mg, 0.90 mmol) in THF (2.3 mL), a solution of NaHCO₃ (227 mg, 2.70 mmol) in water (1 mL) was added at 0 °C and the mixture was stirred. After 10 minutes, benzyl chloroformate (167 µL, 1.17 mmol) was added. Temperature was allowed to reach 25 °C and reaction mixture was stirred for 12 h. Water was added, and the mixture was extracted with EtOAc (3 x 10 mL). Organic phase was dried with NaSO₄, filtered and concentrated under vacuum. The crude was purified by column chromatography on silica gel (PE/EtOAc starting from 3.1 to 1:1) to afford the title compound as a colorless oil (80% yield). ¹H NMR (300 MHz, CDCl₃) δ 7.35 – 7.05 (m, 15H), 5.27 (s, 1H), 5.14 (s, 2H), 3.56 – 3.42 (m, 2H), 3.37 – 3.24 (m, 2H), 1.03 – 0.88 (m, 2H).

Benzyl benzhydryl(4-hydroxybutyl)carbamate (162b). Title compound was prepared according to procedure used for compound **162a** starting from compound **161b** (180 mg, 0.70 mmol), a solution of NaHCO₃ (176 mg, 2.10 mmol) in water (1 mL) and benzyl chloroformate (130 µL, 0.91 mmol) in dry THF (1.8 mL). The crude was purified by column chromatography on silica gel (PE/EtOAc starting from 3:1 to EtOAc) to afford the title compound as a colorless oil (81% yield). ¹H NMR (300 MHz, CDCl₃) δ 7.42 – 7.13 (m, 15H), 5.19 (s, 3H), 3.41 – 3.23 (m, 4H), 1.31 – 1.11 (m, 4H).

Benzyl benzhydryl(3-bromopropyl)carbamate (163). To a solution of compound **162a** (140 mg, 0.37 mmol) in dry DCM (1.2 mL) triphenylphosphine (155 mg, 0.59 mmol), 1-*H*-imidazole (38 mg, 0.56 mmol) and tetrabromomethane (136 mg, 0.41 mmol) were

added. Reaction mixture was stirred for 12 h at room temperature under N_2 atmosphere. The following day, water was added, and the mixture was extracted with DCM (3 x 10 mL). Organic phase was dried with $NaSO_4$, filtered and concentrated under vacuum. The crude was purified by column chromatography on silica gel (PE/EtOAc 5:1) to afford the title compound as a yellowish oil (65% yield). ^{1}H NMR (300 MHz, CDCl$_3$) δ 7.41 – 7.16 (m, 15H), 5.22 (s, 3H), 3.49 – 3.40 (m, 2H), 3.14 – 2.97 (m, 2H), 1.61 – 1.45 (m, 2H).

4-(Benzyhydryl((benzyloxy)carbonyl)amino)butyl methanesulfonate (164). To a solution of compound **162b** (222 mg, 0.57 mmol) in dry DCM (1.4 mL) triethylamine (88 µL, 0.63) and methanesulfonyl chloride (49 µL, 0.63 mmol) were added at 0 °C. Temperature was allowed to reach 25 °C and reaction mixture was stirred for 30 minutes under N_2 atmosphere. After that, a saturated solution of $NaHCO_3$ was added and the mixture was extracted with DCM (3 x 10 mL). The collected organic layers were washed with a saturated solution of NH_4Cl (4 x 10 mL). Organic phase was dried with $NaSO_4$, filtered and concentrated under vacuum. The crude was used in the following step without any further purification (colorless oil, 99% yield). ^{1}H NMR (300 MHz, CDCl$_3$) δ 7.39 – 7.13 (m, 15H), 5.23 (s, 1H), 5.18 (s, 2H), 3.97 – 3.82 (m, 2H), 3.36 – 3.26 (m, 2H), 2.81 (d, J = 12.8 Hz, 3H), 1.46 – 1.28 (m, 4H)

tert-Butyl 4-(3-(benzhydryl((benzyloxy)carbonyl)amino)propyl)pipeazine-1-carboxylate (165a). To a solution of compound **163** (105 mg, 0.24 mmol) in dry THF (1 mL) triethylamine (101 µL, 0.72 mmol) and 1-Boc piperazine (54 mg, 0.29 mmol) were added. Temperature was increased to 75 °C and reaction mixture was stirred for 12 h under N_2 atmosphere. A saturated solution of $NaHCO_3$ was added and the mixture was extracted with EtOAc (3 x 10 mL). Organic phase was dried with $NaSO_4$, filtered and concentrated under vacuum. The crude was purified by column chromatography on silica gel (PE/EtOAc starting from 5:1 to EtOAc) to afford the title compound as a yellowish oil (71% yield). ^{1}H NMR (300 MHz, CDCl$_3$) δ 7.38 – 7.11 (m, 15H), 5.16 (s, 3H), 3.32 – 3.16 (m, 4H), 2.04 – 1.88 (m, 4H), 1.43 (s, 9H), 1.25 – 1.08 (m, 4H), 0.93 – 0.81 (m, 2H).

Benzyl benzhydryl(4-piperazin-1-yl)butyl)carbamate (165b). To a solution of compound **164** (421 mg, 0.98 mmol) in dry MeCN (2.3 mL), K_2CO_3 (135 mg, 0.98 mmol) and 1-Boc piperazine (183 mg, 0.98 mmol) were added. Temperature was increased to 85 °C and reaction mixture was stirred for 12 h under N_2 atmosphere. The following day, solvent was removed under vacuum. The residue was taken up with DCM, quenched with water and the mixture was extracted with DCM (3 x 10 mL). The collected organic layers were washed with a saturated solution of NH_4Cl (2 x 10 mL). Organic phase was dried with $NaSO_4$, filtered and concentrated under vacuum. The crude was purified by column chromatography on silica gel (PE/EtOAc starting from 6:1 to EtOAc) to afford the title compound as a milky oil (72% yield). ^{1}H NMR (300 MHz, CDCl$_3$) δ 7.41 – 7.19 (m, 15H), 5.30 (s, 1H), 5.23 (s, 2H), 3.46 – 3.29 (m, 6H), 2.30 - 2.18 (m, 4H), 2.12 – 2.01 (m, 2H), 1.52 (s, 9H), 1.25 – 1.08 (m, 4H).

Benzyl benzhydyl(3-(piperazin-1-yl)propyl)carbamate (166a). To a solution of compound **165a** (92 mg, 0.17 mmol) in MeOH (10 mL) a solution 1N of HCl/MeOH (170 µL, 0.17 mmol) was added. Temperature was increased to 40 °C and reaction mixture was stirred for 1 h. Solvent was removed under vacuum. The solid residue was taken up with DCM, neutralized with a saturated solution of $NaHCO_3$ and extracted with DCM (3

x 10 mL). Organic phase was dried with NaSO$_4$, filtered and concentrated under vacuum. The crude was used in following step without any further purification (white solid) (94% yield). ^{1}H NMR (300 MHz, CDCl$_3$) δ 7.42 – 7.06 (m, 15H), 5.21 (s, 1H), 5.14 (s, 2H), 3.40 – 3.20 (m, 2H), 2.85 – 2.58 (m, 4H), 2.10 – 1.84 (m, 6H), 1.29 – 1.07 (m, 2H).

*Benzyl benzhydryl(4-piperazin-1-yl)butyl)carbamate **(166b)***. Title compound was prepared according to procedure used for compound **166a** starting from compound **165b** (408 mg, 0.73 mmol) and a solution 1N of HCl/MeOH in MeOH (15 mL). The crude was used in the following step without any further purification (white solid) (99% yield).

*Benzyl (3-(4-(1H-1,2,4-triazole-1-carbonyl)piperazin-1-yl)propyl)(benzhydryl)carbamate **(167a)***. To a solution of compound **166a** (61 mg, 0.14 mmol) in dry DCM (11.5 mL) 1-1- carbonyl di-(1,2,4-triazole) (23 mg, 0.14) was added. Reaction mixture was stirred for 12 h at room temperature under N$_2$ atmosphere. Water was added and the mixture was extracted with EtOAc (3 x 10 mL). Organic phase was dried with NaSO$_4$, filtered and concentrated under vacuum. The crude was purified by column chromatography on silica gel (DCM/MeOH starting from 30:1 to 20:1) to afford the title compound as a colorless oil (43% yield). ^{1}H NMR (300 MHz, CDCl$_3$) δ 8.76 (s, 1H), 7.99 (s, 1H), 7.42 – 7.10 (m, 15H), 5.29 (s, 1H), 5.17 (s, 2H), 3.37 – 3.24 (m, 2H), 2.21 – 1.92 (m, 8H), 1.30 – 1.12 (m, 4H).

*Benzyl(4-(4-(1H-1,2,4-triazole-1-carbonyl)piperazin-1-yl)butyl)(benzhydryl)carbamate **(167b)***. Title compuond was prepared according to procedure used for compound **167a** starting from compound **166b** (156 mg, 0.34mmol) and 1-1'-carbonyl di(1,2,4-triazole) (56 mg, 0.34 mmol) in dry DCM (29 mL). The crude was purified by column chromatography on silica gel (DCM/MeOH starting from 70:1 to 40:1) to afford the title compound as a milky oil (42 %yield.) ^{1}H NMR (300 MHz, CDCl$_3$) δ 8.78 (s, 1H), 7.99 (s, 1H), 7.37 – 7.15 (m, 15H), 5.29 (s, 1H), 5.17 (s, 2H), 3.93 – 3.59 (m, 4H), 3.33 – 3.21 (m, 2H), 2.41 – 2.25 (m, 4H), 2.11 – 2.00 (m, 2H), 1.19 – 0.95 (m, 4H).

*tert-Butyl 4-(3-hydroxypropyl)piperazine-1-carboxylate **(169)***. Compound **169** was prepared according to procedure used for **163** starting from 1-Boc piperazine **168** (200 mg, 1.07 mmol), triethylamine (448 µL, 3.21 mmol) and 3-bromopropan-1-ol (97 µL, 1.07 mmol) in dry THF (4.2 mL). The crude was purified by column chromatography on silica gel (DCM/MeOH 10:1, then DCM/MeOH/NH$_4$OH 10:1:0.1) to afford the title compound as a yellow oil (94% yield). ^{1}H NMR (300 MHz, CDCl$_3$) δ 3.82 – 3.78 (m, 2H), 3.45 – 3.39 (m, 4H), 2.64 – 2.58 (m, 2H), 2.49 – 2.42 (m, 4H), 1.73 (p, *J* = 10.7, 5.4 Hz, 2H), 1.45 (s, 9H).

*tert-Butyl 4-(3-((methylsulfonyl)oxy)propyl)piperazine-1-carboxylate **(170)***. Title compuond was prepared according to procedure for **164** starting from **169** (74 mg, 0.32 mmol), triethylamine (48 µL, 0.35 mmol) and methanesulfonyl chloride (27 µL, 0.35 mmol) in dry DCM (1 mL). The crude was used in the following step without any further purification (yellowish oil) (99% yield). ^{1}H NMR (300 MHz, CDCl$_3$) δ 4.20 (t, *J* = 6.3 Hz,2H), 3.36 – 3.30 (m, 4H), 2.91 (s, 3H), 2.41 (t, *J* = 7.0 Hz, 2H), 2.35 – 2.30 (m, 4H), 1.90 – 1.79 (m, 2H), 1.34 (s, 9H).

*tert-Butyl 4-(3-(dibenzylamino)propyl)piperazine-1-carboxylate **(171)***. Title compuond was prepared according to procedure used for **164** starting from **170** (135 mg, 0.42 mmol), K$_2$CO$_3$ (58 mg, 0.42 mmol) and dibenzylamine (81 µL, 0.42 mmol) in dry MeCN (1 mL).

The crude was purified by column chromatography on silica gel (DCM/MeOH 50:1) to afford a title compound as a yellowish oil (57 % yield). ^{1}H NMR (300 MHz, CDCl$_3$) δ 7.39 – 7.15 (m, 10H), 3.54 (s, 4H), 3.39 – 3.32 (m, 4H), 2.44 (t, J = 7.0 Hz, 2H), 2.32 – 2.24 (m, 6H), 1.73 – 1.61 (m, 2H), 1.45 (s, 9H).

N,N-Dibenzyl-3-(piperazin-1-yl)propan-1-amine (172). Title compound was prepared according to procedure used for **165a** starting from **171** (100 mg, 0.24 mmol) and a solution 1N of HCl/MeOH224 µL, 0.24 mmol) in MeOH (14 mL). The crude was used in the following step without any further purification (yellowish solid, 79% yield). ^{1}H NMR (300 MHz, CDCl$_3$) δ 7.39 – 7.18 (m, 10H), 3.55 (s, 4H), 2.83 (t, J = 4.8 Hz, 4H), 2.44 (t, J = 7.1 Hz, 2H), 2.38 – 2.25 (m, 6H), 1.76 – 1.64 (m, 2H).

tert-Butyl 4-(3-bromopropyl)piperazine-1-carboxylate (173). Title compound was prepared according to procedure used for **163** starting from **169** (92 mg, 0.38 mmol), triphenylphosphine (159 mg, 0.61 mmol), 1-*H*-imidazole (39 mg, 0.57 mmol) and tetrabromomethane (139 mg, 0.42mmol) in dry DCM (1.2 mL). The crude was purified by column chromatography on silica gel (PE/EtOAc starting from 3:1 to 2:1) to afford the title compound as a yellowish oil (47% yield). ^{1}H NMR (300 MHz, CDCl$_3$) δ 3.43 – 3.37 (m, 4H), 2.47 (t, J = 7.1 Hz, 2H), 2.40 – 2.34 (m, 4H), 2.01 (p, J = 6.7 Hz, 2H), 1.42 (s, 9H), 0.93 – 0.80 (m, 2H).

tert-Butyl 4-(3-(phenylamino)propyl)piperazine-1-carboxylate (174). To a solution of aniline (191 mg, 2.05 mmol) in dry DMF (2.5 mL) K$_2$CO$_3$ (62 mg, 0.45 mmol) was added at 0 °C. After stirring for 30 minutes, a solution of compound **173** (126 mg, 0.41 mmol) in DMF (5 mL) was added dropwise. Temperature was allowed to reach 25 °C, then it was increased to 60 °C and reaction mixture was stirred for 2 d under N$_2$ atmosphere. After cooling down to room temperature, a saturated solution of NH$_4$Cl was added and the mixture was extracted with EtOAc (3 x 10 mL). The collected organic layers were washed with a saturated solution of NH$_4$Cl (2 x 10 mL) and a saturated solution of NaCl (1 x 10 mL). Organic phase was dried with NaSO$_4$, filtered and concentrated under vacuum. The crude was purified by column chromatography on silica gel (PE/EtOAc starting from 2:1 to 1:) to afford the title compound as a yellow oil (70% yield). ^{1}H NMR (300 MHz, CDCl$_3$) δ 7.21 – 6.55 (m 5H), 3.51 – 3.40 (m, 4H), 3.19 (t, J = 6.4 Hz, 2H), 2.49 (t, J = 6.6 Hz, 2H), 2.44 – 2.37 (m, 4H), 1.86 – 1.75 (m, 2H), 1.46 (s, 9H).

tert-Butyl 4-(3-(N-phenylbenzamido)propyl)piperazine-1-carboxylate (175). To a solution of **174** (105 mg, 0.33 mmol) in dry dioxane (4.3 mL), triethylamine (50 µL, 0.36 mmol) and benzoyl chloride (38 µL, 0.33 mmol) were added at 0 °C. Temperature was allowed to reach 25 °C, then it was increased to 75 °C and reaction mixture was stirred overnight under N$_2$ atmosphere. The following day, solvent was removed under vacuum. The residue was taken up with DCM, quenched with water and the mixture was extracted with DCM (3 x 10 mL). Organic phase was dried with NaSO$_4$, filtered and concentrated under vacuum. The crude was purified by column chromatography on silica gel (PE/EtOAc starting from 3:1 to EtOAc) to afford the title compound as a colorless oil (56% yield). ^{1}H NMR (300 MHz, CDCl$_3$) δ 7.33 – 7.01 (m, 10H), 4.04 – 3.97 (m, 2H), 3.45 – 3.37 (m, 4H), 2.46 – 2.39 (m, 2H), 2.38 – 2.33 (m, 4H), 1.93 – 1.81 (m, 2H), 1.48 (s, 9H).

N-Phenyl-N-(3-piperazin-1-yl)propyl)benzamide (176). Title compound was prepared according to procedure used for **165a** starting from **175** (83 mg, 0.19 mmol) and a solution 1N of HCl/MeOH (830 µL, 0.19 mmol) in MeOH (5 mL). The crude was used in the following step without any further purification (white solid, 95% yield). ^{1}H NMR (300 MHz, CDCl$_3$) δ 7.30 – 6.93 (m, 10H), 3.95 – 3.88 (m, 2H), 2.80 (t, J = 4.7 Hz, 4H), 2.39 – 2.26 (m, 4H), 1.89 – 1.72 (m, 4H).

3-(Piperidin-1-yl)propan-1-ol (178). To a solution of piperidine **177** (23 mL, 235 mmol) in acetone (200 mL) K$_2$CO$_3$ (32.5g, 235 mmol), KI (26g, 157 mmol) and 3-chloropropan-1-ol (13.1 mL, 157 mmol) were added. Temperature was increased to 65 °C and reaction mixture was stirred for 4 d. After cooling down at room temperature, inorganic salts were removed by filtration and the filtrate was concentrated under vacuum. The crude was purified by means of distillation under reduce pressure (T$_b$ = 65-80 °C at 5 mmbar) to afford the title compound as a white solid (64% yield). ^{1}H NMR (300 MHz, CDCl$_3$) δ 3.80 – 3.76 (m, 2H), 2.57 – 2.51 (m, 2H), 2.48 – 2.29 (m, 4H), 1.72 – 1.64 (m, 2H), 1.60 – 1.51 (m, 4H), 1.47 – 1.36 (m, 2H).

1-(3-Chloropropyl)piperidin-1-ium hydrochloride (179). To a solution of **178** (13 g, 90.76 mmol) in THF (121 mL) thionyl chloride (7.9 mL, 108.91) was added at 0 °C. Temperature was allowed to reach 25 °C, then it was increased to 60 °C and reaction mixture was stirred for 2 h. Then, solvent and SOCl$_2$ were removed by evaporation under vacuum. The crude was purified by recrystallization in isopropanol. The solid residue was washed with diethyl ether to afford the title compound as a slightly brown solid (95% yield). ^{1}H NMR (300 MHz, d$_6$-DMSO) δ 3.74 (t, J = 6.4 Hz, 2H), 3.45 – 3.35 (m, 2H), 3.13 – 3.02 (m, 5.0 Hz, 2H), 2.92 – 2.77 (m, 2H), 2.29 – 2.15 (m, 2H), 1.93 – 1.64 (m, 5H).

4-(3-Piperidin-1-yl)propoxy)benzaldehyde (180). To a solution of **179** (4044 mg, 24.86 mmol) in MeCN (20 mL) K$_2$CO$_3$ (5154 mg, 37.29 mmol) 4-hydroxybenzaldehyde (4,55 g, 37.29 mmol) were added. Temperature was increased to 85 °C and stirred for 2 d. After cooling down to room temperature, inorganic salts were removed by filtration and the filtrate was concentrated under vacuum. A solution 1N of NaOH was added and the mixture was extracted with DCM (3 x 10 mL). The combined organic layers were washed with a solution of NaOH 1N (2 x 10 mL) and a saturated solution of NaCl (1 x 10 mL). Organic phase was dried with MgSO$_4$, filtered and concentrated under vacuum. Purification was achieved by column chromatography on silica gel (DCM/MeOH/NH$_3$ starting from 98:2 to 95:5) to afford the title compound as an orange oil (52% yield). ^{1}H NMR (300 MHz, CDCl$_3$) δ 9.80 (s, 1H), 7.80 – 7.70 (m, 2H), 6.92 (d, J = 8.7 Hz, 2H), 4.04 (t, J = 6.3 Hz, 2H), 2.57 – 2.42 (m, 6H), 2.07 – 1.96 (m, 2H), 1.65 – 1.54 (m, 4H), 1.46 – 1.35 (m, 2H).

tert-butyl (4-hydroxybenzyl)carbamate (182). To a solution of **181** (8.2 mmol, 1000 mg) in DCM (80 mL) cooled at 0 °C, TEA (16.4 mmol, 2280 µL) and di-tertbuthyl bicarbonate (8.9 mmol, 1940 mg) was added. The reaction was allowed to reach 25 °C and it was stirred at this temperature for 12h. NaHCO3 *s.s.* was added and the mixture was extracted with DCM (3 x 30 mL). Organic phase was then washed with 1N HCl, dried over MgSO$_4$, filtered and evaporated. The crude was purified by column chromatography on silica gel (Hexane-EtOAc from 6:1 to 4:1), to afford the title compound as yellow oil (52% yield). ^{1}H NMR (300 MHz, CDCl$_3$) δ 7.12 (d, J = 8.0 Hz, 2H), 6.86 – 6.76 (m, 2H), 6.36 (s, 1H), 4.89 (s, 1H), 4.24 (d, J = 5.9 Hz, 2H), 1.49 (s, 9H).

tert-butyl (4-(3-(piperidin-1-yl)propoxy)benzyl)carbamate (183). Title compound was obtained by using the same procedure described for compound **180**, starting from compound **182** (4.16 mmol, 928 mg), K$_2$CO$_3$, (4.16 mmol, 574 mg), **179** (2.77 mmol, 546 mg), in acetonitrile (6.0 mL). Title compound was used in the next step without any further purification (78 5 yield).^{1}H NMR (300 MHz, CDCl$_3$) δ 7.16 – 7.04 (m, 2H), 6.83 – 6.72 (m, 2H), 4.76 – 4.62 (m, 1H), 4.16 (s, 2H), 3.91 (t, *J* = 6.4 Hz, 2H), 2.49 – 2.20 (m, 7H), 1.95 – 1.81 (m, 2H), 1.58 – 1.45 (m, 5H), 1.39 (s, 9H).

(4-(3-(piperidin-1-yl)propoxy)phenyl)methanamine (184). Title compound was prepared according to procedure used for **165a**, starting from **183** (2.05 mmol, 716 mg) and a solution 1N of HCl/MeOH in MeOH (40 mL). The crude was used in the following step without any further purification (white solid, 99% yield). ^{1}H NMR (300 MHz, CDCl$_3$) δ 7.30 – 6.93 (m, 10H), 3.95 – 3.88 (m, 2H), 2.80 (t, *J* = 4.7 Hz, 4H), 2.39 – 2.26 (m, 4H), 1.89 – 1.72 (m, 4H).

benzyl 4-hydroxybenzoate (186). To a solution of **185** (22 mmol, 3000 mg) in DMF (30 mL) NaHCO$_3$ (33 mmol, 2700 mg) and benzyl bromide (33 mmol, 3900 μL) were added. The reaction was heated to 45 °C and stirred for 12 h. Na4Cl*s.s.* was added, and the mixture was extracted with EtOAc (3 x 30 mL). Organic phase was then washed with brain, dried over MgSO$_4$, filtered, and evaporated. The crude was purified by column chromatography on silica gel (Hexane/EtOAc from 6:1 to 4:1) furnishing title compound as a colorless oil (84%yield).

benzyl 4-(3-(piperidin-1-yl)propoxy)benzoate (187). Title compound was obtained by using the same procedure described for compound **180**, starting from compound **186** (18 mmol, 4230 mg), K$_2$CO$_3$, (18 mmol, 2484 mg), **179** (12 mmol, 2364 mg), in acetonitrile (24.0 mL). Title compound was used in the next step without any further purification (2990 mg, yield 70%).^{1}H NMR (300 MHz, CDCl$_3$) δ 7.99 – 7.89 (m, 2H), 7.42 – 7.22 (m, 5H), 6.88 – 6.78 (m, 2H), 5.25 (s, 2H), 3.97 (t, *J* = 6.4 Hz, 2H), 2.46 – 2.25 (m, 6H), 2.00 – 1.82 (m, 2H), 1.51 (p, *J* = 5.5 Hz, 4H), 1.42 – 1.30 (m, 2H).

4-(3-(piperidin-1-yl)propoxy)benzoic acid (188). To a solution of **187** (8.5 mmol, 2990 mg) in methanol (300 mL), 10% Pd on carbon was added. The reaction was stirred under H$_2$ atmosphere for 6h. The mixture was filtered, and the solvent was then removed *in vacuo*. Title compound was used in the next step without any further purification (2250mg, 99% yield). ^{1}H NMR (300 MHz, Methanol-*d$_4$*) δ 7.94 – 7.75 (m, 2H), 6.93 – 6.79 (m, 2H), 4.09 (t, *J* = 5.9 Hz, 2H), 3.24 – 3.11 (m, 6H), 2.21 (dq, *J* = 11.8, 5.9 Hz, 2H), 1.95 – 1.80 (m, 4H), 1.66 (p, *J* = 5.8 Hz, 2H).

tert-butyl 4-(3-(N-phenyl-4-(3-(piperidin-1-yl)propoxy)benzamido)propyl)piperazine-1-carboxylate (189). To a solution of **188** (1.02 mmol, 266 mg) in THF (14 mL), SOCl$_2$ (14 mmol, 1100 μL) was added at 0 °C. The reaction mixture was stirred for 1h at 75 °C. The reaction was allowed to reach 25 °C and solvent was removed. the residue was washed with DCM (3 x 10 mL) and the solvent was evaporated. To a solution of Chlorine cooled at 0 °C in DCM (6 mL) was added a solution of amine **174** (0.78 mmol, 320 mg) and DIPEA (3.12 mmol, 130 mg) in DCM (6 mL). The reaction was allowed to reach 25 °C and stirred for 1 h. NaHCO3 *s.s* was added, and the mixture was extracted with DCM (3

x 10 mL). the combined organic phases were washed with NH_4Cl *s.s.,* then dried over sodium sulphate and concentrated. The crude was purified by column chromatography on silica gel (from 50:1:0.1 to 20:1:0.1 DCM/MeOH, NH_4OH) to afford the title compound as a yellow oil (21% yield). ^{1}H NMR (300 MHz, $CDCl_3$) δ 7.23 – 6.85 (m, 7H), 6.63 – 6.50 (m, 2H), 3.91 – 3.79 (m, 4H), 3.31 (t, *J* = 5.0 Hz, 4H), 2.40 – 2.18 (m, 12H), 1.91 – 1.71 (m, 4H), 1.49 (p, *J* = 5.5 Hz, 4H), 1.37 (s, 11H).

N-phenyl-N-(3-(piperazin-1-yl)propyl)-4-(3-(piperidin-1-yl)propoxy)benzamide(190).
Title compound was prepared according to procedure used for **165a** starting from compound **189** (136 mg, 0.22 mmol) and a solution 1N of HCl/MeOH in MeOH (40 mL). a colorless solidTitle compound was used in the next step without any further purification (87% yield). ^{1}H NMR (300 MHz, $CDCl_3$) δ 7.19 – 7.11 (m, 4H), 7.09 – 7.02 (m, 1H), 6.98 – 6.93 (m, 2H), 6.60 – 6.51 (m, 2H), 3.86 (q, *J* = 7.3 Hz, 4H), 2.78 (t, *J* = 4.9 Hz, 4H), 2.41 – 2.23 (m, 12H), 2.16 – 2.04 (m, 0H), 1.91 – 1.71 (m, 4H), 1.49 (p, *J* = 5.4 Hz, 4H), 1.35 (q, *J* = 5.9 Hz, 2H).

tert-butyl 4-((4-(3-(piperidin-1-yl)propoxy)benzyl)amino)piperidine-1-carboxylate (191). To a solution of *N*-Boc-piperidone (1.36 mmol, 270 mg) in EtOH (8 mL) amine **184** (2.0 mmol, 508 mg) was added. Temperature was increased to 82 °C and reaction mixture was stirred for 2 h. After cooling down to room temperature, solvent was removed under vacuum. The residue was diluted in MeOH (16 mL) and $NaBH_4$ (50 mg, 1.36 mmol) was added portion wise over 20 minutes at 0 °C. Temperature was allowed to reach 25 °C and reaction mixture was stirred for 12 h. The following day, solvent was removed under vacuum. The residue was taken up with DCM, quenched with a saturated solution of $NaHCO_3$ and reaction mixture was extracted with DCM (3 x 10 mL). Organic phase was dried with $MgSO_4$, filtered and concentrated. The crude was purified by column chromatography on silica gel (from 50:1:0.1 to 20:1:0.1 DCM/MeOH, NH_4OH) to afford the title compound as a yellow oil (21% yield). ^{1}H NMR (300 MHz, $CDCl_3$) δ 7.25 – 7.17 (m, 2H), 6.89 – 6.82 (m, 2H), 3.99 (t, *J* = 6.3 Hz, 4H), 3.75 (s, 2H), 2.80 (t, *J* = 12.3 Hz, 2H), 2.65 (tt, *J* = 10.2, 3.9 Hz, 1H), 2.53 – 2.37 (m, 7H), 2.05 – 1.93 (m, 2H), 1.90 – 1.80 (m, 2H), 1.67 – 1.54 (m, 5H), 1.46 (s, 9H), 1.37 – 1.22 (m, 2H).

tert-butyl 4-(N-(4-(3-(piperidin-1-yl)propoxy)benzyl)benzamido)piperidine-1-carboxylate (192). To a solution of **191** (155 mg, 0.36 mmol) in DCM (2.0 mL) cooled ad 0 °C, TEA (0.54 mmol, 75 μL,) and benzoyl chloride (0.47 mmol, 55 μL) were added. The reaction mixture was allowed to reach 25 °C and stirred for 1 h. $NaHCO_3$ s.s. was added and the mixture was extracted with DCM (3 x 20 mL). The crude was purified by column chromatography on silica gel (from 60:1:0.1 to 20:1:0.1 DCM/MeOH, NH_4OH) to afford the title compound as a yellow oil (41% yield). ^{1}H NMR (300 MHz, $CDCl_3$) δ 7.40 – 7.24 (m, 5H), 7.19 – 6.88 (m, 2H), 6.80 – 6.67 (m, 2H), 4.48 (d, *J* = 5.7 Hz, 2H), 3.92 (t, *J* = 6.1 Hz, 4H), 2.64 (dd, *J* = 16.8, 9.0 Hz, 6H), 2.48 – 2.20 (m, 1H), 2.04 (dq, *J* = 12.5, 6.4 Hz, 2H), 1.74 – 1.40 (m, 12H), 1.35 (s, 9H).

N-(4-(3-(piperidin-1-yl)propoxy)benzyl)-N-(piperidin-4-yl)benzamide (193). Compound **203** was prepared according to procedure used for **165a** starting from compound **192** (85 mg, 0.15 mmol) and a solution 1N of HCl/MeOH in MeOH (10 mL). Colorless oil. Title compound was used in the next step without any further purification (99% yield). ^{1}H NMR (300 MHz, $CDCl_3$) δ 7.45 – 6.95 (m, 6H), 6.88 – 6.66 (m, 3H), 4.72 – 4.32 (m, 2H), 3.98 – 3.81 (m, 2H), 3.08 – 2.81 (m, 3H), 2.50 – 2.21 (m, 8H), 1.99 – 1.81 (m, 2H), 1.75 – 1.46 (m, 8H), 1.38 (q, *J* = 6.1 Hz, 2H).

tert-Butyl 4-(benzylamino)piperidine-1-carboxylate (195). Title compound was prepared according to procedure used for **191** starting from 1-Boc-4-piperidone **194** (502 mg, 2.52 mmol) and benzylamine (550 µL, 5.04 mmol) in EtOH (21 mL) for the first step, then NaBH$_4$ (96 mg,2.55 mmol) in MeOH (42 mL) was used in the second step. The crude was purified by column chromatography on silica gel (DCM/MeOH/NH$_3$ starting from 99:1 to 97:3) to afford the title compound as a yellowish oil (85% yield). ^{1}H NMR (300 MHz, CDCl$_3$) δ 7.37 – 7.28 (m, 5H), 4.02 (d, J = 12.3 Hz, 2H), 3.82 (s, 2H), 2.80 (t, J = 11.5 Hz, 2H), 2.70 – 2.61 (m, 1H), 1.86 (d, J = 10.5 Hz, 2H), 1.45 (s, 9H), 1.38 – 1.21 (m, 2H).

tert-butyl 4-(N-benzyl-4-(piperidin-1-ylmethoxy)benzamido)piperidine-1-carboxylate (196). Title compound was prepared according to the procedure described for compound **189**, starting from **188** (1.2 mmol, 280 mg), SOCl$_2$ (14.5 mmol, 1300 µL), THF (15 mL). The chlorine intermediate reacted with amine **195** (0.78 mmol, 320 mg) and DIPEA (3.12 mmol, 130 mg) in DCM (6 mL). The crude was purified by column chromatography on silica gel (from 50:1:0.1 to 20:1:0.1 DCM/MeOH, NH$_4$OH) to afford the title compound as a yellow oil (21% yield). ^{1}H NMR (300 MHz, CDCl$_3$) δ 7.40 – 7.24 (m, 5H), 7.19 – 6.88 (m, 2H), 6.80 – 6.67 (m, 2H), 4.48 (d, *J* = 5.7 Hz, 2H), 3.92 (t, *J* = 6.1 Hz, 4H), 2.64 (dd, *J* = 16.8, 9.0 Hz, 6H), 2.48 – 2.20 (m, 1H), 2.04 (dq, *J* = 12.5, 6.4 Hz, 2H), 1.74 – 1.40 (m, 12H), 1.35 (s, 9H).

N-benzyl-4-(3-(piperidin-1-yl)propoxy)-N-(piperidin-4-yl)benzamide (197). Title compound was prepared according to procedure used for **165a** starting from compound **196** (120 mg, 0.21 mmol) and a solution 1N of HCl/MeOH in MeOH (40 mL). a colorless solidTitle compound was used in the next step without any further purification (81% yield). ^{1}H NMR (300 MHz, CDCl$_3$) δ 7.35 – 7.09 (m, 7H), 6.88 – 6.74 (m, 2H), 4.59 (s, 2H), 3.94 (t, *J* = 6.4 Hz, 2H), 2.95 (dt, *J* = 12.4, 3.4 Hz, 2H), 2.51 – 2.21 (m, 8H), 1.91 (q, *J* = 6.9 Hz, 2H), 1.83 – 1.71 (m, 2H), 1.67 – 1.44 (m, 8H), 1.37 (q, *J* = 6.1 Hz, 2H).

N-benzyl-1-(4-(3-(piperidin-1-yl)propoxy)phenyl)methanamine (198). Title compound was prepared according to procedure used for **191** starting from benzyamine (2.14, 228 mmol) and **180** (1.07 mmol, 266 mg) in EtOH (7 mL) for the first step, then NaBH$_4$ (1.07 mmol, 40 mg) in MeOH (14 mL) was used in the second step. Solvent was removed under vacuum. The residue was taken up with DCM, quenched with a NaHCO3 s.s. and reaction mixture was extracted with DCM (3 x 10 mL). The combined organic layers were washed with a diluted solution of NH$_4$Cl (3 x 10 mL), then dried over sodium sulphate and evaporated. Title compound was used in the next step without any further purification (61% yield).^{1}H NMR (300 MHz, CDCl$_3$) δ 7.31 – 7.10 (m, 7H), 6.82 – 6.72 (m, 2H), 3.90 (t, *J* = 6.3 Hz, 2H), 3.70 (s, 2H), 3.65 (s, 2H), 2.63 – 2.27 (m, 7H), 1.99 – 1.84 (m, 2H), 1.54 (p, *J* = 5.6 Hz, 4H), 1.37 (q, *J* = 6.1 Hz, 2H).

tert-butyl 4-(benzyl(4-(3-(piperidin-1-yl)propoxy)benzyl)carbamoyl)piperidine-1-carboxylate (199). To a solution of 1-(*tert*-butoxycarbonyl)piperidine-4-carboxylic acid (0.52 mmol, 126 mg) in dry DCM (3 mL) were sequentially added DIPEA (1.03 mmol, 180 uL) and HATU (0.52 mmol, 197), and the reaction mixture was stirred for 10 minutes. Subsequently, a solution of ammine **198** (0.4 mmol, 140 mg) in DCM (3 mL) was added and the reaction mixture was allowed to reach rt and stirred for 12 h. NaHCO$_3$ *s.s.* was added and the mixture was extracted with DCM (3 x 20 mL). The combined organic layers were dried over sodium sulphate and evaporated. The crude was purified by

column chromatography on silica gel (from 60:1:0.1 to 20:1:0.1 DCM/MeOH, NH4OH) to afford the title compound as a yellow oil (98% yield). ^{1}H NMR (300 MHz, CDCl$_3$) δ 7.36 – 7.12 (m, 3H), 7.12 – 6.89 (m, 4H), 6.86 – 6.70 (m, 2H), 4.55 – 4.30 (m, 4H), 4.16 – 4.01 (m, 2H), 3.99 – 3.85 (m, 2H), 3.46 – 3.40 (m, 1H), 2.70 – 2.45 (m, 8H), 2.03 – 1.91 (m, 2H), 1.75 (qt, J = 11.8, 4.5 Hz, 2H), 1.65 – 1.51 (m, 6H), 1.46 – 1.38 (m, 2H), 1.37 (s, 9H).

N-benzyl-N-(4-(3-(piperidin-1-yl)propoxy)benzyl)piperidine-4-carboxamide (200). Title compound was prepared according to procedure used for **165a** starting from compound **199** (103 mg, 0.18 mmol) and a solution 1N of HCl/MeOH in MeOH (40 mL). Colorless oil. (82% yield). Title compound was used in the next step without any further purification (99% yield). ^{1}H NMR (300 MHz, CDCl$_3$) δ 7.45 – 6.95 (m, 6H), 6.88 – 6.66 (m, 3H), 4.72 – 4.32 (m, 2H), 3.98 – 3.81 (m, 2H), 3.08 – 2.81 (m, 3H), 2.50 – 2.21 (m, 8H), 1.99 – 1.81 (m, 2H), 1.75 – 1.46 (m, 8H), 1.38 (q, J = 6.1 Hz, 2H).

tert-butyl 4-(benzyl(4-(3-(piperidin-1-yl)propoxy)benzyl)carbamoyl)piperazine-1-carboxylate (201). To a solution of **198** (0.78 mmol, 267 mg) in DCM (4 mL) and NaHCO$_3$ *s.s. (1 mL) cooled at 0 °C,* a solution of triphosgene (1.56 mmol, 461 mg) in DCM (3 mL) was added in the organic phase. The reaction mixture was stirred for 1h at 25 °C. Water was added and the mixture was extracted with DCM (3 x 20 mL). The combined organic phases were dried over sodium sulphate and concentrated. To a solution of the obtained residue in THF (15 mL), TEA (4.68 mmol, 650 μL) and Boc-piperazine (2.28 mmol, 186 mg) were added. The resulting mixture was stirred 12h at 25°C. NH4Cl *s.s.* was added and the mixture was extracted with ETOAc (3 x 20 mL). The combined organic phases were dried over sodium sulphate and concentrated. The crude was purified by column chromatography on silica gel (from 60:1:0.1 to 20:1:0.1 DCM/MeOH, NH4OH) to afford the title compound as a yellow oil (70% yield). ^{1}HNMR (300 MHz, CDCl$_3$) δ 7.32 – 7.13 (m, 3H), 7.12 – 7.03 (m, 2H), 7.03 – 6.93 (m, 2H), 6.82 – 6.72 (m, 2H), 4.18 (d, J = 13.3 Hz, 4H), 3.93 (t, J = 6.3 Hz, 2H), 3.42 – 3.15 (m, 8H), 2.53 – 2.36 (m, 6H), 2.08 (s, 2H), 2.02 – 1.87 (m, 2H), 1.57 (p, J = 5.5 Hz, 4H), 1.38 (s, 9H).

N-benzyl-N-(4-(3-(piperidin-1-yl)propoxy)benzyl)piperazine-1-carboxamide (202). Title compound was prepared according to procedure used for **165a** starting from compound **202** (0.35 mmol, 160 mg) and a solution 1N of HCl/MeOH in MeOH (10 mL). Colorless oil. Title compound was used in the next step without any further purification (76 mg, 99% yield). ^{1}H NMR (300 MHz, CDCl$_3$) δ 7.31 – 7.05 (m, 5H), 7.01 – 6.94 (m, 2H), 6.83 – 6.71 (m, 2H), 4.17 (d, J = 13.3 Hz, 2H), 3.92 (td, J = 6.3, 2.3 Hz, 2H), 3.33 – 3.17 (m, 3H), 3.01 (s, 2H), 2.80 (dd, J = 5.9, 3.8 Hz, 2H), 2.54 – 2.29 (m, 8H), 2.02 – 1.90 (m, 2H), 1.59 (h, J = 4.9 Hz, 5H), 1.39 (p, J = 6.1 Hz, 2H).

(4-(3-(Benzhydrylamino)propyl)piperazin-1-yl)(1H-1,2,4-triazol-1-yl)methanone (45a)
To a solution of **167a** (30 mg, 0.06 mmol) in Methanol, 10 % palladium on carbon was added. The resulting mixture was stirred under H2 atmosphere for 2 h. The crude was purified by column chromatography on silica gel (DCM/MeOH/NH4OH starting from 30:1:0.1 to 20:1:0.1) to afford the title compound as a milky oil (33% yield). **^{1}H NMR** (300 MHz, CDCl$_3$) δ 8.72 (s, 1H), 7.94 (s, 1H), 7.40 – 7.05 (m, 10H), 4.75 (s, 1H), 2.59 (t, J = 6.6 Hz, 2H), 2.52 – 2.37 (m, 6H), 1.74 – 1.62 (m, 4H), 1.21 – 1.17 (m, 2H). **^{13}C NMR** (75 MHz, CDCl$_3$) δ 152.0, 148.4, 147.0 143.6, 128.5, 127.2, 67.5, 56.8, 52.9, 46.8, 29.7, 26.5. **ESI-MS** *m/z*: 405 [*M*+H]$^{+}$

(4-(4-(Benzhydrylamino)butyl)piperazin-1-yl)(1H-1,2,4-triazol-1-yl)methanone ***(45a)***.
Title compound was obtain following the same procedure described for compound **45a**,
starting from compound **167b** (79 mg, 0.14 mmol) and 10 % palladium on carbon in
EtOAc/MeOH 1:2 (4.0 mL). The crude was purified by column chromatography on silica
gel (DCM/MeOH starting from 50:1 to 20:1) to afford the title compound as a colorless
oil (43% yield). ^{1}H NMR (300 MHz, (CD$_3$)$_2$CO) δ 8.83 (s, 1H), 8.08 (s, 1H), 7.53 – 7.11
(m, 10H), 4.87 (s, 1H), 3.85 – 3.58 (m, 4H), 2.53 – 2.44 (m, 4H), 1.66 – 1.52 (m, 6H),
1.33 – 1.26 (m, 2H). ^{13}C NMR (75 MHz, (CD$_3$)$_2$CO) δ 151.8, 148.4, 146.4, 144.9, 128.2,
127.2, 126.7, 67.4, 57.8, 52.6, 47.7, 27.6, 24.3. ESI-MS *m/z*: 419 [*M*+H]$^+$.

(4-(3-(Dibenzylamino)propyl)piperazin-1-yl)(1H-1,2,4-triazol-1-yl)methanone ***(45c)***.
Title compound was prepared according to procedure used for **167a**, starting from **172**
(60 mg, 0.19 mmol) and 1-1' carbonyl di(1,2,4-triazole) (31 mg, 0.19 mmol) in dry DCM
(15.6 mL). The crude was purified by column chromatography on silica gel (DCM/MeOH
10:1) to afford the title compound as a yellow oil (53% yield). ^{1}H NMR (300 MHz,
CDCl$_3$) δ 8.76 (s, 1H), 7.97 (s, 1H), 7.26 (s, 10H), 3.87 – 3.64 (m, 4H), 3.54 (s, 4H), 2.50
– 2.39 (m, 6H), 2.37 – 2.31 (m, 2H), 1.72 – 1.60 (m, 2H). ^{13}C NMR (75 MHz, CDCl$_3$) δ
151.9, 148.4, 146.6, 140.0, 128.6, 128.1, 126.8, 58.5, 55.9, 52.7, 51.1, 24.4. ESI-MS *m/z*:
419 [*M*+H]$^+$.

N-(3-(4-(1H-1,2,4-Triazole-1-carbonyl)piperazin-1-yl)propyl)-N-phenylbenzamide
(45d). Title compound was prepared according to procedure used for **167a** starting from
176 (15 mg, 0.05 mmol) and 1-1' Carbonyl di(1,2,4-triazole) (8 mg, 0.05 mmol) in dry
DCM (4 mL). The crude was purified by column chromatography on silica gel
(DCM/MeOH starting from 40:1 to 30:1) to afford the title compound as a colorless oil
(20% yield). ^{1}H NMR (300 MHz, CDCl$_3$) δ 8.74 (s, 1H), 7.95 (s, 1H), 7.27 – 6.91 (m,
10H), 4.03 – 3.90 (m, 2H), 2.51 – 2.37 (m, 6H), 1.90 – 1.74 (m, 4H), 1.25 – 1.18 (m, 2H).
^{13}C NMR (75 MHz, CDCl$_3$) δ 170.4, 152.0, 151.9, 148.4, 146.6, 143.4, 136.0, 129.6,
129.2, 128.7, 127.7, 127.6, 126.7, 55.4, 52.7, 48.6, 24.7). ESI-MS *m/z*: 419 [*M*+H]$^+$.

*N-(3-(4-(1H-1,2,4-triazole-1-carbonyl)piperazin-1-yl)propyl)-N-phenyl-4-(3-(piperidin-
1-yl)propoxy)benzamide* ***(46c)***. Title compound was prepared according to procedure
used for **167a**, starting from compound **200** (97 mg, 0.2 mmol) and 1-1' carbonyl di(1,2,4-
triazole) (33 mg, 0.2 mmol) in dry DCM (20 mL). The crude was purified by column
chromatography on silica gel (from 60:1:0.1 to 20:1:0.1 DCM/MeOH, NH$_4$OH) to afford
the title compound as a yellow oil (44 mg, 40% yield). ^{1}H NMR (300 MHz, CDCl$_3$) δ
8.71 (s, 1H), 8.05 (s, 1H), 7.92 (s, 1H), 7.28 – 7.11 (m, 3H), 7.12 – 7.04 (m, 1H), 6.96
(dd, *J* = 7.2, 1.9 Hz, 2H), 6.62 – 6.53 (m, 2H), 3.99 – 3.67 (m, 8H), 2.51 – 2.22 (m, 12H),
1.95 – 1.72 (m, 4H), 1.53 (p, *J* = 5.5 Hz, 4H), 1.38 (q, *J* = 6.1 Hz, 2H). ESI-MS *m/z*: 560
[*M*+H]$^+$.

*N-(1-(1H-1,2,4-triazole-1-carbonyl)piperidin-4-yl)-N-benzyl-4-(3-(piperidin-1-
yl)propoxy)benzamide* ***(46d)***. Title compound was prepared according to procedure used
for **167a**, starting from compound **203** (107 mg, 0.25 mmol) and 1-1' carbonyl di(1,2,4-
triazole) (41 mg, 0.25 mmol) in dry DCM (20 mL). The crude was purified by column
chromatography on silica gel (from 60:1:0.1 to 20:1:0.1 DCM/MeOH, NH$_4$OH) to afford
the title compound as a yellow oil (77 mg, 58% yield). ^{1}H NMR (300 MHz, CDCl$_3$) δ
8.67 (s, 1H), 7.89 (s, 1H), 7.36 – 7.10 (m, 7H), 6.79 (d, *J* = 8.2 Hz, 2H), 4.72 – 4.44 (m,
4H), 4.41 – 4.13 (m, 1H), 3.93 (t, *J* = 6.3 Hz, 2H), 3.06 – 2.70 (m, 2H), 2.44 – 2.25 (m,

6H), 1.96 – 1.70 (m, 6H), 1.51 (p, *J* = 5.5 Hz, 4H), 1.36 (q, *J* = 6.1 Hz, 2H).^{13}C NMR (75 MHz, CDCl$_3$) δ 172.5, 160.2, 152.0, 148.4, 146.6, 138.6, 128.6, 128.5, 128.2, 127.2, 126.5, 114.4, 66.6, 55.8, 54.6, 46.0, 30.1, 26.7, 25.9, 24.4. ESI-MS *m/z*: 531 [*M*+H]$^+$.

N-(1-(1H-1,2,4-triazole-1-carbonyl)piperidin-4-yl)-N-(4-(3-(piperidin-1-yl)propoxy)benzyl)benzamide (46e). Title compound was prepared according to procedure used for **167a**, starting from compound **205** (50 mg, 0.11 mmol) and 1-1' carbonyl di(1,2,4-triazole) (18 mg, 0.11 mmol) in dry DCM (8 mL). The crude was purified by column chromatography on silica gel (from 60:1:0.1 to 20:1:0.1 DCM/MeOH, NH$_4$OH) to afford the title compound as a yellow oil (24 mg, 41% yield). ^{1}H NMR (300 MHz, CDCl$_3$) δ 8.68 (s, 1H), 7.90 (s, 1H), 7.32 (s, 5H), 7.11 – 6.95 (m, 2H), 6.80 – 6.71 (m, 2H), 4.49 (s, 4H), 3.91 (t, *J* = 6.4 Hz, 2H), 3.10 – 2.60 (m, 2H), 2.45 – 2.24 (m, 6H), 2.00 – 1.67 (m, 6H), 1.52 (p, *J* = 5.5 Hz, 5H), 1.37 (q, *J* = 6.0 Hz, 2H). ESI-MS *m/z*: 531 [*M*+H]$^+$.

N-benzyl-N-(4-(3-(piperidin-1-yl)propoxy)benzyl)-1-(1H-1,2,4-triazole-1-carbonyl)piperidine-4-carboxamide (46f). Title compound was prepared according to procedure used for **167a**, starting from compound **208** (118 mg, 026 mmol) and 1-1' carbonyl di(1,2,4-triazole) (42 mg, 0.28 mmol) in dry DCM (20 mL). The crude was purified by column chromatography on silica gel (from 60:1:0.1 to 20:1:0.1 DCM/MeOH, NH$_4$OH) to afford the title compound as a yellow oil (62 mg, 45% yield). ^{1}H NMR (300 MHz, CDCl$_3$) δ 8.74 – 8.65 (m, 1H), 7.92 (s, 1H), 7.39 – 7.21 (m, 3H), 7.13 – 6.93 (m, 4H), 6.87 – 6.72 (m, 2H), 4.56 – 4.32 (m, 6H), 3.93 (q, *J* = 6.7 Hz, 2H), 3.13 – 2.95 (m, 2H), 2.88 – 2.69 (m, 1H), 2.46 – 2.25 (m, 6H), 2.11 – 1.85 (m, 4H), 1.82 – 1.67 (m, 2H), 1.52 (p, *J* = 5.5 Hz, 4H), 1.38 (q, *J* = 5.9 Hz, 2H).^{13}C NMR (75 MHz, CDCl$_3$) δ 174.44, 158.61, 158.38, 151.96, 148.51, 146.57, 137.26, 136.52, 129.56, 129.30, 129.13, 128.70, 128.17, 128.09, 127.85, 127.47, 126.20, 115.07, 114.66, 66.25, 55.84, 54.47, 49.59, 48.13, 47.75, 38.23, 28.67, 26.24, 25.41, 25.31, 23.99. **ESI-MS** *m/z*: 545 [*M*+H]$^+$.

N-benzyl-N-(4-(3-(piperidin-1-yl)propoxy)benzyl)-4-(1H-1,2,4-triazole-1-carbonyl)piperazine-1-carboxamide (46g). Title compound was prepared according to procedure used for **167a**, starting from compound **210** (27 mg, 0.06 mmol) and 1-1' carbonyl di(1,2,4-triazole) (10 mg, 0.06 mmol) in dry DCM (5 mL). The crude was purified by column chromatography on silica gel (from 60:1:0.1 to 20:1:0.1 DCM/MeOH, NH$_4$OH) to afford the title compound as a yellow oil (62 mg, 45% yield). ^{1}H NMR (300 MHz, CDCl$_3$) δ 8.74 (s, 1H), 8.08 (s, 1H), 7.93 (s, 1H), 7.34 – 7.21 (m, 3H), 7.12 – 7.06 (m, 2H), 7.03 – 6.95 (m, 2H), 6.83 – 6.73 (m, 2H), 4.23 (d, *J* = 12.8 Hz, 4H), 3.99 – 3.70 (m, 6H), 3.38 (dd, *J* = 6.7, 3.6 Hz, 4H), 2.59 – 2.38 (m, 8H), 2.04 – 1.92 (m, 2H), 1.60 (p, *J* = 5.6 Hz, 4H), 1.42 (q, *J* = 6.1 Hz, 2H). ESI-MS *m/z*: 545 [*M*+H]$^+$.

9.6. HPLC analysis

A stock solution for each tested compound was prepared dissolving the sample in DMSO to a final concentration of 10 mM. From the stock solution, three samples were prepared: one was used as the standard solution and the other two as the test solu- tions at pH 3.0 and pH 7.4. The samples' concentration of these solutions was 250 mM with a DMSO content of 2.5% (v/v). The standard solution was prepared by dilution of the stock solution in PBS-buffer solution (MeCN/water, 60:40); the dilution of the stock solution in 50mM acetic acid afforded the samples' solution at pH 3.0; and the dilution of the stock solution in 50mM aqueous PBS-buffer afforded the samples' solution at pH 7.4. These suspension/solutions were sealed and left for 24 h at 25 °C under orbital shaking to achieve "pseudothermodynamic equilibrium". After that time the solutions were filtered using PTFE filters and successively diluted 1:2 with the buffer solution used for the preparation of the samples. Then they were analyzed by HPLC/UV/ DAD, using UV detection at 254nm for quantitation. Solubility was calculated by comparing areas of the sample and of the standard:

$$S = \frac{A_{smp} \times FD \times C_{st}}{A_{st}}$$

S = solubility of the compound (µM); Asmp = UV area of the sample (250 mM); Ast = UV area of the standard solution. solution; FD = dilution factor (2); Cst = standard concentration. For each sample the analysis was performed in triplicate and the solubility result reported was obtained from the average of the three values. The same sample solutions were prepared to evaluate the chemical stability of the compounds after 24 h at 25 °C and analyzed by HPLC/UV/DAD, using UV detection at 254nm for quantitation. Stability was calculated by comparing the area of the peak at T0 and the area of the peak

of the same solution after 24 h. A stability percentage value was calculated by this method at pH 3.0 and pH 7.4 for each compound by applying the following formula:

% remaining = $\dfrac{AC_{24}}{AC_{T0}}$

AC_{24} = area of the sample after 24 h at 25 °C; Ac_{T0} = area of the sample at T0. For each sample the analysis was performed in triplicate and the stability result reported was obtained from the average of the three values.

10. Annex

10.1. Collaborations in other projects

During my PhD work I collaborated to other projects in which our research group is involved. Within the context of CNS and neurodegenerative diseases, I contributed to the development of glycogen synthase kinase 3β (GSK-3β) allosteric inhibitors as potential tools for treatment of inherited retinal diseases. This newly sqaramide-based derivatives were obtained through a toxic-free and one-pot synthetic protocol, which employs low-cost goods and avoids any purification step. In this context, my work was dedicated at the characterization of the preliminary drug-like proprieties for the new derivatives, such as solubility and chemical stability. After SAR analysis and computational studies, the allosteric mechanism of action was demonstrated for the most interesting derivatives of the series. Moreover, for our hit compound the GSK-3β inhibition was demonstrated in retinal pigment epithelial (ARPE19) cells *via* T-cell factor/lymphoid enhancer factor (TCF/LEF) binding [162].

The discovery of new anticancer agents also represents a pivotal challenge of our research group. In this framework, our recent research activity was directed toward the identification of new peptide-based parvulin inhibitors as potential anticancer agents. I took part at this project performing the solid phase synthesis of some peptide derivatives. For these compounds, the activity against the target was evaluated whilst to improve cell permeability the most interesting analogues were conjugated with a cell penetrating peptide such as the octa-arginine (R8) stretch. Our R8 conjugated derivatives displayed antiproliferative effects on cancer cell lines compared to non- tumor cells [163].

Keeping in the context of the antitumoral agents, recently we reported the discovery of dual HDAC6/HDAC8 inhibitors as new tools for cancer therapy. Starting from the classic

HDAC inhibitor pharmacophoric structures (consisted of cap group, a linker and a ZBG) we designed innovative azetidine-2-one-based compounds which displayed nanomolar inhibitory profile against the targets of interest together with a good selectivity profile evaluated towards HDAC1 and HDAC10 isoforms. My collaboration in this work, consisted in the synthesis of two derivatives needed to complete the SAR investigation. The most interesting compounds of the series showed antiproliferative activity in U937 and HCT116 cells which overexpressed respectively HDAC6/HDAC8. In this context the activity of our dual compounds resulted better than the selective HDAC6 and HDAC8 inhibitors. Moreover, our compounds did not show any toxicity effects when administrated to zebrafish embryos [164].

11. Bibliography

[1]   G. Appendino, The early history of cannabinoid research, Rend. Lincei. 31 (2020) 919–929. https://doi.org/10.1007/s12210-020-00956-0.

[2]   R. Mechoulam, J.J. Feigenbaum, N. Lander, M. Segal, T.U. Järbe, A.J. Hiltunen, P. Consroe, Enantiomeric cannabinoids: stereospecificity of psychotropic activity., Experientia. 44 (1988) 762–764. https://doi.org/10.1007/BF01959156.

[3]   W.A. Devane, F.A. 3rd Dysarz, M.R. Johnson, L.S. Melvin, A.C. Howlett, Determination and characterization of a cannabinoid receptor in rat brain., Mol. Pharmacol. 34 (1988) 605–613.

[4]   L.A. Matsuda, S.J. Lolait, M.J. Brownstein, A.C. Young, T.I. Bonner, Structure of a cannabinoid receptor and functional expression of the cloned cDNA., Nature. 346 (1990) 561–564. https://doi.org/10.1038/346561a0.

[5]   W.A. Devane, L. Hanus, A. Breuer, R.G. Pertwee, L.A. Stevenson, G. Griffin, D. Gibson, A. Mandelbaum, A. Etinger, R. Mechoulam, Isolation and structure of a brain constituent that binds to the cannabinoid receptor., Science. 258 (1992) 1946–1949. https://doi.org/10.1126/science.1470919.

[6]   A. Papa, S. Pasquini, C. Contri, S. Gemma, G. Campiani, S. Butini, K. Varani, F. Vincenzi, Polypharmacological Approaches for CNS Diseases: Focus on Endocannabinoid Degradation Inhibition, Cells. 11 (2022) 471. https://doi.org/10.3390/cells11030471.

[7]   L. De Petrocellis, V. Di Marzo, An introduction to the endocannabinoid system: from the early to the latest concepts, Best Pract. Res. Clin. Endocrinol. Metab. 23 (2009) 1–15. https://doi.org/10.1016/j.beem.2008.10.013.

[8]   F.A. Iannotti, V. Di Marzo, S. Petrosino, Endocannabinoids and endocannabinoid-related mediators: Targets, metabolism and role in neurological disorders, Prog. Lipid Res. 62 (2016) 107–128. https://doi.org/https://doi.org/10.1016/j.plipres.2016.02.002.

[9]   M.R. Hoehe, L. Caenazzo, M.M. Martinez, W.T. Hsieh, W.S. Modi, E.S. Gershon, T.I. Bonner, Genetic and physical mapping of the human cannabinoid receptor gene to chromosome 6q14-q15., New Biol. 3 (1991) 880–885.

[10]   D. Haspula, M.A. Clark, Cannabinoid receptors: An update on cell signaling, pathophysiological roles and therapeutic opportunities in neurological, cardiovascular, and inflammatory diseases, Int. J. Mol. Sci. 21 (2020) 1–65. https://doi.org/10.3390/ijms21207693.

[11]   W.Y. Ong, K. Mackie, A light and electron microscopic study of the CB1 cannabinoid receptor in primate brain, Neuroscience. 92 (1999) 1177–1191. https://doi.org/https://doi.org/10.1016/S0306-4522(99)00025-1.

[12]   G. Moldrich, T. Wenger, Localization of the CB1 cannabinoid receptor in the rat brain. An immunohistochemical study☆, Peptides. 21 (2000) 1735–1742. https://doi.org/https://doi.org/10.1016/S0196-9781(00)00324-7.

[13]   Y. Kawamura, M. Fukaya, T. Maejima, T. Yoshida, E. Miura, M. Watanabe, T. Ohno-Shosaku, M. Kano, The CB1 cannabinoid receptor is the major cannabinoid receptor at excitatory presynaptic sites in the hippocampus and cerebellum, J. Neurosci. 26 (2006) 2991–3001. https://doi.org/10.1523/JNEUROSCI.4872-05.2006.

[14]   K. Tsou, K. Mackie, M.C. Sañudo-Peña, J.M. Walker, Cannabinoid CB1 receptors are localized primarily on cholecystokinin-containing GABAergic

interneurons in the rat hippocampal formation, Neuroscience. 93 (1999) 969–975. https://doi.org/https://doi.org/10.1016/S0306-4522(99)00086-X.

[15] V.C. Oropeza, K. Mackie, E.J. Van Bockstaele, Cannabinoid receptors are localized to noradrenergic axon terminals in the rat frontal cortex, Brain Res. 1127 (2007) 36–44. https://doi.org/https://doi.org/10.1016/j.brainres.2006.09.110.

[16] S.A. Golech, R.M. McCarron, Y. Chen, J. Bembry, F. Lenz, R. Mechoulam, E. Shohami, M. Spatz, Human brain endothelium: coexpression and function of vanilloid and endocannabinoid receptors, Mol. Brain Res. 132 (2004) 87–92. https://doi.org/https://doi.org/10.1016/j.molbrainres.2004.08.025.

[17] N. Stella, Cannabinoid and cannabinoid-like receptors in microglia, astrocytes, and astrocytomas, Glia. 58 (2010) 1017–1030. https://doi.org/10.1002/glia.20983.

[18] K. Eldeeb, S. Leone-Kabler, A.C. Howlett, No Title, J. Basic Clin. Physiol. Pharmacol. 27 (2016) 311–322. https://doi.org/doi:10.1515/jbcpp-2015-0096.

[19] I. Katona, T.F. Freund, Endocannabinoid signaling as a synaptic circuit breaker in neurological disease, Nat. Med. 14 (2008) 923–930. https://doi.org/10.1038/nm.f.1869.

[20] C. Montero, N.E. Campillo, P. Goya, J.A. Páez, Homology models of the cannabinoid CB1 and CB2 receptors. A docking analysis study, Eur. J. Med. Chem. 40 (2005) 75–83. https://doi.org/https://doi.org/10.1016/j.ejmech.2004.10.002.

[21] A.M. Malfitano, S. Basu, K. Maresz, M. Bifulco, B.N. Dittel, What we know and do not know about the cannabinoid receptor 2 (CB2), Semin. Immunol. 26 (2014) 369–379. https://doi.org/https://doi.org/10.1016/j.smim.2014.04.002.

[22] L. Zhou, S. Zhou, P. Yang, Y. Tian, Z. Feng, X.Q. Xie, Y. Liu, Targeted inhibition of the type 2 cannabinoid receptor is a novel approach to reduce renal fibrosis, Kidney Int. 94 (2018) 756–772. https://doi.org/10.1016/j.kint.2018.05.023.

[23] R.J. Dinis-Oliveira, J.A. Duarte, A. Sánchez-Navarro, F. Remião, M.L. Bastos, F. Carvalho, Paraquat Poisonings: Mechanisms of Lung Toxicity, Clinical Features, and Treatment, Crit. Rev. Toxicol. 38 (2008) 13–71. https://doi.org/10.1080/10408440701669959.

[24] T. Michler, M. Storr, J. Kramer, S. Ochs, A. Malo, S. Reu, B. Göke, C. Schäfer, Activation of cannabinoid receptor 2 reduces inflammation in acute experimental pancreatitis via intra-acinar activation of p38 and MK2-dependent mechanisms, Am. J. Physiol. Liver Physiol. 304 (2013) G181–G192. https://doi.org/10.1152/ajpgi.00133.2012.

[25] R. Roche, L. Hoareau, S. Bes-Houtmann, M.-P. Gonthier, C. Laborde, J.-F. Baron, Y. Haffaf, M. Cesari, F. Festy, Presence of the cannabinoid receptors, CB1 and CB2, in human omental and subcutaneous adipocytes, Histochem. Cell Biol. 126 (2006) 177–187. https://doi.org/10.1007/s00418-005-0127-4.

[26] T.-S. Yu, Z.-H. Cheng, L.-Q. Li, R. Zhao, Y.-Y. Fan, Y. Du, W.-X. Ma, D.-W. Guan, The cannabinoid receptor type 2 is time-dependently expressed during skeletal muscle wound healing in rats, Int. J. Legal Med. 124 (2010) 397–404. https://doi.org/10.1007/s00414-010-0465-1.

[27] P. Lépicier, C. Lagneux, M.G. Sirois, D. Lamontagne, Endothelial CB1-receptors limit infarct size through NO formation in rat isolated hearts, Life Sci. 81 (2007) 1373–1380. https://doi.org/https://doi.org/10.1016/j.lfs.2007.08.042.

[28] I. Nagy, D. Friston, J.S. Valente, J.V. Torres Perez, A.P. Andreou, Pharmacology

of the capsaicin receptor, transient receptor potential vanilloid type-1 ion channel, Prog. Drug Res. 68 (2014) 39—76. https://doi.org/10.1007/978-3-0348-0828-6_2.

[29] H. Sharir, L. Console-Bram, C. Mundy, S.N. Popoff, A. Kapur, M.E. Abood, The endocannabinoids anandamide and virodhamine modulate the activity of the candidate cannabinoid receptor GPR55., J. Neuroimmune Pharmacol. Off. J. Soc. NeuroImmune Pharmacol. 7 (2012) 856–865. https://doi.org/10.1007/s11481-012-9351-6.

[30] H.-C. Lu, K. Mackie, Review of the Endocannabinoid System, Biol. Psychiatry Cogn. Neurosci. Neuroimaging. 6 (2021) 607–615. https://doi.org/https://doi.org/10.1016/j.bpsc.2020.07.016.

[31] J.L. Blankman, G.M. Simon, B.F. Cravatt, A Comprehensive Profile of Brain Enzymes that Hydrolyze the Endocannabinoid 2-Arachidonoylglycerol, Chem. Biol. 14 (2007) 1347–1356. https://doi.org/10.1016/j.chembiol.2007.11.006.

[32] H. Cadas, E. Di Tomaso, D. Piomelli, Occurrence and biosynthesis of endogenous cannabinoid precursor, N- arachidonoyl phosphatidylethanolamine, in rat brain, J. Neurosci. 17 (1997) 1226–1242. https://doi.org/10.1523/jneurosci.17-04-01226.1997.

[33] G.G. Muccioli, Endocannabinoid biosynthesis and inactivation, from simple to complex, Drug Discov. Today. 15 (2010) 474–483. https://doi.org/https://doi.org/10.1016/j.drudis.2010.03.007.

[34] K.-M. Jung, R. Mangieri, C. Stapleton, J. Kim, D. Fegley, M. Wallace, K. Mackie, D. Piomelli, Stimulation of Endocannabinoid Formation in Brain Slice Cultures through Activation of Group I Metabotropic Glutamate Receptors, Mol. Pharmacol. 68 (2005) 1196–1202. https://doi.org/10.1124/mol.105.013961.

[35] U. Anand, B. Pacchetti, P. Anand, M.H. Sodergren, Cannabis-based medicines and pain: a review of potential synergistic and entourage effects, Pain Manag. 11 (2021) 395–403. https://doi.org/10.2217/pmt-2020-0110.

[36] R.A. et al Stone, D., © 19 9 6 Nature Publishing Group, Nature. (1996).

[37] M.H. Bracey, M.A. Hanson, K.R. Masuda, R.C. Stevens, B.F. Cravatt, Structural Adaptations in a Membrane Enzyme That Terminates Endocannabinoid Signaling, Science (80-.). 298 (2002) 1793–1796. https://doi.org/10.1126/science.1076535.

[38] R.K.P. Tripathi, A perspective review on fatty acid amide hydrolase (FAAH) inhibitors as potential therapeutic agents, Eur. J. Med. Chem. 188 (2020) 111953. https://doi.org/https://doi.org/10.1016/j.ejmech.2019.111953.

[39] M. Mileni, S. Kamtekar, D.C. Wood, T.E. Benson, B.F. Cravatt, R.C. Stevens, Crystal Structure of Fatty Acid Amide Hydrolase Bound to the Carbamate Inhibitor URB597: Discovery of a Deacylating Water Molecule and Insight into Enzyme Inactivation, J. Mol. Biol. 400 (2010) 743–754. https://doi.org/https://doi.org/10.1016/j.jmb.2010.05.034.

[40] A.I. Gulyas, B.F. Cravatt, M.H. Bracey, T.P. Dinh, D. Piomelli, F. Boscia, T.F. Freund, Segregation of two endocannabinoid-hydrolyzing enzymes into pre- and postsynaptic compartments in the rat hippocampus, cerebellum and amygdala, Eur. J. Neurosci. 20 (2004) 441–458. https://doi.org/https://doi.org/10.1111/j.1460-9568.2004.03428.x.

[41] G. Labar, C. Bauvois, F. Borel, J.L. Ferrer, J. Wouters, D.M. Lambert, Crystal structure of the human monoacylglycerol lipase, a key actor in endocannabinoid signaling, ChemBioChem. 11 (2010) 218–227. https://doi.org/10.1002/cbic.200900621.

[42] A.J. Hill, C.M. Williams, B.J. Whalley, G.J. Stephens, Phytocannabinoids as novel therapeutic agents in CNS disorders, Pharmacol. Ther. 133 (2012) 79–97. https://doi.org/10.1016/j.pharmthera.2011.09.002.

[43] D. Chanda, D. Neumann, J.F.C. Glatz, The endocannabinoid system: Overview of an emerging multi-faceted therapeutic target, Prostaglandins Leukot. Essent. Fat. Acids. 140 (2019) 51–56. https://doi.org/10.1016/j.plefa.2018.11.016.

[44] T.C. Kirkham, C.M. Williams, F. Fezza, V. Di Marzo, Endocannabinoid levels in rat limbic forebrain and hypothalamus in relation to fasting, feeding and satiation: stimulation of eating by 2-arachidonoyl glycerol, Br. J. Pharmacol. 136 (2002) 550–557. https://doi.org/https://doi.org/10.1038/sj.bjp.0704767.

[45] E. Benarroch, Endocannabinoids in basal ganglia circuits, Neurology. 69 (2007) 306–309. https://doi.org/10.1212/01.wnl.0000267407.79757.75.

[46] M. Sałaga, M. Sobczak, J. Fichna, Inhibition of fatty acid amide hydrolase (FAAH) as a novel therapeutic strategy in the treatment of pain and inflammatory diseases in the gastrointestinal tract, Eur. J. Pharm. Sci. 52 (2014) 173–179. https://doi.org/https://doi.org/10.1016/j.ejps.2013.11.012.

[47] D.J. Hermanson, L.J. Marnett, Cannabinoids, endocannabinoids, and cancer, Cancer Metastasis Rev. 30 (2011) 599–612. https://doi.org/10.1007/s10555-011-9318-8.

[48] Y. Nasser, M. Bashashati, C.N. Andrews, Toward modulation of the endocannabinoid system for treatment of gastrointestinal disease: FAAHster but not "higher," Neurogastroenterol. \& Motil. 26 (2014) 447–454. https://doi.org/https://doi.org/10.1111/nmo.12329.

[49] C. Silvestri, V. Di Marzo, The Endocannabinoid System in Energy Homeostasis and the Etiopathology of Metabolic Disorders, Cell Metab. 17 (2013) 475–490. https://doi.org/https://doi.org/10.1016/j.cmet.2013.03.001.

[50] O. Ofek, M. Karsak, N. Leclerc, M. Fogel, B. Frenkel, K. Wright, J. Tam, M. Attar-Namdar, V. Kram, E. Shohami, R. Mechoulam, A. Zimmer, I. Bab, Peripheral cannabinoid receptor, CB2, regulates bone mass, Proc. Natl. Acad. Sci. U. S. A. 103 (2006) 696–701. https://doi.org/10.1073/pnas.0504187103.

[51] A.S.C. Rice, Should cannabinoids be used as analgesics for neuropathic pain?, Nat. Clin. Pract. Neurol. 4 (2008) 654–655. https://doi.org/10.1038/ncpneuro0949.

[52] D.M. Lambert, C.J. Fowler, The endocannabinoid system: Drug targets, lead compounds, and potential therapeutic applications, J. Med. Chem. 48 (2005) 5059–5087. https://doi.org/10.1021/jm058183t.

[53] A. Gil-Ordóñez, M. Martín-Fontecha, S. Ortega-Gutiérrez, M.L. López-Rodríguez, Monoacylglycerol lipase (MAGL) as a promising therapeutic target, Biochem. Pharmacol. 157 (2018) 18–32. https://doi.org/10.1016/j.bcp.2018.07.036.

[54] V. Chiurchiù, M. van der Stelt, D. Centonze, M. Maccarrone, The endocannabinoid system and its therapeutic exploitation in multiple sclerosis: Clues for other neuroinflammatory diseases, Prog. Neurobiol. 160 (2018) 82–100. https://doi.org/10.1016/j.pneurobio.2017.10.007.

[55] M. van der Stelt, W.B. Veldhuis, P.R. Bär, G.A. Veldink, J.F.G. Vliegenthart, K. Nicolay, Neuroprotection by Δ<sup>9</sup>-Tetrahydrocannabinol, the Main Active Compound in Marijuana, against Ouabain-Induced In Vivo Excitotoxicity, J. Neurosci. 21 (2001) 6475 LP – 6479. https://doi.org/10.1523/JNEUROSCI.21-17-06475.2001.

[56] B.G. Ramírez, C. Blázquez, T. Gómez del Pulgar, M. Guzmán, M.L. de Ceballos,

Prevention of Alzheimer's disease pathology by cannabinoids: neuroprotection mediated by blockade of microglial activation., J. Neurosci. Off. J. Soc. Neurosci. 25 (2005) 1904–1913. https://doi.org/10.1523/JNEUROSCI.4540-04.2005.

[57] M. Moreno-Martet, A. Feliú, F. Espejo-Porras, M. Mecha, F.J. Carrillo-Salinas, J. Fernández-Ruiz, C. Guaza, E. de Lago, The disease-modifying effects of a Sativex-like combination of phytocannabinoids in mice with experimental autoimmune encephalomyelitis are preferentially due to Δ9-tetrahydrocannabinol acting through CB1 receptors, Mult. Scler. Relat. Disord. 4 (2015) 505–511. https://doi.org/https://doi.org/10.1016/j.msard.2015.08.001.

[58] D.K. Nomura, B.E. Morrison, J.L. Blankman, J.Z. Long, S.G. Kinsey, M.C.G. Marcondes, A.M. Ward, Y.K. Hahn, A.H. Lichtman, B. Conti, B.F. Cravatt, Endocannabinoid Hydrolysis Generates Brain Prostaglandins That Promote Neuroinflammation, Science (80-.). 334 (2011) 809–813. https://doi.org/10.1126/science.1209200.

[59] J. Paloczi, Z. V. Varga, G. Hasko, P. Pacher, Neuroprotection in Oxidative Stress-Related Neurodegenerative Diseases: Role of Endocannabinoid System Modulation, Antioxidants Redox Signal. 29 (2018) 75–108. https://doi.org/10.1089/ars.2017.7144.

[60] H. Khan, F.K. Ghori, U. Ghani, A. Javed, S. Zahid, Cannabinoid and endocannabinoid system: a promising therapeutic intervention for multiple sclerosis, Mol. Biol. Rep. 49 (2022) 5117–5131. https://doi.org/10.1007/s11033-022-07223-5.

[61] R.J.M. Franklin, C. Ffrench-Constant, Regenerating CNS myelin - From mechanisms to experimental medicines, Nat. Rev. Neurosci. 18 (2017) 753–769. https://doi.org/10.1038/nrn.2017.136.

[62] H. Zéphir, Progress in understanding the pathophysiology of multiple sclerosis, Rev. Neurol. (Paris). 174 (2018) 358–363. https://doi.org/https://doi.org/10.1016/j.neurol.2018.03.006.

[63] H.L. Weiner, A shift from adaptive to innate immunity: a potential mechanism of disease progression in multiple sclerosis, J. Neurol. 255 (2008) 3–11. https://doi.org/10.1007/s00415-008-1002-8.

[64] I. Mitroulis, V.I. Alexaki, I. Kourtzelis, A. Ziogas, G. Hajishengallis, T. Chavakis, Leukocyte integrins: Role in leukocyte recruitment and as therapeutic targets in inflammatory disease, Pharmacol. Ther. 147 (2015) 123–135. https://doi.org/https://doi.org/10.1016/j.pharmthera.2014.11.008.

[65] G.G. Ortiz, F.P. Pacheco-Moisés, O.K. Bitzer-Quintero, A.C. Ramírez-Anguiano, L.J. Flores-Alvarado, V. Ramírez-Ramírez, M.A. Macias-Islas, E.D. Torres-Sánchez, Immunology and Oxidative Stress in Multiple Sclerosis: Clinical and Basic Approach, Clin. Dev. Immunol. 2013 (2013) 708659. https://doi.org/10.1155/2013/708659.

[66] T.O. Tobore, Oxidative/Nitroxidative Stress and Multiple Sclerosis, J. Mol. Neurosci. 71 (2021) 506–514. https://doi.org/10.1007/s12031-020-01672-y.

[67] Á. Arévalo-Martín, J.M. Vela, E. Molina-Holgado, J. Borrell, C. Guaza, Therapeutic action of cannabinoids in a murine model of multiple sclerosis, J. Neurosci. 23 (2003) 2511–2516. https://doi.org/10.1523/jneurosci.23-07-02511.2003.

[68] M. Brindisi, S. Maramai, S. Gemma, S. Brogi, A. Grillo, L. Di Cesare Mannelli, E. Gabellieri, S. Lamponi, S. Saponara, B. Gorelli, D. Tedesco, T. Bonfiglio, C. Landry, K.M. Jung, A. Armirotti, L. Luongo, A. Ligresti, F. Piscitelli, C.

Bertucci, M.P. Dehouck, G. Campiani, S. Maione, C. Ghelardini, A. Pittaluga, D. Piomelli, V. Di Marzo, S. Butini, Development and Pharmacological Characterization of Selective Blockers of 2-Arachidonoyl Glycerol Degradation with Efficacy in Rodent Models of Multiple Sclerosis and Pain, J. Med. Chem. 59 (2016) 2612–2632. https://doi.org/10.1021/acs.jmedchem.5b01812.

[69] A. Llorente-Berzal, A.L.B. Terzian, V. di Marzo, V. Micale, M.P. Viveros, C.T. Wotjak, 2-AG promotes the expression of conditioned fear via cannabinoid receptor type 1 on GABAergic neurons, Psychopharmacology (Berl). 232 (2015) 2811–2825. https://doi.org/10.1007/s00213-015-3917-y.

[70] M.O. Klein, D.S. Battagello, A.R. Cardoso, D.N. Hauser, J.C. Bittencourt, R.G. Correa, Dopamine: Functions, Signaling, and Association with Neurological Diseases, Cell. Mol. Neurobiol. 39 (2019) 31–59. https://doi.org/10.1007/s10571-018-0632-3.

[71] V. Micale, J. Stepan, A. Jurik, F.A. Pamplona, R. Marsch, F. Drago, M. Eder, C.T. Wotjak, Extinction of avoidance behavior by safety learning depends on endocannabinoid signaling in the hippocampus, J. Psychiatr. Res. 90 (2017) 46–59. https://doi.org/https://doi.org/10.1016/j.jpsychires.2017.02.002.

[72] D.P. Covey, Y. Mateo, D. Sulzer, J.F. Cheer, D.M. Lovinger, Endocannabinoid modulation of dopamine neurotransmission, Neuropharmacology. 124 (2017) 52–61. https://doi.org/https://doi.org/10.1016/j.neuropharm.2017.04.033.

[73] L. Adermark, D.M. Lovinger, Retrograde endocannabinoid signaling at striatal synapses requires a regulated postsynaptic release step, Proc. Natl. Acad. Sci. 104 (2007) 20564–20569. https://doi.org/10.1073/pnas.0706873104.

[74] L. Adermark, G. Talani, D.M. Lovinger, Endocannabinoid-dependent plasticity at GABAergic and glutamatergic synapses in the striatum is regulated by synaptic activity, Eur. J. Neurosci. 29 (2009) 32–41. https://doi.org/https://doi.org/10.1111/j.1460-9568.2008.06551.x.

[75] C. Sagheddu, A.L. Muntoni, M. Pistis, M. Melis, Chapter Seven - Endocannabinoid Signaling in Motivation, Reward, and Addiction: Influences on Mesocorticolimbic Dopamine Function, in: L. Parsons, M. Hill (Eds.), Endocannabinoids, Academic Press, 2015: pp. 257–302. https://doi.org/https://doi.org/10.1016/bs.irn.2015.10.004.

[76] X. Viñals, E. Moreno, L. Lanfumey, A. Cordomí, A. Pastor, R. de La Torre, P. Gasperini, G. Navarro, L.A. Howell, L. Pardo, C. Lluís, E.I. Canela, P.J. McCormick, R. Maldonado, P. Robledo, Cognitive Impairment Induced by Delta9-tetrahydrocannabinol Occurs through Heteromers between Cannabinoid CB1 and Serotonin 5-HT2A Receptors, PLOS Biol. 13 (2015) 1–40. https://doi.org/10.1371/journal.pbio.1002194.

[77] P. Morales, P.H. Reggio, An Update on Non-CB1, Non-CB2 Cannabinoid Related G-Protein-Coupled Receptors, Cannabis Cannabinoid Res. 2 (2017) 265–273. https://doi.org/10.1089/can.2017.0036.

[78] R.M. Vitale, F.A. Iannotti, P. Amodeo, The (Poly)Pharmacology of Cannabidiol in Neurological and Neuropsychiatric Disorders: Molecular Mechanisms and Targets, Int. J. Mol. Sci. 22 (2021). https://doi.org/10.3390/ijms22094876.

[79] J. Mestres, E. Gregori-Puigjané, Conciliating binding efficiency and polypharmacology, Trends Pharmacol. Sci. 30 (2009) 470–474. https://doi.org/10.1016/j.tips.2009.07.004.

[80] A. Anighoro, J. Bajorath, G. Rastelli, Polypharmacology: Challenges and Opportunities in Drug Discovery, J. Med. Chem. 57 (2014) 7874–7887. https://doi.org/10.1021/jm5006463.

[81] A. Cavalli, M.L. Bolognesi, A. Minarini, M. Rosini, V. Tumiatti, M. Recanatini, C. Melchiorre, Multi-target-Directed Ligands To Combat Neurodegenerative Diseases, J. Med. Chem. 51 (2008) 347–372. https://doi.org/10.1021/jm7009364.

[82] A.A. Antolin, P. Workman, J. Mestres, B. Al-lazikani, week 6 - PM_Portfolio.pdf, (2016) 6935–6945. https://doi.org/10.2174/1381612822666160923.

[83] Y. Hu, J. Bajorath, High-resolution view of compound promiscuity [version 1; peer review: 3 approved], F1000Research. 2 (2013). https://doi.org/10.12688/f1000research.2-144.v1.

[84] H. Gühring, M. Hamza, M. Sergejeva, M. Ates, C.E. Kotalla, C. Ledent, K. Brune, A role for endocannabinoids in indomethacin-induced spinal antinociception, Eur. J. Pharmacol. 454 (2002) 153–163. https://doi.org/https://doi.org/10.1016/S0014-2999(02)02485-8.

[85] M. Cipriano, E. Björklund, A.A. Wilson, C. Congiu, V. Onnis, C.J. Fowler, Inhibition of fatty acid amide hydrolase and cyclooxygenase by the N-(3-methylpyridin-2-yl)amide derivatives of flurbiprofen and naproxen, Eur. J. Pharmacol. 720 (2013) 383–390. https://doi.org/https://doi.org/10.1016/j.ejphar.2013.09.065.

[86] O. Sasso, K. Wagner, C. Morisseau, B. Inceoglu, B.D. Hammock, D. Piomelli, Peripheral FAAH and soluble epoxide hydrolase inhibitors are synergistically antinociceptive, Pharmacol. Res. 97 (2015) 7–15. https://doi.org/https://doi.org/10.1016/j.phrs.2015.04.001.

[87] L.H. Parsons, Y.L. Hurd, Endocannabinoid signalling in reward and addiction, Nat. Rev. Neurosci. 16 (2015) 579–594. https://doi.org/10.1038/nrn4004.

[88] G. Spadoni, A. Bedini, L. Furiassi, M. Mari, M. Mor, L. Scalvini, A. Lodola, A. Ghidini, V. Lucini, S. Dugnani, F. Scaglione, D. Piomelli, K.-M. Jung, C.T. Supuran, L. Lucarini, M. Durante, S. Sgambellone, E. Masini, S. Rivara, Identification of Bivalent Ligands with Melatonin Receptor Agonist and Fatty Acid Amide Hydrolase (FAAH) Inhibitory Activity That Exhibit Ocular Hypotensive Effect in the Rabbit, J. Med. Chem. 61 (2018) 7902–7916. https://doi.org/10.1021/acs.jmedchem.8b00893.

[89] M. Seierstad, J.G. Breitenbucher, Discovery and Development of Fatty Acid Amide Hydrolase (FAAH) Inhibitors, J. Med. Chem. 51 (2008) 7327–7343. https://doi.org/10.1021/jm800311k.

[90] D.L. Boger, H. Sato, A.E. Lerner, M.P. Hedrick, R.A. Fecik, H. Miyauchi, G.D. Wilkie, B.J. Austin, M.P. Patricelli, B.F. Cravatt, Exceptionally potent inhibitors of fatty acid amide hydrolase: The enzyme responsible for degradation of endogenous oleamide and anandamide, Proc. Natl. Acad. Sci. 97 (2000) 5044–5049. https://doi.org/10.1073/pnas.97.10.5044.

[91] A.H. Lichtman, D. Leung, C.C. Shelton, A. Saghatelian, C. Hardouin, D.L. Boger, B.F. Cravatt, Reversible inhibitors of fatty acid amide hydrolase that promote analgesia: Evidence for an unprecedented combination of potency and selectivity, J. Pharmacol. Exp. Ther. 311 (2004) 441–448. https://doi.org/10.1124/jpet.104.069401.

[92] D.L. Boger, H. Miyauchi, W. Du, C. Hardouin, R.A. Fecik, H. Cheng, I. Hwang, M.P. Hedrick, D. Leung, O. Acevedo, C.R.W. Guimarães, W.L. Jorgensen, B.F. Cravatt, Discovery of a potent, selective, and efficacious class of reversible α-ketoheterocycle inhibitors of fatty acid amide hydrolase effective as analgesics, J. Med. Chem. 48 (2005) 1849–1856. https://doi.org/10.1021/jm049614v.

[93] G. Tarzia, A. Duranti, A. Tontini, G. Piersanti, M. Mor, S. Rivara, P.V. Plazzi, C.

Park, S. Kathuria, D. Piomelli, Design, Synthesis, and Structure−Activity Relationships of Alkylcarbamic Acid Aryl Esters, a New Class of Fatty Acid Amide Hydrolase Inhibitors, J. Med. Chem. 46 (2003) 2352–2360. https://doi.org/10.1021/jm021119g.

[94] M. Mor, S. Rivara, A. Lodola, P.V. Plazzi, G. Tarzia, A. Duranti, A. Tontini, G. Piersanti, S. Kathuria, D. Piomelli, Cyclohexylcarbamic Acid 3'- or 4'-Substituted Biphenyl-3-yl Esters as Fatty Acid Amide Hydrolase Inhibitors: Synthesis, Quantitative Structure−Activity Relationships, and Molecular Modeling Studies, J. Med. Chem. 47 (2004) 4998–5008. https://doi.org/10.1021/jm031140x.

[95] J.P. Alexander, B.F. Cravatt, Mechanism of Carbamate Inactivation of FAAH: Implications for the Design of Covalent Inhibitors and In Vivo Functional Probes for Enzymes, Chem. Biol. 12 (2005) 1179–1187. https://doi.org/10.1016/j.chembiol.2005.08.011.

[96] S. Kathuria, S. Gaetani, D. Fegley, F. Valiño, A. Duranti, A. Tontini, M. Mor, G. Tarzia, G. La Rana, A. Calignano, A. Giustino, M. Tattoli, M. Palmery, V. Cuomo, D. Piomelli, Modulation of anxiety through blockade of anandamide hydrolysis, Nat. Med. 9 (2003) 76–81. https://doi.org/10.1038/nm803.

[97] S. Butini, M. Brindisi, S. Gemma, P. Minetti, W. Cabri, G. Gallo, S. Vincenti, E. Talamonti, F. Borsini, A. Caprioli, M.A. Stasi, S. Di Serio, S. Ros, G. Borrelli, S. Maramai, F. Fezza, G. Campiani, M. MacCarrone, Discovery of potent inhibitors of human and mouse fatty acid amide hydrolases, J. Med. Chem. 55 (2012) 6898–6915. https://doi.org/10.1021/jm300689c.

[98] R. Kaur, P. Sidhu, S. Singh, What failed BIA 10–2474 Phase I clinical trial? Global speculations and recommendations for future Phase I trials, J. Pharmacol. Pharmacother. 7 (2016) 120–126. https://doi.org/10.4103/0976-500X.189661.

[99] C.N. Kapanda, J. Masquelier, G. Labar, G.G. Muccioli, J.H. Poupaert, D.M. Lambert, Synthesis and Pharmacological Evaluation of 2,4-Dinitroaryldithiocarbamate Derivatives as Novel Monoacylglycerol Lipase Inhibitors, J. Med. Chem. 55 (2012) 5774–5783. https://doi.org/10.1021/jm3006004.

[100] A.G. Hohmann, R.L. Suplita, N.M. Bolton, M.H. Neely, D. Fegley, R. Mangieri, J.F. Krey, J. Michael Walker, P. V Holmes, J.D. Crystal, A. Duranti, A. Tontini, M. Mor, G. Tarzia, D. Piomelli, An endocannabinoid mechanism for stress-induced analgesia, Nature. 435 (2005) 1108–1112. https://doi.org/10.1038/nature03658.

[101] J.Z. Long, W. Li, L. Booker, J.J. Burston, S.G. Kinsey, J.E. Schlosburg, F.J. Pavón, A.M. Serrano, D.E. Selley, L.H. Parsons, A.H. Lichtman, B.F. Cravatt, Selective blockade of 2-arachidonoylglycerol hydrolysis produces cannabinoid behavioral effects, Nat. Chem. Biol. 5 (2009) 37–44. https://doi.org/10.1038/nchembio.129.

[102] B.M. Ignatowska-Jankowska, S. Ghosh, M.S. Crowe, S.G. Kinsey, M.J. Niphakis, R.A. Abdullah, Q. Tao, S.T. O'Neal, D.M. Walentiny, J.L. Wiley, B.F. Cravatt, A.H. Lichtman, In vivo characterization of the highly selective monoacylglycerol lipase inhibitor KML29: Antinociceptive activity without cannabimimetic side effects, Br. J. Pharmacol. 171 (2014) 1392–1407. https://doi.org/10.1111/bph.12298.

[103] N. Aaltonen, J.R. Savinainen, C.R. Ribas, J. Rönkkö, A. Kuusisto, J. Korhonen, D. Navia-Paldanius, J. Häyrinen, P. Takabe, H. Käsnänen, T. Pantsar, T. Laitinen, M. Lehtonen, S. Pasonen-Seppänen, A. Poso, T. Nevalainen, J.T.

Laitinen, Piperazine and piperidine triazole ureas as ultrapotent and highly selective inhibitors of monoacylglycerol lipase, Chem. Biol. 20 (2013) 379–390. https://doi.org/10.1016/j.chembiol.2013.01.012.

[104] J.S. Cisar, O.D. Weber, J.R. Clapper, J.L. Blankman, C.L. Henry, G.M. Simon, J.P. Alexander, T.K. Jones, R.A.B. Ezekowitz, G.P. O'Neill, C.A. Grice, Identification of ABX-1431, a Selective Inhibitor of Monoacylglycerol Lipase and Clinical Candidate for Treatment of Neurological Disorders, J. Med. Chem. 61 (2018) 9062–9084. https://doi.org/10.1021/acs.jmedchem.8b00951.

[105] C. Schalk-Hihi, C. Schubert, R. Alexander, S. Bayoumy, J.C. Clemente, I. Deckman, R.L. DesJarlais, K.C. Dzordzorme, C.M. Flores, B. Grasberger, J.K. Kranz, F. Lewandowski, L. Liu, H. Ma, D. Maguire, M.J. Macielag, M.E. McDonnell, T. Mezzasalma Haarlander, R. Miller, C. Milligan, C. Reynolds, L.C. Kuo, Crystal structure of a soluble form of human monoglyceride lipase in complex with an inhibitor at 1.35 Å resolution, Protein Sci. 20 (2011) 670–683. https://doi.org/https://doi.org/10.1002/pro.596.

[106] T.F. Gamage, B.M. Ignatowska-Jankowska, P.P. Muldoon, B.F. Cravatt, M.I. Damaj, A.H. Lichtman, Differential effects of endocannabinoid catabolic inhibitors on morphine withdrawal in mice, Drug Alcohol Depend. 146 (2015) 7–16. https://doi.org/https://doi.org/10.1016/j.drugalcdep.2014.11.015.

[107] R. Greco, C. Demartini, M. Francavilla, A.M. Zanaboni, C. Tassorelli, Dual Inhibition of FAAH and MAGL Counteracts Migraine-like Pain and Behavior in an Animal Model of Migraine, Cells. 10 (2021). https://doi.org/10.3390/cells10102543.

[108] J.E. Schlosburg, B.L.A. Carlson, D. Ramesh, R.A. Abdullah, J.Z. Long, B.F. Cravatt, A.H. Lichtman, Inhibitors of Endocannabinoid-Metabolizing Enzymes Reduce Precipitated Withdrawal Responses in THC-Dependent Mice, AAPS J. 11 (2009) 342–352. https://doi.org/10.1208/s12248-009-9110-7.

[109] J.Z. Long, D.K. Nomura, R.E. Vann, D.M. Walentiny, L. Booker, X. Jin, J.J. Burston, L.J. Sim-Selley, A.H. Lichtman, J.L. Wiley, B.F. Cravatt, Dual blockade of FAAH and MAGL identifies behavioral processes regulated by endocannabinoid crosstalk in vivo, Proc. Natl. Acad. Sci. 106 (2009) 20270–20275. https://doi.org/10.1073/pnas.0909411106.

[110] S. Butini, S. Gemma, M. Brindisi, S. Maramai, P. Minetti, D. Celona, R. Napolitano, F. Borsini, W. Cabri, F. Fezza, L. Merlini, S. Dallavalle, G. Campiani, M. MacCarrone, Identification of a novel arylpiperazine scaffold for fatty acid amide hydrolase inhibition with improved drug disposition properties, Bioorganic Med. Chem. Lett. 23 (2013) 492–495. https://doi.org/10.1016/j.bmcl.2012.11.035.

[111] A. Grillo, F. Fezza, G. Chemi, R. Colangeli, S. Brogi, D. Fazio, S. Federico, A. Papa, N. Relitti, R. Di Maio, G. Giorgi, S. Lamponi, M. Valoti, B. Gorelli, S. Saponara, M. Benedusi, A. Pecorelli, P. Minetti, G. Valacchi, S. Butini, G. Campiani, S. Gemma, M. Maccarrone, G. Di Giovanni, Selective Fatty Acid Amide Hydrolase Inhibitors as Potential Novel Antiepileptic Agents, ACS Chem. Neurosci. 12 (2021) 1716–1736. https://doi.org/10.1021/acschemneuro.1c00192.

[112] A. Grillo, G. Chemi, S. Brogi, M. Brindisi, N. Relitti, F. Fezza, D. Fazio, L. Castelletti, E. Perdona, A. Wong, S. Lamponi, A. Pecorelli, M. Benedusi, M. Fantacci, M. Valoti, G. Valacchi, F. Micheli, E. Novellino, G. Campiani, S. Butini, M. Maccarrone, S. Gemma, Development of novel multipotent compounds modulating endocannabinoid and dopaminergic systems, Eur. J. Med. Chem. 183 (2019) 111674. https://doi.org/10.1016/j.ejmech.2019.111674.

[113] A. Papa, S. Pasquini, F. Galvani, M. Cammarota, C. Contri, G. Carullo, S. Gemma, A. Ramunno, S. Lamponi, B. Gorelli, S. Saponara, K. Varani, M. Mor, G. Campiani, F. Boscia, F. Vincenzi, A. Lodola, S. Butini, Development of potent and selective FAAH inhibitors with improved drug-like properties as potential tools to treat neuroinflammatory conditions, Eur. J. Med. Chem. 246 (2023) 114952. https://doi.org/10.1016/j.ejmech.2022.114952.

[114] S. Butini, M. Brindisi, S. Gemma, P. Minetti, W. Cabri, G. Gallo, S. Vincenti, E. Talamonti, F. Borsini, A. Caprioli, M.A. Stasi, S. Di Serio, S. Ros, G. Borrelli, S. Maramai, F. Fezza, G. Campiani, M. MacCarrone, Discovery of potent inhibitors of human and mouse fatty acid amide hydrolases, J. Med. Chem. 55 (2012) 6898–6915. https://doi.org/10.1021/jm300689c.

[115] J.L. Blankman, G.M. Simon, B.F. Cravatt, A Comprehensive Profile of Brain Enzymes that Hydrolyze the Endocannabinoid 2-Arachidonoylglycerol, Chem. Biol. 14 (2007) 1347–1356. https://doi.org/https://doi.org/10.1016/j.chembiol.2007.11.006.

[116] T. Bertrand, F. Augé, J. Houtmann, A. Rak, F. Vallée, V. Mikol, P.F. Berne, N. Michot, D. Cheuret, C. Hoornaert, M. Mathieu, Structural Basis for Human Monoglyceride Lipase Inhibition, J. Mol. Biol. 396 (2010) 663–673. https://doi.org/10.1016/j.jmb.2009.11.060.

[117] J.Z. Long, D.K. Nomura, B.F. Cravatt, Characterization of Monoacylglycerol Lipase Inhibition Reveals Differences in Central and Peripheral Endocannabinoid Metabolism, Chem. Biol. 16 (2009) 744–753. https://doi.org/10.1016/j.chembiol.2009.05.009.

[118] E.J. Barreiro, Chapter 1: Privileged scaffolds in medicinal chemistry: An introduction, RSC Drug Discov. Ser. 2016-Janua (2016) 1–15. https://doi.org/10.1039/9781782622246-00001.

[119] A. Safrygin, D. Dar'in, O. Bakulina, M. Krasavin, Synthesis of spirocyclic tetrahydroisoquinolines (spiroTHIQs) via the Castagnoli-Cushman reaction, Tetrahedron Lett. 61 (2020) 152408. https://doi.org/10.1016/j.tetlet.2020.152408.

[120] K. Hiesinger, D. Dar'In, E. Proschak, M. Krasavin, Spirocyclic Scaffolds in Medicinal Chemistry, J. Med. Chem. 64 (2021) 150–183. https://doi.org/10.1021/acs.jmedchem.0c01473.

[121] G. Campiani, C. Cavella, J.D. Osko, M. Brindisi, N. Relitti, S. Brogi, A.P. Saraswati, S. Federico, G. Chemi, S. Maramai, G. Carullo, B. Jaeger, A. Carleo, R. Benedetti, F. Sarno, S. Lamponi, P. Rottoli, E. Bargagli, C. Bertucci, D. Tedesco, D. Herp, J. Senger, G. Ruberti, F. Saccoccia, S. Saponara, B. Gorelli, M. Valoti, B. Kennedy, H. Sundaramurthi, S. Butini, M. Jung, K.M. Roach, L. Altucci, P. Bradding, D.W. Christianson, S. Gemma, A. Prasse, Harnessing the Role of HDAC6 in Idiopathic Pulmonary Fibrosis: Design, Synthesis, Structural Analysis, and Biological Evaluation of Potent Inhibitors, J. Med. Chem. 64 (2021) 9960–9988. https://doi.org/10.1021/acs.jmedchem.1c00184.

[122] A.S. Bhathiwal, A. Bendi, A. Tiwari, A study on synthesis of benzodiazepine scaffolds using biologically active chalcones as precursors, J. Mol. Struct. 1258 (2022) 132649. https://doi.org/10.1016/j.molstruc.2022.132649.

[123] J.F. Fisher, S. Mobashery, Chapter 3: The b-lactam (azetidin-2-one) as a privileged ring in medicinal chemistry, 2016. https://doi.org/10.1039/9781782622246-00064.

[124] M. Brindisi, S. Brogi, S. Maramai, A. Grillo, G. Borrelli, S. Butini, E. Novellino, M. Allarà, A. Ligresti, G. Campiani, V. Di Marzo, S. Gemma, Harnessing the pyrroloquinoxaline scaffold for FAAH and MAGL interaction: Definition of the

structural determinants for enzyme inhibition, RSC Adv. 6 (2016) 64651–64664. https://doi.org/10.1039/c6ra12524g.

[125] L.E. Hebert, J. Weuve, P.A. Scherr, D.A. Evans, Alzheimer disease in the United States (2010{\textendash}2050) estimated using the 2010 census, Neurology. 80 (2013) 1778–1783. https://doi.org/10.1212/WNL.0b013e31828726f5.

[126] K.A. Jellinger, Recent advances in our understanding of neurodegeneration, J. Neural Transm. 116 (2009) 1111–1162. https://doi.org/10.1007/s00702-009-0240-y.

[127] R. Stevenson, E. Samokhina, I. Rossetti, J.W. Morley, Y. Buskila, Neuromodulation of Glial Function During Neurodegeneration, Front. Cell. Neurosci. 14 (2020) 1–23. https://doi.org/10.3389/fncel.2020.00278.

[128] N. Govindarajan, P. Rao, S. Burkhardt, F. Sananbenesi, O.M. Schlüter, F. Bradke, J. Lu, A. Fischer, Reducing HDAC6 ameliorates cognitive deficits in a mouse model for Alzheimer's disease, EMBO Mol. Med. 5 (2013) 52–63. https://doi.org/https://doi.org/10.1002/emmm.201201923.

[129] P. Lopresti, The selective HDAC6 inhibitor ACY-738 sneaks into memory and disease regulation in an animal model of multiple sclerosis, Front. Neurol. 10 (2019). https://doi.org/10.3389/fneur.2019.00519.

[130] A. Fontana, I. Cursaro, G. Carullo, S. Gemma, S. Butini, G. Campiani, A Therapeutic Perspective of HDAC8 in Different Diseases: An Overview of Selective Inhibitors, Int. J. Mol. Sci. 23 (2022). https://doi.org/10.3390/ijms231710014.

[131] K. Ververis, T.C. Karagiannis, Overview of the Classical Histone Deacetylase Enzymes and Histone Deacetylase Inhibitors, ISRN Cell Biol. 2012 (2012) 130360. https://doi.org/10.5402/2012/130360.

[132] X.-J. Yang, E. Seto, HATs and HDACs: from structure, function and regulation to novel strategies for therapy and prevention., Oncogene. 26 (2007) 5310–5318. https://doi.org/10.1038/sj.onc.1210599.

[133] M. Brindisi, A.P. Saraswati, S. Brogi, S. Gemma, S. Butini, G. Campiani, Old but Gold: Tracking the New Guise of Histone Deacetylase 6 (HDAC6) Enzyme as a Biomarker and Therapeutic Target in Rare Diseases, J. Med. Chem. 63 (2020) 23–39. https://doi.org/10.1021/acs.jmedchem.9b00924.

[134] C. Cook, T.F. Gendron, K. Scheffel, Y. Carlomagno, J. Dunmore, M. DeTure, L. Petrucelli, Loss of HDAC6, a novel CHIP substrate, alleviates abnormal tau accumulation, Hum. Mol. Genet. 21 (2012) 2936–2945. https://doi.org/10.1093/hmg/dds125.

[135] C. Kim, H. Choi, E.S. Jung, W. Lee, S. Oh, N.L. Jeon, I. Mook-Jung, HDAC6 Inhibitor Blocks Amyloid Beta-Induced Impairment of Mitochondrial Transport in Hippocampal Neurons, PLoS One. 7 (2012) 1–7. https://doi.org/10.1371/journal.pone.0042983.

[136] I. Taes, M. Timmers, N. Hersmus, A. Bento-Abreu, L. Van Den Bosch, P. Van Damme, J. Auwerx, W. Robberecht, Hdac6 deletion delays disease progression in the SOD1G93A mouse model of ALS, Hum. Mol. Genet. 22 (2013) 1783–1790. https://doi.org/10.1093/hmg/ddt028.

[137] R. Frye, M. Myers, K.C. Axelrod, E.A. Ness, R.L. Piekarz, S.E. Bates, S. Booher, Romidepsin: a new drug for the treatment of cutaneous T-cell lymphoma., Clin. J. Oncol. Nurs. 16 (2012) 195–204. https://doi.org/10.1188/12.CJON.195-204.

[138] K. Chen, X. Zhang, Y.-D. Wu, O. Wiest, Inhibition and Mechanism of HDAC8 Revisited, J. Am. Chem. Soc. 136 (2014) 11636–11643.

https://doi.org/10.1021/ja501548p.

[139] M. Brindisi, C. Cavella, S. Brogi, A. Nebbioso, J. Senger, S. Maramai, A. Ciotta, C. Iside, S. Butini, S. Lamponi, E. Novellino, L. Altucci, M. Jung, G. Campiani, S. Gemma, Phenylpyrrole-based HDAC inhibitors: synthesis, molecular modeling and biological studies, Future Med. Chem. 8 (2016) 1573–1587. https://doi.org/10.4155/fmc-2016-0068.

[140] N. Relitti, A.P. Saraswati, G. Chemi, M. Brindisi, S. Brogi, D. Herp, K. Schmidtkunz, F. Saccoccia, G. Ruberti, C. Ulivieri, F. Vanni, F. Sarno, L. Altucci, S. Lamponi, M. Jung, S. Gemma, S. Butini, G. Campiani, Novel quinolone-based potent and selective HDAC6 inhibitors: Synthesis, molecular modeling studies and biological investigation, Eur. J. Med. Chem. 212 (2021) 112998. https://doi.org/https://doi.org/10.1016/j.ejmech.2020.112998.

[141] A.P. Saraswati, N. Relitti, M. Brindisi, J.D. Osko, G. Chemi, S. Federico, A. Grillo, S. Brogi, N.H. McCabe, R.C. Turkington, O. Ibrahim, J. O'Sullivan, S. Lamponi, M. Ghanim, V.P. Kelly, D. Zisterer, R. Amet, P. Hannon Barroeta, F. Vanni, C. Ulivieri, D. Herp, F. Sarno, A. Di Costanzo, F. Saccoccia, G. Ruberti, M. Jung, L. Altucci, S. Gemma, S. Butini, D.W. Christianson, G. Campiani, Spiroindoline-Capped Selective HDAC6 Inhibitors: Design, Synthesis, Structural Analysis, and Biological Evaluation, ACS Med. Chem. Lett. 11 (2020) 2268—2276. https://doi.org/10.1021/acsmedchemlett.0c00395.

[142] S.J. Hill, J.G. Baker, Histaminergic System, in: S. Offermanns, W. Rosenthal (Eds.), Encycl. Mol. Pharmacol., Springer Berlin Heidelberg, Berlin, Heidelberg, 2008: pp. 588–591. https://doi.org/10.1007/978-3-540-38918-7_74.

[143] P. Lieberman, The basics of histamine biology., Ann. Allergy, Asthma Immunol. Off. Publ. Am. Coll. Allergy, Asthma, Immunol. 106 (2011) S2-5. https://doi.org/10.1016/j.anai.2010.08.005.

[144] S. Corbel, E. Schneider, F.M. Lemoine, M. Dy, Murine hematopoietic progenitors are capable of both histamine synthesis and uptake., Blood. 86 (1995) 531–539.

[145] H. Ericson, A. Blomqvist, C. Köohler, Origin of neuronal inputs to the region of the tuberomammillary nucleus of the rat brain, J. Comp. Neurol. 311 (1991) 45–64. https://doi.org/https://doi.org/10.1002/cne.903110105.

[146] P. Panula, S. Nuutinen, The histaminergic network in the brain: basic organization and role in disease, Nat. Rev. Neurosci. 14 (2013) 472–487. https://doi.org/10.1038/nrn3526.

[147] L. Cheng, J. Liu, Z. Chen, The histaminergic system in neuropsychiatric disorders, Biomolecules. 11 (2021). https://doi.org/10.3390/biom11091345.

[148] W. Hu, Z. Chen, The roles of histamine and its receptor ligands in central nervous system disorders: An update, Pharmacol. Ther. 175 (2017) 116–132. https://doi.org/https://doi.org/10.1016/j.pharmthera.2017.02.039.

[149] K. Karlstedt, A. Senkas, M. Åhman, P. Panula, Regional expression of the histamine H2 receptor in adult and developing rat brain, Neuroscience. 102 (2001) 201–208. https://doi.org/https://doi.org/10.1016/S0306-4522(00)00464-4.

[150] H.L. Haas, O.A. Sergeeva, O. Selbach, Histamine in the Nervous System, Physiol. Rev. 88 (2008) 1183–1241. https://doi.org/10.1152/physrev.00043.2007.

[151] H. Haas, P. Panula, The role of histamine and the tuberomamillary nucleus in the nervous system, Nat. Rev. Neurosci. 4 (2003) 121–130. https://doi.org/10.1038/nrn1034.

[152] S.N. Rahman, D.A. Mcnaught-flores, Y. Huppelschoten, C. Pereira, A. Christopoulos, R. Leurs, C.J. Langmead, Structural and Molecular Determinants

for Isoform Bias at Human Histamine H 3 Receptor Isoforms, (2022). https://doi.org/10.1021/acschemneuro.2c00425.

[153] J.M. Arrang, M. Garbarg, J.C. Schwartz, Auto-inhibition of brain histamine release mediated by a novel class (H3) of histamine receptor., Nature. 302 (1983) 832–837. https://doi.org/10.1038/302832a0.

[154] C. Pillot, A. Heron, V. Cochois, J. Tardivel-Lacombe, X. Ligneau, J.-C. Schwartz, J.-M. Arrang, A detailed mapping of the histamine H(3) receptor and its gene transcripts in rat brain., Neuroscience. 114 (2002) 173–193. https://doi.org/10.1016/s0306-4522(02)00135-5.

[155] G.B. Fox, J.B. Pan, R.J. Radek, A.M. Lewis, R.S. Bitner, T.A. Esbenshade, R. Faghih, Y.L. Bennani, M. Williams, B.B. Yao, M.W. Decker, A.A. Hancock, Two novel and selective nonimidazole H3 receptor antagonists A-304121 and A-317920: II. In vivo behavioral and neurophysiological characterization., J. Pharmacol. Exp. Ther. 305 (2003) 897–908. https://doi.org/10.1124/jpet.102.047241.

[156] C.R. Ganellin, F. Leurquin, A. Piripitsi, J.M. Arrang, M. Garbarg, X. Ligneau, W. Schunack, J.C. Schwartz, Synthesis of potent non-imidazole histamine H3-receptor antagonists., Arch. Pharm. (Weinheim). 331 (1998) 395–404. https://doi.org/10.1002/(sici)1521-4184(199812)331:12<395::aid-ardp395>3.0.co;2-7.

[157] K. Szczepańska, T. Karcz, S. Mogilski, A. Siwek, K.J. Kuder, G. Latacz, M. Kubacka, S. Hagenow, A. Lubelska, A. Olejarz, M. Kotańska, B. Sadek, H. Stark, K. Kieć-Kononowicz, Synthesis and biological activity of novel tert-butyl and tert-pentylphenoxyalkyl piperazine derivatives as histamine H(3)R ligands., Eur. J. Med. Chem. 152 (2018) 223–234. https://doi.org/10.1016/j.ejmech.2018.04.043.

[158] K. Szczepanska, K. Kuder, K. Kiec-Kononowicz, Histamine H3 Receptor Ligands in the Group of (Homo)piperazine Derivatives., Curr. Med. Chem. 25 (2018) 1609–1626. https://doi.org/10.2174/0929867325666171123203550.

[159] D. Mahmood, Histamine H(3) receptors and its antagonism as a novel mechanism for antipsychotic effect: a current preclinical & clinical perspective., Int. J. Health Sci. (Qassim). 10 (2016) 564–575.

[160] F. Jadidi-Niaragh, A. Mirshafiey, Histamine and histamine receptors in pathogenesis and treatment of multiple sclerosis, Neuropharmacology. 59 (2010) 180–189. https://doi.org/10.1016/j.neuropharm.2010.05.005.

[161] F. Imeri, B. Stepanovska Tanturovska, A. Zivkovic, G. Enzmann, S. Schwalm, J. Pfeilschifter, T. Homann, B. Kleuser, B. Engelhardt, H. Stark, A. Huwiler, Novel compounds with dual S1P receptor agonist and histamine H3 receptor antagonist activities act protective in a mouse model of multiple sclerosis, Neuropharmacology. 186 (2021) 108464. https://doi.org/10.1016/j.neuropharm.2021.108464.

[162] G. Carullo, L. Bottoni, S. Pasquini, A. Papa, C. Contri, S. Brogi, V. Calderone, M. Orlandini, S. Gemma, K. Varani, S. Butini, F. Galvagni, F. Vincenzi, G. Campiani, Synthesis of Unsymmetrical Squaramides as Allosteric GSK-3β Inhibitors Promoting β-Catenin-Mediated Transcription of TCF/LEF in Retinal Pigment Epithelial Cells, ChemMedChem. (2022). https://doi.org/10.1002/cmdc.202200456.

[163] N. Relitti, A. Prasanth Saraswati, G. Carullo, A. Papa, A. Monti, R. Benedetti, E. Passaro, S. Brogi, V. Calderone, S. Butini, S. Gemma, L. Altucci, G. Campiani, N. Doti, Design and Synthesis of Oligopeptidic Parvulin Inhibitors,

ChemMedChem. 17 (2022) 1–14. https://doi.org/10.1002/cmdc.202200050.

[164] S. Federico, T. Khan, A. Fontana, S. Brogi, R. Benedetti, F. Sarno, G. Carullo, A. Pezzotta, A.P. Saraswati, E. Passaro, L. Pozzetti, A. Papa, N. Relitti, S. Gemma, S. Butini, A. Pistocchi, A. Ramunno, F. Vincenzi, K. Varani, V. Tatangelo, L. Patrussi, C.T. Baldari, S. Saponara, B. Gorelli, S. Lamponi, M. Valoti, F. Saccoccia, M. Giannaccari, G. Ruberti, D. Herp, M. Jung, L. Altucci, G. Campiani, Azetidin-2-one-based small molecules as dual hHDAC6/HDAC8 inhibitors: Investigation of their mechanism of action and impact of dual inhibition profile on cell viability, Eur. J. Med. Chem. 238 (2022) 114409. https://doi.org/10.1016/j.ejmech.2022.114409.